Cardiff University
School of Medicine
Systems Immunity Research Institute

Prifysgol Caerdydd
Yr Ysgol Meddygaeth
Sefydliad Ymchwil Ststemau Imiwnedd

Novel Unconventional T-cells in Response to Bacteria and Cancer

A Thesis Submitted in Fulfilment of the Requirements for the Degree of Doctor of Philosophy of Cardiff University

Michael Douglas Crowther

August 2018

DECLARATION

This work has not been submitted in substance for any other degree or award at this or any other university or place of learning, nor is being submitted concurrently in candidature for any degree or other award.

Signed …… (candidate) Date ……

STATEMENT 1

This thesis is being submitted in partial fulfilment of the requirements for the degree of PhD.

Signed …… (candidate) Date ……

STATEMENT 2

This thesis is the result of my own independent work/investigation, except where otherwise stated, and the thesis has not been edited by a third party beyond what is permitted by Cardiff University's Policy on the Use of Third Party Editors by Research Degree Students. Other sources are acknowledged by explicit references. The views expressed are my own.

Signed …… (candidate) Date ……

STATEMENT 3

I hereby give consent for my thesis, if accepted, to be available online in the University's Open Access repository and for inter-library loan, and for the title and summary to be made available to outside organisations.

Signed …… (candidate) Date ……

STATEMENT 4: PREVIOUSLY APPROVED BAR ON ACCESS

I hereby give consent for my thesis, if accepted, to be available online in the University's Open Access repository and for inter-library loans after expiry of a bar on access previously approved by the Academic Standards & Quality Committee.

Signed …… (candidate) Date ……

Acknowledgements

I would like to thank my supervisor **Professor Andrew Sewell**, for recognising that Liverpool fans can make good scientists. His continuous support and opportunities provided by him have greatly advanced my development as a researcher. However, without **Dr Garry Dolton**, none of this would have been possible.

I would like to thank all those who have helped with experiments and advice through my time in Cardiff; to **Dr Meriem Attaf** and **Cristina Rius Rafael** for assistance with T-cell receptor sequencing; **Garry Dolton**, **Sarah Galloway** and **Katie Tungatt** for tissue culture; **Dr Mateusz Legut** for helping with whole genome CRISPR; **Dr Angharad Lloyd** for molecular biology assistance; **Dr Catherine Naseriyan** (CBS, Cardiff University) for cell sorting; **Dr Barbara Szomolay** for NGS data analysis; and **Thomas Whalley** for help removing background sequencing data. Outside of Cardiff University, I would also like to thank **Dr Marco Donia**, **Professor Inge Marie Svane**, and **Professor Per Thor Straten** (CCIT, Copenhagen) for patient samples; **Colin Farrell** and **Professor John Phillips** (University of Utah) for deconvolution of whole genome CRISPR and HiSeq; and **Professor Jamie Rossjohn** (Cardiff University/Monash University) who provided MR1 monomers and experimental advice.

The rest of the **T-cell Modulation Group** at Cardiff have all been invaluable. From the early days of **2F04** featuring **Val**, **Angharad**, **Alicia**, **Katie** and **Juneid**; to last of us with **Sarah**, **Tom** and **Aaron**, thanks to all support both inside and outside of work.

This journey would not have been possible without **Mum**, **Dad**, **Keith, Jenny**, **Immy**, **Laura**, **Bruce**, **Chris, Adam**, and **Emma** for their emotional support when it was needed.

Publications

Tungatt, K., V. Bianchi, **M.D. Crowther**, W. E. Powell, A. J. Schauenburg, A.Trimby, M. Donia, A. Skowera, J. J. Miles, C. J. Holland, D. K. Cole, A. J. Godkin, M. Peakman, P. T. Straten, I. M. Svane, G, Dolton and A.K. Sewell (2015) Antibody stabilization of peptide-MHC multimers reveals functional T-cells bearing extremely low affinity TCRs. ***Journal of Immunology*** **194**, 463-74

Laugel, B., A. Lloyd, E.W. Meermeier, **M.D. Crowther**, T.R. Connor, G. Dolton, J.J. Miles, S.R. Burrows, M.C. Gold, D.M. Lewinsohn and A.K. Sewell (2016). Engineering of isogenic cells deficient for MR1 with a CRISPR/Cas9 lentiviral system: tools to study microbial antigen processing and presentation to human MR1-restricted T cells. ***Journal of Immunology***, **197**, 971-82

David K. Cole, Hugo A. van den Berg, Angharad Lloyd, **Michael D. Crowther**, Konrad Beck, Julia Ekeruche-Makinde, John J. Miles, Anna M. Bulek, Garry Dolton, Andrea J. Schauenburg, Aaron Wall, Anna Fuller, Mathew Clement, Bruno Laugel, Pierre J. Rizkallah, Linda Wooldridge and Andrew K. Sewell. (2016). Structural Mechanism Underpinning Cross-reactivity of a CD8 T-cell Clone That Recognizes a Peptide Derived from Human Telomerase Reverse Transcriptase. ***Journal of Biological Chemistry,*** **292**, 802-13

Sophie V. Pageona, Thibault Tabarina, Yui Yamamoto, Yuanqing Ma, Philip R. Nicovich, John S. Bridgeman, André Cohnene, Carola Benzing, Yijun Gao, **Michael D. Crowther**, Katie Tungatt, Garry Dolton, Andrew K. Sewell, David A. Price, Oreste Acuto, Robert G. Parton, J. Justin Gooding, Jérémie Rossy, Jamie Rossjohn, and Katharina Gaus. (2016). Functional role of T-cell receptor nanoclusters in signal initiation and antigen discrimination. ***PNAS,*** **113,** E5454-63

Fuller A, Wall A, Crowther MD, Lloyd A, Zhurov A, Sewell AK, Cole DK, Beck K. (2017). Thermal Stability of Heterotrimeric pMHC Proteins as Determined by Circular Dichroism Spectroscopy. ***Bio-protocol, 7(13),*** e2366

Summary

Background - Conventional T-cells respond to peptide antigens presented by person-specific Human Leukocyte Antigens (HLAs) and therefore therapies that harness such cells may only be applicable to a minority of individuals. Unconventional T-cells could bypass this limitation to provide an opportunity for population-wide disease treatments. Exploitation of such T-cells first requires a detailed study of the unconventional T-cells involved in the immune response. I therefore sought to characterise novel invariant T-cells generated in response to varied disease agents.

Results – An optimised protocol for procurement of disease-relevant unconventional T-cells was established and used to generate T-cell lines and clones of interest. T-cell receptor (TCR) sequencing of unconventional T-cell populations revealed a predominance of mucosal-associated invariant cells and Vγ9Vδ2 T-cells. Enrichments for other shared TCR clonotypes included TRAV21 and TRAV13-1 genes, which have some evidence of an invariant nature. I identified an interesting T-cell clone that was capable of recognising a broad range of target cells through a novel mechanism. The ligand recognised by these T-cells was identified using a whole genome CRISPR approach. Further studies confirmed the nature of the ligand and that recognition was dependent on a new subtype of TCR that was present in all donors tested.

Conclusions - The field of unconventional T-cells is rapidly expanding, with novel invariant T-cells proving to be a much greater part of the T-cell repertoire than previously estimated. New and undiscovered invariant T-cell subsets are likely to provide exciting novel immunotherapies and bypass the limitation of HLA-restriction that is associated with conventional T-cell recognition of peptide-major histocompatibility complex ligands.

Abbreviations

ACT – adoptive cell transfer
AIRE – autoimmune regulator
APC – antigen presenting cells
APCy – allophycocyanin
BTN – butyrophilin
C – constant
CAR – chimeric antigen receptor
CD – cluster of differentiation
cDNA – complementary DNA
CDR – complementarity-determining region
CRISPR – clustered regularly interspaced short palindromic repeats
crRNA – CRISPR RNA
D – diversity
DC – dendritic cell
DMEM – Dulbecco modified eagle's minimum essential media
DMSO – dimethylsulfoxide
DN – double negative
DNA – deoxyribonucleic acid
dNTP – deoxyribonucleotide
DTT – dithiothreitol
E:T – effector to target ratio
EBV – Epstein-barr virus
EDTA – ethylenediaminetetraacetic acid
EF – elongation factor
ELISA – enzyme-linked immunosorbent assay
EPCR – endothelial protein C receptor
ER – endoplasmic reticulum
FACS – fluorescence activated cell sorting
FBS – foetal bovine serum
FcRn – neonatal Fc receptor
FITC – fluorescein isothiocyanate
FMO – fluorescence minus one
FSC – forward scatter
αGalCer – α-galactosylceramide
GeCKO – genome-wide CRISPR knock-out
GMP – good manufacturing practice
HeBS – HEPES-buffered saline
HEPES - 4-(2-hydroxyethyl)-1-piperazineethanesulfonic acid
HIV – human immunodeficiency virus
HFE – human hemochromatosis protein
HLA – human leukocyte antigen
HMBPP – (*E*)-4-Hydroxy-3-methyl-but-2-enyl pyrophosphate
ICS – intracellular cytokine staining
IFN-γ – interferon-γ
IL – interleukin
IPP – isopentenyl pyrophosphate
J – joining

JAK – Janus kinase
KO – knock-out
LB – lysogeny broth
LCL – lymphoblastoid cell line
MACS – magnetic activated cell sorting
MaGECK – model-based analysis of genome-wide CRISPR/Cas9 knockout
MAIT – mucosal associated invariant T
MFI – mean fluorescence intensity
MHC – major histocompatibility complex
MIC – minimum inhibitory concentration
MICA/B – MHC Class I polypeptide-related sequences A and B
MIP – macrophage inflammatory protein
MM – malignant melanoma
MOI – multiplicity of infection
MR1 – MHC-related protein 1
MSH – MutS homologue
N – non-template
NGS – next generation sequencing
NKG2D – natural killer group 2 member D
NKT – natural killer T
ns – not significant
nt – nucleotide
OD – optical density
ORF – open reading frame
P – palindromic
PAM – protospacer adjacent motif
PB – pacific blue
PBS – phosphate buffered saline
PBMC – peripheral blood mononuclear cell
PCR – polymerase chain reaction
PD – programmed death
PDB – protein database
PE – phycoerythrin
PerCP – Peridinin chlorophyll protein
PHA – phytohemagglutinin
PKI – protein kinase inhibitor
RACE – rapid amplification of cDNA ends
RBC – red blood cell
RCC – renal cell carcinoma
RFX – regulatory factor X
RFXANK – RFX associated ankyrin containing protein
RFXAP – RFX associated protein
RPMI – Roswell Park Memorial Institute medium
RNA – ribonucleic acid
SEM – standard error of the mean
SMARTer – switching mechanism at 5’ end of RNA transcript
SSC – side scatter
TAPI – TNFα processing inhibitor
TCR – T-cell receptor
TE – tris-EDTA
TIL – tumour infiltrating lymphocytes

TNF – tumour necrosis factor
traccrRNA – trans-activating CRISPR RNA
ULBP – UL-16 binding protein
wt – wildtype
ZAG – zinc-alpha-2-glycoprotein
β_2M – β-2-microglobulin

Table of Contents

List of Figures

List of Tables

Chapter 1. Introduction

1.1 The Immune System

The immune system is responsible for clearance of the multitude of pathogens that humans are exposed to daily. It is a complex system that can be broadly divided into two response groups that work in tandem to eliminate harmful threats: the innate and adaptive immune system. The vast majority of pathogens are prevented from establishing an infection by the non-specific broad range of the innate immune system alone. If a pathogen overcomes the innate response, the adaptive immune system comprised of B-cells and T-cells, is triggered. Primary adaptive immune responses are slower to develop compared to the innate response. Secondary exposure to the pathogen is stronger as a result of immunological memory, where B- and T-cells can differentiate into memory cells that persist in secondary lymphoid organs from where they can rapidly proliferate and respond to clear the pathogen. B- and T-cells are both initially stimulated by antigen-presenting cells (APCs) through recognition of their corresponding antigen, mediated by B-cell receptors and T-cell receptors (TCR) encoded by highly diverse somatically rearranged genes. This study focuses on T-cells, which can express either αβ or γδ TCRs depending on which genes are used to form the rearranged antigen receptor.

1.2 Generation of TCR Diversity by VDJ Recombination

The diversity produced by the TCR gene rearrangements in both αβ and γδ T-cells is fundamental for the clearance of pathogens and abnormal cells (Messaoudi et al. 2002). Precursors of T-cells are produced by haematopoietic stem cells in the bone marrow and

then migrate to the thymus, where the generation of diversity of the TCR occurs. Thymic T-cell development results in production of T-cells each with a unique TCR upon egress into the periphery. Both αβ- and γδ-TCRs possess the same immunoglobulin-like structure but appear to have strikingly different specificities despite evolving at roughly the same time (Hayday 2000; Hirano et al. 2013). The highly diverse nature of these two TCR types is produced via somatic recombination of germline clustered gene segments termed Variable (V), Diversity (D), and Joining (J) genes which are alternatively spliced to a Constant (C) domain in a process known as V(D)J recombination (**Figure 1.1**). When translated into protein, recombined VDJ genes form the TCR structure capable of recognising specific antigens. Historically, the *trg*, *trd* and *trb* loci were thought to rearrange concomitantly, however next generation sequencing of TCR chains has identified sequential rearrangement of chains, beginning with the *trd*, followed by *trg*, which if unsuccessful lead to *trb* rearrangement (Dik et al. 2005; Sherwood et al. 2011). If a *trb* rearrangement proves functional (through pairing with a surrogate α chain, termed pre-Tα), the thymocyte commits to an αβ-T-cell lineage and *tra* rearrangement occurs. The number of segments present in each TCR locus is highlighted in **Table 1.1**.

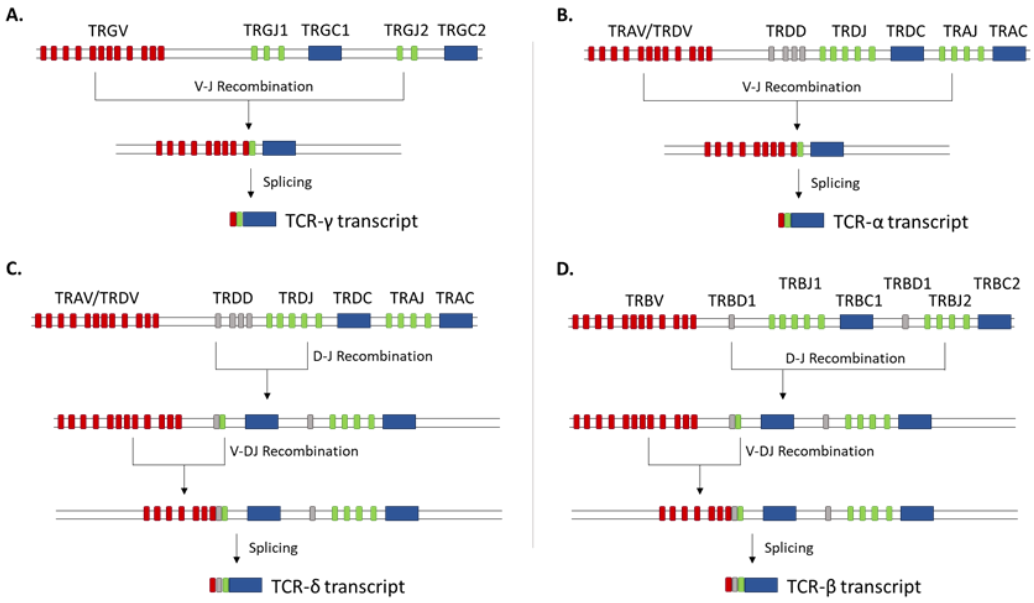

Figure 1.1 - Schematic Overview of V(D)J Recombination of human TCR locus

(**A** & **B**) The recombination of the *trg* and *tra* loci occurs between Variable (V) and Joining (J) segments with non-germline insertions of P- and N- nucleotides at this junction. The resulting transcript is spliced to the Constant (C) segment to result in a mature TCR-γ or TCR-α transcript. (**C** & **D**). The first recombination event occurs between Diversity (D) and J segments (with *trd* able to recombine multiple D segments). The DJ segment is then able to recombine with V segment and produce a full TCR-δ or TCR-β transcript after splicing to the C segment. P- and N- nucleotide additions can occur at both the V-DJ intersection and the DJ intersection, greatly increasing diversity. As the *trd* locus is contained within the *tra* locus, a successful recombination at the *tra* locus results in deletion of the *trd* segments, however there is some promiscuity between TRAV and TRDV segments. Figure shows a representative number of segments, and is adapted from (Attaf et al. 2015).

Table 1.1 - Germline diversity in TCR genes

	αβ-TCR		**γδ-TCR**	
	α	**β**	**γ**	**δ**
Variable (V) Segments	45	48	6	3 (8*)
Diversity (D) Segments	-	3	-	3
Joining (J) Segments	57	14	6	4
Potential Diversity	$10^{16\text{-}20}$		$10^{18\text{-}22}$	

*includes an additional 5 promiscuous TRAV genes that can be incorporated in the δ-chain. Number of gene segments from IMGT database (Lefranc et al. 2015), potential diversity from (Zarnitsyna et al. 2013; Sewell 2012; Chien et al. 2014; Davis et al. 1988).

The *trg* and *tra* (forming the γ-chain and α-chain TCRs respectively) recombine V and J segments, followed by splicing to the C segment for a full TCR chain transcript (**Figure 1.1**). At the junction of the V-J segment, deletion of germline nucleotides, as well as insertions of palindromic (P-) or non-templated (N-) nucleotides occur serving to increase diversity of the resulting TCR. In the *trd* and *trb* locus, an additional D segment is recombined with a J segment before joining to a V segment, forming a full TCR transcript when spliced to the C domain (**Figure 1.1**). P- and N- nucleotides as well as germline deletions can occur at both the D-J intersection and the V-DJ intersection, increasing diversity in these TCR chains. Moreover, as TRDD segments can be read in all three reading frames, the *trd* locus can incorporate up to three D segments in the final TCR with each join able to contain non-germline additions/deletions (Elliott et al. 1988). The resulting TCR proteins result in a vast potential germline T-cell repertoire (**Table 1.1**). An additional source of variability among TCRs not included in these estimates is the possibility for hybrid TCRs, where recombination of segments from different chains occurs. In one particular example, a TRDV segment (not one of the five promiscuous TRAV/TRDV segments, **Table 1.1**) recombines with a TRAJ segment, spliced to a TRAC segment and paired with a TCR-β chain resulting in a functionally viable δ/αβ TCR (Pellicci et al. 2014). Other hybrid TCRs have also been documented, including TRGV/TRBJ and TRGV/TRBD rearrangements that are functionally responsive to TCR stimulation (Bowen et al. 2014). However, due to the genomic location of the *trd* locus within the *tra* locus (**Figure 1.1**), α-chain recombination can result in complete deletion of the entire *trd* gene segments.

TCR rearrangements lead to the formation of a unique binding domain of each TCR. Each chain (α, β, γ or δ) has three loops termed Complementarity Determining Regions (CDRs) (**Figure 1.2**). CDR1 and CDR2 are embedded within the germline-encoded V segments, whereas the CDR3 is termed hypervariable as it is composed of the junction between the V

and C segments (including the J segment and any deletions or insertions, as well as any D segments if applicable) (**Figure 1.2**). Each T-cell clone will therefore have a unique CDR3, but can be more generally defined by their V, D and J segments when conducting repertoire analyses. The CDR loops generated during this process are vital to T-cell-mediated immunity as they form the majority, if not the entirety, of TCR-ligand contacts (Attaf et al. 2015). In most cases, the CDR3 loop is responsible for the antigen specificity of the TCR.

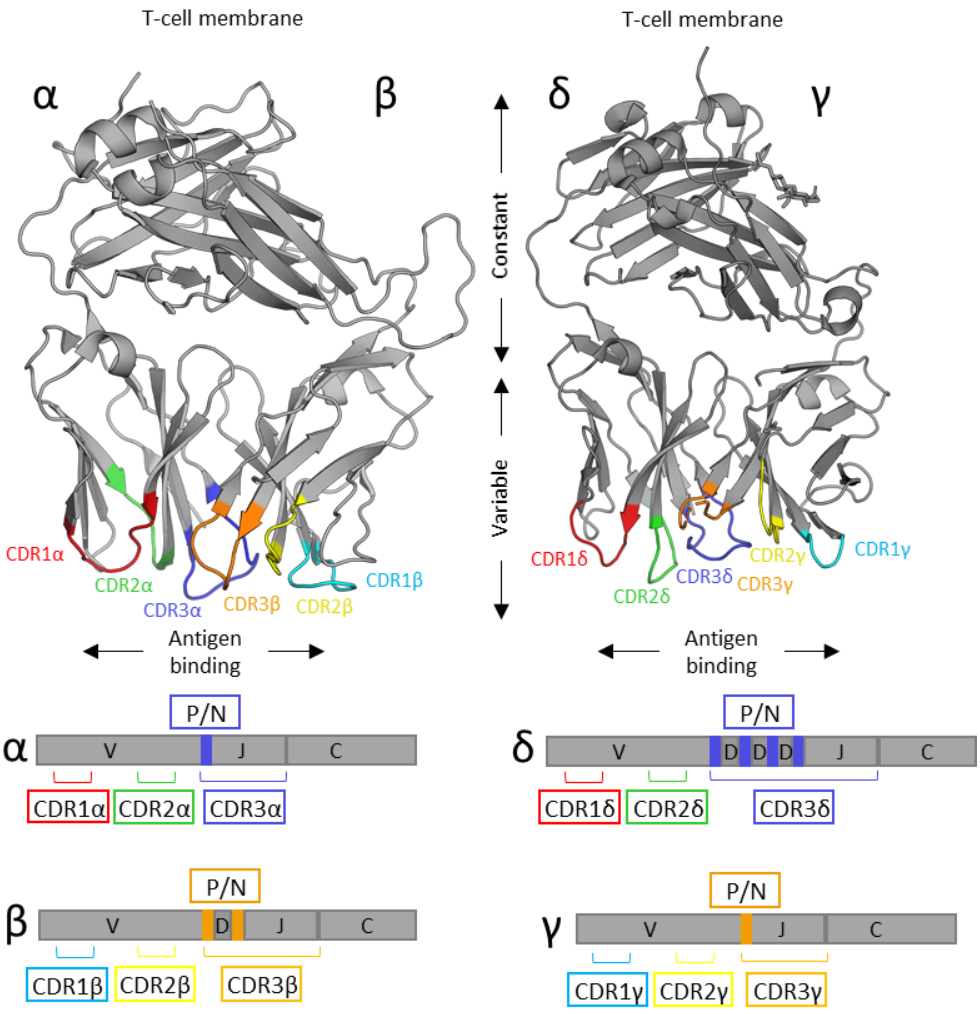

Figure 1.2 - Structure of TCR proteins and mRNA schematic
(Top) αβ and γδ crystal structures adopt similar quaternary structures comprised of six complementarity-determining regions (CDR) positioned at the membrane distal end of the structure. (Bottom) mRNA schematic show CDR1 and CDR2 loops are germline encoded in the variable (V) gene. CDR3 is comprised of the segment between the V and constant (C) segments, including a Joining (J) segment, and Diversity (D) segments (only in TCR-δ and TCR-β). Included in this junction are palindromic (P) and non-germline (N) nucleotide additions. Adapted from (Attaf et al. 2015). PDB codes: αβ TCR – 4MNQ, γδ TCR – 4LFH.

After TCR recombination, T-cells must survive positive and negative selection ensuring T-cells are functional but not self-reactive, respectively. Regarding conventional αβ-T cell development, after V(D)J recombination, a functional TCR-β pairs with a surrogate α chain, termed pre-Tα, enabling the immature $CD4^{neg}$ $CD8^{neg}$ thymocyte to rearrange its *tra* locus. Upon successful TCR-α chain rearrangement, the thymocyte becomes double positive ($CD4^{+}$ $CD8^{+}$) and is selected via survival signals for recognising peptide-Major Histocompatibility Complex (pMHC) at low levels (positive selection) or deleted due to recognising self-pMHC too strongly (negative selection), mostly regulated by autoimmune regulatory element (AIRE). Thymocytes that survive selection (approximately 2%) then lose their expression of either CD8 or CD4, dependent on their MHC-restriction (MHC Class-I or MHC-II respectively). The mechanisms of γδ T-cell selection however remain poorly understood, due to the limited availability of purported ligands. While essential in conventional αβ thymocyte selection, absence of AIRE has no effect on γδ T-cell development (Tuovinen et al. 2009). Experiments in mice show Skint-1 protein is essential for the development of certain γδ T-cell subsets, however there is no human Skint-1 homologue (Barbee et al. 2011; Salim et al. 2016).

1.3 Conventional T-cells

While T-cells are defined by their expression of TCR chains, they are further subdivided based on their antigen specificity, particularly the restricting molecule that facilitates recognition. The most extensively studied subsets of T-cells are those that recognise peptides restricted by specific MHC molecules. These 'conventional' T-cells typically express a broad repertoire of the αβ TCRs and form the majority of circulating peripheral blood T-cells but are also found in tissues and lymph nodes. Conventional T-cells subsets are defined by their surface expression of coreceptors; $CD8^{+}$ and $CD4^{+}$ T-cells. Broadly speaking, $CD8^{+}$ T-cells induce targeted killing of infected or transformed cells and are therefore also known as cytotoxic T-

cells, whereas $CD4^+$ T-cells are responsible for facilitating and regulating the immune response and are also known as helper T-cells.

MHC-I is the main presenting molecule to $CD8^+$ T-cells and presents a wide range of 8-14 amino acid length peptides on its three human family members; Human Leukocyte Antigen (HLA)-A, -B or -C. MHC-I is a heterodimer comprised of a polymorphic HLA-α chain non-covalently paired with a non-polymorphic β_2-microglobulin (β_2M) chain that is not involved in the direct presentation of antigen to T-cells. In contrast, MHC-II is formed of a heterodimer of an α and β chain that combine to form an antigen binding cleft capable of presenting peptides of 12-20 amino acids in length to $CD4^+$ T-cells. The MHC-II presentation of peptides is usually limited to professional APCs where it presents exogenous peptides. The human presenting molecules in MHC-II are HLA- DP, -DQ and -DR.

1.4 Unconventional αβ T-cells

Unconventional T-cells are so named because they do not follow the normal paradigm of αβ T-cell recognition of pMHC. Unconventional T-cells can express either an αβ or γδ TCR. TCR-αβ antigens include a range of antigen presenting MHC-I related genes, comprised of MHC-Ib (located within the MHC locus) or MHC-like molecules (located outside the MHC locus). The majority of known antigens for γδ TCRs do not appear to conform to the standard model of presentation, instead recognising some MHC-I related genes in addition to soluble antigens, haptens and ectopically expressed proteins. The MHC-Ib and MHC-like genes show extensive evolutionary conservation as well as restricted polymorphic diversity, contrasting the classical MHC molecules (Rodgers et al. 2005; Godfrey et al. 2015). The MHC-Ib and MHC-like molecules form a similar structure to MHC-I, in that they possess a heavy chain consisting of three α subunits non-covalently linked to β2M, with unique features in their respective

antigen binding groove. The range of known MHC-Ib molecules, MHC-like molecules and the TCRs that recognise them are shown in **Table 1.2**. The unconventional αβ T-cells are described in further detail in **Figure 1.3**, with γδ T-cells discussed later. In addition to those that are recognised by human TCRs, proteins such as haemochromatosis protein (HFE), Neonatal Fc Receptor (FcRn) and alpha-2-glycoprotein 1 (AZGP1, also known as ZAG) all have this MHC-Ib morphology, yet no human TCR has currently been identified that binds these molecules. Of note however, both human and murine HFE are able to activate a subset of murine $CD8^+$ T-cells (Rohrlich et al. 2005). Additional murine MHC-Ib molecules include H2-M3 which presents N-formylated peptides (Chiu et al. 1999; Seaman et al. 2000) and H2-Q9 known to present polyomavirus and tumour peptides (Swanson et al. 2008; Chiang et al. 2005); these however appear to have no human homologue.

Table 1.2 - Ligands and restricting molecules for unconventional T-cells

Restricting Molecule	Ligand	αβ TCR	γδ TCR
Annexin A2	N/A	Unknown	Vγ8Vδ3
BTN3A1	HMBPP	Unknown	Vγ9Vδ2
CD1a	Lipids	Diverse	Unknown
CD1b	Lipids/GMM	Diverse/ TRAV1-2 TRAJ9/ TRBV4-1	Unknown
CD1c	Lipids	Diverse	Vδ1*
CD1d	α-GalCer/lipids	TRAV10 TRAJ18 TRBV25/ Diverse	Vγ4Vδ1/ Vγ5Vδ1
EPCR	Lipids/ protein C	Unknown	Vγ4Vδ5
HLA-E	MHC-I Leader/ mycobacterial peptides	Diverse	Unknown
MICA/B	-	Unknown	Vδ1
MR1	Vitamin B metabolites	TRAV1-2 TRAV12/20/33	Unknown
MSH2	-	Unknown	Vδ2
ULBPs	-	Unknown	Vγ9Vδ2

*as part of a γδ-TCR or as a δ-αβ TCR hybrid. HMBPP, (E)-4-hydroxy-3-methyl-but-2-enyl pyrophosphate; GMM, glucose monomycolate; α-GalCer, α-galactosylceramide; EPCR, epithelial protein receptor C; MSH2, Muts homolog 2; ULBPs, UL-16 binding proteins.

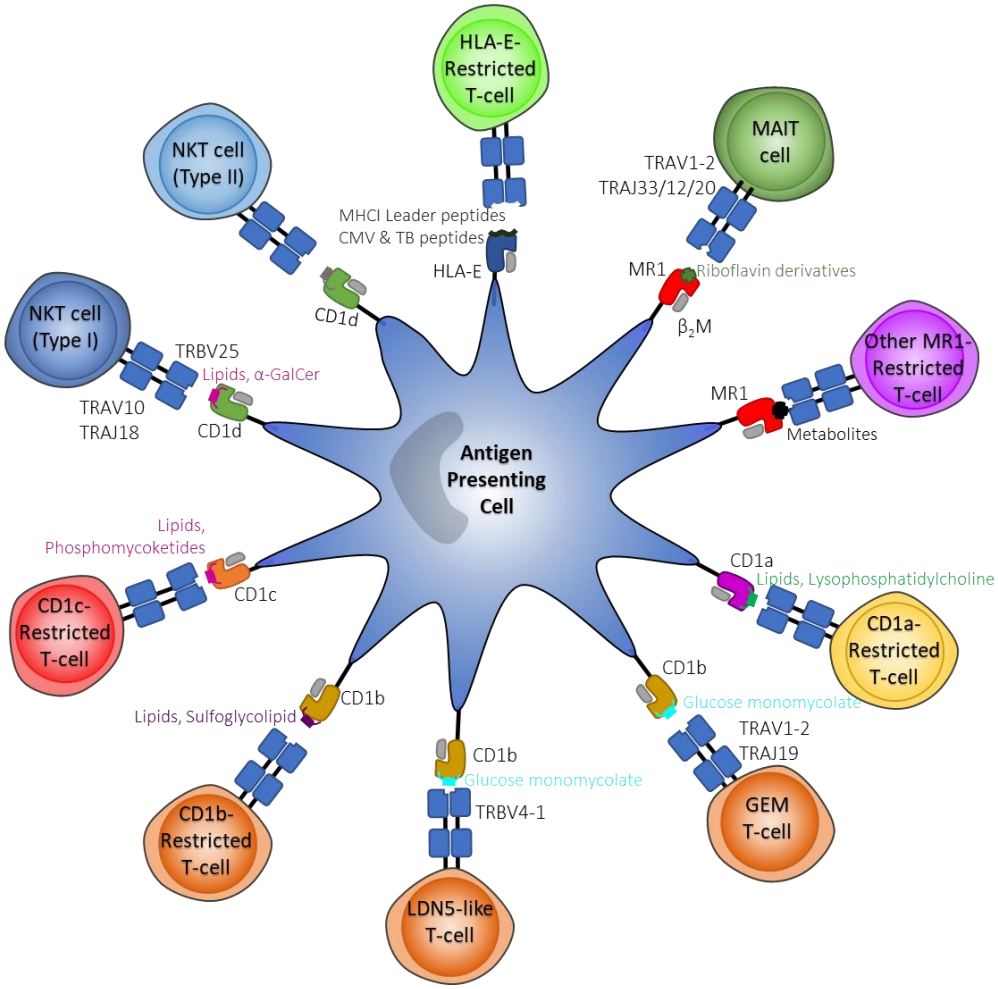

Figure 1.3 - Unconventional human αβ T-cell family
Interactions of unconventional αβ T-cell TCRs with their antigen presenting molecule. Each presenting molecule shows its cognate ligand, with antigens and TCR receptor usage described if known. β_2M, β_2-microglobulin; α-GalCer, α-galactosylceramide; CMV, cytomegalovirus; TB, tuberculosis.

1.4.1 HLA-E-restricted T-cells

HLA-E is an MHC-Ib molecule that is found within the MHC locus of the genome on chromosome 6. It is the most homologous to classical MHC-I molecules of the MHC-Ib proteins in that it binds and presents peptides. However, unlike classical MHC-I molecules, HLA-E is a conserved gene with a very limited range of polymorphisms; only 13 allelic variants have been officially recognised worldwide with only HLA-E*01:01 and *01:03 contributing to HLA-E function (Felício et al. 2014). HLA-E has a putative role in homeostasis by binding peptides from the leader sequence of classical MHC-I molecules that are presented to NK

cell-expressed NKG2A, -B and -C, to indicate any changes in MHC expression induced by viruses or cellular stress (Braud et al. 1997; Braud et al. 1998). However, there is extensive evidence of HLA-E-restricted T-cells reactive to peptides from cytomegalovirus (CMV) (Pietra et al. 2003), Epstein-Barr Virus (EBV) (Romagnani et al. 2002), Hepatitis C Virus (HCV) (Schulte et al. 2009), Human Immunodeficiency Virus (HIV) (Hannoun et al. 2018), *Salmonella enterica Typhi* (S. Typhi) (Salerno-Goncalves et al. 2004) and *Mycobacterium tuberculosis* (*M. tuberculosis)* (Caccamo et al. 2015; Heinzel et al. 2002; Mcmurtrey et al. 2017). HLA-E-restricted T-cells tend to possess an enrichment of arginine residues in the CDR3β despite diverse gene segment usage (Hoare et al. 2006). Of note, HLA-E restricted T-cells are very specific for peptide antigens, with one example showing activation by the CMV-peptide VMAPRTL**I**L but not the self-peptide VMAPRTL**V**L (Pietra et al. 2003). Interestingly, tumours often overexpress HLA-E, but low tumour-HLA-E expression is indicative of a better prognosis when using T-cell-related therapies (Yazdi et al. 2016).

1.4.2 MR1-restricted T-cells

1.4.2.1 MAITs

Mucosal-associated invariant T (MAIT)-cells are an unconventional T-cell subset that are restricted by MHC-related protein (MR)1 (**Figure 1.3**), which unlike HLA-E is located outside the MHC locus on chromosome 1 (Hashimoto et al. 1995). MR1 is monomorphic as the only known polymorphisms are silent or intronic (Parra-Cuadrado et al. 2000; Seshadri et al. 2016). Furthermore, MR1 has 90% sequence homology in the antigen binding groove between human and mouse molecules (Riegert et al. 1998) resulting in high cross-reactivity between mammalian species as both human and mouse MAIT cells recognise mammalian MR1 orthologs (Huang et al. 2009).

MAIT cells were first described by their invariant chain usage of TRAV1-2 TRAJ33 as a dominant TCR rearrangement in the $CD4^{neg}$ $CD8^{neg}$ T-cell pool (Porcelli et al. 1993) across multiple donors (between 1 and 10% of circulating T-cells), with a consensus CDR3 sequence CAVXDSNYQL (Tilloy et al. 1999). The MAIT cell TCR-β shows predominant usage of TRBV6 and TRBV20 (Tilloy et al. 1999) but a wide range of TCR-β pairings are possible (TRBV4-2, 4-3, 11-2, 15, 19, 24, 25 and 28) (Reantragoon et al. 2013). The production of MR1 tetramers extended the repertoire of MAIT cells to include TCRs containing TRAJ12 and TRAJ20; these show a greater presence in the peripheral tissues compared to the TRAV1-2 TRAJ33 MAITs, indicating the potential for different MAIT-cell subsets (Lepore, Kalinicenko, et al. 2014). MAIT TCRs possessing TRAJ33, TRAJ12 and TRAJ20 segments all possess a conserved tyrosine at position 95 (Tyr95α) that is crucial for the activation of majority of TRAV1-2-expressing MAIT cells (Reantragoon et al. 2012; Patel et al. 2013; Eckle et al. 2014), although more recent evidence suggests there are TCRs where this is not the case and other residues such as asparagine can be used instead (Gold et al. 2014; Gherardin et al. 2016; Meermeier et al. 2016).

MAIT cells possess an effector memory phenotype ($CD45RO^{+}$, $CD62L^{low}$, $CD95^{high}$, $CD122^{int}$, $CD127^{int}$ $CCR7^{low}$) expressing tissue-homing chemokine receptors CCR5, CCR6 and CXCR6 (Dusseaux et al. 2011), in addition to high expression of the NK receptor CD161 with varying expression of CD4 and CD8 (majority being the latter) (Le Bourhis et al. 2010).

Activation of MAIT cells can occur through their TCR via MR1 or through the activation of a cytokine receptor. In the context of TCR activation, MAIT cells require a MR1-presented microbial-derived Vitamin-B metabolite to induce recognition (**Figure 1.4**). Importantly, humans cannot synthesise these ligands; they are only produced by certain microorganisms. A list of bacterial and fungi species known to stimulate MAIT cells is provided in **Table 1.3**.

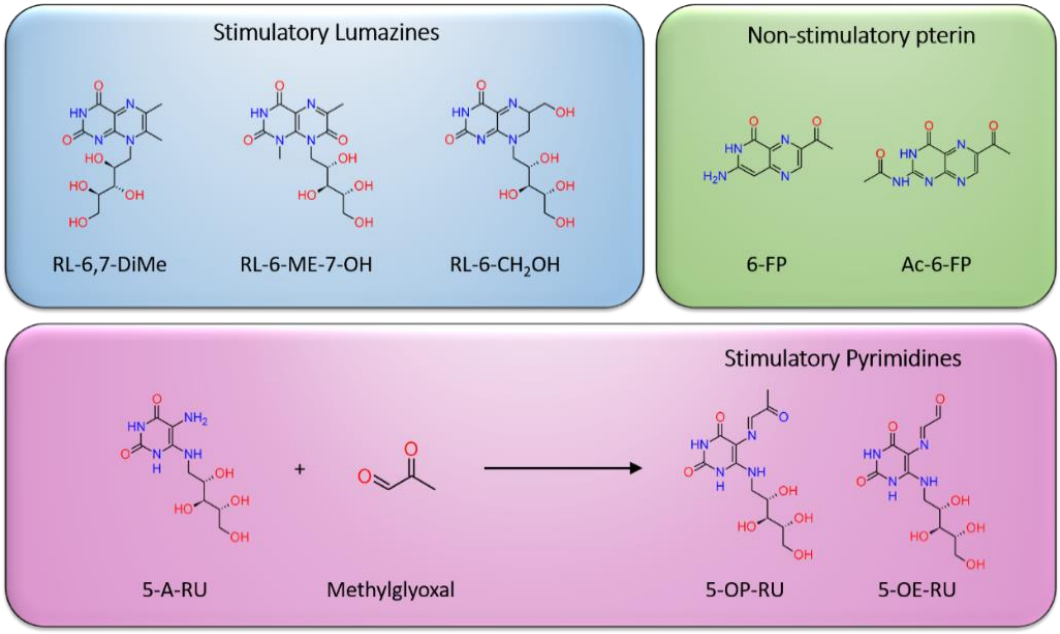

Figure 1.4 - Vitamin ligands known to bind MR1 and their ability to activate MAIT cells

The first identified MR1 ligands – 6-formylpterin (6-FP) and acetyl-6-formylpterin (Ac-6-FP) do not stimulate MAIT cells. The first MAIT stimulatory ligands were lumazines: 6,7-dimethyl-8-D-ribityllumazine (RL-6,7-DiMe), 7-hydroxy-6-methyl-8-D-ribityllumazine (RL-6-Me-7-OH) and reduced 6-hydroxymethyl-8-D-ribityllumazine (rRL-6-CH_2OH). The most potent MAIT cell activating ligands are pyrimidines produced by the condensation reaction between 5-amino-6-D-ribitylaminouracil (5-A-RU) and methylglyoxal, to produce 5-(2-oxoethylideneamino)-6-D-ribitylaminouracil (5-OE-RU) or 5-(2-oxopropylideneamino)-6-D-ribitylaminouracil (5-OP-RU).

Table 1.3 - Riboflavin synthesising microbes able to activate MAIT cells.

Type	Species
Acid Fast bacteria	*Mycobacterium tuberculosis**
Gram^{+} bacteria	*Corynebacterium diphtheriae**
	*Clostridium difficile**
	Staphylococcus aureus$^{\#}$
Gram^{neg} bacteria	*Escherichia coli**
	*Pseudomonas aeruginosa**
	*Klebsiella pneumoniae**
	*Helicobacter pylori**
	*Legionella pneumophila**
	*Leptospira interrogans**
	*Salmonella enterica**
Fungi	*Candida albicans*
	Candida glabrata
	Saccharomyces cerevisiae

*also activate Vγ9Vδ2 γδ T-cells. $^{\#}$activate Vγ9Vδ2, do not possess MEP pathway. Adapted from (Liuzzi et al. 2015; Le Bourhis et al. 2010; Heuston et al. 2012).

Alternatively, MR1-independent activation of MAIT cells occurs via cytokine receptor binding of interferon (IFN)-γ, IFNα/β, IL-12 and various other cytokines that are produced by virally infected cells (**Figure 1.5**) (Le Bourhis et al. 2010). Indeed, MAIT cells have been implicated in HIV infections, involving HIV-induced changes in MAIT cell frequencies and changes in activatory ability (Cosgrove et al. 2013; Leeansyah et al. 2013; Fernandez et al. 2015). MAIT cells have also been shown to be activated in individuals infected by Dengue, Hepatitis C and Influenza viruses, via a TCR-independent mechanism involving IL-18 acting in synergy with IL-12, IL-15 and IFNα/β (Wilgenburg et al. 2016). MAIT cells have also been shown to have a role in sterile inflammation with reports of MAIT cell infiltrations in various tumour types (Zabijak et al. 2015; Ling et al. 2016; Haeryfar et al. 2018), multiple sclerosis (MS) (Treiner et al. 2015), psoriasis (Teunissen et al. 2014), ankylosing spondylitis (Gracey et al. 2016) and inflammatory bowel diseases (Serriari et al. 2014). MAIT cells also contribute to protection against lethal influenza infection *in vivo* (Wilgenburg et al. 2018).

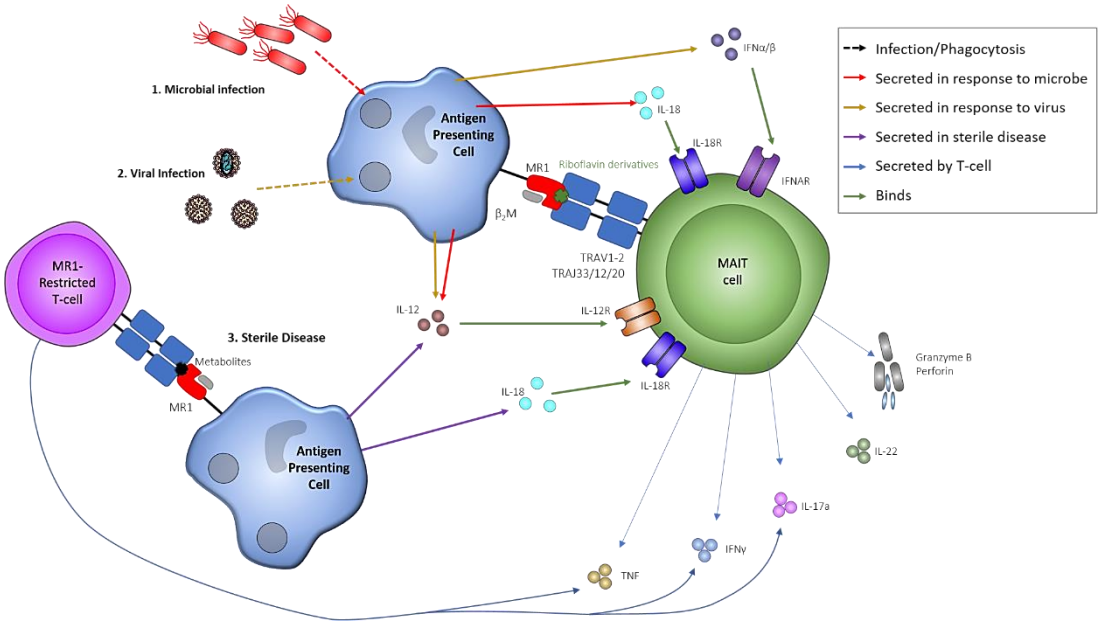

Figure 1.5 - Activation of MAIT and MR1-restricted T-cells in infection and sterile disease
(**1**) Riboflavin-synthesising bacteria and yeast infect or are phagocytosed by antigen presenting cells (APCs). When bacteria are degraded in endosomes, bacterial antigens are released. Riboflavin antigens from these microbes are presented via MR1 to induce activation of TRAV1-2 TRAJ33/12/20 TCRs expressed by MAIT cells. Microbes also stimulate release of IL-18 and IL-12 by the APCs activating MAIT cells independent of TCR. (**2**). Viruses can also stimulate release of IL-12, IL-18 and additionally IFNα/β via Toll-Like Receptors (TLRs) expressed by APCs in order to activate MAITs in a TCR-independent manner. (**3**). In sterile disease such as autoimmunity and cancer, metabolites can be bound by MR1 and presented to MR1-restircted T-cells. IL-12 and IL-18 can also be secreted by APCs to activate MAITs independently of TCR. Activated MAITs can secrete a range of cytokines such as TNF, IFNγ, IL-17a, IL-22 and express Granzyme B and Perforin. MR1-restricted T-cells so far have been shown to secrete cytokines such as TNF, IFNγ and IL-17a.

In response to both MR1-mediated and cytokine driven activation, MAIT-cells have a diverse range of effector functions. MAIT cells can directly lyse bacterially-infected cells upon recognition of microbial vitamin B-metabolites on MR1 through perforin and granzyme B expression; secretion of pro-inflammatory cytokines IFNγ, TNF, and IL-17a; as well as expression of multidrug resistance gene ABCB1 suggestive of resistance to xenobiotics secreted by gut commensal bacteria (Dusseaux et al. 2011) (**Figure 1.5**).

1.4.2.2 Other MR1-restricted T-cells

While canonical MAITs are known to recognise 5-OP-RU and other ligands from the riboflavin synthesis pathway, additional ligands are known to bind MR1 (**Figure 1.4**). In fact, the first discovered ligand, Acetyl-6-Formylpterin (Ac-6-FP), a photodegradation product of folic acid, does not activate canonical MAITs, despite binding MR1 (as shown in crystal structures) and induction of MR1 surface expression *in vitro* (Kjer-Nielsen et al. 2012). Indeed, MR1 tetramers loaded with Ac-6-FP activated TRAV1-2 TRAJ33^{neg} T-cells (i.e. non-canonical MAIT cells) (Gherardin et al. 2016). Furthermore, with the advent of an MR1 knockout phagocytic lung epithelial cell line, A549 (Laugel et al. 2016), studies on non-MAIT MR1 reactive T-cells were further realised through the discovery of an MR1-restricted TRAV12-2/TRAJ39 TRBV29-1/TRBJ1-5 TCR stimulated by *Streptococcus pyogenes,* a bacterial species that does not possess the riboflavin synthesis pathway and is therefore unable to produce the current known stimulatory MR1-restricted ligands (Meermeier et al. 2016). Likewise, MR1-restricted T-cells expressing non-canonical MAIT TCRs (TRAV1-2 TRAJ33^{neg}) have also been shown to directly recognise non-microbial endogenous-derived ligands presented on MR1 (**Figure 1.5**) (Lepore et al. 2017). These T-cells (termed MR1T cells) were stimulated to produce a range of cytokines including IFNγ and increase surface expression of CD69 upon recognition of MR1 on cultured cell lines.

These studies highlight that a wider range of TCRs recognise MR1 and that this molecule presents a more extensive range of ligands than previously realised. Indeed, the crystal structure of MR1 shows a deep hydrophobic cradle able to bind much larger ligands than those currently known (Andrew N. Keller et al. 2017).

1.4.3 CD1a-restricted T-cells

Like MR1, the CD1 family of molecules are MHC-like molecules that are located on chromosome 1. The CD1 molecules have deep hydrophobic antigen binding pockets that are suited to binding large lipid antigens (**Figure 1.6**, (Koch et al. 2005; Zeng et al. 1997). There are four CD1 molecules responsible for activation of T-cells split into two groups; Group I (comprised of CD1a, CD1b and CD1c) is mostly only found in primates; Group II is solely comprised of CD1d and is conserved across many species. CD1a possesses the smallest antigen-binding grooves of the CD1 isoforms (Zajonc et al. 2003) and its expression is limited to Langerhans cells in the skin where it presents lipids and glycolipids. The most well studied and most frequent CD1a-restricted T-cells are those that respond to CD1a bound to self-antigens, forming a normal component of the αβ T-cell repertoire (de Jong et al. 2010; De Lalla et al. 2011). CD1-bound self-antigens appear to stabilise surface expression of CD1a, with TCRs recognising the A' roof of CD1a independent of ligand (Birkinshaw et al. 2015; Cotton et al. 2018). Non-permissive self-antigens can also bind CD1a where occlusion of the TCR-CD1a contact zone prevents CD1a recognition by T-cells. Commonalities between sequences of auto-reactive CD1a-restricted TCRs include tyrosine residues in the CDR1α and CDR2α loops, small residues in the CDR3α loop, and hydrophobic residues in the CDR3β loop (Birkinshaw et al. 2015). Regarding non-self-antigens, CD1a has been shown to present a class of lipopeptides from *M. tuberculosis*, the didehydroxymycobactins, inducing activation of αβ T-cells (Moody et al. 2004; Zajonc et al. 2005). Mutations in CD1a have also been implicated in susceptibility to tuberculosis, indicating this molecule may be important in T-cell mediated control of *M. tuberculosis* infections (Seshadri et al. 2014).

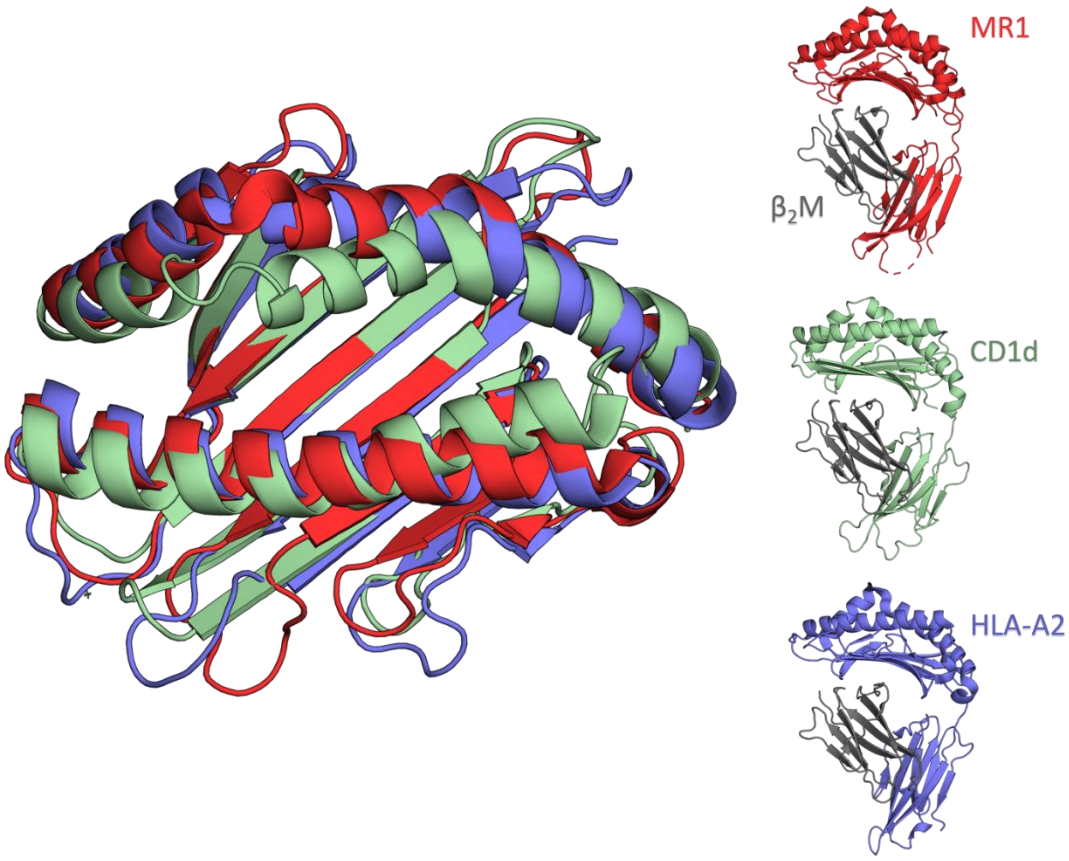

Figure 1.6 - Structural comparison of MR1, CD1 and HLA-A2
The antigen binding grooves of MR1, CD1d and HLA-A2 overlaid shows high structural homology formed by a corridor of α-helices with a β-sheet floor. B_2-microglobuin (β_2M) shown in grey. In MR1, current known ligands are small bacterial metabolites; in CD1 lipids can bind due to an extended β-sheet floor to accommodate larger hydrophobic molecules; HLA-A2 binds peptides of 8-14 amino acid length. PDB Codes: MR1 – 4GUP, CD1d – 1ZT4, HLA-A2 – 5NMH.

1.4.4 CD1b-restricted T-cells

CD1b-restricted T-cells have only recently been identified, divided into three subsets depending on the diversity of the TCR. Germline-encoded mycolyl-reactive (GEM) T-cells are a conserved $CD4^+$ T-cell subset that recognise the mycobacterial antigen glucose monomycolate (GMM) bound to CD1b (**Figure 1.3**) (Van Rhijn et al. 2013). This subset expresses an invariant TCR consensus CDR3α sequence CAVRNTGGFKTIF formed recombination of TRAV1-2 with TRAJ9 and no P-/N- additions (hence the eponym germline-encoded). Although the TCR-β chain of GEM T-cells lack strict sequence conservation, there

are biases of TRBV6-2 and TRBV30. Interestingly, despite expressing an invariant TCR-α chain, antigen specificity is mediated by the TCR-β (Van Rhijn et al. 2013). The interaction between GEM TCRs and CD1b-GMM is very strong, with a dissociation constant of approximately 1 μM. In addition to GEM T-cells, a similar subset of T-cells reactive to GMM-CD1b with an invariant TRAV17 TRBV4-1 TCR is known as LDN5-like T-cells (**Figure 1.3**) (Kasmar et al. 2011; Van Rhijn et al. 2013; Van Rhijn et al. 2014).

The final characterised subset of CD1b-restricted T-cells are those with diverse usage of TCR genes responsive to a diverse range of ligands (**Figure 1.3**); one identified ligand is known as phosphatidylglycerol (PG). T-cells reactive to this phospholipid were unable to distinguish mammalian from bacteria-derived PG (Van Rhijn et al. 2015). However, PG is rare in cellular membranes that carry CD1b proteins in contrast to bacterial membranes that are rich in PG, thus enabling sensing of foreign antigen. This indicates these self- and foreign-reactive CD1b restricted T-cells offer immune-mediated detection of infection.

Lipid antigens are loaded onto CD1b with the help of a fifth CD1 molecule known as CD1e which is expressed intracellularly and is not involved in direct antigen presentation (Garcia-Alles et al. 2011; Facciotti et al. 2011).

1.4.5 CD1c-restricted T-cells

The least studied of the CD1-restricted T-cells are those that recognise CD1c. The recent development of CD1c tetramers has identified populations of T-cells able to recognise phosphomycoketides and lipids in both the αβ (Ly et al. 2013; Roy et al. 2014) and γδ (Roy et al. 2016) T-cell compartments. The αβ-T-cells reactive to CD1c-phosphomycoketides show an overrepresentation of TRBV7-8 and TRBV7-9, indicating potentially invariant populations

in the TCR-β repertoire. A recent study found TRBV4-1^{+} autoreactive cells responding to endogenous lipids presented by CD1c (Guo et al. 2017). Interestingly, this is the same TRBV associated with the CD1b-restricted LDN5-like T-cells. Autoreactive T-cells that recognised CD1c independent of bound antigen were also recently identified (Wun et al. 2018), suggesting surface expression of CD1c may act as a stress marker. CD1c has also been implicated in cancers where it was shown to present methyl-lysophosphatidic acids, a lipid that accumulates in leukaemia cells, to CD1c restricted T-cells (Lepore, de Lalla, et al. 2014).

1.4.6 CD1d-restricted T-cells

CD1d-restricted T-cells are also known as Natural Killer T (NKT)-cells and these are the most studied of the CD1-restricted T-cell pool (Reviewed (Tupin et al. 2007). NKT cells bridge properties of Natural Killer cells and T-cells, evidenced by their expression of surface markers of NK receptors such as NKG2D and NK1.1 (CD161), and an αβ TCR. There are two main types of NKT-cells, the most characterised of which is the Type I or *invariant* NKT (iNKT) cells that have a canonical TRAV10 TRAJ18 TCR-α (CDR3α consensus sequence CVVSDRGSTLGRLYF) paired to TRBV25-1 (Porcelli et al. 1993; Dellabona et al. 1994) (**Figure 1.3**), and are stimulated by the *Agelas mauritianus* marine sponge-derived prototypical ligand α-galactosylceramide (α-GalCer) bound to CD1d in both mice and humans (Kawano et al. 1997; Brossay et al. 1998; Matsuda et al. 2001) (**Figure 1.7**). αGalCer however is not the only iNKT ligand; glycolipids and glycosphingolipids from bacteria (Kinjo et al. 2011; Kinjo et al. 2005); glycosphingolipids from fungi (Albacker et al. 2013); and self-lipids such as lysophosphatidylcholine and β-glucosylceramide are all known iNKT ligands when presented on CD1d (López-Sagaseta et al. 2012; Pellicci et al. 2011) (**Figure 1.7**). Indeed, despite being originally derived from a marine sponge, α-GalCer homologues have been found in mammalian cells where they play a role in regulating iNKT-cell responses (Kain et al. 2014).

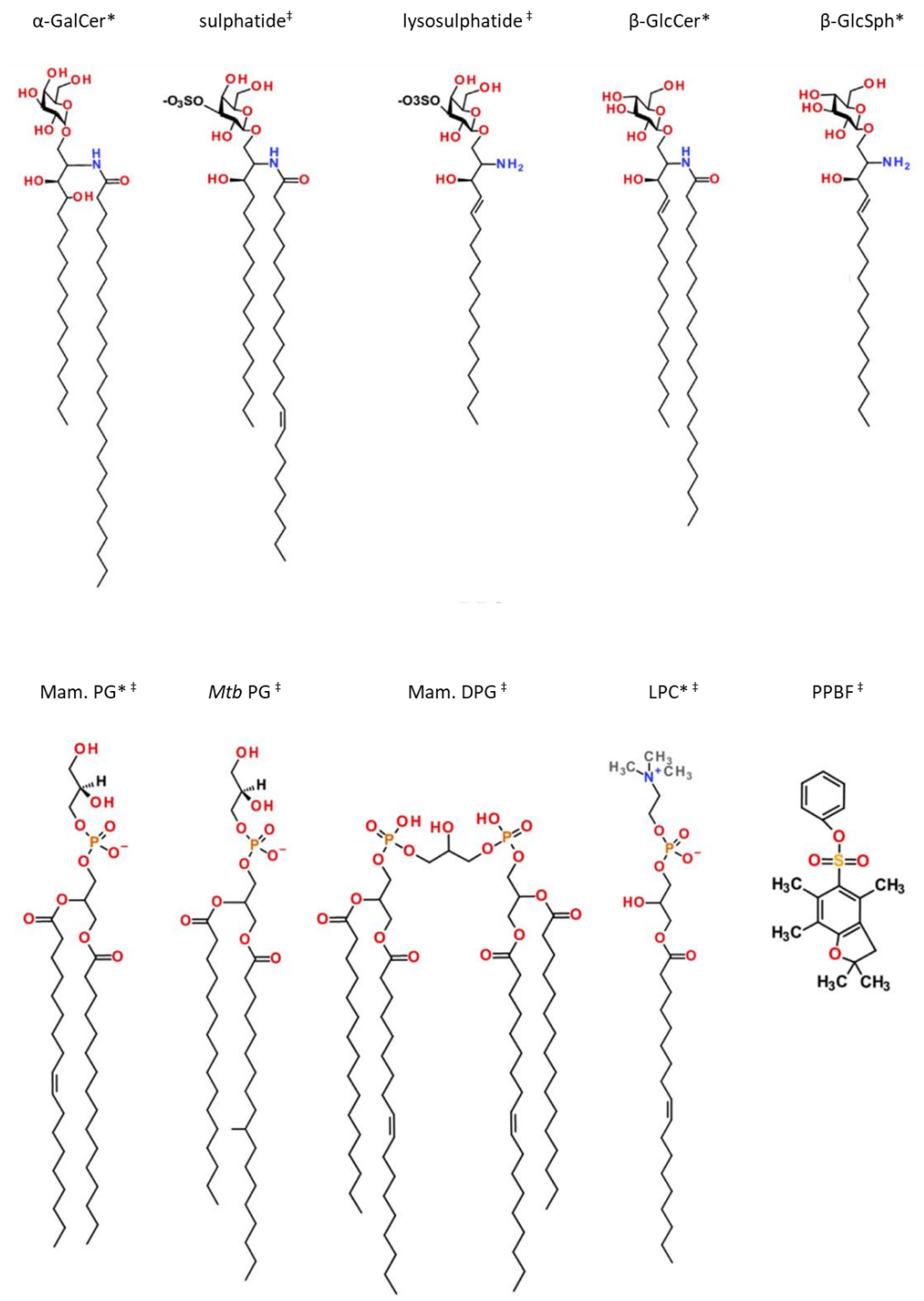

Figure 1.7 - Antigens recognised by CD1d restricted T-cells
Chemical structures of lipid antigens responsible for activation of Type I* or Type II‡ CD1d-restricted T-cells. α-GalCer, α-galactosylceramide; phosphatidylglycerol, PG (mammalian or *Mycobacterium tuberculosis* derived, mam and *Mtb* respectively); mammalian diphosphatidylglycerol, Mam. DPG; lysophosphotidylcholine, LPC; phenyl 2,2,4,6,7-pentamethyldihydrobenzofuran-5-sulphonate, PPBF. Figure adapted from (Macho-Fernandez et al. 2015).

The canonical iNKT TCR binds to CD1d parallel to the lipid binding groove in a manner unlike all current TCR-pMHC-I structures determined so far (Burrows et al. 2010; Godfrey et al. 2008). Additionally, there are 'atypical' Type I NKT TCRs, including αβ-TCRs such as TRAV21 TRAJ18 (Le Nours et al. 2016), γδ-TCRs (Uldrich et al. 2013), as well as δ/αβ TCR hybrids (Pellicci et al. 2014) that constitute a major pool of CD1d-αGalCer-reactive T-cells (***Table 1.4***).

Table 1.4 - Overview of CD1d-restricted T-cells

	Type I NKT Cells	**'Atypical' Type I**	**Type II NKT Cells**	**γδ and δ/αβ TCR**
CD1d dependent	Yes	Yes	Yes	Yes
α-GalCer reactive	All	All	No	Some
Sulphatide reactive	No	No	Some	Some
TCR-α/δ chain	TRAV10 TRAJ18	Diverse with TRAJ18 enrichment	Diverse	Vδ1, Vδ3 Diverse TRAJ
TCR-β/ chain	TRBV25-1	Diverse	Diverse	TRBV25-1^{neg}
NK1.1 (CD161)	+	+	+/-	low

NK1.1 (CD161) is a Natural killer cell marker expressed on subsets of T-cells. α-GalCer, α-alpha-galactosylceramide. Adapted from (Macho-Fernandez et al. 2015).

iNKT cells have been shown to be important mediators in tumour control (Fujii et al. 2013) through CD1d mediated recognition of lipids resulting in tumour lysis, as well as secretion of cytokines that activate NK cells to induce death of MHC^{neg} tumour cells and activate DCs (Fujii et al. 2003). Control of tumour growth has also been evidenced in T-cell lymphomas *in vitro* and *in vivo* in mice (Bassiri et al. 2014) but conflicting reports implicate NKT-cells in aiding tumour growth, by supressing T_H1 immunity and promoting regulatory T-cell (T_{reg}) recruitment and activation in mice (Wang et al. 2018).

The second group of NKT cells, known as Type II or *diverse* NKT cells (dNKT cells), recognise CD1d but utilise a wider range of TCR chains and do not respond to α-GalCer (Balato et al. 2009) (**Table 1.3**). The best characterised ligand for murine dNKT cells is sulphatide (Yang et al. 2011; Fuss et al. 2014), but other ligands such as lysophosphatidylcholine (also an iNKT ligand) (Fox et al. 2009; López-Sagaseta et al. 2012) and PG from both microbial and mammalian sources (Wolf et al. 2015; Tatituri et al. 2013) have been identified (**Figure 1.7**). Additional non-lipid antigens have also been found to stimulate Type II NKT cells, such as the sulphur-containing small molecule PPBF (Van Rhijn et al. 2004). Despite antigens from bacteria being identified as dNKT cell ligands, their role in host defence against pathogens is still unclear. For example, while not essential in *Staphylococcus aureus* control, dNKT cells activated by sulphatide-CD1d led to a reduction in pathogen-induced cytokine storm and subsequent improved survival of infected mice (Kwiecinski et al. 2013). Moreover, *Listeria monocytogenes*-derived PG has been shown to be a more potent stimulator of dNKT cells compared to mammalian PG (Wolf et al. 2015), thus suggesting a role in differentiating between self and non-self.

Due to the limited availability of known antigens that stimulate dNKT cells, the specificity and function of these cells is less well understood compared to their iNKT counterparts. Their role has been suggested as antagonistic to iNKT cells in the context of tumour rejection in mice (Berzofsky et al. 2008), whereas iNKT and dNKT cells appear to work concomitantly against Hepatitis B (Zeissig et al. 2012). Structural studies have also shown that dNKT TCRs do not bind to CD1d in the parallel manner that iNKT TCR binds, instead docking orthogonally above the A' pocket of CD1d (Girardi et al. 2012).

1.5 γδ T-Cells

The final group of unconventional T-cells are those that utilise a γδ-TCR. Some established γδ T-cell ligands include CD1 molecules, MHC class I chain-related protein A and B (MICA/B), UL16 binding proteins (ULBPs) and Endothelial protein C receptor (EPCR) from the MHC-Ib and MHC-like molecules, as outlined in **Figure 1.8**. In addition, γδ T-cells have a more extensive range of ligands not associated with the standard model of antigen presentation; they can directly recognise molecules such as phycoerythrin (Zeng et al. 2012), haptens (only murine T-cells) (Zeng et al. 2014) and some ectopically expressed self-proteins often associated with cellular stress in an antibody-like manner such as annexin A2 and MutS Homolgue 2 (MSH2) (as reviewed in (Vermijlen et al. 2018; Vantourout et al. 2013)). There is also some historical evidence of γδ-TCR recognition of soluble proteins and small peptides (Guo et al. 1995; Kim et al. 1995). Upon recognition of their cognate ligand, γδ T-cells secrete a range of cytokines similar to αβ T-cells, but are noted potent producers of IL-17a (Roark et al. 2008), as well as able to direct lyse target cells (Munk et al. 1990; Davodeau et al. 1993). Ligands recognised by γδ T-cells have however remained elusive and hard to characterise; the few that have been defined provide a useful mechanism of dividing γδ T-cells into subsets based on their cognate antigen.

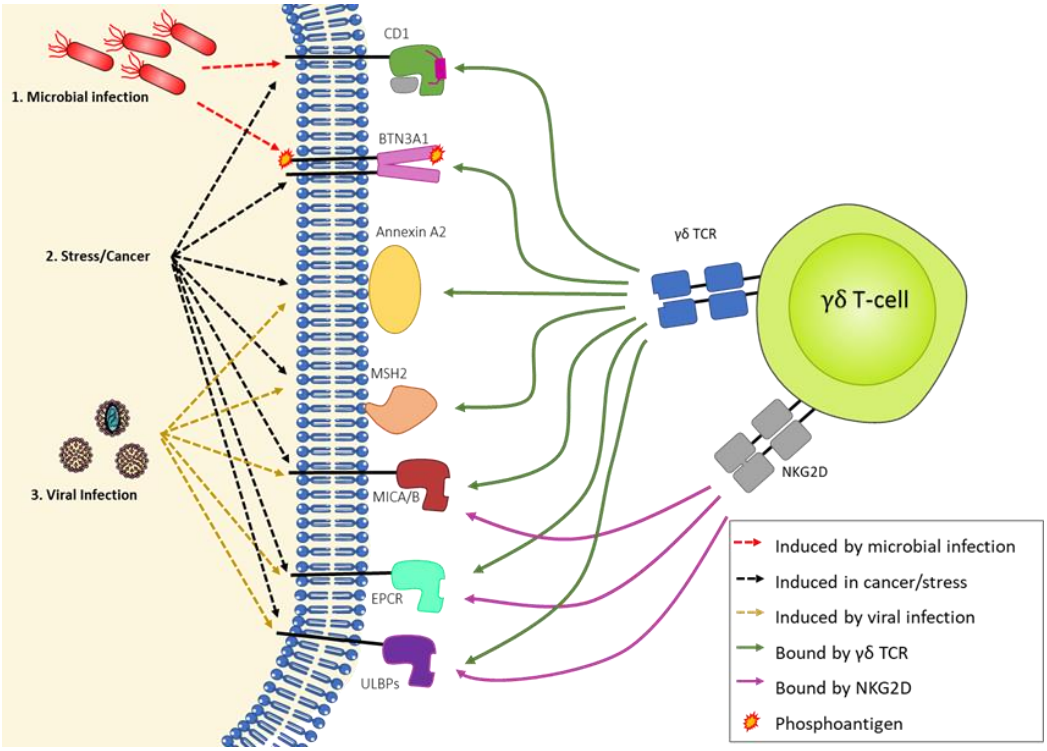

Figure 1.8 - Overview of major ligands involved in γδ T-cell recognition
The wide range of γδ ligands have been confirmed through biophysical or structural complexes. CD1, and in particular CD1d, can present diverse lipids to γδ T-cells linked to bacteria and cancer. Likewise, BTN3A1 is able to bind metabolic antigens produced by bacteria and in stress or cancer, however this binding induces a conformational shift in the molecule resulting in γδ T-cell activation. The mechanism of presentation however is contested in the literature. Annexin A2, MSH2, MICA/B, EPCR and ULBPs are upregulated in cellular stress/cancer or in viral infection that is recognised by γδ T-cells. Furthermore, MSH2, MICA/B and ULPBPs are also bound by NKG2D contributing to γδ T-cell mediated stress sensing. BTN3A1, butyrophilin 3A1; MSH2, MutS homolog 2; ULBPs, UL-16 binding proteins; MICA/B, major histocompatibility complex class-I related chain A/B; EPCR, endothelial protein C receptor; NKG2D, natural-killer group 2 member D.

1.5.1 Phosphoantigen-specific γδ T-cells

One of the first and best studied γδ T-cell antigens was isolated from phosphatase-sensitive mycobacterial precipitates that retained activatory ability despite protease treatment (Holoshitz et al. 1989). These lysates stimulated Vγ9Vδ2 (also known as Vγ2Vδ2 T-cells under Arden nomenclature (Arden et al. 1995)) T-cell clones, the dominant γδ T-cell subset in adult peripheral blood (>70 % of all peripheral blood γδ T-cells (Hannani et al. 2012)). The specific antigen was identified as (E)-4-hydroxy-3-methyl-but-2-enyl pyrophosphate (HMBPP) – an intermediate of the microbial 2-C-methyl-D-erythritol 4-phosphate (MEP) pathway (also

known as the non-mevalonate pathway) (Eberl et al. 2002; Hintz et al. 2001). While HMBPP was initially identified in mycobacterial lysates, it is also found in other pathogenic bacteria (***Table 1.3***) (Puan et al. 2007), protozoans such as *Plasmodium* species responsible for causing malaria (Giulia et al. 2011), *Brucella melitensis* (Bertotto et al. 1993), *Leishmania* species (Russo et al. 1993), *Toxoplasma gondii* (Scalise et al. 1992), *Listeria monocytogenes* (Jouen-Beades et al. 1997) and *Legionella* (Kroca et al. 2001). HMBPP induces a strong response in Vγ9Vδ2 cells and acts as metabolic indicator of infection with each of these pathogens. However, HMBPP is unable to stimulate γδ T-cells directly and requires presentation by Butyrophilin 3A1 (BTN3A1) to induce activation (Harly et al. 2012) (**Figure 1.8**). There is contrasting literature on the mechanism of phosphoantigen presentation however; it is either through intracellular binding of phosphoantigen resulting in extracellular conformation changes (Sandstrom et al. 2014), through antigen presentation to γδ T-cells analogous to MHC (Vavassori et al. 2013) or a combination of these two mechanisms (Legut, Dolton, et al. 2018).

The Vγ9Vδ2 γδ T-cell subset has also been shown to recognise some human cancer cell lines such as Daudi cells (Davodeau et al. 1993) via the endogenously produced activating ligand isopentenyl pyrophosphate (IPP). IPP is an intermediate of the mevalonate pathway that accumulates as a result of metabolic dysregulation that can occur in cancer (Gober et al. 2003) but it is a less potent stimulator of Vγ9Vδ2 cells compared to HMBPP (>10,000 fold (Eberl et al. 2009)), requiring excessive accumulation to activate Vγ9Vδ2 cells. IPP also binds to BTN3A1, and like in the bacterial mode of recognition, can result in direct lysis of tumour upon γδ TCR recognition (Uchida et al. 2007; Gober et al. 2003). Moreover, treatment of tumour cells with inhibitory molecules targeting the endogenous mevalonate pathway such as zoledronate and pamidronate, leads to accumulation of IPP thus inducing Vγ9Vδ2 T-cells *in vivo* with a clinically significant outcome (Meraviglia et al. 2010). Interestingly,

phosphoantigens like HMBPP can also be presented by mitochondrial F1-adenosine triphosphatase (ATPase) when it is expressed ectopically on the cell surface, resulting in stimulation of Vγ9Vδ2 cells (Scotet et al. 2005). Indeed, treatment of tumour cells with zoledronate results in concomitant ectopic expression of F1-ATPase and accumulation of IPP, facilitating recognition by Vγ9Vδ2 cells (Mookerjee-Basu et al. 2010).

Additionally, the Vγ9Vδ2 γδ subset has been shown to function as professional antigen presenting cells, termed γδ T-APCs, whereby Vγ9Vδ2 T-cells are able to cross-present ligands to αβ T-cell compartment (Brandes et al. 2005) resulting in priming and activation of $CD8^+$ T-cells (Brandes et al. 2009). Cross-presentation requires phosphoantigen-induced activation of Vγ9Vδ2 cells combined with additional stimuli such as opsonised cell targets (Himoudi et al. 2012). The resulting presentation licensing has been shown to occur in physiological conditions and can inhibit T_{reg} mediated immunosuppression (Mao et al. 2014). These γδ T-APCs can be readily generated from peripheral blood T-cells highlighting a potential therapeutic target (Khan et al. 2014).

1.5.2 EPCR-restricted γδ T-cells

Some of the less dominant γδ subsets have been identified with specific ligand reactivity. One notable human γδ T-cell ligand is the Endothelial Protein C Receptor (EPCR), recognised by Vγ4Vδ5 expressing γδ-TCRs with an antibody-like moiety (i.e. independent of presenting molecule) (Willcox et al. 2012). EPCR is upregulated on cytomegalovirus (CMV) infected cells and on tumours acting as a stress-induced marker (**Figure 1.8**), with Vγ4Vδ5 EPCR-restricted T-cells able to cross react between CMV-infected cells and cancer cells. Furthermore, EPCR is able to bind and present phospholipids in its antigen binding groove (Oganesyan et al. 2002) though this does not appear to induce γδ TCR binding.

1.5.3 MICA/B-restricted γδ T-cells

MICA/B proteins show high structural similarity to MHC-I; however, they do no associate with β_2M and do not present antigens. In humans, MICA/B have been described as stress-ligands expressed on tumours (Groh et al. 1999), viral infections (Groh et al. 2001), in mycobacterial infection (Das et al. 2001) as well as in other infections and activate both NK cells and γδ T-cells (Groh et al. 1998). NK cells are activated through the NKG2D receptor (Bauer et al. 1999); whereas γδ T-cells are activated by MICA/B through Vδ1 γδ TCRs as well as co-stimulatory activity through γδ T-cell expressed NKG2D (**Figure 1.8**) (Xu et al. 2011; Qi et al. 2003). Indeed, MICA/B can also act as co-stimulatory molecules for αβ T-cell activation (Groh et al. 2001). The frequency of Vδ1 γδ T-cells in tumours expressing MICA was significantly increased compared to MICA/B^{neg} (Bauer et al. 1999). Additionally, loss of MIC molecules is an immune evasion strategy employed by cancers (Groh et al. 2002) and CMV infections (Fielding et al. 2014).

1.5.4 ULBP-restricted γδ T-cells

ULBPs are stress-inducible markers that bind to the eponymous CMV-associated UL-16 protein (Cosman et al. 2001), however they can also be overexpressed in cancers (Kong et al. 2009; Lança et al. 2010; Sutherland et al. 2006). In both cases, ULBPs induce activation of NK cells via NKG2D recognition. Interestingly, ULBPs can also activate γδ T-cells via both the NKG2D receptor as well as the γδ TCR (Kong et al. 2009). The main γδ T-cell subset known to recognise ULBPs, in particular ULBP4, is the phosphoantigen-specific Vγ9Vδ2 subset (Kong et al. 2009).

1.5.5 CD1-restricted γδ T-cells

Another major set of ligands for γδ T-cells are the CD1 molecule presentation of natural and synthetic phospholipids (Russano et al. 2007). In particular, CD1c can present bacterial phosphomycoketides as well as cancer-derived methyl-lysophosphatidic acids to γδ T-cells, all of which express Vδ1 chains with diverse Vγ chains (Faure et al. 1990; Roy et al. 2016; Lepore, de Lalla, et al. 2014). CD1d on the other hand has been shown in a structural complex presenting sulphatide to a Vγ4Vδ1 TCR (Luoma et al. 2013), and the structure of CD1d-αGalCer complexed with a Vγ5Vδ1 TCR has also been solved (Uldrich et al. 2013). CD1d has further been shown to induce recognition by $V\delta1^+$ γδ T-cells independent of bound antigen, suggesting CD1d can act as a stress-induced marker recognised by γδ T-cells (Uldrich et al. 2013). The Vδ1 subset has also been shown to recognise CD1d-sulphatide (Bai et al. 2012). Additionally, the δ/αβ hybrid TCR known to bind CD1d-αGalCer utilises a Vδ1 segment recombined to a range of TRAJ segments (***Table 1.4***), with a higher binding affinity than iNKT cells (Pellicci et al. 2014).

1.5.6 γδ T-cell recognition of ectopically expressed proteins

During active CMV-infection and in oxidative stress, Annexin A2 has been shown to be ectopically expressed on the extracellular membrane (Derry et al. 2007) resulting in activation of human Vγ8Vδ3 γδ T-cells (Marlin et al. 2017). Annexin-A2 specific γδ T-cells are readily available in the PBMC pool potentially acting in a stress surveillance role. In a similar manner, surface-expressed MSH2 can also induce responses in γδ T-cells expressing Vδ2 TCRs (normally associated with phosphoantigen recognition), independent of phosphoantigens. Activation of γδ T-cells is mediated is via both the TCR and NKG2D in the context of both tumour transformation and EBV infection (Dai et al. 2012) (**Figure 1.8**), analogous to MICA/B activation of γδ T-cells.

The unconventional T-cells discussed so far have a wide range of roles in the human body, being implicated in autoimmune diseases as well as other sterile pathologies such as cancer. Their primary role however appears to be in controlling of microbial infection, with innate-like sensing of microbes via a diverse range of receptor-mediated activation of TCRs.

1.6 Aims

With increasing levels of antibiotic resistance among microbes, novel approaches to develop treatments for the clearance of these organisms must be adopted. As bacteria could rapidly become resistant to a new class of antibiotics, improving immune responses to these dangerous pathogens is a possible avenue for exploration. As unconventional T-cells are conserved across the population, these cells make ideal targets for pan-population immunotherapeutics. I hypothesised that commonalities could be found in the T-cells responding to different bacteria through antigens comprised of non-pMHC ligands. The function, clonotypic architecture and phenotype of unconventional bacteria-reactive T-cells should therefore be studied to identify the T-cell subsets most important in clearing of pathogens. For my first results chapter, **Chapter 3**, I sought to optimise a system for isolating bacteria-reactive T-cells from healthy donors. With this system, I could link the phenotype, function and clonotypic architecture of these cells.

The potential for such unconventional T-cell subsets however is not limited to bacteria – there is extensive evidence that these T-cells may be important in control of sterile diseases such as cancer. As with unconventional T-cells reactive to bacteria, those that recognise cancer could potentially be exploited in all individual without the need for patient-specific personalisation through HLA-matching. Therefore, I also sought to characterise novel subsets

of cancer-reactive T-cells that are restricted by evolutionarily conserved antigen presenting molecules. These studies consequently form the basis of **Chapters 4** and **5.**

Chapter 2. Materials and Methods

2.1. Bacterial Cell Culture

Table 2.1 - Buffers and media used in the culture of bacteria

Buffer	Reagents
Lysogeny Broth (LB) Medium	10 g/L tryptone (Fisher Scientific), 5 g/L yeast extract (Fisher Scientific), 5 g/L NaCl (Fisher Scientific)
LB Agar	10 g/L tryptone, 5 g/L yeast extract, 5 g/L NaCl, 10 g/L agar bacteriological (Oxoid)
Lemco Culture Medium	5 g/L Lemco powder (Oxoid), 10 g/L tryptone, 5 g/L NaCl, 0.5 mL/L Tween-80 (Sigma-Aldrich)
Lemco Agar	5 g/L Lemco powder, 10 g/L tryptone, 5 g/L NaCl, 15 g/L agar bacteriological
Bacteria Freezing Buffer	75% LB medium, 25% glycerol (Fisher Scientific)

2.1.1. *Mycobacterium smegmatis* (*M. smegmatis*)

The mc2155 strain of *M. smegmatis* was kindly donated by Dr Matthias Eberl (Cardiff University). To culture this strain, a loop of glycerol stock was streaked onto a plate of Lemco agar and incubated for 48 hours (h) at 37 °C. 20 mL of Lemco medium was inoculated with a single colony from the plate. The inoculated medium was then placed in an orbital shaker incubator at 37 °C, 150 revolutions per minute (RPM) for a minimum 72 h. The optical density was taken and used to determine the colony forming unit (CFU) density and phase growth by comparing to a standard growth curve, giving the units CFU/mL (**Figure 2.1**). Aliquots of the inoculated medium were frozen in bacteria freezing buffer at 10,000 CFU per vial. Aliquots were defrosted and used to inoculate 20 mL Lemco media with OD growth monitoring before being used in experiments.

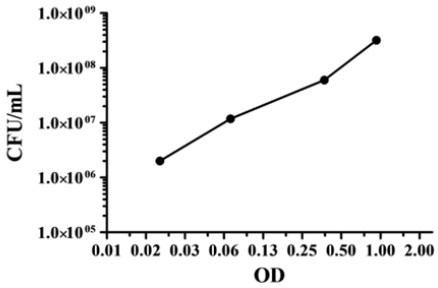

Figure 2.1 – Standard curve of optical density to determine M. smegmatis growth
M. smegmatis was grown in 20 mL Lemco media for 72 h. The optical density (600 nm) was taken at regular intervals with a matched sample plated on Lemco agar plates to establish CFU/mL. This protocol was optimised by Johanne Pentier.

2.1.2. *Salmonella enterica subspecies enterica serovar typhimurium* (*S. typhimurium*) and Staphylococcus aureus (*S. aureus*).

S. typhimurium (strain 08-2885) and *S. aureus* (strain USC9) clinical isolates (kindly provided by Professor Timothy Walsh, Cardiff University) were initially cultured by inoculating 20 mL of LB medium with individual colonies from a streaked plate of either *S. typhimurium* or *S. aureus*. 1 mL of inoculated media was added to beaded bacterial cryovials (Pro-Lab Diagnostics) which was inverted, the 1 mL of media was removed and the vial frozen at -80 °C. For culture, a bead was removed from a defrosted vial of *S. typhimurium* or *S. aureus* and added to 20 mL LB media. After 4 h, the media was serially diluted and plated on LB agar. Plates were incubated at 37 °C for 6 h or overnight and colonies counted to determine CFU/mL.

2.2. Mammalian Cell Culture

Table 2.2 - Buffers used in the culture of mammalian cell lines

Buffer	Reagents
Freezing Buffer	90% FBS, 10% Endotoxin-tested Dimethyl-sulfoxide (DMSO) (Sigma-Aldrich)
Red Blood Cell Lysis (RBC Lysis)	155 mM NH_4Cl (Fisher Scientific), 10 mM $KHCO_3$ (VWR), 0.1 mM Ethylenediaminetetraacetic acid (EDTA) (Sigma-Aldrich), dH_2O (final solution adjusted to pH 7.2-7.4).
PBS-EDTA	Phosphate buffered saline (PBS) (Oxoid), 2 mM EDTA
MACS	DPBS (Life Technologies), 0.5% Bovine Serum Albumin (BSA) (Sigma Aldrich), 2 mM EDTA

Table 2.3 - Media used in the culture of mammalian cell lines

Cell Media	Reagents
R0	RPMI-1640 (Life Technologies), 100 U/mL Penicillin (Life Technologies), 100 µg/mL Streptomycin (Life Technologies), 2 mM L-Glutamine (Life Technologies)
R5	RPMI-1640, 100 U/mL Penicillin, 100 µg/mL Streptomycin, 2 mM L-Glutamine, 5% Heat-inactivated Foetal Bovine Serum (FBS) (Life Technologies)
R10	RPMI-1640, 100 U/mL Penicillin, 100 µg/mL Streptomycin, 2 mM L-Glutamine, 10% FBS
Antibiotic-free R10	RPMI-1640, 2 mM L-Glutamine, 10% FBS
D10	Dulbecco's Modified Eagle Medium (DMEM) (Life Technologies), 100 U/mL Penicillin, 100 µg/mL Streptomycin, 2 mM L-Glutamine, 10% FBS
20IU T-Cell Medium (TCM)	RPMI-1640, 100 U/mL Penicillin, 100 µg/mL Streptomycin, 2 mM L-Glutamine, 10% FBS, 25 ng/mL interleukin (IL)-15 (Peprotech Inc), 20 IU/mL IL-2 (Proleukin), 1x non-essential amino acids (Life Technologies), 1mM Sodium Pyruvate (Life Technologies), 1 mM HEPES Buffer (Life Technologies)

200IU TCM	RPMI-1640, 100 U/mL Penicillin, 100 µg/mL Streptomycin, 2 mM L-Glutamine, 10% FBS, 25 ng/mL IL-15, 200 IU/mL IL-2, 1x non-essential amino acids, 1 mM Sodium Pyruvate, 1 mM HEPES Buffer
20IU Priming TCM	RPMI-1640, 100 U/mL Penicillin, 100 µg/mL Streptomycin, 2 mM L-Glutamine, 10% FBS, 20 IU/mL IL-2, 1x non-essential amino acids, 1 mM Sodium Pyruvate, 1 mM HEPES Buffer
Smooth Muscle Cell Medium (SMCM)	Smooth Muscle Cell Medium (SCMC 1101) (ScienCell), 100 U/mL Penicillin, 100 µg/mL Streptomycin, 2 mM L-Glutamine, 10% FBS
Epithelial Cell Medium (EpiCM)	Human Renal Epithelial Cell Medium (EpiCM 4101) (ScienCell), 100 U/mL Penicillin, 100 µg/mL Streptomycin, 2 mM L-Glutamine, 10% FBS
Hepatocyte Medium (HCM)	Hepatocyte Medium (HM 5201) (ScienCell), 100 U/mL Penicillin, 100 µg/mL Streptomycin, 2 mM L-Glutamine, 10% FBS

All tissue culture media and buffers were sterilised using 0.22 µm syringe (Merck) or 0.2 µm Stericup filter bottles (Merck). Cells were cultured in 6, 24, 48 or 96 (flat and U-well) plates (Greiner Bio-One) or in T25, T75 and T175 flasks (Greiner Bio-One). Regular screening was carried out on cell lines for Mycoplasma using MycoAlert Kit (Lonza) following manufacturer's instructions.

2.2.1. Cell Lines

Cells lines were grown in 5 % CO_2 at 37 °C in appropriate media (**Table 2.3**). Cells were split when approaching 90% confluency or when turning media yellow indicating a build-up of waste. Adherent cells were split by replacing media with PBS-EDTA and incubating at 37 °C for 5 min or until all cells had dissociated from the flask. For strongly adherent cells, a 10 min incubation with TrpLE Express (Life Technologies) at 37 °C was required. Detached cells were transferred to a 50 mL tube (Greiner Bio-One) and centrifuged at 400 x *g*. The resulting pellet was resuspended in appropriate media and seeded into culture flasks at required density.

Table 2.4 - Cell lines used throughout this thesis

Cell Line	Culture condition	Cell Type
(HEK)-293T, RCC-117	D10, Adherent	Embryonic Kidney
A549	R10, Adherent	Non-small cell lung carcinoma
C1R, T2	R10, Suspension	B-cell lymphoma
CIL-1	EpiCM, Adherent	Normal ciliary epithelial
FM45, Mel624, MM909.11, MM909.15, MM909.24, SK-Mel-28	R10, Adherent	Malignant melanoma
HCT-116	R10, Adherent	Colorectal Carcinoma
HeLa, SIHA	R10, Adherent	Cervical carcinoma
Hep2	HCM, Adherent	Normal hepatocyte
Jurkat E6.1, Molt3	R10, Suspension	T-cell leukaemia
LnCAP	R10, Suspension	Prostate carcinoma
MCF-7, T47D, MDA-MB-231	R10, Adherent	Breast adenocarcinoma
MRC5	R10, Suspension	Normal lung fibroblast
pt146	R10, Suspension	Lymphoblastoid cell line (LCL)
SMC-3	SMCM, Adherent	Normal smooth muscle
THP1	R10, Suspension	Monocytic leukaemia
TK-143B, U2OS	R10, Adherent	Bone osteosarcoma
U266	R10, Suspension	Multiple myeloma

MM909.11, MM909.15 and MM909.24 are tumour cell lines derived from biopsies of tumours excised from patients with metastatic melanoma, kindly donated by I. M. Svane from Copenhagen University Hospital. CIL-1, Hep2 and SMC-3 were supplied by ScienCell. All other cell lines originated from the American Type Culture Collection (ATCC) and subsequently stored as laboratory stocks.

2.2.2. Cell counting

Cells were washed and diluted to an appropriate density. 10 µL of cell suspension was thoroughly mixed 1:1 with Trypan Blue 0.4% solution (STEMCELL Technologies). The solution was loaded onto a haemocytometer and the number of viable cells counted using a

brightfield microscope. The total density of cells was then determined using the following formula: Number of viable cells x dilution factor x 0.01 = number of viable cells x 10^6.

2.2.3. Cryopreservation and thawing of cells

Cells were counted and subsequently centrifuged. The pellet was resuspended in an appropriate volume of freezing buffer at 1 mL per vial and transferred to 1 mL cryovials (Greiner Bio-One) which were stored in CoolCell Freezing Pot (Biocision) at -80 °C for 24 h. For long-term storage, cryovials were transferred to vapour-phase liquid nitrogen storage.

Frozen cryovials were thawed briefly in a 37 °C water bath before transferring to a Universal Tube (Greiner Bio-One) containing 19 mL R0. The cells were centrifuged, media discarded and resuspended in appropriate media before counting. Cells were transferred to an appropriate flask or plate for culture dependent on cell density.

2.2.4. Isolation of Peripheral Blood Mononuclear Cells (PBMCs) from whole blood

Buffy coats were obtained from the Welsh Blood Service (WBS) in accordance with local ethical approval and the Human Tissue Act (2004). The WBS ensure samples are seronegative for HIV-1, HBV and HCV. Buffy coats were diluted 1 in 2 in R10 and left rotating overnight. 33 mL was then added to a SepMate Tube (StemCell Technologies) containing 13 mL of Lymphoprep (StemCell Technologies). The tubes were centrifuged at 1200 x *g* for 10 min and the top layer moved to a 50 mL falcon tube, topped up to 50 mL with R0 and centrifuged at 700 x *g* for 10 min. The supernatant was discarded, the pellet resuspended in 25 mL RBC lysis buffer (if multiple tubes per donor were used, these were combined at this stage) and incubated at 37 °C for 10 min. The tubes were then topped up to 50 mL with R0 and

centrifuged at 700 x *g* for 5 min. The pellet was resuspended in R10 and counted. Isolated allogenic PBMCs were subsequently used as irradiated feeders for T-cell expansions (proliferation stimulated by HLA-mismatch and secreted factors), for T-cell priming (**Section 2.2.7**) or for lentiviral transduction (**Section 2.5.6**).

2.2.5. Cloning, expansion and culture of T-cells

Isolated T-cells were single cell cloned by diluting in appropriate media to a density of 0.5 cells/100 µL, with 100 µL added to each well of a 96-well plate to ensure that less than 1 cell is present in each well. Single cells were expanded in 20IU medium with 50,000 irradiated mixed 'feeder' PBMC supplemented with 1 µg/mL phytohaemagglutinin (PHA, Fisher Scientific), a plant lectin that acts as a mitogen and triggers T-cell division. Once cells had grown to sufficient numbers they were moved to appropriate culture vessels for further clonal expansion. 1 x 10^6 T-cells were transferred to a T25 flask containing 20 IU TCM supplemented with 1.5 µg/mL PHA. 15 x 10^6 irradiated PBMCs were added (from three donors irradiated using a Cesium-137 source for 3100 centigrays (cGy)), the flask tilted at 45° and cultured at 37 °C for 5 days. Half of media was replaced with fresh 20 IU TCM and incubated for a further 48 h. Cells were harvested, counted and plated in 200 IU at either 3.5 x 10^6 T-cells per well in a 24- well plate, or 1 x 10^6 per well in a 48- well plate. T-cells were routinely expanded in this manner.

2.2.6. Bacterial loading onto A549 cells

A549 cells were washed with R0 and cultured in antibiotic-free R10 overnight. Medium was then replaced with fresh antibiotic-free R10 medium. Bacterial density was determined and added to A549 cells, at a multiplicity of infection (MOI) of 100:1 (bacteria to cells) for *M. smegmatis* or 25:1 for *S. typhimurium* and *S. aureus*, in antibiotic-free R10 for 2 h at 37 °C.

The supernatant was discarded, and cells were washed with R0 three times. Cells were then cultured for a further 2 h in R10. For *S. aureus* loading of cells, R10 media was supplemented with 0.05 µg/mL rifampicin for all subsequent culture. Cells were detached from flask and washed three times in R0 before either plating at 2 x 10^5 cells per well of a 24 well plate for T-cell priming or freezing in freezing buffer at a density of 2 x 10^6.

2.2.7. T-Cell Priming

A549 cells loaded with bacteria (as described in **Section 2.2.6**) were plated at 2 x 10^5 per well of a 24-well plate in R10 medium and allowed to adhere for 1 hour. 6 x 10^6 isolated PBMC (**Section 2.2.4**) were added in R10 to each well, at a total volume of 2 mL. Medium was replaced after 24 hr with priming medium. Cells were cultured for 2 weeks before phenotypic analysis and sorting, with media change every 2-3 days. For C1R priming, culture conditions were consistent with A549 priming, but C1R cells were irradiated (3100 cGy) before being added to a 24-well plate at 3 x 10^5 with no adherence step.

2.2.8. MACS separation of $CD4^+$ and $CD8^+$ T-cells from PBMCs

Anti-CD8 microbeads (Miltenyi Biotec) were used to purify CD8+ T-cells from isolated PBMCs (**Section 2.2.4**) following the manufacturers guidelines. In brief, counted cells were centrifuged at 300 x *g* for 10 min and resuspended in 80 µL of cold MACS buffer per 10^7 cells. 20 µL of anti-CD8 microbeads was added per 10^7 cells and incubated for 15 min at 4 °C. Cells were washed in PBS and resuspended in 500 µL cold MACS buffer. Up to 2 x 10^8 cells were applied to an MS column that had been pre-rinsed with MACS buffer and attached to a magnet. The column was drained by gravity and was subsequently washed in 500 µL cold MACS buffer 3 times. The column was removed from the magnet and the cells were eluted

in 1 mL cold MACS buffer. The cells were centrifuged for 10 min and resuspended in 200 IU TCM and plated in 48- well plates. This process can be combined with anti-CD4 beads to enrich for CD4+ and CD8+ T-cells, where in addition to the 20 µL anti-CD8 microbeads, 20 µL of anti-CD4 microbeads was also added to cells resuspended in 60 µL MACS buffer. For other MACS sorting criteria, antibodies conjugated to PE were used to label cells, followed by addition of anti-PE microbeads. Protocol then followed $CD8^+$ cell isolation.

2.3. Flow Cytometry and Functional Assays

Expression of cell surface markers and intracellular cytokines were monitored using fluorochrome conjugated antibodies, in addition to the use of pMHC and MR1 tetramer staining. Samples were acquired on a BD FACSCanto II flow cytometer (BD Biosciences) or BD FACSAria (BD Biosciences) for cell sorting, with data collection through the FACSDiva software (BD Biosciences). Data analysis was performed on FlowJo V10 (TreeStar Inc.). Compensations were achieved using anti-mouse Igκ antibody capture beads. All staining was carried out in the dark on ice unless otherwise stated.

Table 2.5 - Buffers used in flow cytometry staining

Buffer	Reagents
FACS Buffer	PBS, 2% FBS
Paraformaldehyde (PFA)	PBS, 4% PFA

2.3.1. Surface marker labelling with antibodies

For flow cytometry analysis, cells were stained with a combination of antibodies and a cell viability marker. Prior to staining, cells were counted and transferred to a Fluorescence-Activated Cell Sorting (FACS) tube (Greiner Bio-one) or 96-well plate. Cells were washed once

in FACS buffer followed by PBS. The supernatant was discarded, and cells stained with either Violet or Aqua LIVE/DEAD stain (Life Technologies) at room temperature in the dark for 5 min. If Fc blocking was required, 10 µL of Fc Block (Miltenyi Biotech) was added to cells and then incubated for 10 min on ice in the dark. Cells were then stained with a premixed cocktail of antibodies (**Table 2.6**) and incubated on ice for 20 min. 3 mL of FACS buffer was added and cells centrifuged at 700 x *g,* after which the supernatant was discarded and cells resuspended in either 50 µL FACS buffer if used directly on the BD FACSCanto II, or fixed in PFA for 20 min.

Table 2.6 - Conjugated antibodies and dyes used in flow cytometry

Marker	Fluorochrome	Brand	Clone
CD8	APCy APCy-Vio770 PE	Miltenyi Biotech	BW 135/80
CD4	PE-Vio770	Miltenyi Biotech	VIT4
CD3	PercP	Biolegend	UCHT1
αβ TCR	PE	Biolegend	IP26
γδ TCR	FITC APC	Miltenyi	REA591
Rat CD2	PE FITC	Biolegend	OX-34
MR1	PE	Biolegend	26.5
Vα7.2	APC	Miltenyi Biotech	REA179
IFN-γ	APC	Miltenyi Biotech	45-15
CD107a	PE FITC	BD Biosciences	H4A3
TNF-α	PE-Vio770	Miltenyi Biotech	Mab11
Vβ11	FITC	Beckman Coulter	C21
LiveDead*	Vivid (PB) Aqua (AmCyan)	Life Technologies	

*LiveDead is a cell viability stain that covalently binds to amines in proteins. APCy, allophycocyanin; PE, phycoerythrin; FITC, Fluorescein isothiocyanate; PercP, Peridinin Chlorophyll Protein Complex; PB, pacific blue.

2.3.2. Intracellular Cytokine Staining (ICS)

T-cells were rested overnight in R5 media, then washed twice in R0 prior to activation. Subsequently, T-cells were cultured with and without target cells at a ratio of 1 effector to 1 target cells. Monensin and Brefeldin A (GolgiStop and GolgiPlug respectively, BD Biosciences) were added alongside anti-CD107a antibody and cultured at 37 °C for a minimum of 4 h. Cells were stained with Live/Dead and cell surface markers and prepared for ICS by addition of Cytofix/Cytoperm (BD Biosciences) according to manufacturer's instructions. TNF-α and IFN-γ antibodies were added for 20 min on ice to stain intracellular cytokines. Cells were washed and resuspended in 50 µL PBS.

2.3.3. TAPI-based Assay

The following assay is an alternative to ICS and enables isolation of viable cells based on membrane bound TNF. Unlike most cytokines, TNF is produced as a membrane-bound form that is subsequently cleaved by TNF converting enzyme to release the soluble form. Inhibition of this cleavage event using TNF processing inhibitor 0 (TAPI-0) retains the membrane-bound form of TNF at the surface of activated T-cells where it can be stained with antibody (Haney et al. 2011). In brief, cells were rested overnight in R5 media, then washed twice in R0 prior to activation. Subsequently cells were cultured with and without target cells at a ratio of 1:1 effector to target cells. CD107a and TNF-α conjugated antibodies were added to cells in addition to 30 µM of TAPI-0 (Sigma Aldrich). Cells were incubated in the dark at 37 °C for a minimum of 4 h before washing followed by LiveDead and cell surface marker staining. Stained cells could then be used for cell sorting by flow cytometry on BD FACS Aria through Central Biotechnology Services (CBS) (Cardiff University) as cell viability is preserved. Isolated cells be subsequently cultured in lines, single cell cloned or clonotyped (**Section 2.4**). The TAPI-0 assay can be used in conjunction with staining for CD107a as a surrogate marker of T-cell degranulation (Betts et al. 2003).

2.3.4. Tetramer Staining

Biotinylated MR1 monomers were kindly provided by Prof. Jamie Rossjohn (Monash University), biotinylated p-MHC monomers were produced in house. MR1 or p-MHC tetramers were assembled by adding 0.6 µL of streptavidin PE backbone (Life Technologies) every 20 min five times to 0.95 µg of MR1 biotinylated monomer or 5 µg pMHC-I biotinylated monomer whilst incubating on ice. Tetramer staining was boosted as described in (Tungatt et al. 2014). Briefly, up to 1 x 10^6 cells were rested overnight in R5 medium, washed in FACS tubes with FACS buffer at 700 x *g* before resuspending in 50 µL PBS. 50 µL of 100 nM Protein Kinase Inhibitor (PKI) Dasatinib (Axon Medchem) was added to make a final concentration of 50 nM PKI and incubated for 30 min at 37 °C (Lissina et al. 2009). Without washing, 0.03 µg to 0.5 µg of tetramer was added at a concentration ranging from 0.04 µg/µL to 0.5 µg/µL. Following tetramer addition, cells were incubated on ice in the dark for 30 min. Cells were then washed in FACS buffer and labelled with 0.5 µg Mouse Anti-PE anti-fluorochrome unconjugated primary antibody (Clone PE001, Biolegend) for 20 min on ice in the dark, at a concentration of 10 µg/mL. Cells were then stained with cell surface markers and viability staining as described in **Section 2.3.1**.

2.3.5. Antibody Blocking

Blocking antibodies were preincubated with APCs for 1 h at 37 °C at a final concentration of 10 µg/mL, before addition of effector cells. The following antibodies were used for blocking assays: biotinylated anti-MR1 (clone 26.2, provided by Ted Hansen); anti-HLA-A, -B and -C (clone W6/32, Biolegend); anti-HLA-DR, -DP, -DQ (clone Tü39, Biolegend). APCs were then used in a T-cell activation assay (**Section 2.3.6**).

2.3.6. T-cell Activation Assay

T-cells were washed in R0 and rested in R5 medium overnight. T-cells were counted and added to 96-well plate at 3 x 10^4 with 6 x 10^4 APCs in a final volume of 100 µL. T-cells alone and T-cells with 1 µg/mL PHA were included as negative and positive controls respectively, and cells were incubated overnight. Cells were pelleted by centrifugation at 700 x *g* for 4 min. 50 µL of supernatant was harvested from each well and diluted with 70 µL of R5 medium. Supernatants were harvested and cytokine secretion was quantified by ELISA (**Section 2.3.7**).

2.3.7. ELISA

Table 2.7 - Buffers used in ELISA

Buffer	Reagents
ELISA Wash Buffer	0.05% Tween-20 in PBS
Reagent Diluent	1% Bovine Serum Albumin (BSA) (Oxoid) in PBS

MIP-1β, TNF-α and IFN-γ Enzyme-Linked ImmunoSorbent Assays (ELISA) were performed using DuoSet human ELISA kit (R&D Systems) according to manufacturer's instructions. All washes were performed in triplicate using an automated microplate washer with 190 µL of ELISA Wash Buffer, with blotting after the final wash to remove excess liquid. Accessory reagents (all supplied by R&D Systems) include Streptavidin-Horseradish Peroxidase (Streptavidin-HRP), Reagent A (tetramethylbenzidine), Reagent B (hydrogen peroxide) and Stop Solution (2N sulphuric acid). Assays were performed in duplicate or triplicate as stated. All incubations were performed at room temperature. In brief, 96-well half area flat bottom plates (Greiner Bio-One) were coated with either mouse anti-human MIP-1β, TNF-α or IFN-γ capture antibody diluted to 1.5 µg/mL in PBS and incubated at room temperature overnight. Plates were washed then blocked with 150 µL of reagent diluent for 1 h. Plates were washed

and 50 µL of supernatant from a T-cell activation assay added to appropriate wells. In addition, 50 µL of a titrated MIP-1β, TNF-α or IFN-γ recombinant standard was added ranging from 2 ng/mL to 15.6 pg/mL diluted in reagent diluent with a reagent diluent alone well included. This allowed production of a sample curve to determine concentration of cytokine. Plates were subsequently incubated for 75 min after which supernatants and standards were discarded, plate washed, and biotinylated goat anti-human MIP-1β, TNF-α or IFN-γ detection antibody diluted in reagent diluent at 50 ng/mL added to each well. Plates were incubated for 75 min followed by washing and addition of streptavidin-HRP prediluted 1:40 in reagent diluent for 20 min. Plates were washed and 50 µL of a 1:1 solution of reagent A and reagent B was aliquoted into each well, then incubated in the dark for up to 20 min until there was an observable colour change. With no washing step, 25 µL stop solution was added. Optical density (OD) readings were taken at 450 nm with a correction set to 570 nm using an iMark microplate reader (Bio-Rad). The results were analysed in Microsoft Excel and displayed in GraphdPad Prism 6 software.

2.3.8. MACS Separation of TNF/IFNγ-expressing cells

To enrich T-cell lines for antigen-specific TNF/IFNγ reactivity, TNF/IFNγ based magnetic pull-out was performed according to manufacturer's protocols (TNF/IFNγ Secretion Assays, Miltenyi Biotec). T-cells were rested by extensive washing in R0 followed by overnight culture in R5 medium. Rested T-cells were then co-incubated with target cells at 1:1 ratio (typically 100,000 T-cells and target cells each per well in a 96-U well plate). After 5 h, cells were harvested and washed twice with MACS buffer (400 x *g* for 5 min at 4 °C). Washed cells were resuspended in MACS buffer and TNF and IFNγ catch reagents added for 5 min on ice. These catch reagents bind to surface markers on all lymphocytes and capture TNF/IFNγ upon secretion from the activated T-cells. TNF capture was either used alone or combined with

IFNγ catch reagents to maximise the number of recovered antigen-specific T-cells. The cells were subsequently diluted in R5 medium and incubated for 45 min at 37 °C under slow continuous rotation. Cells were then washed with MACS buffer and incubated with PE-conjugated TNF/IFNγ detection antibodies for 10 min on ice. Cells were again washed with MACS buffer and incubated at 4 °C for 15 min with anti-PE microbeads. After another wash step, the microbead-labelled cells were separated on an appropriate magnetic column placed in a magnetic field. Column-bound cells were eluted into 20IU TCM and the following day were either expanded as a line or single cell cloned.

2.3.9. Chromium^{51} (Cr^{51}) Release Cytotoxicity Assay

T-cell specific killing assays were carried out by measuring Chromium^{51} release from target cells. Effector T-cells were washed in R0 and rested overnight in R5 medium. The following day, approximately 1 x 10^6 target cells were washed in R0 and all media removed from cells. Target cells were then labelled with 30 µCr^{51} (Sodium Chromate in saline, Perkin Elmer) per 1 x 10^6 cells for 1 h. Target cells were then washed, resuspended in R10 and allowed to leach for 1 h at 37 °C to remove excess Cr^{51}. Leached cells were subsequently washed and plated at a density of 2000 cells/well in a 96-well plate together with effector T-cells at the desired effector to target ratio in a final volume of 150 µL. Target cells were also incubated with medium alone, in addition to wells containing 5% Triton X-100 detergent to give spontaneous and maximum Cr^{51} release respectively. After 4-, 6- and/or 18-h incubation at 37 °C, 15 µL of supernatant was harvested and mixed with 150 µL of Optiphase Supermix Scintillation Cocktail (Perkin Elmer) in flexible 96-well polyethylene terephthalate (PET) microplate (Perkin Elmer) and sealed. The Cr^{51} release was measured using 1450-Microbeta counter (Perkin Elmer) which measures gamma radioactivity (indirect). The specific target lysis by T-cells was calculated by: $$\frac{\text{experimental release - spontaneous release}}{\text{maximal release-spontaneous release}} \times 100$$

2.4. TCR Clonotyping

T-cells were sorted by flow cytometry on BD FACS Aria (Becton Dickson) with the help of Dr Catherine Naseriyan (Central Biotechnology Services, CBS), based on function and phenotype (**Section 2.3.3**). All centrifugation steps were performed at 8000 x *g* unless otherwise stated.

2.4.1. mRNA Extraction from T-cells

RNA was extracted using RNeasy Plus Mini Kit (Qiagen), as per manufacturer's instructions. Briefly, isolated cells were lysed using 350 µL RLT Lysis Buffer and mixed. Samples were then added to gDNA eliminator tubes and centrifuged for 30 secs. 350 µL 70% ethanol was added to the flow through and mixed. Each sample was then transferred to a MinElute column, centrifuged for 30 secs and flow through discarded. 700 µL of buffer RW1 was added to column followed by a 30 secs centrifugation. Flow through was discarded and 500 µL 80% ethanol was added. The sample was centrifuged for 2 min and the flow through discarded. The column was transferred to a new collection tube and dried by centrifugation for 5 min at full speed. The dry column was transferred to a 1.5 mL Eppendorf tube, 30 µL RNase-free water added and centrifuged for 1 min at 16,800 x *g.* The flow through now contains mRNA and was stored at -80 °C until required.

2.4.2. cDNA Synthesis

The isolated mRNA was converted to cDNA using the SMARTer (Switching Mechanism At 5' end of RNA Transcript) RACE (Rapid Amplification of cDNA Ends) PCR cDNA Synthesis Kit (Takara Bio, ClonTech). This kit uses a primer that binds to the poly(A) tail of mRNA initially, with reverse transcriptase adding non-templated resides at the 5' end of the mRNA transcript. The second step anneals to the added non-templated residues on the synthesised

cDNA. Subsequent newly generated cDNA molecules therefore contain a universal anchor at the 5' end. To achieve this, 10 µL of defrosted mRNA sample was added to 1 µL SMART 5' CDS Primer IIA and placed into a thermocycler for 3 min, followed by a 2 min incubation at 42 °C. The annealed product was then added to the following mastermix which was made up for appropriate number of reactions:

Reagents	**Volume (µL)**
5X First Strand Buffer	4
DTT (100 mM)	0.5
dNTP (10 mM)	1
SMARTer IIA Oligonucleotide (12 µM)	1
RNase Inhibitor	0.5
SMARTScribe Reverse Transcriptase	2

The sample was then incubated in a thermocycler for 90 min at 42 °C, followed by 10 min at 70 °C, after which samples were stored at -20 °C.

2.4.3. Step-out and Nested PCR

To allow unbiased amplification of only TCR chains within the sample, a set of forward primers specific for the universal anchor on the cDNA molecules, combined with a reverse primer specific for each TCR constant chain were used to capture the whole variable region of each TCR chain. Sample-free controls were set up alongside samples to test for contaminations. The initial step out PCR uses following PCR mastermix:

Reagents	**Volume (µL)**
5X HF Buffer	10
DMSO	0.5
dNTP (10 mM)	1
Primer A	5
Constant Region Primer R1*	1
Phusion Tag	0.25
RNase-free H_2O	29.75
Sample	2.5

*C-α, C-β, C-δ or C-γ depending on the chain being sequenced (Synthesised by Eurofins).

The PCR cycle was carried out as followed:

Temperature °C	**Time (min:sec)**	
94	5:00	
94	0:30	x 30 cycles
Variable*	0:30	
72	1:30	
72	7:00	

*Temperature dependant on TCR constant region: C-α at 63 °C, C-β at 66 °C, C-δ at 57 °C or C-γ at 60 °C.

The Nested PCR was then carried out using 2.5 µL of the step-out PCR product, the thermocycler settings from the Step-out PCR maintained, using the following mastermix:

Reagents	**Volume (µL)**
5X HF Buffer (Green)	10
DMSO	0.5
dNTP (10 mM)	1
Primer Short‡	1
Constant Region Primer R2*‡	1
Phusion Tag	0.25
RNase-free H_2O	33.75

*C-α, C-β, C-δ or C-γ depending on the chain being sequenced (Eurofins).

2.4.4. Agarose Gel Electrophoresis

Table 2.8 - Buffers used for agarose gel electrophoresis

Buffer	Reagents
1x Tris Acetate EDTA (TAE)	40 mM Tris (pH 8.1), 20 mM acetic acid, 1 mM EDTA, ddH_2O
1% Agarose Gel	0.6 g agarose, 60 mL TAE

Nested PCR products were purified using gel electrophoresis. 1% agarose gel was cast by dissolving 0.6 g agarose (Invitrogen) in 60 mL TAE and gentle heating in a microwave. Midori green nucleic acid stain (Nippon Genetics) was added as gel was cooling before pouring into gel mould containing appropriate sized combs. A 1 kb DNA hyperladder (Bioline) was loaded alongside DNA fragments to determine fragment size. If required, 5x DNA Loading Buffer Blue (Bioline) was added to DNA samples and ran on the gel at 80 V for 45 min. Fragments were visualised in a transilluminator (Modern Biology Inc) and DNA was extracted using QIAEX II Gel Extraction Kit (Qiagen). Briefly, 3 volumes of Buffer QX1 was added to gel slice along with 10 µL QIAEX II beads. The resulting mixture was incubated at 50 °C for 10 min with vortexing every 2 min. Samples were centrifuged for 30 secs at 16,000 x *g* and supernatant discarded. The pellet was washed in 500 µL Buffer QX1 by centrifugation at 16,000 x *g.* The

pellet was washed twice with 700 µL Buffer PE by centrifugation at 16,000 x *g*. The pellet was air-dried until white. 20 µL of ddH_2O was used to resuspend the pellet and then the sample centrifuged for 30 secs at 16,000 x *g.* The supernatant was harvested and transferred to a new tube.

2.4.5. Barcoding and Sequencing of Samples

Purified products were barcoded using NEBNext Ultra Library Preparation Kit (New England Biolabs) to attach Illumina sequencer adaptors. The samples were then pooled and sequenced with 2x250 base-pair paired end reads on an Illumina MiSeq instrument using the MiSeq v2 reagent kit (Illumina, Cambridge, UK) by Dr Meriem Attaf or Cristina Rius Raphael. NGS output files were initially analysed with MiXCR software by Dr Meriem Attaf or Cristina Rius. Output files were then converted using VDJtools for analysis with VDJViz (Bagaev et al. 2016). Singletons were not included in analysis. NGS clonotypes from A549-reactive T-cells were removed from bacterial NGS samples with the help of Thomas Whalley (**Appendix, Figure 8.2**).

2.4.6. Clonotyping individual T-cell clones

mRNA was extracted, converted to cDNA, amplified by nested and step-out PCRs and PCR products extracted by gel electrophoresis as described above (**Sections 2.4.1**-**2.4.4**). PCR products were then inserted into the Zero Blunt TOPO PCR Cloning Kit (Invitrogen), according to manufacturer's instructions. TOP10 bacteria cells were then transformed with the Zero Blunt cloning product. In brief, 5 µL Zero Blunt product was added to 25 µL TOP10 bacteria cells, incubated for 30 min on ice, heat shocked for 30 sec at 42 °C and then returned to ice. 250 µL SOC medium was added and incubated for 1 hr at 37 °C to allow bacteria to recover. The bacteria suspension was then plated on LB agar plates supplemented with 50 µg/mL

kanamycin and cultured at 37 °C overnight. To confirm resistant colonies had taken the correct insert, a colony PCR was performed by inoculating a PCR reaction tube with a colony containing the following mastermix:

Reagents	**Volume (µL)**
M13 F	1
M13 R	1
DreamTaq 2x Mastermix	12.5
RNase-free H_2O	10.5

A PCR reaction was then carried out:

Temperature °C	**Time (min:sec)**	
94	10:00	
94	0:20	x 27 cycles
57	0:20	
72	0:45	
72	5:00	

PCR products were analysed for insert by performing a 1% agarose gel electrophoresis step (**Section 2.4.4**). Colonies that were positive for insert were then sequenced using the Eurofins PlateSeq service, according to manufacturer's instructions. Cα-R3 and Cβ-R3 primers (**Appendix, Table 8.1**) were used for sequencing.

2.5. Lentiviral transduction of cells

2.5.1. Vector Design

Genes to be expressed via lentiviral transduction were cloned into the 3rd generation lentiviral vector pELNS (kindly provided by Dr. James Riley (Richardson et al. 2008)), using XbaI and XhoI/SalI restriction sites (**Figure 2.2a**). This vector places the gene to be expressed

under the elongation factor (EF)-1α promoter. In addition, the pELNS vector contains rCD2 used as a marker for transduction separated from the transgene(s) by a self-cleaving 2A sequence (Szymczak et al. 2004). When TCRs were required as transgenes, the individual α and β chains were separated by another 2A sequences to ensure stoichiometric expression of both TCR chains. The secondary 2A sequence also contains a SmaI restriction site for exchange of chains if required. The native MR1 and K43A transgenes were cloned into pELNS vector using XBaI and SalI restriction sites thus removing the rCD2 transduction marker. For MR1 knockout, a Clustered Regularly Interspaced Short Palindromic Repeats (CRISPR)/CRISPR associated protein 9 (Cas9) single guide (sg)RNA targeting exon 2 of human MR1 was cloned into the pRRLSIN.cPPT.WPRE backbone (Addgene plasmid # 12252) with a pCDNA.3-TOPO_WT-Cas9 (Addgene plasmid # 41815) insert, resulting in an 'all-in-one' CRISPR lentiviral plasmid (Laugel et al. 2016).

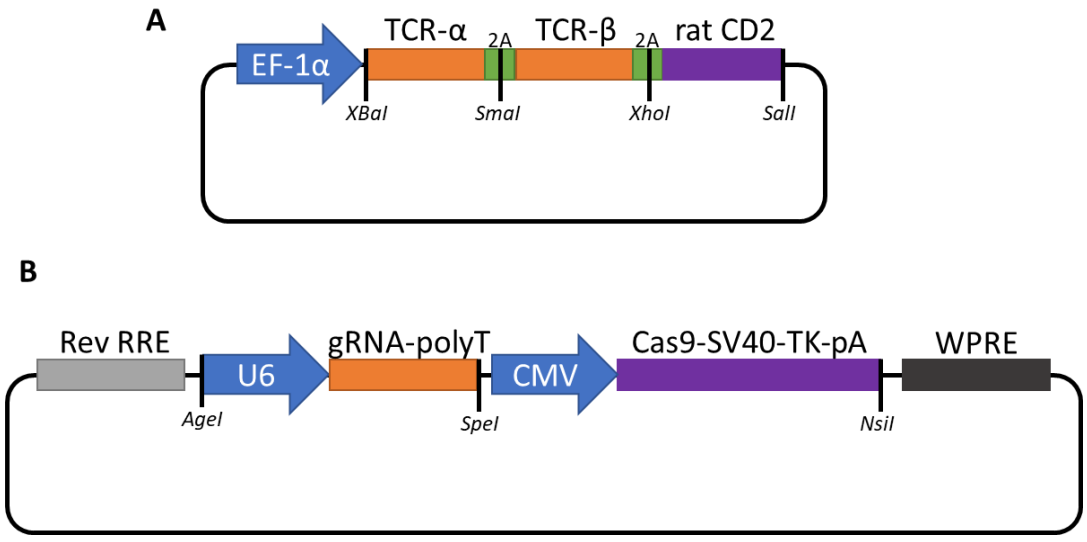

Figure 2.2 - Schematic of lentivirus gene transfer plasmids used in this thesis
(**A**). pELNS plasmid. TCR α and β chains were cloned into plasmid using unique restriction enzyme sites XbaI, SmaI and XhoI. Each gene was separated by 2A self-cleaving peptide sequencing. Genes were under Elongation Factor 1α (EF-1α) promotor. If MR1 was used as transgene, XBaI and SalI were used as restriction sites. (**B**). pRRLSIN.cPPT.WPRE backbone with pCDNA.3-TOPO_WT-Cas9 insert. MR1 gRNA was inserted at the SpeI restriction site and under U6 promotor control. Cas9 nuclease was under SV40 CMV promotor control.

2.5.2. Gene cloning into plasmid vectors

All gene constructs were synthesised by Genewiz in the pUC57 vector. MR1 used the native sequence, whereas TCRs and MR1 K43A used were codon optimised for *Homo sapiens* expression. Vectors were digested for 1-2 h at 37 °C with the following reaction mixture:

Table 2.9 - Reaction mix for removing genes from pUC57 vector

Reagents	**Amount**
Plasmid DNA	1 µg
10X FastDigest buffer (Thermo Scientific)	2 µL
XBaI (FastDigest, Thermo Scientific)	1 µL
XhoI/SalI (FastDigest, Thermo Scientific)	1 µL
Nuclease-free H_2O	To 20 µL

Digested plasmids were purified on 1% agarose gel electrophoresis at 80V for 1 h. The vector and insert were cut from the gel and DNA extracted using Wizard SV Gel and PCR Clean-up System (Promega), according to manufacturer's instructions. Briefly, the excised gel was dissolved in 100 µL membrane binding solution per 100 mg of gel slice and dissolved at 65 °C. The solution was transferred to a mini-column and incubated at room temperature for 1 min, followed by centrifugation at 16,000 x *g* for 1 min and the flow through discarded. The column was washed twice with wash buffer (700 µL followed by 500 µL with centrifugation at 16,000 x *g*). The flow-through was discarded and the column dried by centrifugation for 1 min at 16,000 x *g*. DNA was eluted from the column in 20 µL of dH_2O and the concentration of DNA determined using a Nanodrop ND1000 (Thermo Scientific). The fmol concentration was determined using the online tool http://www.promega.com/a/apps/biomath/. The vector and insert were then ligated, with the reaction mix described in **Table 2.10**, conducted for 2 h at room temperature. A control ligation was also set up with no insert.

Table 2.10 - Reaction mix for ligation of plasmids

Reagents	**Amount**
Vector	30 fmol
Insert	150 fmol
10X T4 DNA Ligase Buffer (Thermo Sceintific)	2 µL
T4 Ligase (Thermo Scientific)	1 µL
Nuclease-free H_2O	To 20 µL

Escherichia coli (*E. coli*) XL-10 Gold (Agilent Technologies, Fisher Scientific) were transformed with the ligation mix according to manufacturer's guidelines. These cells are endonuclease and recombination deficient, preventing loss of insert in lentiviral vectors that contain long terminal repeats. In brief, 20 µL of competent cells were thawed on ice, to which up to 100 ng of DNA was added (or 5 µL of a ligation mix). After a 30 min incubation on ice, the cells and DNA were heat shocked at 42 °C for 30 s followed by 5 min on ice. The cells were then incubated in an orbital shaker incubator for one hour at 37 °C at 220 RPM in 100 µL super optimal broth (SOC) media (Invitrogen) before streaking onto LB agar plates supplemented with 100 µg/mL carbenicillin (Carbenicillin Direct) overnight at 37 °C. Colonies were harvested for miniprep/maxiprep (**Section 2.5.3**).

2.5.3. Miniprep/Maxiprep Plasmid DNA Extraction

To confirm sequence of plasmids, transformed XL-10 Gold bacteria were cultured in 5 mL LB medium overnight and plasmids isolated with PureLink Quick Plasmid Miniprep Kit (Invitrogen), followed by sequencing by Eurofins. In brief, transformed XL-10 Gold bacteria were pelleted and resuspended in R3 buffer containing RNase A, then lysed in pre-warmed L7 buffer, neutralised with N4 buffer and added to an equilibrated spin column. The column was washed then eluted in 75 µL TE buffer. pELNS plasmids were sequenced using pELNS F2 and R3 primers, and the pRRLSIN.cPPT.WPRE.TOPO_WT-Cas9 was sequenced with pLKO.1-A

and gRNAcolPCR_R primers (Genewiz). Bacteria cultures with confirmed plasmid sequences were then cultured in 250 mL LB supplemented with 100 µg/mL ampicillin at 37 °C with orbital shaking at 220 RPM overnight. Cultures were pelleted by centrifugation at 4,000 x *g* for 10 min and plasmids extracted PureLink HiPure Plasmid Filter Maxiprep Kit (Invitrogen). This uses the same buffers and protocols as the PureLink Quick Plasmid Miniprep Kit but on a larger scale. The concentration of DNA was measured using a Nanodrop ND1000 (Thermo Scientific). An aliquot was tested for correct sequence by Sanger Sequencing (Eurofins), with the remaining samples stored at -20 °C.

2.5.4. $CaCl_2$ transfection of 293T cells for lentivirus particles production

Table 2.11 - Composition of plasmids required for production of 2nd and 3rd generation lentiviruses

Plasmid Generation	Transfer Plasmid	Envelope Plasmid	Packaging Plasmid
2nd	pRRLSIN.cPPT.WPRE (16 µg)	pMD2.G (8 µg)	pCMV-dR8.74\\ (12 µg)
3rd	pELNS (15 µg)	pMD2.G (7 µg)	pMDLg/pRRE (18 µg), pRSV-REV (18 µg)

Quantities given per 1 x T175 flask.

Table 2.12 - Buffers used in transfection of lentiviral plasmids

Buffer	Reagents
0.1x TE Buffer	1 mM Tris, 0.1 mM EDTA, ddH_2O. pH 8.0
Buffered water	125 µL 1M HEPES, 50 mL ddH_2O. pH 7.3
$CaCl_2$ (2.5M)	9.18 µg $CaCl_2.2H_2O$, 25 mL H_2O
2xHeBS (HEPES-buffered Saline)	0.28 M NaCl, 0.05 M HEPES, 1.5 mM anhydrous Na_2HPO_4, ddH_2O. pH to 7.00 (using NaOH).

Each buffer was 0.2 µm sterile filtered.

2 x 10^7 293T cells were plated in a T175 flask in 25 mL of D10 and cultured overnight until 80% confluent. 4 h prior to transfection, the medium was replaced with 15 mL D10. A transfection mix was made by combining either 2nd or 3rd generation plasmids (**Table 2.11**). To this, 1.1 mL of 0.1x TE and 580 µL of buffered water were added, followed by 188 µL $CaCl_2$

and mixed by pipetting (**Table 2.12**). 1.9 mL 2xHeBS was added dropwise under agitation by vortexing followed by a 20 min room-temperature incubation. The transfection mix was added dropwise to the flask containing 293T cells followed by overnight culture. Medium was discarded and 20 mL fresh D10 was added with cells cultured again overnight. Supernatant was harvested and 0.45 μm filtered (Millipore) and stored at 4 °C (48 hr harvest), with 20 mL fresh D10 added to cells. After another overnight culture, the supernatant was harvested and 0.45 μm filtered (72 hr harvest). The supernatant harvests were pooled and either left unconcentrated or concentrated using 70% IMS sterilised polyallomer ultracentrifuge tubes (Beckman Coulter) centrifugated at 140,000 x *g* for 2 hr at 4 °C. The pellet was resuspended in 1 mL of appropriate media – either 20 IU TCM or R10 depending on the target for transduction. Lentivirus was then either stored at 4 °C if used for transduction within 7 days, or aliquoted into cryotubes and snap frozen on dry ice before transferring to -80 °C.

2.5.5. Transduction of cell lines

Cells were plated at 1 x 10^6 cells per well in a 24- well plate in 500 μL of R10 or D10. For suspension cells, 8 μg/mL was added and left in culture for 2 h and for adherent cells 8 μg/mL of polybrene was added at the same time as the lentivirus. Up to 500μL of concentrated lentivirus or 1 mL of unconcentrated lentivirus was added to cells and spinfected by centrifugation at 500 x *g* for 2 h. After 24 h, the media was replaced with media supplemented with 1 μg/mL puromycin (for selection of cells carrying the plasmid containing the puromycin resistance gene), or with fresh media alone.

To knock out MR1, an 'all-in-one' lentiviral CRISPR/Cas9 system was developed (Laugel et al. 2016). A549 cells were transiently lipofected by Dr Bruno Laugel and Dr Angharad Lloyd

produced stable MR1 knockouts in THP1 and MM909.24 cell lines using lentivirus. For the MM909.24 MR1 knockout clone (c4), a round of selection for MR1 knockout was carried out using the MR1-restricted T-cell clone MC.7.G5. MC.7.G5 cells were cultured with CRISPR-treated MM909.24 cells at a 1:2 ratio for 7 days in 20 IU TCM. MC.7.G5 T-cells were subsequently removed by washing and further culture with R10, thus removing IL-2 required in T-cell culture. Any remaining T-cells would therefore die due IL-2 neglect. MM909.24 cells were consequently enriched with a biallelic MR1 knock out, and all tested clones produced were $MR1^{neg}$.

2.5.6. Transduction of primary T-cells

T-cells are considered difficult to transduce, however efficiency can be significantly increased if T-cells are actively proliferating, as induced through TCR and co-receptor stimulation (Bilal et al. 2015). Isolated T-cells, as described in **Section 2.2.4**, were activated with anti-CD3 anti-CD28 magnetic Dynabeads (Life Technologies) at a ratio of 3:1 beads to T-cells for 24 h at a density of 0.5 x 10^6 cells per well of a 48-well plate, in 1 mL of 200 IU TCM. 800 µL of media was replaced with up to 300 µL of concentrated lentivirus in addition to 8 µg/mL of polybrene. The T-cells were incubated overnight after which 500 µL of 200IU TCM supplemented with an additional 10 % FBS (total 20% FBS) was added. Transduced cells were fed with this medium every 2-3 days. 13 days post-transduction, TCR transduced cells were purified using anti-rat CD2-PE antibody and anti-PE magnetic beads sorting by MACS (**Section 2.2.8**). Transduced CD8+ T-cells were expanded after 14 days (**Section 2.2.5**), after which they were screened for transduction efficiency and used in functional assays.

2.6. Whole Genome CRISPR

Human Whole Genome CRISPR/Cas9 screening, using Genome-scale CRISPR Knock-Out (GeCKO) v2 libraries (Addgene plasmid ##1000000048, kindly provided by Feng Zhang) was used in this study in collaboration with Mat Legut (a fellow PhD student). The GeCKO library is formed of 6 independent CRISPR gRNAs (each binding to the first 5' protein-coding exon of a given gene) targeting 19,050 protein-coding genes in the human genome, as well as 1,864 micro-RNAs (miRNAs) targeted with 4 gRNAs each, with all guides split into two sub-libraries termed Library A and B. Included in the library are 1,000 gRNAs that do not target any region in the human genome which are used as controls for non-specific target cell survival. This results in a full library of 123,411 gRNAs. Due to the pooled library containing a large number of unique gRNAs, maintenance of proper representation of gRNA population throughout the library preparation, screening and sequencing is crucial. The following methods are based on methods published by Feng Zhang and colleagues on www.genome-engineering.org website (Joung et al. 2017).

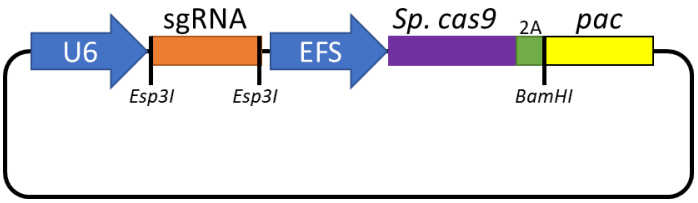

Figure 2.3 - Schematic of lentiCRISPR v.2 lentivirus plasmid used in whole genome CRISPR
U6 and EFS promotors shown by arrows with transgenes as bars. A single sgRNA from GeCKO libraries were inserted at Esp3I restriction sites. EFS, short elongation factor; pac, puromycin N-acetyltransferase; *Sp. Cas9*, *Streptococcus pyogenes cas9* gene.

2.6.1. Library Amplification

Ready to use lentivirus, along with starting aliquots that were amplified by Mat Legut were provided by Professor John Phillips (University of Utah). In brief, the sub-libraries were

amplified by transforming 100 ng library per 25 µL of ElectroCompetent Endura cells (Lucigen) (5 transformations per sub-library). To achieve this, plasmid libraries were added to bacteria and pulsed at 1,800 V (Bio-Rad MicroPulser, programme Ec1). Immediately after pulsing, 975 µL of room-temperature Recovery Medium (Lucigen) was added. The transformed bacteria were transferred to a 15 mL tube and placed in an orbital shaker at 37 °C, 220 RPM for 1 h, followed by plating on LB agar plates supplemented with 100 µg/mL ampicillin. Each sub-library was plated on 20 LB plates. To calculate transformation efficiency, an additional plate was inoculated with an aliquot of transformed bacteria diluted 40,000 x. The plates were incubated at 32 °C for 14 h, and the CFU counted on the dilution plate. The transformation was considered successful if more than 75 colonies were present, as this gives an estimated 3 x 10^6 colonies per sub-library and therefore 50x coverage of gRNAs. The transformed bacteria were then harvested from the plates and the plasmid DNA extracted using the PureLink HiPure Plasmid Filter Maxiprep kit (Invitrogen), as described in **Section 2.5.3**. The maximum bacterial pellet added to an individual HiPure Filter column was 500 mg.

2.6.2. Library Setup and Screening

293T and MM909.24 cell lines were used for screening with the GeCKO v2 library. Puromycin sensitivity of these cell lines was determined prior to library screening: 1 x 10^6 cells per well were plated in a 12- well plate for 24 h, after which puromycin (Thermo Scientific) was added to the cells at a concentration range of 0.1 to 10 µg/mL and cultured for 3 days. Cells were then detached and re-plated for 24 h, after which they were again detached and counted. The lowest concentration of puromycin that resulted in no cell survival was used as the selecting concentration for cells transduced with the GeCKO v2 library. The GeCKO v2 lentivirus was titrated in each cell line to ensure a MOI of approximately 0.4, decreasing the possibility of transducing a single cell with more than one viral particle. Briefly, 3 x 10^6 cells

per well in a 6-well plate were transduced with 0, 25, 50 or 100 µL of lentivirus in the presence of 8 µg/mL polybrene by spinfection (500 x *g*, 2 h, 37 °C). After 18 h, the medium was replaced. After a further 2 days, the cells were split across two wells and the appropriate concentration of puromycin added to one of the wells. 3 days later the cells were detached and re-plated, and after a further 24 h the cells were harvested and counted. The MOI was calculated according to the following formula:

$$\text{MOI} = \frac{\text{number of viable cells treated with puromycin}}{\text{number of viable cells not treated with puromycin}}$$

40 x 10^6 target cells (either 293T or MM909.24) were then transduced, as this gives more than 100x coverage of each sub-library if MOI = 0.3-0.5. The transduced cells were cultured for 14 days, after which half of the cells from each sub-library were frozen down, the remaining cells were used for screening by co-incubating with the MC.7.G5 T-cell. For this, 50,000 target cells per well were plated in a 96-well flat bottom plate in T-cell priming medium, with T-cells at a predetermined effector to target ratio of 0.25:1. Several wells of untransduced target cells were plated in parallel to serve as a control ensuring that all target cells were killed by T-cells at the given ratio. After 14 days of co-incubation, surviving target cells were pooled and re-plated with T-cells at a 2x effector to target ratio of 0.5:1. After the second round of T-cell selection, target cells were cultured to a sufficient cell number for sequencing, functional assays and freezing for preservation of library representation.

2.6.3. Library sequencing

T-cell selection resulted in a limited number of surviving cells from which genomic DNA was isolated, and the lentiviral inserts barcoded and sequenced with sample multiplexing on MiSeq or HiSeq (Illumina). Two rounds of PCR were performed on the entirety of the isolated genomic DNA as described below.

1st round PCR:

Reagents	Amount
NEBNEXT High Fidelity PCR Master Mix 2x (NEB)	25 µL
Adaptor F (10 µM)	2.5 µL
Adaptor R (10 µM)	2.5 µL
Genomic DNA	2.5 µg
H_2O	To 50 µL

Multiple separate reactions were set up to process genomic DNA from 20 x 10^6 cells per sub-library, which were pooled before using in 2nd round PCR.

2nd round PCR:

Reagents	Volume (µL)
NEBNEXT High Fidelity PCR Master Mix 2x (NEB)	25
Illumina F01-04 (10 µM)*	2.5
Illumina R, barcoded (10 µM)‡	2.5
PCR Product	2.5
H_2O	17.5

*Staggered primers to increase diversity of sequenced library. ‡Contain sample specific barcodes. Sequences described in Appendix, Table 8.1.

Both PCR cycles were carried out as followed:

Temperature °C	Time (min:sec)
98	0:30
98	0:10
60	0:10
72	0:15
72	2:00

1st PCR run for 18 cycles, 2nd PCR run for 24 cycles.
PCR products were then run on a 2% agarose gel and extracted as described in **Section 2.4.4**.

MiSeq sequencing was carried by Dr Meriem Attaf and HiSeq sequencing was performed by University of Utah (courtesy of John Phillips), with 80 cycles of read 1 and 8 cycles of index 1. To achieve a normalised gRNA count, the following formula was used:

$$\frac{\text{number of reads per given gRNA}}{\text{number of reads in the sample}} \text{ X } 10^6$$

The NGS data for GeCKO v2 libraries were analysed using a bespoke web tool (courtesy of Dr. Barbara Szomolay, Cardiff University). Model-based Analysis of Genome-wide CRISPR/Cas9 Knockout (MAGeCK) was performed by Colin Pharrell (University of Utah) where genes are prioritised by robust rank aggregation of P-values of enriched sgRNAs (Li et al. 2014). MAGeCK outperforms other sgRNA analysis methods by maintaining a low false discovery rate (FDR) with high sensitivity.

Chapter 3. Bacterial activation of unconventional T-cells

3.1 Background

Since the discovery of antibiotics, human morbidity and mortality have greatly reduced leading to an extension of average human lifespan. There are a broad range of antibiotics targeting protein synthesis, DNA and RNA synthesis, damage to bacterial cell walls or altering the metabolism of a bacterial cell. However, bacterial infections have now once again become a threat, due to the evolution of resistance by a range of mechanisms to each of the current antibiotics used clinically and agriculturally. According to the Centres for Disease Control (CDC), many gram-negative bacteria and to a lesser extent gram-positive bacteria, have developed resistance to nearly all current commercial antibiotics (CDC 2013). The threat of growing antibiotic resistance is particularly problematic for immunocompromised individuals, such as those who undergo organ transplant or are infected with HIV (Anuwatnonthakate et al. 2013; Spellberg et al. 2008). Bacterial immune-evasion strategies and inefficient vaccines (such as the Bacille Calmette-Guérin (BCG) vaccine against pulmonary Tuberculosis (TB) (Pereira et al. 2007)) highlight the need to identify novel prophylactic and therapeutic treatments to prevent the spread of potentially fatal infections. Since there have been few advances in the field of novel antibiotics (CDC 2013) and with little encouragement from pharmaceutical companies to invest further, targeting the immune system to better deal with pathogenic infections is a viable alternative, in particular taking advantage of shared, HLA-independent, unconventional T-cell responses.

Unconventional T-cell recognition of non-peptidic antigens bound by evolutionally-conserved proteins have a role in bacterial clearance (Gao et al. 2015; Liuzzi et al. 2016). Conserved presenting molecules are much less polymorphic than classical MHC proteins, and

therefore offer an attractive means to develop population-wide therapeutics (Godfrey et al. 2015). The current invariant TCRs known to bind to these presenting molecules are outlined in **Table 3.1**. For my studies I aimed to study donor-shared T-cell based responses to three morphologically distinct bacteria species – *Mycobacterium smegmatis* (*M. smegmatis*), *Salmonella enterica subsp. enterica serovar typhimurium* (*S. typhimurium*), and *Staphylococcus aureus* (*S. aureus*).

Table 3.1 - Invariant TCR gene usage

Cell Type (TCR)	Invariant TCR	Restriction molecule	Antigen
MAIT (αβ)	**CAVMDSNYQLIW*** TRAV1-2 TRAJ33/12/20	MR1	Riboflavin metabolites
GEM (αβ)	**CAVRNTGGFKTIF*** TRAV1-2 TRAJ9	CD1b	GMM
LDN5 (αβ)	TRAV17 TRBV4-1	CD1b	GMM
CD1c-restricted (αβ)	TRBV7-8/7-9	CD1c	Phosphomycoketides
iNKT (αβ)	**CVVSDRGSTLGRLYF*** TRAV10 TRAJ18 TRBV25-1	CD1d	αGalCer
EPCR-specific (γδ)	TRGV4 TRDV5	-	EPCR
CD1d-restriced (γδ)	TRGV4 TRDV1	CD1d	Sulphatide
CD1d-restriced (γδ)	TRGV5 TRDV1	CD1d	αGalCer
δ/αβ (hybrid)	TRDV1	CD1d	αGalCer

*Consensus sequence – slight variations can occur.

3.1.1. Mycobacterium smegmatis

M. smegmatis is a model organism used to study *Mycobacterium tuberculosis* (*M. tuberculosis*), an acid fast (**Figure 3.1a**) pathogenic bacterium that causes Tuberculosis disease (TBD). In 2016, an estimated 10.4 million people fell ill with TBD, and it is currently the ninth leading cause of death worldwide and the leading cause of death from a single infectious agent (WHO 2017). Resistance to the first line antibiotic Rifampicin is increasing

with over 600,000 new resistant cases of TB in 2016, 82% of which had multi-drug resistance (WHO 2017). Identification of a novel pathogen-specific target could be very helpful in the search for a protective vaccine (Colditz et al. 1994). Current vaccination strategies have sought to improve the efficacy of BCG, however these have shown limited improvements in protection from TBD (Tameris et al. 2013).

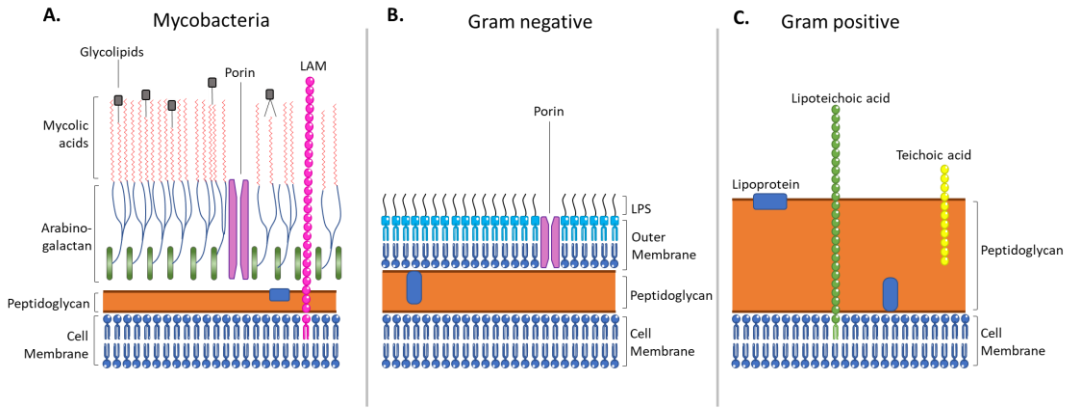

Figure 3.1 - Cell wall structure of Mycobacteria, gram-positive and gram-negative bacteria
(**A**). Surrounding the cell membrane of mycobacteria, the cell wall consists of a thin layer of peptidoglycan, arabinogalactan and a thick layer of mycolic acids. Glycolipids, lipoproteins and lipoarabinomannan (LAM) are also present. These surface proteins and lipids prevent gram staining of the peptidoglycan layer. (**B**). Gram negative bacteria have a thin layer of peptidoglycan surrounding the cell membrane, followed by a lipid bilayer forming an outer membrane, which contains lipopolysaccharides (LPS). Also present are transport channels such as porins. (**C**). Gram positive bacteria have a single lipid bilayer surrounded by a thick wall of peptidoglycan, with lipoteichoic acid and teichoic acids present. LAM, lipoarabinomannan; LPS, lipopolysaccharide. Adapted from (Brown et al. 2015).

The cellular response is vital for controlling mycobacterial infection (Cooper 2009); responses from conventional αβ T-cells, γδ T-cells and unconventional αβ T-cells have specificity to mycobacterial antigens. MAIT, GEM, iNKT, HLA-E-restricted and CD1a-d-restricted T-cells (reviewed in (Rodgers et al. 2005) all recognise distinct mycobacterial antigens presented by their restricting molecules. Indeed, several of these targeted antigens are abundant structural components of the mycobacterial cell wall, making them attractive immune targets (Barry et al. 1998).

3.1.2. Salmonella enterica subsp. enterica serovar Typhimurium

Salmonella enterica is species of gram-negative rod-shaped bacilli (**Figure 3.1b**), a number of whose serovars can cause serious foodborne disease in both livestock and humans. *Salmonella* infection resulted in in 19,336 hospitalisations and 378 deaths per year in the US alone from the nontyphoidal *Salmonella spp.*, more than any other recognised foodborne disease (Scallan et al. 2011). Non-typhoidal *Salmonella* causes 25% of global cases of diarrhoea each year with a stable population of bacteria resistant to first line antibiotics ciprofloxacin and ceftriaxone (reviewed in (Helke et al. 2017; WHO 2016; Medalla et al. 2017). Typhoidal *Salmonella* infections caused by *Salmonella enterica* serovar Typhi (*S.* Typhi), leads to an estimated 20 million infections and 200,000 death a year in developing countries (Mogasale et al. 2014).

3.1.1.1 S. *Typhi vaccine*

A vaccine for the prevention of Typhoid diseases caused by *S.* Typhi has recently gained prequalification from the WHO for use in ages from 6 months and above (World Health Organization 2018). The Capsular Vi-tetanus toxoid conjugated (Vi-TT) vaccine prevents 54.6% of typhoid infections, however this rises to up to 87% efficacy when using field definitions of typhoid fever (Jin et al. 2017). Field vaccinations efficacy may increase further due to pre- and post-vaccine exposure to *S.* Typhi. However, this vaccine is ineffective against other strains of *Salmonella* including the non-typhoidal pathogens.

Like in mycobacterial infections, γδ, MAIT cells, and iNKT cells have all been implicated in the clearance of *Salmonella* infection (Berntman et al. 2005; Gold et al. 2010; Hara et al. 1992); both bacteria share similarities in bacterial antigen production of unconventional T-cell ligands, such as phosphoantigens for the stimulations of γδ T-cells (Heuston et al. 2012; Liuzzi

et al. 2016) and riboflavin-derivatives bound to MR1 that are able to stimulate MAIT cells (Le Bourhis et al. 2013).

3.1.3. Staphylococcus aureus

S. aureus is a gram-positive round-shaped firmicute (**Figure 3.1c**) that is an opportunistic pathogen and forms part of the normal flora of the body. *S. aureus* can lead to a wide range of conditions such as boils, cellulitis, skin abscesses but also is a causative agent for more serious illness including but not limited to endocarditis, pneumonia, sepsis and toxic shock syndrome (Nizet et al. 2015). Methicillin-resistant *S. aureus* (MRSA) is an established antibiotic resistant strain that is a challenging problem in health care facilities where infections are most commonly acquired due to large volumes of circulating antibiotics (Klevens et al. 2007) and variations in toxicity among different isolates (Laabei et al. 2014). Current vaccination trials have proven ineffective but have targeted antibodies (Fowler et al. 2014) despite the dominant *S. aureus* response being associated with T-cells (reviewed in (Bröker et al. 2016)).

Unconventional T-cell responses are less well studied in response to *S. aureus* infections compared to *Mycobacterium* and *Salmonella* species, however the dominant immune response is linked with T-cells producing IL-17a, focused on T_H17 cells (Montgomery et al. 2014; Yu et al. 2018). Furthermore, both γδ and MAIT cells are known potent IL-17a producers, and these have also been implicated in the response to staphylococcal infections (Gold et al. 2010; Murphy et al. 2014). Interestingly, despite *S. aureus* being deficient in the MEP pathway and therefore unable to produce HMBPP (Heuston et al. 2012), Vγ9Vδ2 T-cells are activated in response to infection with *S. aureus*, mediated by accumulation of

alternative less-stimulatory phosphoantigens such as IPP (Montgomery et al. 2014; Wang et al. 2001; Heuston et al. 2012).

Each of these bacteria cause different pathologies, however all are able to survive within mammalian host cells (Garcia-del Portillo et al. 1993; Fraunholz et al. 2012; Sharma et al. 2012). Bacteria that have developed the ability to survive within a host can manipulate cellular pathways and immune responses that the immune system would normally use to control pathogenic infections; examples include downregulation of classical MHC molecules at the cell surface (Pecora et al. 2009; Cheminay et al. 2005), shielding from host antibodies, and secretion of superantigens to induce non-specific activation of T-cells (Marrack et al. 1990). Unconventional T-cells show conservation across the population and enable focused targeting of immune responses. Therefore, targeting unconventional T-cells could provide a novel approach for induction of bacterial clearance in all individuals against a variety of pathogens.

3.1.4. Aims

The majority of known unconventional T-cell responses are mediated by non-polymorphic antigen-presenting molecules. Antigens presented by these molecules could be shared between bacteria with unconventional T-cells able to respond to lipid or metabolic antigens that could be less prone to mutation than peptide antigens. Identifying the nature of specific T-cell subsets that are involved in bacterial recognition could reveal novel targets for therapies. Modern developments in high-throughput sequencing and computation now make it possible to examine the clonotypic architecture of bacterially-induced T-cell receptors (TCRs) for the first time. For my first results chapter, my aims were to:

- Dissect the phenotype of T-cell subsets reactive to bacterial antigens from unrelated bacteria species in a non-HLA-matched system using phagocytosed bacteria.
- Assess functionality of bacteria-reactive T-cells.
- Identify dominant clonotypes from multiple donors reactive to bacterial antigens, including identifying if there are clonotypic trends shared between donors and T-cells reactive to different bacterial species.

3.2 Results

3.2.1. Bacterial loading of cellular targets

To ensure bacterial antigens were processed and presented to T-cells, I examined the use of phagocytic/pinocytic cell lines (Wasylnka et al. 2002; García-Pérez et al. 2008) to ingest bacteria before culturing with donor PBMCs. Two epithelial phagocytic/pinocytic cell lines were available: (1) the monocyte-like phagocytic cell line THP1 and (2) the epithelial cell line A549. THP1, like most blood-derived cell lines, grow as suspension cells. Initial experiments with THP1 showed that it was difficult to wash off extracellular bacteria before addition of T-cells thereby allowing the complication of direct bacteria-T-cell interaction. Moreover, THP1 cells express HLA-A2 (Battle et al. 2013), the most common HLA (in ~40% of donors), giving potential for activation of conventional HLA-A2-restricted T-cells. Due to these problems with THP1 cells I therefore opted to use A549 cells to present antigen in my experiments.

M. smegmatis loading of A549 cells had previously been optimised in my laboratory by Dr Johanne Pentier, with *M. smegmatis* specific T-cells identified by co-culture with PBMCs at an effector to target ratio of 30:1, using CFSE as a marker of proliferation or ICS as readouts. CFSE covalently binds intracellular proteins that is diluted as cells proliferate, thus acting as a surrogate marker of activation of T-cells. ICS lyses cells and stains for intracellular cytokines, however mRNA cannot be used from lysed and fixed cells. As I aimed to clonotype bacteria-reactive T-cells, requiring the cells to be live and healthy, initial experiments were conducted using CFSE-labelled PBMCs activated with *M. smegmatis*-loaded A549 cells (**Figure 3.2**).

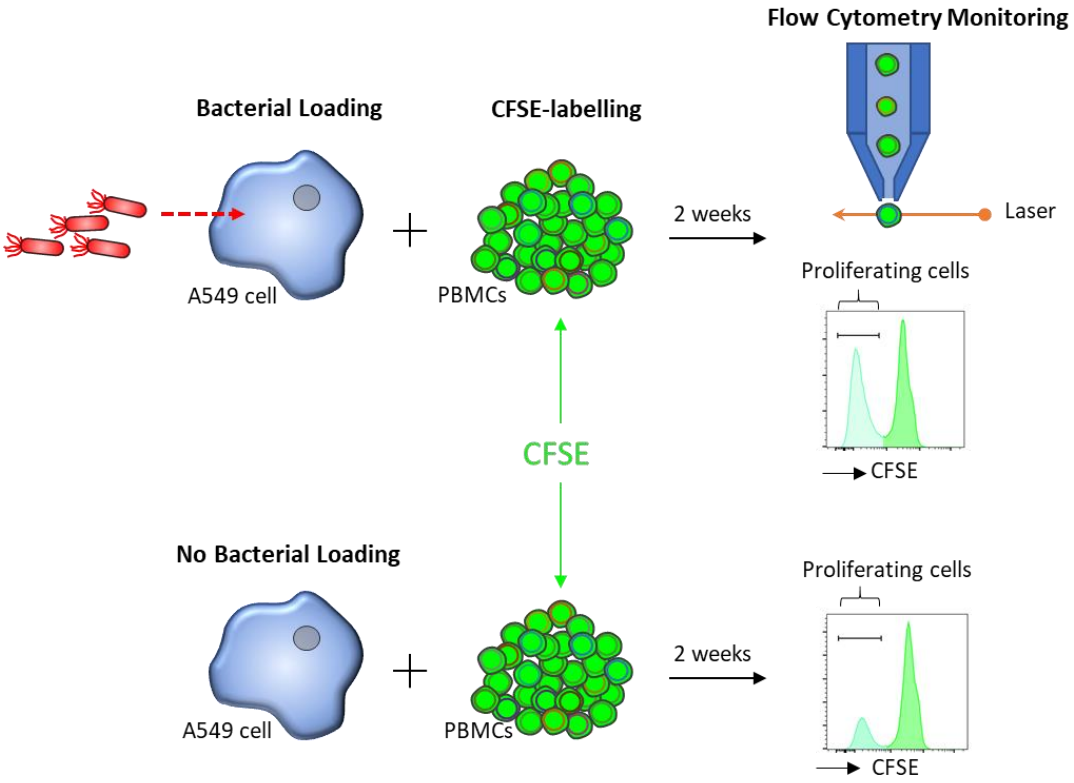

Figure 3.2 - Experimental overview of CFSE-labelling to identify bacteria-reactive T-cells
A549 cells loaded with *M. smegmatis* at a multiplicity of infection of 100:1 bacteria to A549 cell (top row) were co-cultured with CFSE-labelled PBMC at an effector to target ratio of 30:1 to prime bacteria-specific T-cells. A549 cells without loading of bacteria were also used to prime PBMCs as a negative control (bottom row). Priming cultures were stained for surface markers and monitored by flow cytometry after two weeks. Cells with low CFSE had proliferated evidenced by dilution of dye between cells, and these were taken through for further analysis.

3.2.2. High background proliferation is observed using CFSE-labelling

M. smegmatis-loaded A549 cells appeared to induce greater proliferation of T-cells over two weeks compared to bacteria-free A549 cells (**Figure 3.3**), however this difference was not statistically significant across multiple donors (**Figure 3.4a**). The $CFSE^{low}$ T-cells primed in *M. smegmatis*-loaded A549 cells were enriched for $CD4^{neg}$ (**Figure 3.4b**); *M. smegmatis*-loaded A549 cells induced 20.6 % ± 5.98 co-receptor double negative and 26.5 % ± 7.8 $CD8^{+}$ T-cells. On the other hand, T-cells primed without bacteria and without A549 cells were mostly $CD4^{+}$ – 90.0 % ± 14.3 (**Figure 3.4b**). Bacteria-free A549 cells also primed $CD4^{+}$ T-cells - 75.1 % ± 15.1, but as PBMCs were not HLA-matched I was interested in investigating the molecular

basis of the CD4^{neg} reactivity. One T-cell clone isolated from the CD4^{neg} population, designated MC.7.G5, showed non-HLA mediated recognition of multiple cancer cell lines. The nature of this HLA-agnostic recognition of cancer cell lines is of interest and forms the basis of **Chapter 4**.

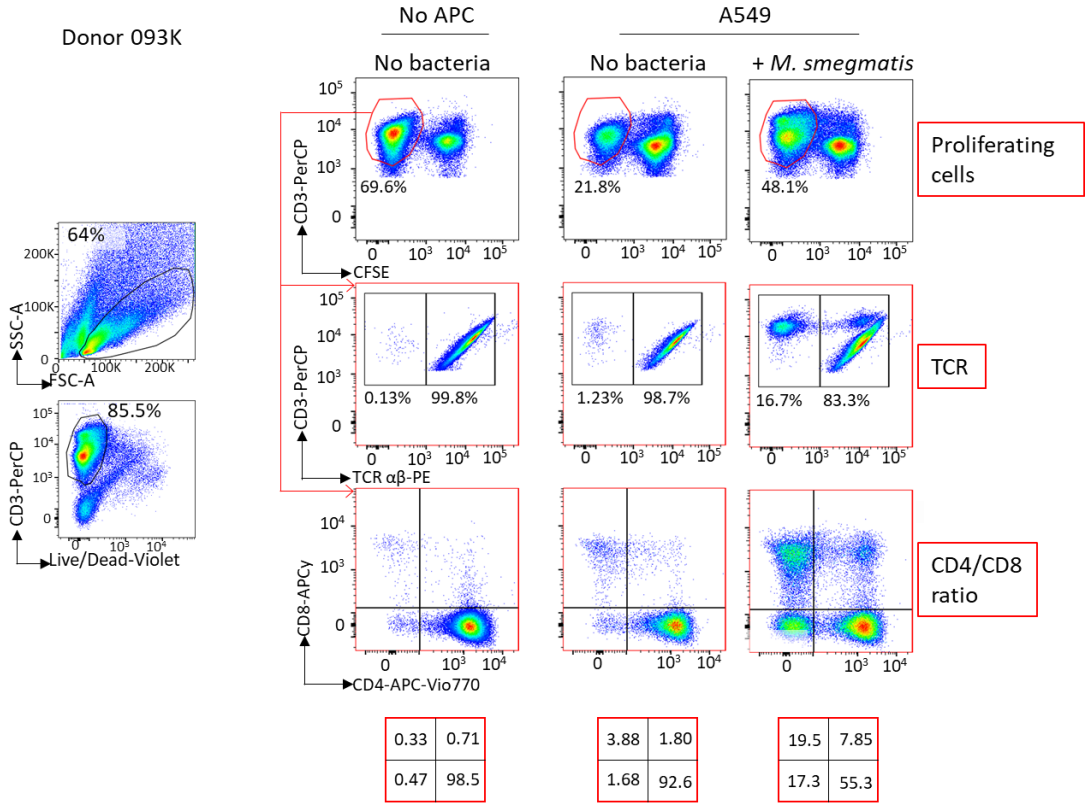

Figure 3.3 - Mycobacterium smegmatis-loaded A549 cells activate different subsets of CFSE-labelled T-cells compared to bacteria-free conditions.
After two weeks of priming CFSE-labelled healthy donor (093K) PBMCs with A549 cells loaded with or without *Mycobacterium smegmatis*, or without A549 cells were stained for surface markers. Cells were previously gated on CD3^{+} alive lymphocytes (shown on left). (Top row) Cells were gated on CFSE^{low} for proliferating cells. To identify T-cell subsets, cells were gated on either TCR-αβ (middle row) or CD4/CD8 expression (bottom row). CD4/CD8 quadrant percentages shown in red boxes.

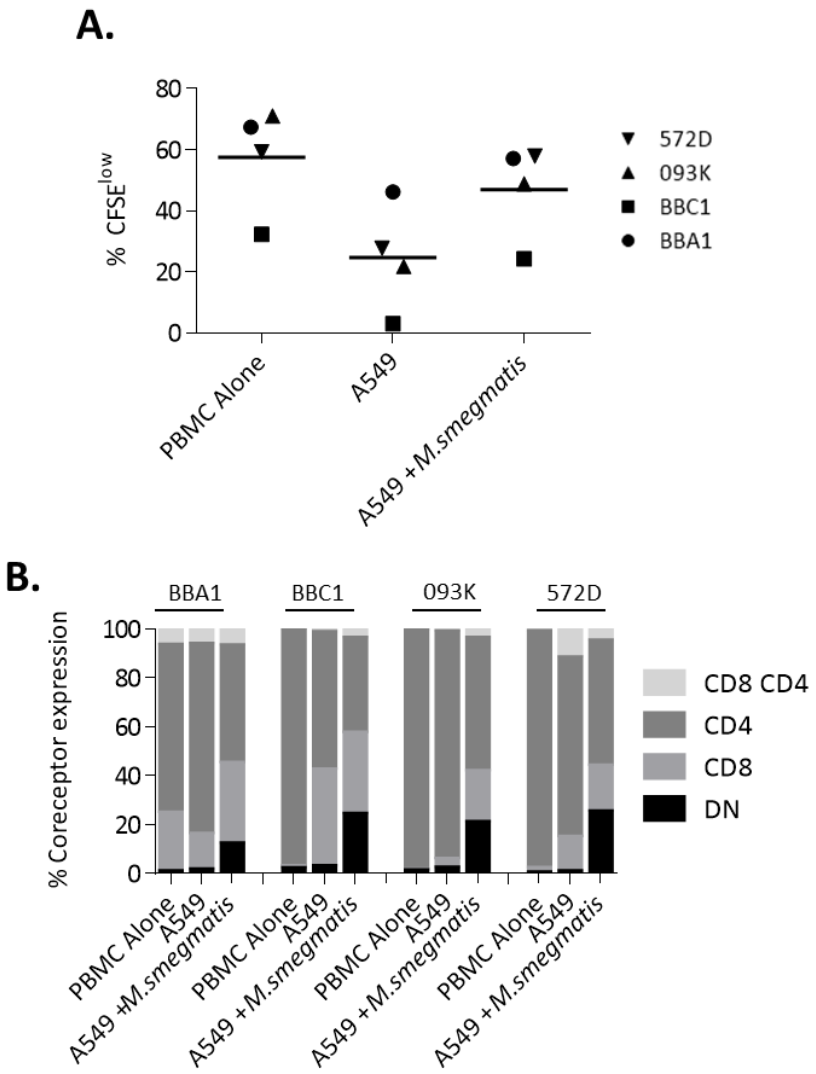

Figure 3.4 - CFSE and co-receptor staining of T-cells from the PBMC of four healthy donors
(**A**). PBMCs labelled with CFSE were co-cultured with A549 cell loaded with or without *M. smegmatis*, or without A549 cells. After two weeks, cells were analysed by flow cytometry for CFSE dilution with previous gating on $CD3^+$ alive lymphocytes. Results were not significant, $p > 0.1$ in unpaired t-test. (**B**). $CFSE^{low}$ cells from (A) were stained for CD4 and CD8 co-receptor expression.

Due to the high background of proliferation, CFSE-labelling was not specific enough to allow for true identification of bacteria-reactive T-cells. I therefore sought an alternative method to more reliably identify bacteria-reactive unconventional T-cells.

3.2.3. Frozen bacteria-loaded A549 cells activate MAITs and enable captured cytokine isolation of bacteria-reactive cells

Identification of bacteria-reactive T-cells has in my laboratory previously been achieved by ICS. However, this results in lysis of cells and therefore is not suitable to procurement and expansion of T-cells clones or for further TCR sequencing. A viable alternative is to use TAPI-O based sorting (Haney et al. 2011), where cells remain intact after sorting to ensure mRNA for clonotyping is undamaged. TAPI-O prevents cell surface cleavage of TNF enabling staining of activated TNF-producing cells with anti-TNF antibodies (**Figure 3.5a**). I adapted this protocol to include the surrogate killing, cellular degranulation marker CD107a (**Figure 3.5b**) (Betts et al. 2003), with sorting of T-cells reactive to *M. smegmatis*, as well as *S. typhimurium* and *S. aureus*, thus enabling isolation of viable cells by flow cytometry in two dimensions (TNF^+ and $CD107a^+$). Cells sorted this way remained viable and could be subsequently subjected to clonotypic analyses (**Figure 3.6**).

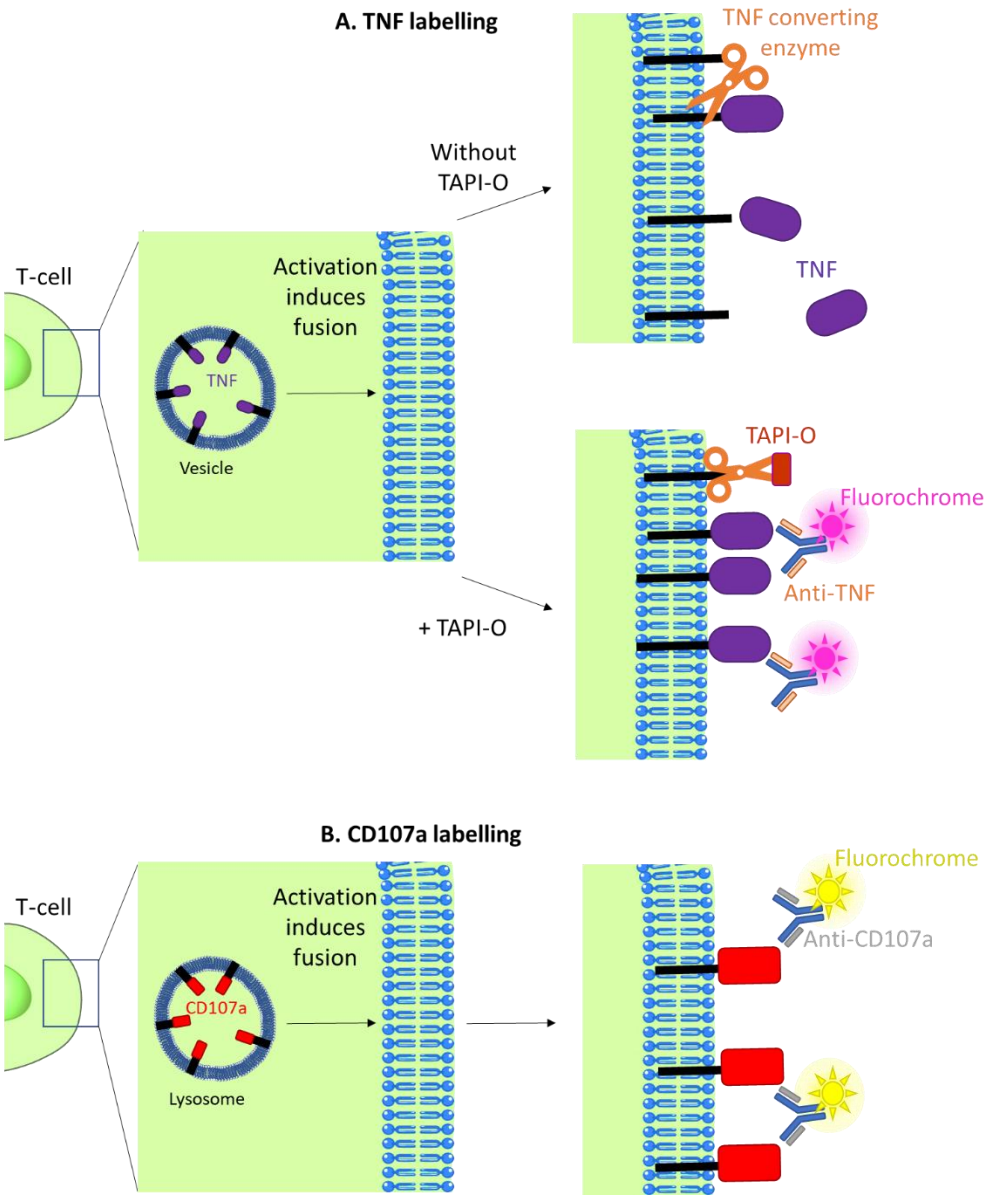

Figure 3.5 - Schematic of C107a and TAPI-based staining rationale
(**A**). TNF is membrane bound on intracellular vesicles. Upon T-cell activation, vesicles fuse with cell membrane, TNF is cleaved from the membrane by TNF-converting enzyme resulting in cellular secretion of TNF, thus cells cannot be stained with anti-TNF antibodies. TNF-converting enzyme can be inhibited with TAPI-O, resulting in surface bound TNF which can then be stained with fluorochrome-conjugated anti-TNF antibodies. (**B**). CD107a is expressed intracellularly on the inner side of lysosomal membranes. Upon T-cell activation, lysosomes fuse with cell membrane thus releasing lytic proteins such as perforin and granzymes, resulting in short-term surface expression of CD107a. Surface CD107a can then be stained with fluorochrome-conjugated antibodies. A combination of these techniques allows the sorting of viable, activated T-cells in two dimensions by flow cytometry. T-cells sorted in this way can then be clonotyped as shown in Figure 3.6.

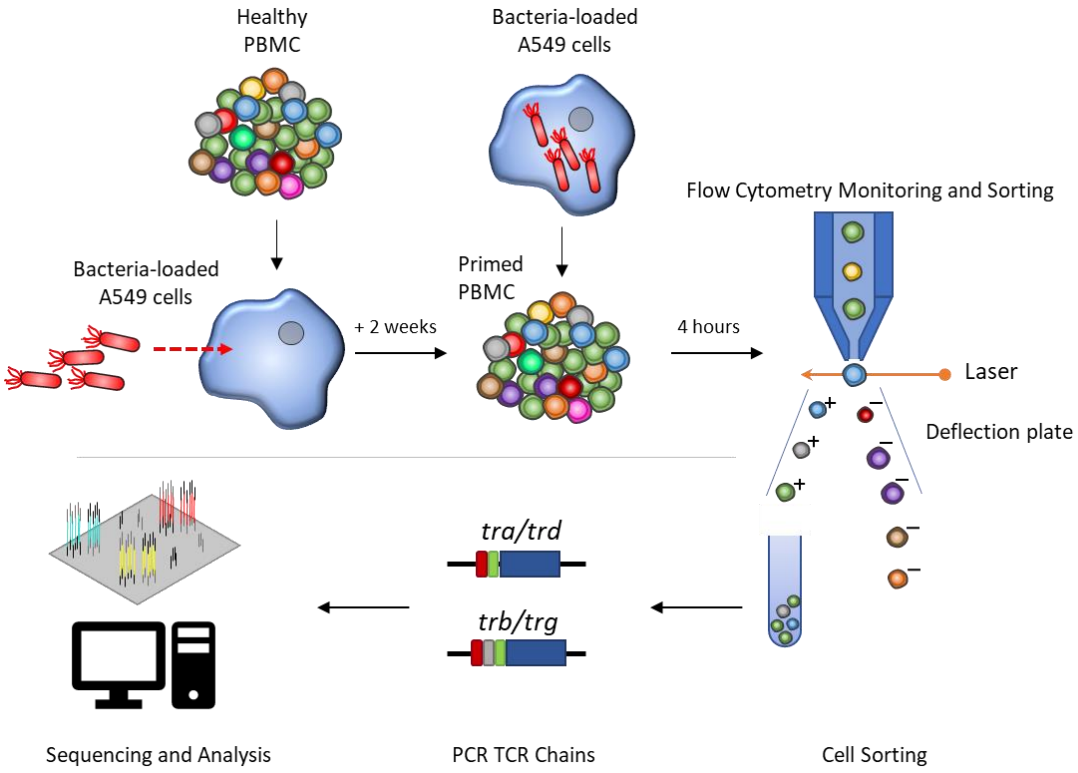

Figure 3.6 - Outline of methods used to identify bacteria-specific T-cells.
Schematic of experimental design. *Mycobacterium smegmatis, Salmonella enterica subs. Enterica serovar Typhimurium,* and *Staphylococcus aureus* were loaded onto the phagocytic cell line A549 (100:1, 25:1 and 25:1 MOI respectively). Bacteria-loaded A549 were cultured with healthy donor PBMCs at 30 PBMCs to 1 A549 cell, with monitoring by flow cytometry over two weeks, after which PBMCs were restimulated with their respective bacteria-loaded A549 cells in a TAPI-based TNF/CD107a activation assay (Figure 3.5), gating on alive $CD3^+$ lymphocytes expressing $CD107^+$ and TNF^+. TCR chains were amplified by PCR with Illumina sequence adapters and barcodes added, followed by next generation sequencing on an Illumina MiSeq.

The assay described above required bacterial loading of targets, T-cell activation and sorting of activated T-cells. Due to the length of each step it was not possible to undertake the entire assay in a single day. This was especially problematic as I was required to finish the cell sorting before 5 pm while expert technical assistance was available (PhD students are not allowed to run this specialist equipment unassisted). I therefore examined ways to simplify and standardise the assay to make it more reproducible and of shorter duration. As there was no way of easily shortening the T-cell activation, I focused on accelerating the bacterial loading. Specifically, I examined using fixed, stored bacteria with a known density or using a uniform frozen stock of A549 targets that were pre-loaded with bacteria (**Figure 7a**). Fixed

M. smegmatis induced recognition by a MAIT clone but at a reduced level compared to pre-loaded frozen cell samples. Fixed *S. typhimurium* and *S. aureus* were poor at inducing MAIT cell activation when compared to their frozen counterparts. As a result of these experiments, frozen stocks of bacteria-loaded A549 were used for further bacterial priming and experiments, enabling reduction of experimental time by 4.5 hours (**Figure 3.7b**).

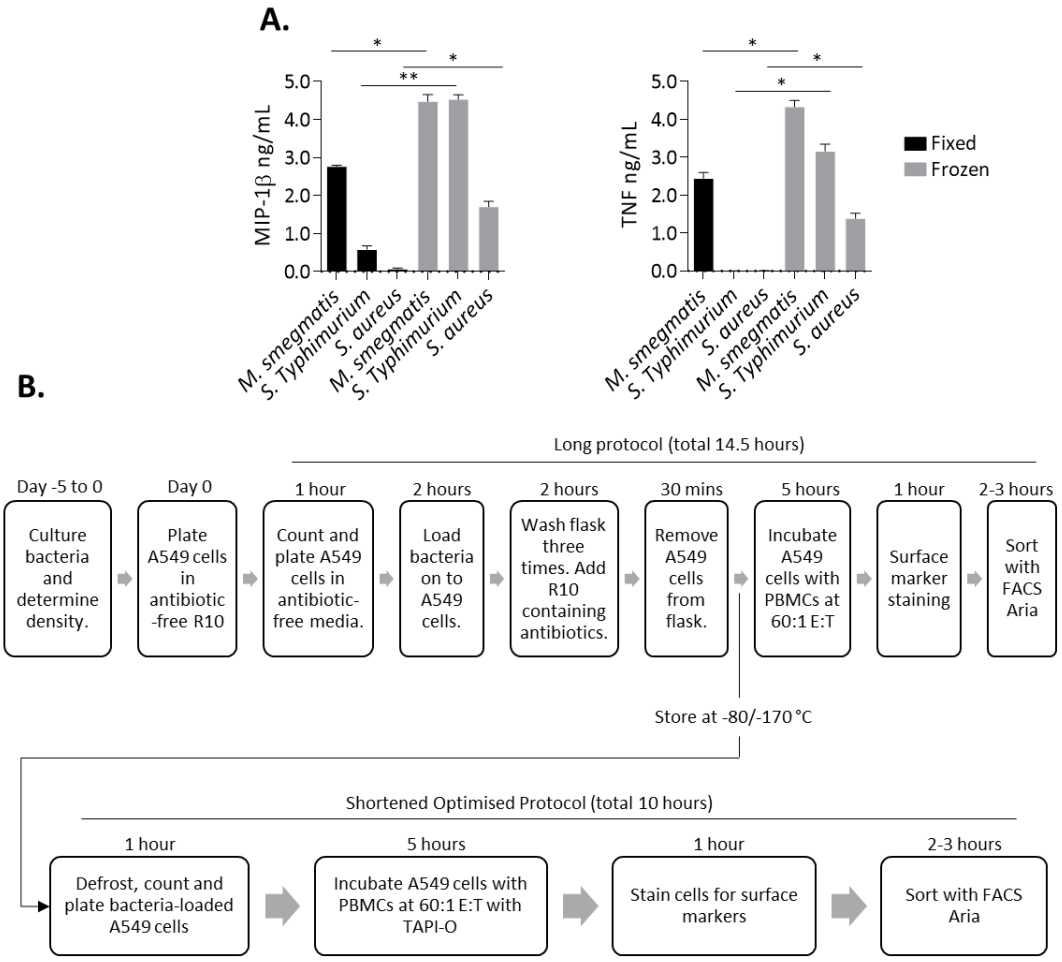

Figure 3.7 - Frozen A549 cells loaded with live bacteria activate MAIT-cells and shorten experimental set up time

(**A**). *Mycobacterium smegmatis, Salmonella enterica subs. Enterica serovar Typhimurium,* and *Staphylococcus aureus* (either fixed in 4% paraformaldehyde or live) were loaded onto the phagocytic cell line A549 (100:1, 25:1 and 25:1 MOI respectively) for two hours in antibiotic free media, followed by 2 hours with antibiotic. A549 cells loaded with live bacteria were then frozen. Bacteria-loaded A549 were then cultured with a MAIT clone in an overnight T-cell activation assay with supernatants analysed for MIP-1β and TNF concentration by ELISA. Assay performed in duplicate with error bars and t-test results shown, *p<0.01, **p<0.001. (**B**). Timeline of TAPI-O and CD107a based activation of T-cells. Top row shows original experimental design, bottom row shows optimised activation protocol using aliquots of frozen bacteria-loaded A549 cells stored at either -80 or -170 °C. Sorting by FACS Aria must be completed before 5pm due to the requirement of a dedicated specialist technical help.

3.2.4. *Staphylococcus aureus* are resistant to standard mammalian culture antibiotics

While an overnight assay sufficiently activated MAIT cells, prolonged culture during priming experiments resulted in extracellular outgrowth of *S. aureus* leading to death of APCs and PBMCs. I tested several antibiotics for their ability to inhibit growth of *S. aureus* without being toxic to the A549 target cells. Of the antibiotics tested, only Rifampicin - a bacteriostatic antibiotic that prevents RNA synthesis, controlled *S. aureus* at levels that were not toxic to A549 cells (**Table 3.2**). 0.05 μg/ml Rifampicin was therefore selected for use in subsequent experiments with *S. aureus.*

Table 3.2 - Antibiotics screening for prevention of* Staphylococcus aureus *growth

Antibiotic	**Penicillin/Streptomycin**			**Tetracycline**			**Gentamicin**			**Rifampicin**		
Concentration (μg/ mL)*	10x	5x	1x	26	2.6	0.26	50	5	0.5	5	0.5	0.05
Toxic to *S. aureus*	N	N	N	Y	N	N	Y	N	N	Y	Y	Y
Toxic to A549 cells	N	Y	Y	N	N	Y	N	Y	Y	Y	Y	Y

Toxicity to *S. aureus* determined by microscopic analysis of extracellular bacteria, toxicity to A549 cells determined by trypan blue exclusion. *For penicillin/streptomycin, concentrations at 1x were 100 U/mL Penicillin, 100 μg/mL Streptomycin.

3.2.5. TAPI/CD107a Staining specifically identifies bacteria-reactive cells

T-cells primed for two weeks with A549 cells loaded with bacteria were activated as outlined in **Figure 3.6**. The flow cytometry gating strategy for identification of bacteria-reactive T-cells is described in **Figure 3.8.** Across three donors, *M. smegmatis*-loaded A549 cells induced surface CD107a and TNF expression in 10.9 % ± 2.4 of single, live $CD3^+$ T-cells, *S. typhimurium* induced 30.0 % ± 1.7 and *S. aureus* induced 3.1 % ± 0.5 of T-cells (**Figure 3.9a**). Bacteria-free A549 cells induced 0.3 % ± 0.2 cells. Thus, TAPI/CD107a identification of bacteria-reactive T-

cells is considerably more specific than CFSE-labelling (**Figure 3.4**). T-cells were also stained for CD8, αβ-TCR and γδ-TCR expression to identify if each individual bacteria species induced phenotypically different subpopulations of T-cells (**Figure 3.8 & Figure 3.9b**). I did not stain for CD4 due to channel/fluorochrome limitations. *M. smegmatis* reactive T-cells were skewed towards $CD8^+$ αβ-TCR subsets – 67.2 % ± 13.1 $CD8^+$ αβ-TCR^+, 7.3 % ± 0.2 $CD8^{neg}$ αβ-TCR^+, and 25.2 % ± 1.8 γδ-TCR^+. *S. typhimurium* reactive cells were more skewed to γδ-TCR expressing T-cells – 19.0 % ± 10.3 $CD8^+$ αβ-TCR^+, 2.7 % ± 1.0 $CD8^{neg}$ αβ-TCR^+ and 75.8 % ± 7.0 γδ-TCR^+. Lastly, *S. aureus* reactive T-cells were also dominated by a γδ-T-cell response – 2.9 % ± 3.3 $CD8^+$ αβ-TCR^+, 5.2 % $CD8^{neg}$ αβ-TCR^+, and 88.3 % ± 4.8 γδ-TCR^+.

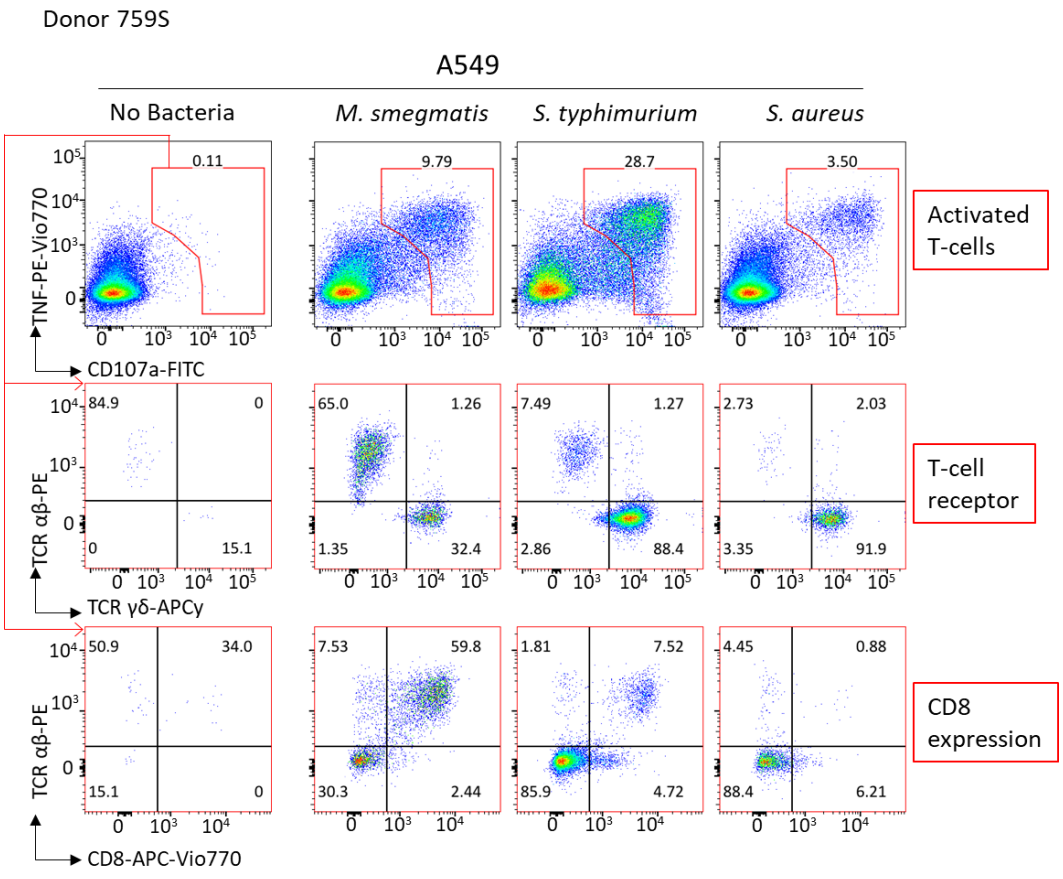

Figure 3.8 - Bacteria-loaded A549 cells activate different subsets of T-cells in CD107a/TNF assays
Healthy donor PBMCs (Donor 759S) were cultured with A549 cells loaded with *Mycobacterium smegmatis, Salmonella enterica subs. Enterica serovar Typhimurium,* and *Staphylococcus aureus*; after two weeks of culture were activated in a TAPI assay using bacteria-loaded A549 cells. Cells were previously gated on single alive $CD3^+$ lymphocytes, followed by activation markers CD107a and TNF expression (top row). Middle row shows T-cell receptor αβ (TCR-αβ) and TCR-γδ expression of activated cells, bottom row shows proportion of activated cells with CD8/TCR-αβ expression.

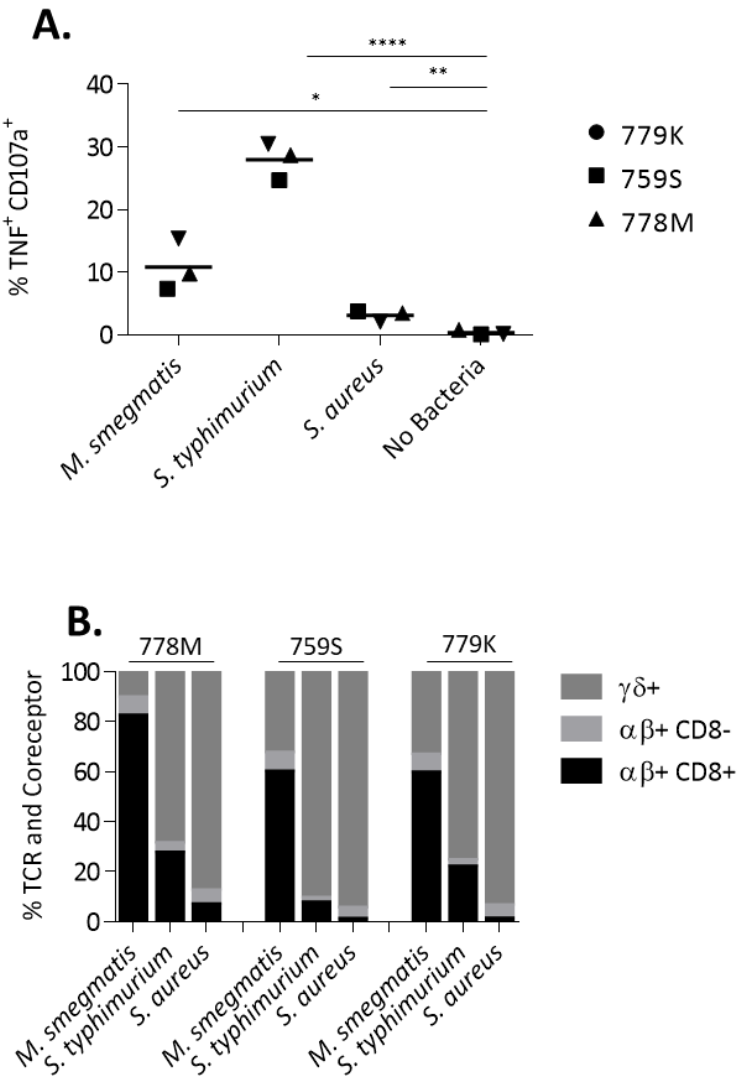

Figure 3.9 – M. smegmatis, S. typhimurium and S. aureus activate different T-cell subsets.
(**A**). The percentage of $CD107^+$ and TNF expressing cells was determined across three donors. Two tailed unpaired t test performed. * p= 0.017, ** p = 0.008, *** p < 0.0001. Previously gated on alive $CD3^+$ lymphocytes. (**B**). The CD8 coreceptor, TCR-αβ and TCR-γδ expression of CD107a and TNF expressing live $CD3^+$ lymphocytes in the $TNF^+CD107a^+$ gate after exposure to A549 cells loaded with indicated bacteria (as indicated in the top row of Figure 3.8).

3.2.6. TCR gene rearrangements of bacteria-specific T-cells

Clonotyping of T-cells identifies genetic similarities and differences in the antigen-specific T-cell receptor pool. The V, D (β and δ chains only) and J genes used to form the TCR can be analysed in addition to the T-cell clone-specific CDR3 sequence. To identify the repertoire of T-cells involved in recognition of bacteria, TNF^+ and $CD107a^+$ T-cells were sorted and sequenced from three donors (**Figure 3.9**) using the gates shown in **Figure 3.8,** with the total number of sorted and sequenced TCR chains shown in the **Appendix, Table 8.4**. T-cells that were activated by bacteria-free A549 cells were also sorted and sequenced. These TCRs are not bacteria specific and are most likely allogenic responses to non-self MHC molecules. Sequences that were observed in the TNF^+ $CD107a^+$ gate in the absence of bacteria were removed from the datasets that included bacteria using a python script written by Thomas Whalley (**Appendix, Figure 8.2**).

Clonotyping of responses in donor 778M showed there was a striking enrichment for gene rearrangements using TRAV1-2 recombined to TRAJ33 with all bacteria, while TRAV21 and TRAV13-1 with varying TRAJ genes were also enriched. TRBV20-1 was the most common TRBV gene across all bacteria (**Figure 3.10**). Donors 759S and 779K showed similar enrichments, however *S. aureus* did not enrich for the TRAV1-2/TRAJ33 recombination as strongly as in donor 778M (**Appendix, Figure 8.3**).

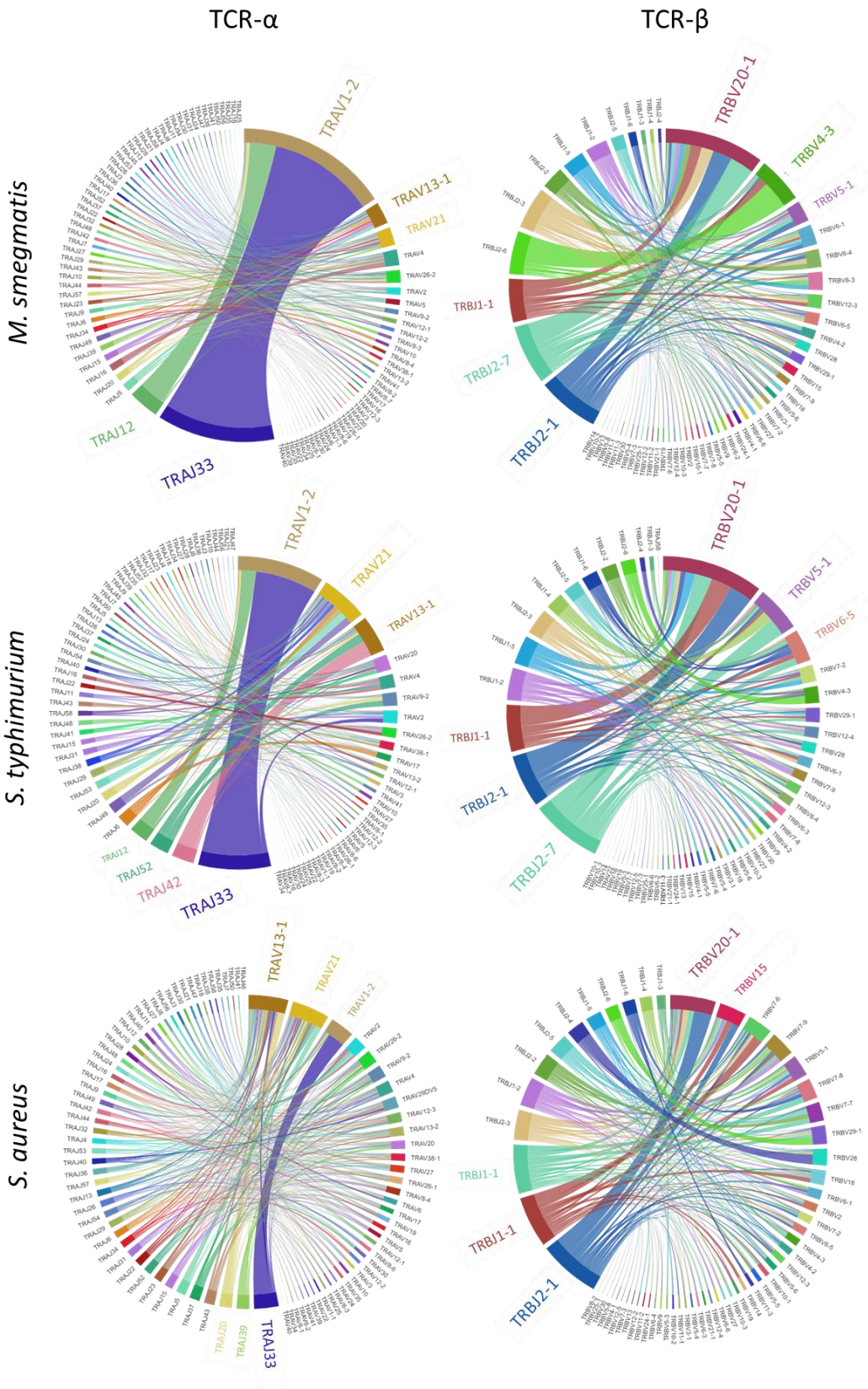

Figure 3.10 – αβ-TCR gene rearrangements in bacteria-responsive T-cell lines from Donor 778M
TCR gene rearrangements enriched in response to specific bacteria. Arcs on the right of a wheel dictate how common a variable gene is, arcs on the left of a wheel indicate Joining genes, with the link between the two showing how common genes are rearranged to each other. Plots were generated using VDJViz (Bagaev et al. 2016).

Analysis of TCR-γδ chains in each donor showed dominant enrichments of TRGV9/TRGJP rearrangements (**Figure 3.11**). The non TRGV9 genes differed between bacteria in Donor 778M (**Figure 3.11**), with *M. smegmatis* priming more TRGV4 and TRGV8 expressing T-cells, contrasting to *S. typhimurium* TRGV2 enrichments (other donors shown in **Appendix, Figure 8.5**). The second most common TRGV gene across most donors and bacteria was TRGV10. Interestingly, TRGV10 has previously been described as a pseudogene resulting from a mutation resulting in incorrect splicing of an intron (Sherwood et al. 2011; Zhang et al. 1994). The presence of this pseudogene could be due to errors in sequencing, allelic polymorphism enabling expression in some individuals (as in the case with some TRBV genes (Lefranc et al. 2015)) or a rearrangement that does not produce a TCR to facilitate positive thymic selection thus leading to subsequent alternative TCR rearrangements. To identify if TRGV10 was expressed as a surface-expressed TCR chain, I performed another bacterial-priming and flow cytometry sorted for $CD107a^{+}TNF^{+}CD3^{+}$γδ-TCR^{+} cells and sequenced the TCR-γ chains. This ensured sequenced γδ TCRs were from T-cells expressing surface γδ TCRs. When compared to TCR-γ chains from donor 759S which were not sorted on TCR-$γδ^{+}$, there was a striking reduction in the presence of the TRGV10/Vγ10 gene (**Figure 3.11**). The reduction of TRGV10 rearrangements in T-cell staining with a γδ TCR antibody compared to bulk $CD3^{+}$ cells suggests that TRGV10 may not be forming a functional γδ TCR in these cells. Failure to generate a functional γδ TCR could then cause these cells to channel into the αβ-TCR development pathway. Formal testing of this hypothesis would require sequencing of the Vγ chains in T-cells sorted with αβ-TCR antibody. I did not undertake such testing so while it seems unlikely that TRGV10 could produce a functional TCR chain this still remains a possibility. TCR-δ rearrangements were almost exclusively TRDV2 recombined with TRDJ1 (**Appendix, Figure 8.6**).

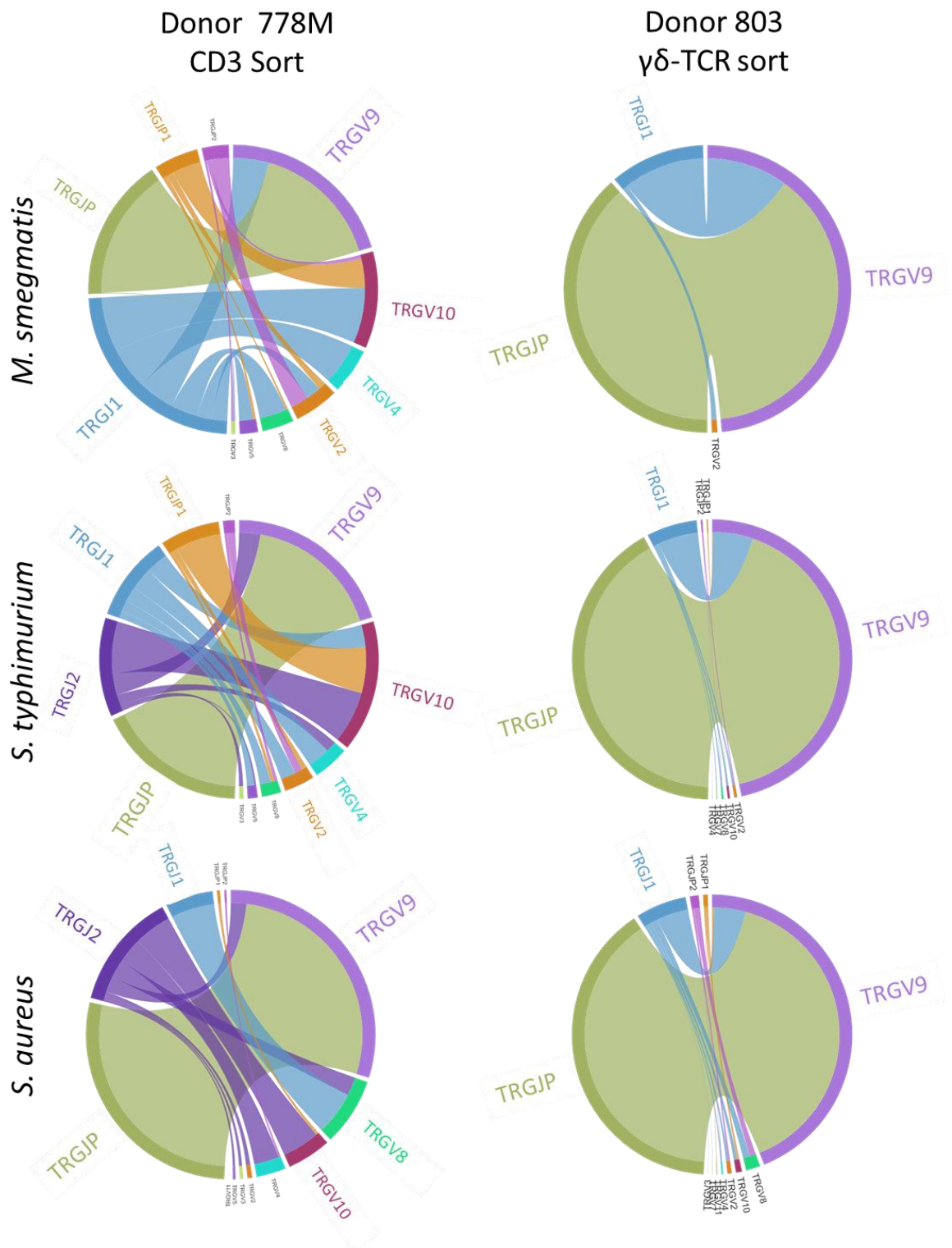

Figure 3.11 - TRGV/TRGJ gene rearrangements differ when sorting on surface expressed γδ-TCR
T-cells were activated in response to bacteria and sorted by flow cytometry either on single cell $CD3^+$ TNF and CD107a expression, or with the same parameters plus TCR-γδ antibody. TCR-γ chains were sequenced and VDJViz used to visualise TRGV/TRGJ gene rearrangements.

3.2.7. Gene enrichments are shared across donors and bacteria

While previous analyses focused on the general T-cell populations in each donor to each bacteria species, I next wanted to identify if there were any commonalities between TCR chains present across samples. I therefore compared all CDR3 sequences in each donor across bacteria (**Figure 3.12a**), using a list comparison tool (http://barc.wi.mit.edu). While the majority of CDR3 sequences from *M. smegmatis, S. typhimurium* and *S. aureus* in individual donors were unique, each donor showed the presence of the same TCRs in at least two bacteria-specific populations in all TCR chains (shared), intimating the presence of a pool of TCRs able to recognise multiple bacteria species. Almost 25% of TCR-γ and TCR-δ showed TCRs present in more than one bacteria-species, whereas TCR-β showed the least amount of shared TCRs (**Figure 3.12a**).

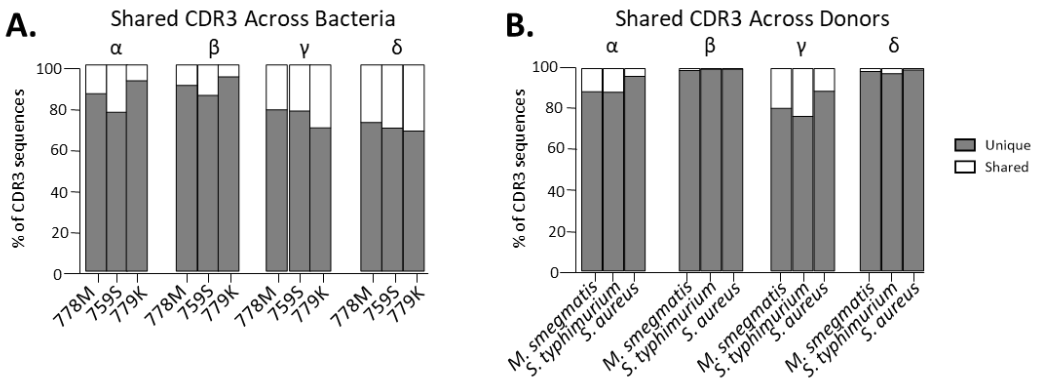

Figure 3.12 - Percentage of shared CDR3 sequences
(**A**). Per donor, percentage of CDR3 sequences present in a bacteria reactive-T-cell pool that are also present in at least one other bacteria-reactive T-cell pool. CDR3 from all four TCR-chains (α, β, γ, and δ) shown. (**B**). Per bacteria, percentage of CDR3 sequences present in a bacteria reactive-T-cell pool from one individual donor that are also present in at least one other donor. CDR3 from all four TCR-chains (α, β, γ, and δ) shown. Public TCRs found in more than one donor.

There was a decreased amount of sharing of TCRs across multiple donors to a specific bacterial species (i.e. interdonor) (**Figure 3.12b**). In contrast to shared cross-bacteria CDR3 sequences (**Figure 3.12a)**, the TCR-β and TCR-δ showed the least amount of sharing, probably

mediated by the inclusion of donor specific P-/N- additions surrounding the D segment, suggesting TCR-β and TCR-δ possess more private TCR chains.

3.2.8. The repertoire of cross bacteria-reactive TCR-α chains is dominated by MAIT cell TCR TRAV1-2 TRAJ33

To determine if CDR3 sequences were present in my cohort that respond to multiple bacteria in multiple individuals, I used VDJViz (Bagaev et al. 2016) to map all shared CDR3 sequences and align them based on frequency within each donor and bacteria. For the α-chain, the vast majority (68.6%) of shared CDR3 sequences across all donors and all bacteria were the canonical MAIT cell TRAV1-2 TRAJ33 rearranged TCR-α chain (**Figure 3.13**). While MAITs form the dominant shared response in this system, there is scope for the identification of other invariant CDR3 sequences. For example, the CAVFSGGYNKLIF CDR3α sequence composed of a TRAV2 TRAJ4 rearrangement is present in donors 778M and 759S responding to *M. smegmatis*, as well as in donor 759S responding to *S. typhimurium* and donor 778M responding to *S. aureus*. TRAV21 rearranged TCRs also are one of the most abundant non-MAIT TCRs across the shared clonotypes, albeit with differing TRAJ genes. In particular, an enriched shared clonotype using a TCR with a CDR3α CAVNDYKLSF (TRAV21/TRAJ20) sequence was shared in *M. smegmatis, S. aureus and S. typhimurium* in two independent donors. This TCR has been previously identified in non-biased (i.e. with no described function) TCR sequencing of 8 donors indicating a novel invariant T-cell population (Kitaura et al. 2016). Therefore, I have identified a potential function for this invariant clonotype in response to infection with multiple bacterial species. Interestingly, this CDR3α shows striking similarity to TRAJ20^{+} MAIT cell CDR3α sequences (e.g. CAVRDNYKLSF, (Lepore, Kalinicenko, et al. 2014; Reantragoon et al. 2013)) and possesses a Tyr95α, important for MAIT cell recognition of MR1 (Reantragoon et al. 2013). Another interesting shared TCR that was

enriched in T-cells responding to *M. smegmatis* and *S. typhimurium,* CAGGNNARLMF (TRAV21/TRAJ31), has previously been shown to respond to CMV and influenza virus (Chen et al. 2017). TRAV2, TRAV13-1, TRAV21 and TRAV8-3 all are enriched non-MAIT shared clonotypes (**Table 3.3**) and therefore may have a role in the non-MAIT antibacterial immune response (**Figure 3.13**).

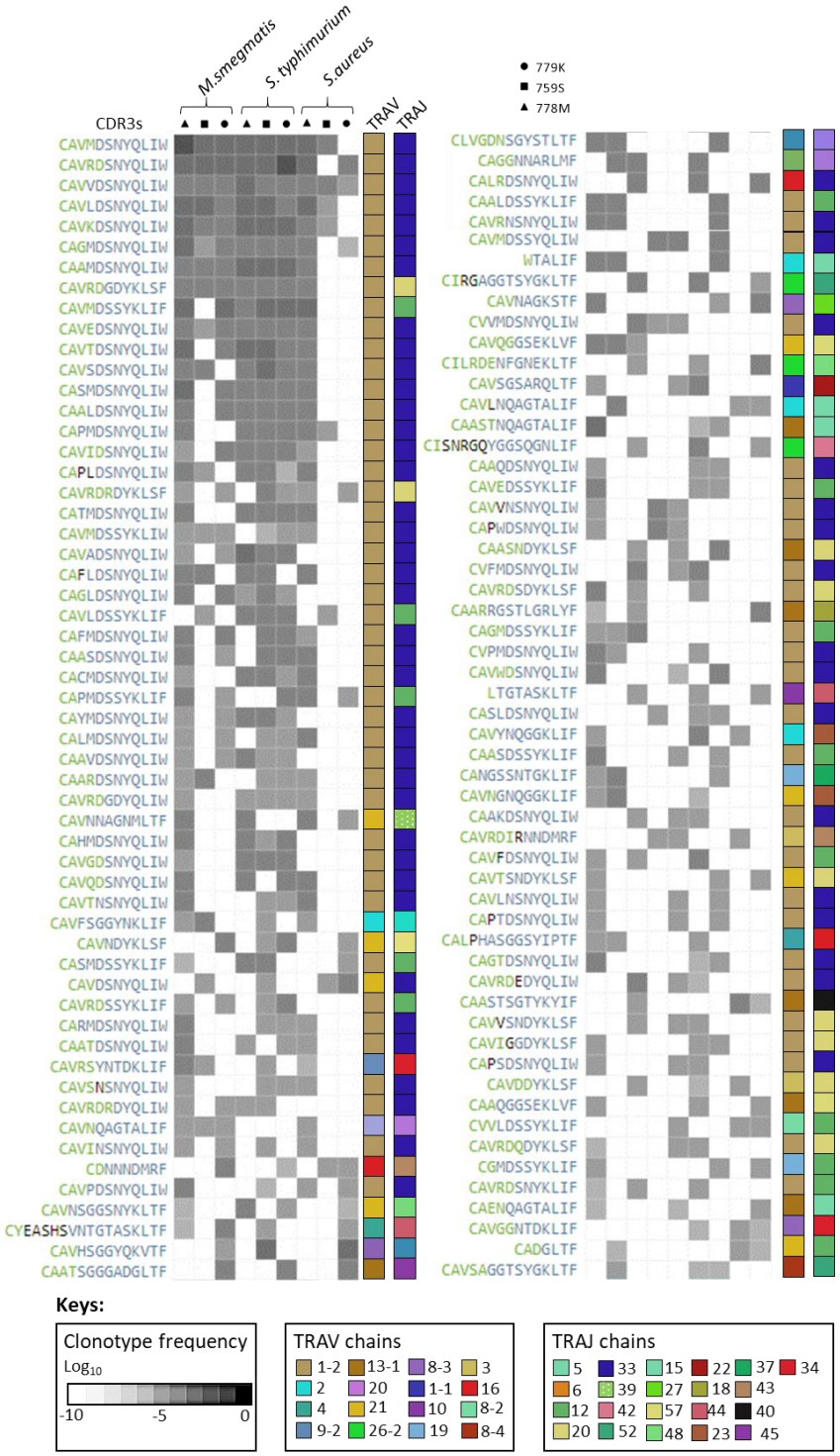

Figure 3.13 - CDR3 and TCR-α gene usage of shared CDR3 sequences between three donors responding to M. smegmatis, S. typhimurium, and S. aureus.

Cells were sorted on TNF and CD107a expression in response to activation with three bacteria. CDR3 sequences were compared across all three bacteria and all three donors to identify public CDR3 sequences. Green text indicates TRAV sequence, blue text indicates TRAJ sequences, with black text indicating non-germline additions. Shade of grey on squares indicates frequency of clonotypes in each sample. Coloured squares indicate TRAV/TRAJ gene usage. CDR3 ordered in hierarchy dependent on average frequency across all samples. Only CDR3 shared in more than 3 samples were included in analysis.

Table 3.3 - Shared non-MAIT CDR3α sequences

	M. smegmatis			*S. typhimurium*			*S. aureus*			
CDR3	*778M*	*759S*	*779K*	*778M*	*759S*	*779K*	*778M*	*759S*	*779K*	**Published**
CAVRSYNTDKLIF **(TRAV41/TRAJ34)**	x	x			x		x			(Thorsson et al. 2018)*
CALRDSNYQLIW **(TRAV16/TRAJ33)**			x			x			x	(Thorsson et al. 2018)
CAGGNNARLMF **(TRAV21/TRAJ31)**		x	x			x				(Chen et al. 2017; Thorsson et al. 2018)
CAVNAGKSTF **(TRAV8-3/TRAJ27)**	x						x		x	(Thorsson et al. 2018)
CAVQGGSEKLVF **(TRAV21/TRAJ57)**	x	x	x							(Thorsson et al. 2018)
CAASNDYKLSF **(TRAV13/TRAJ20)**			x		x		x			(Thorsson et al. 2018)
CAVFSGGYNKLIF **(TRAV2 TRAJ4)**	x	x			x		x			(Kitaura et al. 2016)
CAARDSNYQLIW **(TRAV13-1/TRAJ33)**	x	x			x	x	x			(Thorsson et al. 2018)
CAVNNAGNMLTF **(TRAV21 TRAJ39)**	x			x			x		x	(Thorsson et al. 2018)
CAVNDYKLSF **(TRAV21 TRAJ20)**			x		x	x			x	(Kitaura et al. 2016)
CAVDSNYQLIW **(TRAV21/TRAJ33)**		x			x			x	x	(Thorsson et al. 2018)
CAVNSGGSNYKLTF **(TRAV21/TRAJ53)**	x			x		x			x	(Thorsson et al. 2018)
CAVHSGGYQKVTF **(TRAV8-3/TRAJ13)**			x		x				x	(Thorsson et al. 2018)
CAVSGSARQLTF **(TRAV1-1/TRAJ22)**	x				x	x				(Thorsson et al. 2018; Sims et al. 2016)
CAVLNQAGTALIF **(TRAV2/TRAJ15)**		x						x	x	(Thorsson et al. 2018; Sims et al. 2016)
CAVTSNDYKLSF **(TRAV21/TRAJ20)**	x						x		x	(Thorsson et al. 2018)
CAASTSGTYKYIF **(TRAV13-1 TRAJ40)**			x					x	x	(Thorsson et al. 2018)
CAVDDYKLSF **(TRAV3/TRAJ20)**			x			x		x		(Thorsson et al. 2018; Sims et al. 2016)
CAAQGGSEKLVF **(TRAV13-1/TRAJ57)**	x					x			x	(Sun et al. 2016)
CAENQAGTALIF **(TRAV13-2/TRAJ15)**	x				x				x	(Chen et al. 2017; Thorsson et al. 2018)
CAVSAGGTSYGKLTF **(TRAV8-4/TRAJ52)**		x			x	x				(Thorsson et al. 2018)
CALPHASGGSYIPTF **(TRAV16/TRAJ6)**	x	x				x				-
CAVRDIRNNDMRF **(TRAV3/TRAJ43)**				x	x			x		-
CAATSGGGADGLTF **(TRAV13-1/TRAJ45)**			x			x			x	-
CLVGDNSGYSTLTF **(TRAV4 TRAJ11)**	x	x					x			-
CIRGAGGTSYGKLTF **(TRAV26-2/TRAJ52)**			x			x			x	-
CILRDENFGNEKLTF **(TRAV26-2/TRAJ48)**			x			x			x	-
CAASTNQAGTALIF **(TRAV13-1/TRAJ15)**	x					x	x			-
CISNRGQYGGSQGNLIF **(TRAV26-2/TRAJ42)**			x			x			x	-
CAARRGSTLGRLYF **(TRAV13-1/TRAJ18)**	x		x						x	-
CAVYNQGGKLIF **(TRAV2/TRAJ23)**	x					x		x		-
CANGSSNTGKLIF **(TRAV19/TRAJ37)**	x	x					x			-
CAVNGNQGGKLIF **(TRAV21 TRAJ23)**	x	x				x				-
CVVLDSSYKLIF **(TRAV8-2 TRAJ12)**					x			x	x	-
CGMDSSYKLIF **(TRAV19/TRAJ12)**	x						x		x	-
CAVGGNTDKLIF **(TRAV8-3/TRAJ34)**						x		x	x	-

Previous publications identified through PubMed or VDJdb (Shugay et al. 2018). *(Thorsson et al. 2018) TCR sequences are from tumour infiltrating lymphocytes, but do not describe TRAV/TRAJ usage so CDR3 sequences may be convergently produced by different genes. (Kitaura et al. 2016) CDR3 sequenced PBMCs. (Chen et al. 2017) CDR3 sequences in response to CMV or

influenza virus. (Sun et al. 2016) CDR3 sequences in HIV escape mutants. (Sims et al. 2016) CDR3s in glioma-infiltrating lymphocytes. Green box, frequency >0.01; red box, frequency >0.001; blue box, frequency >0.0001; white box, frequency <0.0001; clear box without x, not detectable in sample.

Unexpectedly, there was only one sample in which the iNKT TCR (CDR3α sequence CVVSDRGSTLGRLYF, TRAV10/TRAJ18) was present (Donor 759S, *S. typhimurium,* <0.0002 frequency, 2 reads) despite this T-cell subset being known to respond to mycobacterial ligands (Sada-Ovalle et al. 2008) and having a role in *Salmonella* and *Staphylococcal* infections (Noto Llana et al. 2017; Hayworth et al. 2012). However, A549 cells do not appear to express CD1d as they cannot induce activation of an iNKT clone when loaded with the prototypical iNKT ligand αGalCer (**Appendix, Figure 8.1**). Additionally, GEM TCRs (CDR3α sequence CAVRNTGGFKTIF, TRAV1-2/TRAJ9) were only present once (Donor 778M, *M. smegmatis*, <0.0001 frequency) despite known antigen specificity to mycobacterial antigens, indicating A549 cells may poorly express CD1b.

3.2.9. TCR-β sequencing shows reduced numbers of public TCRs

There was a reduced degree of TCR-β chain sharing compared to TCR-α across all bacteria and donors (**Figure 3.14**). This is likely due, as previously mentioned, to the added diversity provided by the addition of the P-/N- nucleotides during V(D)J rearrangement, despite almost exclusive use of TRBD2. The majority of the shared TCR-β TRBV chains possessed TRBV20-1 and TRBV6 genes, the most common TRBV genes used in MAIT-cell TCRs. The MAIT TCR-β has previously been shown to be oligoclonal and private, with the TCR-β providing MR1-presented ligand specificity in response to distinct pathogens (Gold et al. 2014). Contrastingly, here I have described public TCR-β chains that are likely associated with MAIT cells that respond to three different bacteria (**Figure 3.14**). The most frequent shared TCR-β clonotype possesses a CDR3β sequence of CASSELAGGPDTQYF (TRBV6-1 TRBD2 TRBJ2-3), shared across multiple bacteria and donors. This particular clonotype has previously been

described as persistent across age, indicating it may be important in the immune response (Britanova et al. 2014).

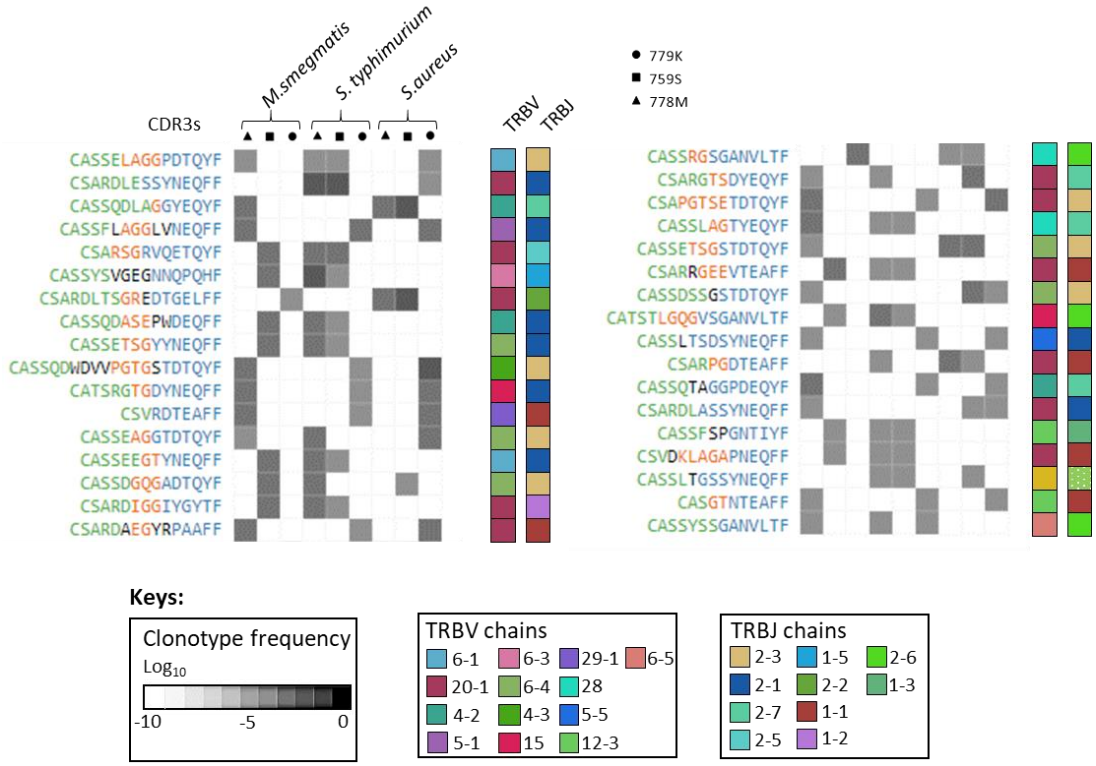

Figure 3.14 - CDR3 and TCR-β gene usage of shared CDR3 sequences between three donors responding to M. smegmatis, S. typhimurium, and S. aureus.
Cells were sorted on TNF and CD107a expression in response to activation with three bacteria. CDR3 sequences were compared across all three bacteria and all three donors to identify shared CDR3 sequences. Green text indicates TRBV sequence, blue text indicates TRBJ sequences, orange text indicates TRDV sequence, with black text indicating non-germline additions. Shade of grey on squares indicates frequency in each sample. Coloured squares indicate TRBV/TRBJ gene usage. TRBD sequence were exclusively TRBD2. CDR3 ordered in hierarchy dependent on average frequency across all samples. Only CDR3 shared in more than 3 samples were included in analysis.

Regarding TCR-β chains that do not possess a MAIT-associated TCR-β, one example shared CDR3β with the CATSRGTGDYNEQFF sequence, previously unpublished, is composed of a TRBV15 TRBD2 TRBJ2-1 TCR and is present in two donors in all three bacteria. This could indicate a cross bacteria-specific public TCR-β that is previously not associated with MAIT cells.

3.2.10. TCR-γ chains are enriched for TRGV9/Vγ9

As γδ T-cells also formed a significant population of bacteria-reactive T-cells, I also investigated the clonotypic architecture of the shared TCR-γδ CDR3 sequences across all donors and bacteria (**Figure 3.15**). 24 out of 52 of the shared CDR3γ sequences were comprised of TRGV9/Vγ9 rearranged with TRGJP, correlating with the fact that the bacteria used in these experiments lead to phosphoantigen-mediated activation of Vγ9Vδ2 T-cells. Indeed, when investigating the CDR3γ sequences by length, 16 amino acid length CDR3 sequences possessed a conserved Vγ9 CALWEXXELGKKIKVF motif. TRGV8 is also shared across samples, with one previously unpublished clonotype with the sequence CATWDLYYKKLF being found across all donors responding to *M. smegmatis* and *S. typhimurium.* The majority of shared TRGV8 CDR3γ sequences appear to have short CDR3 sequences and are not previously published. TRGV8 has previously been associated with CMV infection (Vermijlen et al. 2010), with the public CDR3γ CATWDTTGWFKI also found in the Donor 759S *M. smegmatis* sample. Interestingly, the TCR-γ response to *S. aureus* was much more diverse and private than the TCR-γ CDR3 sequences in response to *M. smegmatis* and *S. typhimurium*, possibly due to the overall T-cell response being dominated by γδ-T-cells (**Figure 3.8**). As seen in **Figure 3.11**, TRGV10/Vγ10 was enriched in shared CDR3γ (**Figure 3.16**); the 4th most frequent shared clonotype (CAAWDYTTGWFKIF) and the majority of the lesser shared clonotypes utilised the TRGV10 segment (**Figure 3.15**). It is interesting that TRGV10 can be found not only rearranged, but also the same clonotype shared across donors and bacteria, meaning the role these rearrangements play may not yet be fully elucidated.

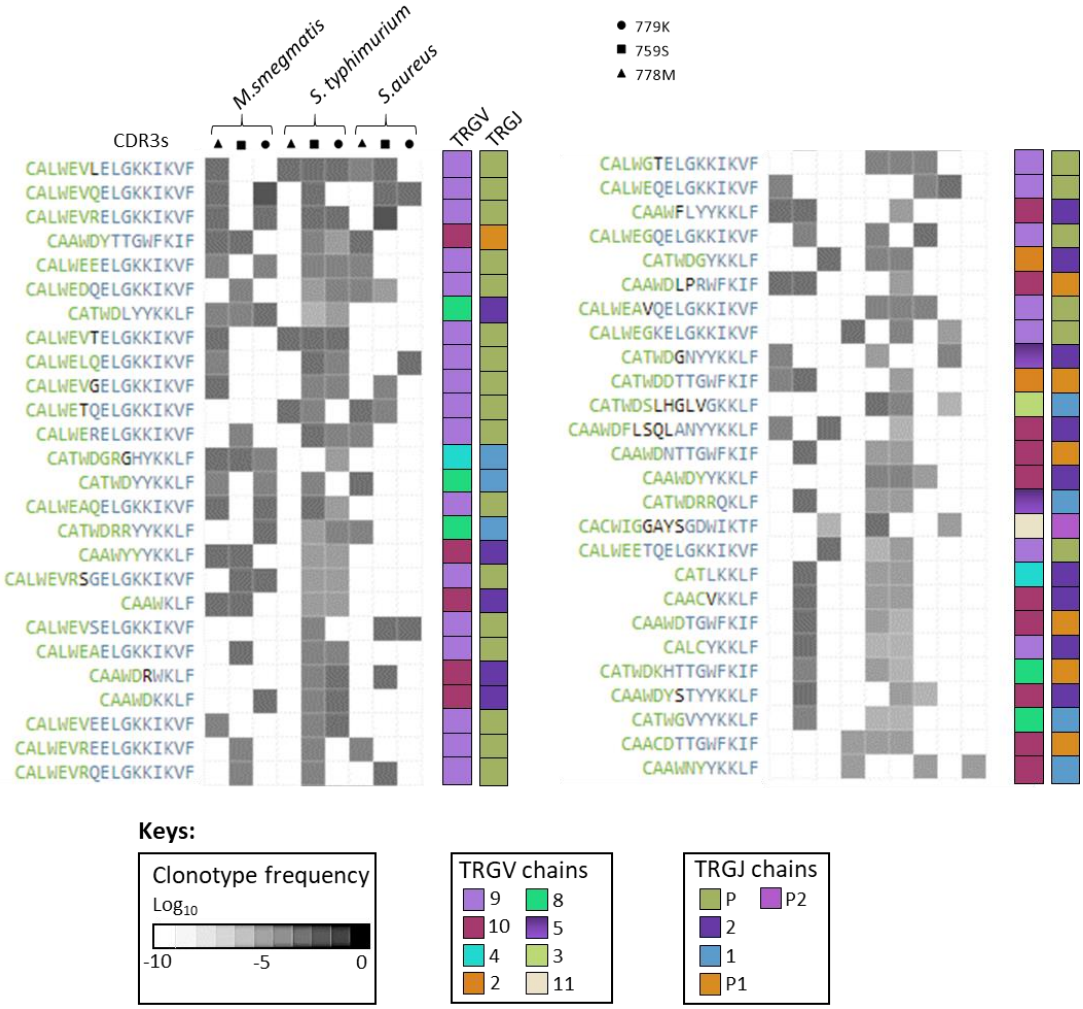

Figure 3.15 - CDR3 and TCR-γ gene usage of shared CDR3 sequences between three donors responding to M. smegmatis, S. typhimurium, and S. aureus.

Cells were sorted on TNF and CD107a expression in response to activation with three bacteria. CDR3 sequences were compared across all three bacteria and all three donors to identify shared CDR3 sequences. Green text indicates TRGV sequence, blue text indicates TRGJ sequences, with black text indicating non-germline additions. Shade of grey on squares indicates frequency in each sample. Coloured squares indicate TRGV/TRGJ gene usage. CDR3 ordered in hierarchy dependent on average frequency across all samples. Only CDR3 shared in more than 3 samples were included in analysis.

3.2.11. Diverse TCR-δ chains consist solely of TRDV2/Vδ2

Similar to the TCR-β chain, the TCR-δ chains showed limited sharing of CDR3 sequences. Despite the use of the TRDV2 being ubiquitous across the shared CDR3δ sequences, both the length and diversity of the CDR3δ sequences was variegated, possibly due to added diversity associated with the inclusion of TRDD genes, despite all CDR3δ sequences using the TRDD3

gene (**Figure 3.16**). The most frequent shared clonotype, CACDTVGGTDKLIF, has been included as part of a recent patent identifying anti-tumour and anti-infective TCR-δ chains (patent application number WO2017212074A1). Interestingly however, shared CDR3δ showed low numbers of P-/N- additions, implying enrichment of public germline-like TCRs that could be important for the hosts' natural immunity.

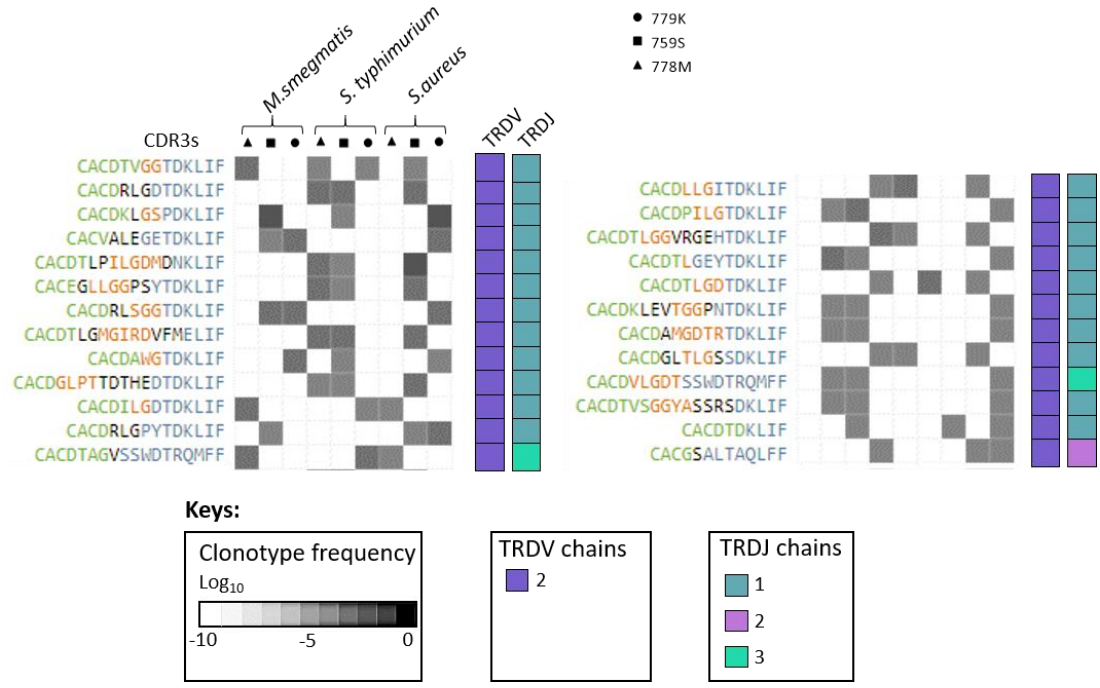

Figure 3.16 - CDR3 and TCR-δ gene usage of shared CDR3 sequences between three donors responding to M. smegmatis, S. typhimurium, and S. aureus.

(**A**). Cells were sorted on TNF and CD107a expression in response to activation with three bacteria. CDR3 sequences were compared across all three bacteria and all three donors to identify shared CDR3 sequences. Green text indicates TRDV sequence, blue text indicates TRDJ sequences, blue text indicates TRDJ sequences, with black text indicating non-germline additions. Shade of grey on squares indicates frequency in each sample. Coloured squares indicate TRDV/TRDJ gene usage. TRDD sequences were exclusively TRDD3. CDR3 ordered in hierarchy dependent on average frequency across all samples. Only CDR3 shared in more than 3 samples were included in analysis.

3.3. Discussion

3.3.1. The burden of bacteria in the modern world

Increasing antibiotic resistance could enable common infections to become killers once again, greatly increasing the risks in many common medical procedures (World Health Organization 2015). Too few antibacterial agents are currently in development to meet the challenge of resistance (World Health Organization 2015) with only two new classes of antibiotics having been discovered since 1987, teixobactin and malacidins (Ling et al. 2015; Hover et al. 2018). Vaccines have already proven useful in the fight against antibiotic resistance; *Haemophilus influenzae*, *Streptococcus pneumoniae*, and *Neisseria meningitidis* showed increasing levels of resistance that have reduced since the adoption of population-wide vaccination schemes (Lipsitch et al. 2016). However, some vaccination strategies have proved problematic with limited efficacy, particularly in the case of pulmonary adult tuberculosis (Pereira et al. 2007) and *S. aureus* (Jansen et al. 2013). A more targeted vaccination strategy, such as those targeting population-wide conserved antibacterial unconventional T-cells may yield more efficacious results.

3.3.2. Unconventional T-cell responses to bacteria

Unconventional T-cells have a well-established role in clearing of bacterial infections. The molecules responsible for the restriction of unconventional αβ T-cells include HLA-E, MR1, CD1a, CD1b, CD1c and CD1d. HLA-E has been shown to present peptides from *M. tuberculosis* (Prezzemolo et al. 2017) and *S. typhi* (Salerno-Goncalves et al. 2004). MR1 presents riboflavin biosynthetic antigens to TRAV1-2 TRAJ33 TCR-expressing MAIT cells during mycobacterial, salmonella and staphylococcal infections (Gold et al. 2010). CD1 molecules are also known to present ligands derived from these three bacteria (Roy et al. 2014; Birkinshaw et al. 2015;

Kronenberg et al. 2013; Hayworth et al. 2012). CD1a is stabilised by exogenous lipid antigens, whereas CD1b, CD1c and CD1d all present bacterial lipids to T-cells. CD1 proteins also present ligands to subsets of γδ T-cells; CD1c presents phosphomycoketides from mycobacterial species, with CD1d presenting phosphatidylglycerol and sulphatide lipids from all three species outlined in this chapter (Macho-Fernandez et al. 2015). Furthermore, the most well documented γδ T-cell ligand implicated in bacterial infection is BTN3A1 with bound phosphoantigens, particularly HMBPP. HMBPP is a metabolite produced by both mycobacterial and salmonella species, whereas staphylococcal species induce accumulation of alternative phosphoantigens such as IPP leading to γδ T-cell activation (Montgomery et al. 2014; Wang et al. 2001; Heuston et al. 2012). The field of unconventional T-cells is constantly expanding as new invariant T-cells are discovered along with new conserved antigens that require further investigation.

3.3.3. Clonotyping reveals enriched TCR genes in bacterial immunity

This work represents a robust method for identifying HLA-independent bacteria-reactive T-cells with the ability to combine both phenotyping and clonotyping. I have demonstrated that frozen aliquots of bacteria-loaded A549 cells prime and activate unconventional T-cells, with function, phenotype and clonotype as readouts across multiple donors. With this system, I identified T-cell subsets that were conserved across donors to specific bacteria, in addition to responding to morphologically distinct species of bacteria. To identify the TCRs used by unconventional T-cells in response to these bacteria, I employed NGS to analyse the clonotypic architecture of these bacteria-reactive T-cells. The most common αβ-TCR clonotypes shared in these responses consisted of TRAV1-2 TCRs likely paired with a limited range of TCR-β chains, forming the well-known MAIT-cell subset, however other invariant T-cells were also identified. In particular, TCR-α chains containing TRAV21 and TRAV13-1 were

enriched across bacteria and donors, with some TCR chains previously being published further evidencing the potential invariant nature of these TCRs across the population. Vγ9Vδ2 cells dominated the shared γδ-TCR repertoire, likely due to the use of peripheral blood as the T-cell source, where these cells are known to be dominant. Initial samples also showed enrichments of TCR-γ chains including TRGV10, previously described as a pseudogene. There may be multiple reasons for enriched gene combinations using TRGV10, such as rearrangements occurring in αβ T-cells where the TCR-γ is non-functional, or it could be an allelic polymorphism that in some people is a genuinely expressed TCR-chain, as with some TCR-β chains (Lefranc et al. 2015). Sequencing of TCR-γ cells from prior sorting on TCR-$\gamma\delta^+$ revealed a reduction in the presence of TRGV10, suggesting rearranged TRGV10 genes are indeed non-functional and potentially lead to αβ-T cell development. However, I did not sequence the αβ T-cell pool for γδ-TCRs to confirm this. TCR-δ chains were exclusively TRDV2 but showed varying lengths of CDR3 loop in the shared repertoire across donors and bacteria, with reduced numbers of P-/N- additions suggesting a more germline-like repertoire in the shared TCR pool.

3.3.4. Further research

The system of bacterial activation of T-cells that I pioneered in this chapter could be applied to a wider range of donors and bacteria. For example, while here I used the model bacteria *M. smegmatis*, it would be more useful to study the pathogen *M. tuberculosis*. However, as *M. tuberculosis* has a biosafety category of 3, culture would require a specialist laboratory set up. Additionally, other intracellular microorganisms could be used such as *Cryptococcus neoformans (C. neoformans)*, one of the most common causes of fungal meningitis in immunocompromised individuals (Rajasingham et al. 2017). The unconventional T-cell repertoire has not previously been investigated in response to *C. neoformans* however one

study showed NKT cell recruitment and activation in *C. neoformans* lung infection (Kawakami et al. 2001).

If expanding donors and bacterial species, it may be prudent to use THP1 cells as opposed to A549 cells or to compare both APC, potentially using CRISPR/Cas9 technology to knock out the HLA-A2 gene to prevent classical immune responses. Indeed, while A549 cells are adherent and therefore more convenient to wash off extracellular bacteria, they do not express CD1d which resulted in a lack of iNKT cell representation in my clonotyping. THP1 cells have previously been shown to express CD1d (Nicol et al. 2000). The dominance of MAITs in the response to all bacteria might mask other important invariant T-cell responses. Removal of MR1 from the APC or gating out TRAV1-2-expressing cells during flow cytometry could be used to exclude MAITs from the analyses. Indeed, I have already helped in the development of MR1 knockouts in both A549 and THP1 cells (Laugel et al. 2016). In the same manner, elucidation of the non-Vγ9Vδ2 bacteria-reactive T-cells could be identified using knockout BTN3A1 in A549 or THP1 cells, thus preventing phosphoantigen-mediated activation of Vγ9Vδ2 T-cells. Alternatively, using T-cells derived from peripheral tissues such as skin or gut as opposed to PBMCs would also enrich for non-Vγ9Vδ2 cells, as well as providing a source of T-cells closer to a source of infection. Furthermore, these T-cells would likely be tissue-resident effector memory T-cells that are already primed and with effector phenotypes. Lymph nodes could also provide an enriched source of both naïve T-cells and central memory cells that could be excluded by only investigating the blood T-cell pool.

TCR NGS provided me with an extensive list of diverse TCRs that are activated in response to bacteria. The output of CDR3 sequences provides information on specific TCR chains that are important in the bacterial response. It is not unlikely that unconventional T-cells possessing public TCRs would be previously published due to their potential ubiquitous nature.

However, publications of sequencing data lack standardisation in CDR3 descriptions, and often CDR3 sequences are included in figures and therefore are not searchable through standard means. Furthermore, there multiple historic nomenclatures for describing TCRs, however the IMGT database (Lefranc et al. 2015) is now becoming the standard (and used in this thesis). A requirement to include all published CDR3 sequences onto a shared database, such as VDJdb (Shugay et al. 2018), or as supplementary materials would aid in analysis of public TCR sequences in future.

While it is useful to study the total TCR repertoire in general, the method used in this chapter does not provide information on the full surface-expressed TCR i.e. the TCR chain pairing. Newer high-throughput single cell sequencing technologies such as Drop-Seq (Macosko et al. 2015) or 10X Genomics Chromium (Zheng et al. 2017) would enable TCR chain pairing. Both of these technologies work in a similar manner, with individual droplets containing an individual cell plus a bead coated with TCR constant region-specific primers, thus acting as small PCR reaction chambers enabling individual barcoding of both TCR chains with the same barcode (Zheng et al. 2016; Zheng et al. 2017; Macosko et al. 2015). The PCR products can then be sequenced on conventional sequencing systems such as the Illumina platform. An alternative much lower throughput method involves single cell cloning of T-cells followed by Sanger sequencing. Each of these methods could be combined with functionality studies such as full cytokine characterisation in addition to identification of bacterial killing capabilities. Chain pairing with a more extensive functional phenotyping panel could provide more detailed information on the T-cell subsets involved in this system of bacteria-induced T-cell responses. Activation markers of IL-2, IL-17A and perforin, along with other markers such as CD161 (MAIT/NKT cells), PD-1 (exhausted/T_{reg} cells), FOX-P3 (T_{reg}), CD45RA (naïve T-cells) and CD45RO (memory T-cells) could help identify the T-cell subsets involved in bacterial infection. Clonal analysis could also enable identification of restricting ligands by whole

genome CRISPR to identify targets of bacteria-specific T-cells. This approach was successfully applied in Chapter 4 to reveal the restricting element of the MC.7.G5 T-cell discovered during my initial CSFE-based analyses in this Chapter.

In summary I have shown identification of bacteria-specific unconventional T-cells can be achieved through combination of phenotyping, functional outputs and clonotyping. These methods can be applied to multiple donors and reveal potentially new invariant T-cells. Invariant T-cells could provide new population-wide vaccination targets to reduce the burden of antibiotic resistance. My studies in this chapter discovered a T-cell clone that recognised A549 cells in the absence of bacterial loading. This recognition was shown to be HLA-agnostic. Studies on the mechanism by which this T-cell clone recognises and destroys a variety of cancer cell lines form the basis of Chapter 4.

Chapter 4. Ubiquitous Cancer Cell Killing Via MR1

4.1 Introduction

As described in **Section 3.2.2**, I grew a T-cell line that responded to A549 cells without the need for bacterial infection. An αβ T-cell clone from this line, designated MC.7.G5, was found to display HLA-independent recognition of the A549 cancer cell line despite HLA-mismatching. This clone, and its TCR, represented a promising candidate for providing broad anti-tumour recognition without the need for a specific HLA. This unexpected finding changed the course of my research project as I set out to understand how the MC.7.G5 T-cell recognised target cells.

4.1.1 T-cell based cancer immunotherapy

Conventional αβ CD8 T-cells recognise short peptides presented by MHC molecules at the cell surface of almost all nucleated cells, allowing $CD8^+$ T-cells to scan the internal proteome for anomalies such as pathogen-derived proteins or dysregulated gene expression associated with cancer cells. The ability of $CD8^+$ T-cells to directly recognise and destroy cancer cells makes them powerful weapons in the fight against cancer, evidenced by the recent success of T-cell checkpoint blockade for some cancers in some patients (Pardoll 2012). These success stories have proved that the immune system can eradicate established cancer and have rekindled strong interest in T-cell-based cancer immunotherapies.

To improve the efficacy of cancer immunotherapies, one avenue of exploration involves adoptively transferring $CD8^+$ T-cells equipped with cancer-specific receptors. This approach

has shown promising success for soluble, B-cell-derived haematological cancers using chimeric antigen receptors (CARs) based on anti-CD19 antibodies in chronic lymphocytic leukaemia (CLL) and acute lymphocytic leukaemia (ALL) (Porter et al. 2011; Grupp et al. 2013). To date however, CARs have shown disappointing results with solid tumours (Mirzaei et al. 2017). Targets for CARs so far have been limited to cell lineage-specific markers; such targets are unsuitable for most peripheral tissues. Genetic engineering with TCRs provides another way to redirect T-cells as TCRs can recognise a far wider range of targets including intracellular antigens (Molloy et al. 2005).

Cancer-specific TCRs that target over-expressed or aberrantly expressed self-proteins can be used to redirect T-cells through gene transfer. T-cells that can recognise self-antigens strongly are culled during negative thymic selection to limit potential for autoimmunity (Xing et al. 2012). This process is presumably responsible for the fact that natural anti-cancer TCRs bind to their cognate antigens weakly (Cole et al. 2007). TCR binding affinity and half-life are critical determinants of the sensitivity and function of cancer-specific T-cells, meaning natural anti-cancer TCRs often fail to recognise the low copy number of peptide epitopes found at the tumour cell surface (Tan et al. 2015; Tan et al. 2017). Various strategies can be used to overcome this deficiency by optimising TCRs (reviewed by (Legut and Sewell 2018). One example showed engineered T-cells with enhanced affinity TCRs can mediate sustained anti-tumour effects in myeloma (Rapoport et al. 2015). Despite this success, the HLA-restriction of conventional TCRs remains a major drawback as any given TCR can only ever be used to treat a minority of patients. Another source of cancer-specific TCRs include those that target neoantigens arising from mutated self-proteins, however again these are still restricted by HLA (Balachandran et al. 2017). An alternative approach would be to use cancer-specific unconventional T-cells that bypass HLA-restriction and potentially recognise cancer cells from any individual. Other advantages to using unconventional T-cells in cancer

immunotherapy include their inherent ability to secrete a rapid burst of cytokines without the need for clonal expansion, their ability to activate multiple arms of the immune system and many unconventional T-cells express tissue-homing markers thereby increasing their potential to target solid cancers in non-lymphoid tissues. Unfortunately, little is known about cancer-specific unconventional T-cells or the mechanism by which they recognise their targets (reviewed in (Godfrey et al. 2018)). Here I took the unexpected opportunity to determine how the MC.7.G5 T-cell recognises cancer targets without responding to healthy cells and without the requirement for a specific HLA.

4.2 Aims

Cancer-specific unconventional T-cells and their targets have the potential to transform cancer immunotherapies. My unexpected discovery of a broadly tumoricidal T-cell clone while I was undertaking studies of bacteria-specific T-cell responses warranted further exploration. The fact that this T-cell recognised a broad range of targets without the requirement for a specific HLA meant that it might recognise a new broadly-expressed non-polymorphic cancer-specific target. In this chapter I aimed to:

- Phenotype the MC.7.G5 T-cell clone and investigate its pan-cancer reactivity
- Identify the molecular target for MC.7.G5 T-cell clone
- Confirm that recognition occurred via the MC.7.G5 TCR

4.3 Results

4.3.1 MC.7.G5 T-cell clone recognises A549 cells in an HLA-independent manner

T-cells that proliferated in response to epithelial lung carcinoma A549 cells independent of bacterial loading were discovered while attempting to characterise T-cell responses to bacteria (**Section 3.2.2**; **Figure 4.1a**), evidenced by dilution of the proliferation marker CFSE. I hypothesised that this population of T-cells might recognise A549 cells independent of classical pMHC-presentation due lack of an HLA match between A549 cells and the donor PBMC. The A549-reactive T-cell line was sorted by flow cytometry gating on $CFSE^{low}$ $CD3^{+}$ $CD4^{neg}$ cells, in order to exclude the high background proliferation of $CD4^{+}$ T-cells in response to the media alone (evidenced in control samples). Subsequently, the sorted population was cloned by limiting dilution and expanded. Only one clone isolated from these cells, designated MC.7.G5, maintained A549 cell reactivity that was not reduced by blocking antibodies to pan-HLA-I and pan-HLA-II, indicating recognition was not allogenic in nature (**Figure 4.1b**). Phenotypic analysis by flow cytometry showed that the MC.7.G5 T-cell clone was $\alpha\beta\text{-TCR}^{+}$ $\gamma\delta\text{-TCR}^{neg}$ $CD8\alpha^{+}$ $CD8\beta^{low}$ $CD4^{neg}$. (**Figure 4.1c**).

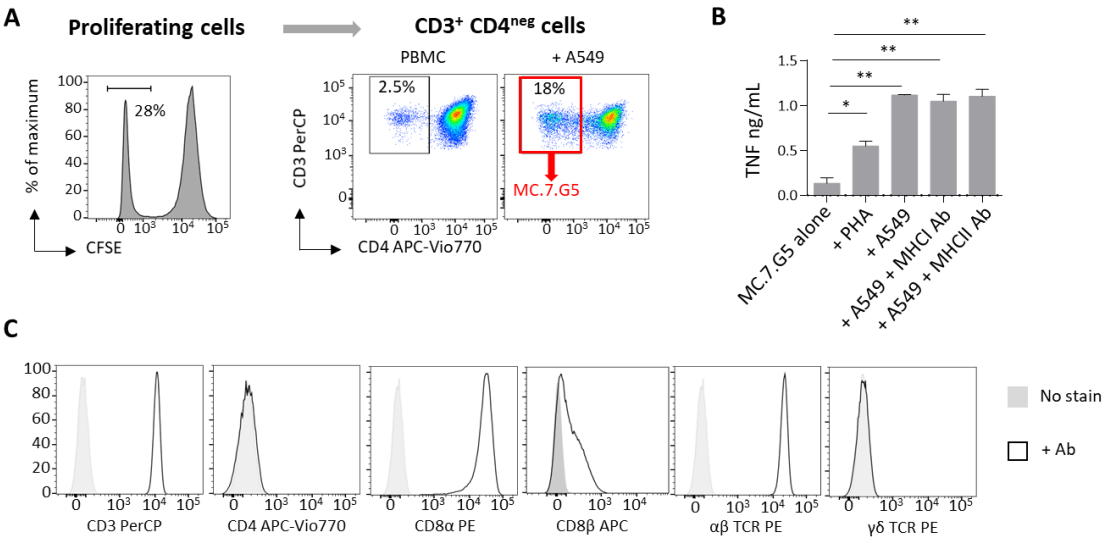

Figure 4.1 - Isolation and characterisation of A549-reactive T-cell clone MC.7.G5
(**A**). T-cells from PBMCs from a healthy donor proliferated in response to A549 cells without bacterial loading. CFSE-labelled PBMCs were primed against HLA-mismatched A549 cells for 14 days, then proliferating ($CFSE^{low}$) $CD3^+$ $CD4^{neg}$ cells (red gate) were sorted by flow cytometry and single cell cloned. Previous gating on alive single $CD3^+$ lymphocytes. (**B**). To exclude allorecognition of A549 cells, a T-cell activation assay in the presence of anti-pan-MHC-I and anti-pan-MHC-II blocking antibodies was performed, with secreted TNF quantified by ELISA. PHA used as a positive control. Standard errors shown, with assay performed in duplicate. Representative of two repeats. (**C**). Flow cytometry-based phenotyping identified MC.7.G5 as αβ-TCR^+ γδ-TCR^{neg} $CD8α^+$ $CD8β^{low}$ $CD4^{neg}$. No stain shown in grey, antibody shown in black line. * $p < 0.02$; ** $p < 0.006$, student's t-test. Representative of two repeats.

4.3.2 MC.7.G5 recognises a broad range of cancer cell lines

MC.7.G5 did not recognise A549 cells through MHC-I or MHC-II, intimating recognition was not via classical MHC. I hypothesised that MC.7.G5 could potentially recognise tumour associated antigens that may be shared across multiple cancer cell lines. Screening by cytokine secretion showed that MC.7.G5 recognised most cancer cell lines tested by MIP-1β and TNF ELISA irrespective of tissue source and HLA-allotype (**Figure 4.2a**), whilst remaining inert to healthy smooth muscle, epithelia, and hepatocyte cell lines (SMC3, CIL-1 and Hep2 respectively) (**Figure 4.2b**). MC.7.G5 also exhibited cytotoxicity against a broad range of cancer cell lines from a variety of tissues at a T-cell to target cell ratio of 1:1 and 5:1 after four hours (**Figure 4.2c**). MC.7.G5 did not appear to show an obvious pattern in its recognition of multiple cancer cell lines and recognition could not be attributed to a specific HLA molecule.

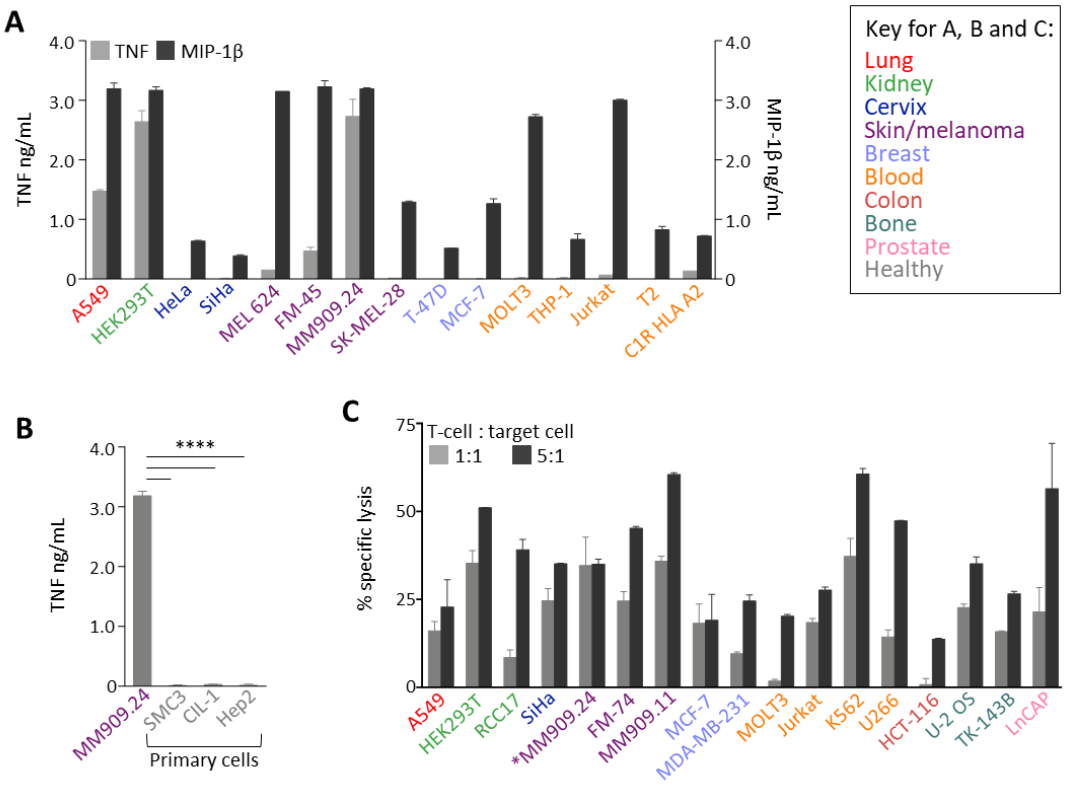

Figure 4.2 - MC.7.G5 has broad cancer cell reactivity

(**A**). MC.7.G5 was cultured with a range of cancer cell lines from various tissue types in an overnight T-cell activation assay. Secreted MIP-1β and TNF were quantified by ELISA. Assay performed in duplicate. (**B**). T-cell activation assay of MC.7.G5 recognition of healthy cell lines: SMC3 (smooth muscle); CIL-1 (ciliated epithelium); and Hep2 (hepatocyte). Melanoma MM909.24 was used as a positive control. Secreted TNF analysed by ELISA. Assay performed in triplicate. (**C**). Chromium release cytotoxicity assay conducted over 4 hours shows MC.7.G5 killing of a range of cancer cell lines. Assay performed at either 1:1 or 5:1 T-cell to target ratio. All assays performed in duplicate with error bars shown. *MM909.24 was incubated at an alternative T-cell: target cell of either 1.5:1 or 6:1. Assay performed in duplicate. **** $p < 0.0001$, student's t-test. All assays were performed once.

4.3.3 Whole genome CRISPR as a tool to discover MC.7.G5 ligands

I next set out to find the non-HLA-restricted ligand that MC.7.G5 was recognising across these unrelated cancer cell lines. For conventional αβ T-cells, HLA-restriction can be determined using blocking HLA blocking antibodies and/or partially HLA-matched cell lines. The peptide recognised in the context of a given HLA can be predicted using combinatorial peptide libraries cross-referenced to protein databases (Wooldridge et al. 2010). This approach is not useful for ligand discovery with unconventional T-cells like MC.7.G5. Existing methodologies for ligand discovery with unconventional T-cells are laborious and expensive. For instance, despite the TRAV1-2 TRAJ33 invariant TCR being discovered in 1993 (Porcelli et al. 1993), it took a decade to identify MR1 as the restricting molecule through elaborate series of murine gene knockouts. For this, the presence of mVα19-Jα33 (murine MAIT TCR) mRNA transcripts was identified in knockouts of TAP/Invariant chain (Ii) -/- mice, Immunoglobulin-μ (IgM) -/- mice, and CD1 -/- mice, but the mVα19-Jα33 transcripts were lacking in β_2M -/- and germ-free mice indicating TCR restriction to a non-classical CD1-like MHC important in bacterial infection, that was found to be MR1 (Tilloy et al. 1999; Treiner et al. 2003). An alternative approach to ligand identification used murine immunisation with target human cancer cells, resulting in antibody generation to cell-surface components (Marlin et al. 2017; Willcox et al. 2012). These antibodies were subsequently screened for their ability to block T-cell recognition and identify potential TCR targets. Here, I applied a different approach that used the new whole genome CRISPR technology in combination with a forward genetic screen. This approach is outlined in (**Figure 4.3**).

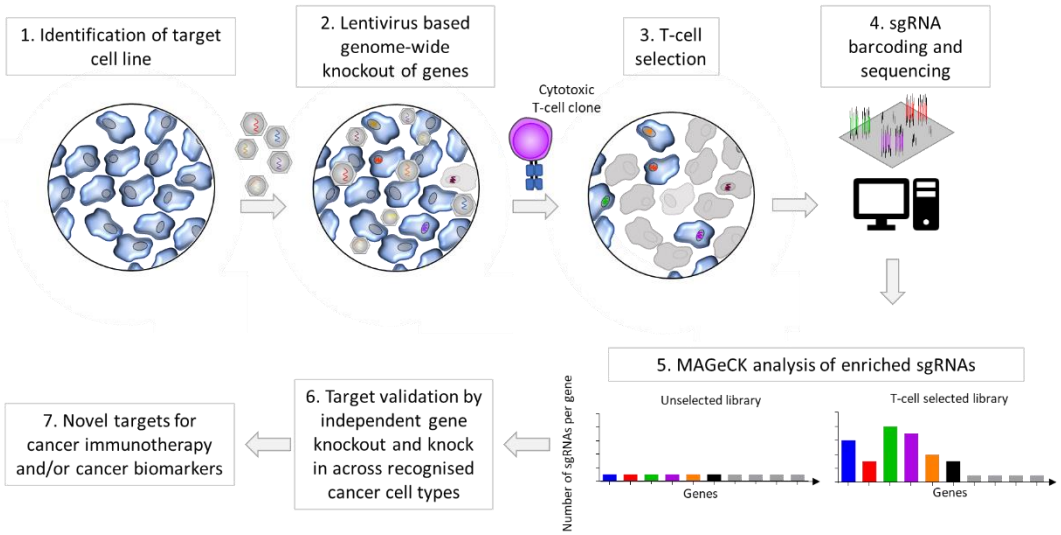

Figure 4.3 - Genome-scale CRISPR-Cas Knockout screening with cytotoxic T-cells
(**1**). Transducable cell line targeted by cytotoxic T-cell identified. (**2**). Target cell line is transduced with lentivirus pool containing single guide (sg)RNAs targeting the whole human genome producing a heterogeneous pool of isogenic cells, each containing a CRISPR-Cas9 mediated knockout of one gene. (**3**). The library of knockout cells is then co-incubated with a T-cell clone to enrich for cells that are resistant to T-cell-mediated lysis over two rounds of selection. Resistance to T-cell lysis can be through knockout of the cognate antigen or a component of the pathway that leads to antigen generation or surface expression. (**4**). The sgRNAs of T-cell-lysis-resistant enriched cell lines and control cell lines are then extracted and barcoded for next-generation sequencing (NGS). (**5**). Enriched sgRNAs are identified by comparison to unselected control library. (**6**). Gene targets are validated through independent gene knockouts using alternative sgRNAs and transgene expression in knockout cells. (**7**). Identified proteins are examined as novel targets for cancer immunotherapy.

Whole genome CRISPR approaches in cancer have led to the discovery of a range of genes involved in drug resistance (Wang et al. 2014; Shalem et al. 2014), proliferation (Hart et al. 2015; Wang et al. 2015) and metastasis (Wang et al. 2015). More recently, and after I initiated my studies, the whole genome CRISPR approach was extended to identify genes that are responsible for antigen recognition by T-cells, linking the loss of genes in cancer cells with resistance to effector $CD8^+$ T-cell function and therefore non-responsiveness to immunotherapies (Patel et al. 2017).

I used genome-scale CRISPR-Cas9 Knock-Out (GeCKO) originally developed by the Feng Zhang laboratory (Shalem et al. 2014) to screen for the MC.7.G5 ligand. The GeCKO library consists of a pool of lentiviruses containing plasmids that each contain a sgRNA targeting the 5' region of exons in one of 19,050 protein-coding genes. There are six sgRNAs per gene split over two

sub-libraries, A and B, with an additional 4 sgRNAs per microRNA only in sub-library A. The library was used to produce a heterogeneous pool of genome edited cells known to act as targets for the MC.7.G5 T-cell, each target cell with a different single gene knockout (**Figure 4.3**). Two rounds of selection by lysis by MC.7.G5 T-cells produced a population of lysis-resistant targets theoretically enriching for cells missing genes that played a prominent role in T-cell-mediated destruction. These genes were identified by sequencing the sgRNAs within the lysis-resistant cancer target lines compared to control cells that did not undergo T-cell selection.

4.3.4 Pilot whole genome CRISPR experiments indicate that tumour recognition by MC.7.G5 requires β2M

I initially tested the GeCKO v.2 library by transducing the melanoma MM909.24 cell line with only Library A. Clones produced after MC.7.G5-based selection were screened against MC.7.G5 showing minimal TNF secretion (**Figure 4.4**). Sequencing of these clones yielded two genes of interest – β_2M (clones 2 and 9) and CORO1b (Coronin actin binding protein 1b; clones 10, 14 and 15). β_2M associates with MHC-I, MHC-Ib and MHC-like molecules indicating that recognition of the cancer cell was might occur via one of these known antigen-presentation platforms. CORO1b on the other hand has no known role in antigen presentation and is associated with regulation of cell migration and actin-binding (Williams et al. 2012). CORO1b has been shown to be mutated in gastric cancer (Zhang et al. 2015). Interestingly, the two clones with β_2M knockout did not stimulate MC.7.G5 to produce MIP-1β or TNF, whereas CORO1b knockout clones stimulated MIP-1β but not TNF secretion by MC.7.G5 (**Figure 4**). It is possible that CORO1b is important in immunological synapse formation (Comrie et al. 2015), which could be tested by assessing activation of a conventional T-cell clone.

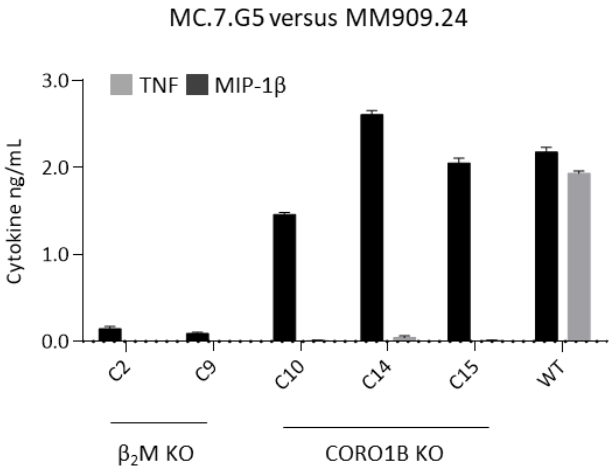

Figure 4.4 – β2M and CORO1b knockout GeCKO clones do not induce TNF recognition by MC.7.G5
GeCKO treated MM909.24 cells were cloned and screened in an overnight T-cell activation assay with MC.7.G5. Secreted MIP-1β and TNF were quantified by ELISA. Assay performed once in duplicate with error bars shown. All data were statistically significant at $p < 0.02$ when comparing knock out clones to WT, except MIP-1β secretion by clone 15 – $p = 0.14$. Two-tailed unpaired Student's t-test.

I next used the full complement of guides (Library A and B) using the same MM909.24 melanoma cell line. The enriched sgRNAs after two rounds of MC.7.G5 selection were sequenced with Illumina MiSeq and are shown in **Table 4.1**, revealing a wider range of genes that were mostly associated with cytoskeleton and membrane associated proteins. This is not unexpected as the cytoskeleton is known to play a role in T-cell recognition of antigen, particularly in forming the immunological synapse (Compeer et al. 2014; Verboogen et al. 2016). Indeed, MHC presentation pathway molecules, adhesion molecules, and JAK/STAT signalling pathways have been all been previously identified as important to T-cell-mediated lysis in whole genome CRISPR screens (Patel et al. 2017).

Table 4.1 - Whole genome CRISPR results from MM909.24

Library	Gene ID	Total Hits	Function
A	DPY19L3	6107	C-mannosylation of Trp
A	JAK1	5240	Tyrosine Kinase
A	HHIP	4251	Hedgehog signalling
A	SLC2A8	1563	Glucose transporter GLUT8
B	MARCKSL1	465	Cytoskeleton regulation, PKC and calmodulin signalling
B	AGAP2	10	Activate nuclear PI3K, mediates anti-apoptotic effects of nerve growth factor
B	CCDC88C	6	Negative regulator of Wnt signalling
B	LCE1A	5	Involved in cornified envelope assembly in the skin
B	MSGN1	5	Transfers N-acetyl galactosamine to serine/threonine
B	BLOC1S5	5	Involved in biogenesis of organelles such as melanosomes
B	GALNT3	3	Part of the mesodermal commitment pathway, chromatin binding and transcriptional activator activity

Genes shown with >2 hits (number of times sequenced). Gene function information from www.genecards.org

4.3.5 A complete whole genome CRISPR screen using 293T targets identified MR1 as required for target recognition by MC.7G5

As no obvious ligand was identified through pilot screening with MM909.24, I next undertook an extensive whole genome CRISPR screening with cancer cell line 293T as the target and increasing sequencing coverage with Illumina HiSeq sequencing. After MC.7.G5 selection (**Figure 4.3**), I confirmed loss of reactivity by T-cell activation quantification of TNF secretion (**Figure 4.5a**). Sequencing of enriched sgRNAs compared to the unselected control sgRNAs identified over 300 individual sgRNAs. To increase stringency, only sgRNAs that were present more than once for a single gene were included, decreasing the chance of a gene being a false positive hit (Shalem et al. 2014). Only six genes were represented by more than one sgRNA; β_2M (five sgRNAs), MR1 (two sgRNAs), signal transducer and activator of transcription 6 (STAT6, two sgRNAs), regulatory factor X (RFX, five sgRNAs), RFX associated ankyrin containing protein (RFXANK, five sgRNAs), and RFX associated protein (RFXAP, three sgRNAs) (**Figure 4.5b**). RFX, RFXANK and RFXAP are essential components of the protein complex responsible for transactivating β_2M, MHC-I and MHC-II (Reith et al. 2005). Combined with the fact that MR1 and β_2M heterodimerise to present antigen to T-cells, this strongly suggested that MC.7.G5 recognised cancer targets via MR1. **Figure 4.5c** shows how the genes identified might be involved in recognition by the MC.7G5 T-cell clone.

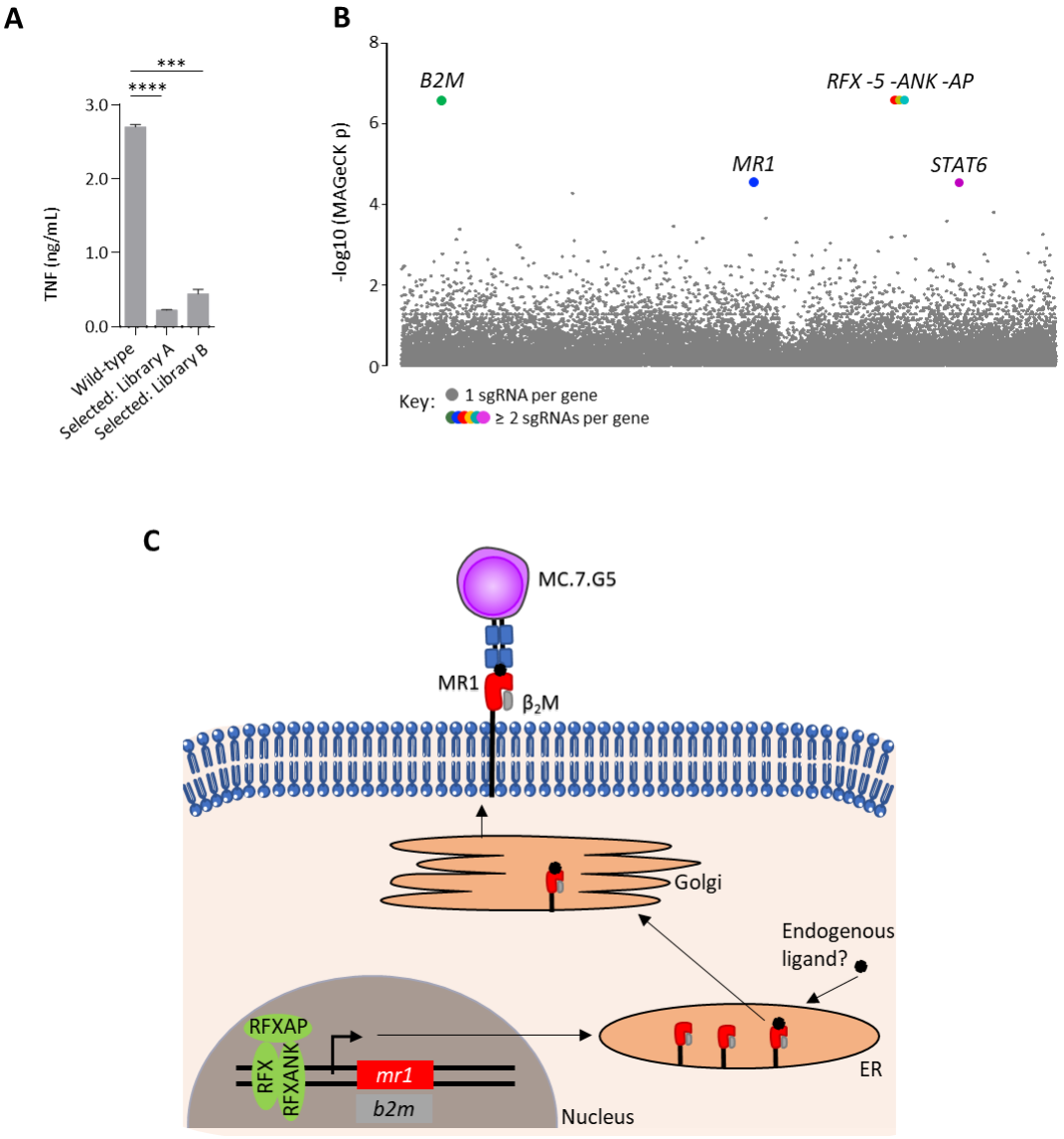

Figure 4.5 - Whole genome CRISPR identifies MR1 as the ligand for MC.7.G5

(**A**). 293T cells treated with whole genome CRISPR library and selected by MC.7.G5. T-cell activation assay performed in duplicate of untreated wildtype 293T compared to GeCKO v2 library A and library B treated. Secreted TNF quantified by ELISA with errors bars shown. Assay performed once in duplicate. **** $p < 0.0001$; *** $p = 0.0005$; two-tailed unpaired t-test. (**B**). MAGeK analysis of deep sequencing of sgRNAs from whole genome CRISPR identifying genes with >2 sgRNAs enriched in selected 293T cells. (**C**). Schematic overview of putative MR1 presentation pathway to MC.7.G5; all nuclear components were identified in whole genome sequencing. ER, endoplasmic reticulum. Sample preparation for sgRNA sequencing was undertaken by a colleague, Mateusz Legut. Colin Farrell and Dr Barbara Szomolay assisted with the bioinformatics and data analysis to create panel B.

4.3.6 Confirmation of MR1 as MC.7.G5 restricting ligand

To validate MR1 restriction of MC.7.G5, I performed an antibody blocking assay that showed anti-MR1 antibody impeded target recognition whereas anti-MHC-I and anti-MHC-II antibodies had no effect (**Figure 4.6a**). I next tested if knocking out the MR1 gene in cancer cells would disrupt recognition using an 'all-in-one' CRISPR/Cas9 MR1 knockout system developed in my laboratory (Laugel et al. 2016). Removal of the MR1 gene from the strongly recognised target MM909.24 abrogated recognition by MC.7.G5 (**Figure 4.6b**). A549 cells also acted as a good target for MC.7.G5, and the corresponding MR1 knockout clone A549 C9 (Laugel et al. 2016) was not recognised (**Figure 4.6b**). Additionally, a chromium release assay showed MR1 knockout MM909.24 and A549 cells were protected from MC.7.G5 mediated lysis (**Figure 4.6b**).

I next examined if introduction of an MR1 transgene into cancer cell lines that were poorly recognised by MC.7.G5 like HeLa and C1R (**Figure 4.2**) could induce recognition. The native MR1 gene was cloned into the 3rd generation lentiviral plasmid pRRLSIN.cPPT.PGK-GFP.WPRE, lentivirus produced and HeLa and C1R cells were transduced with the MR1 transgene. Over-expression of MR1 increased killing of both HeLa and C1R cells in comparison to their wildtype (WT) counterparts. Introduction of the MR1 transgene into MM909.24 also increased MC.7.G5-mediated lysis (**Figure 4.6c**). Transduction of A549 MR1-/- knockout cells (Laugel et al. 2016) with the MR1 lentivirus restored recognition of these targets (**Figure 4.6d**).

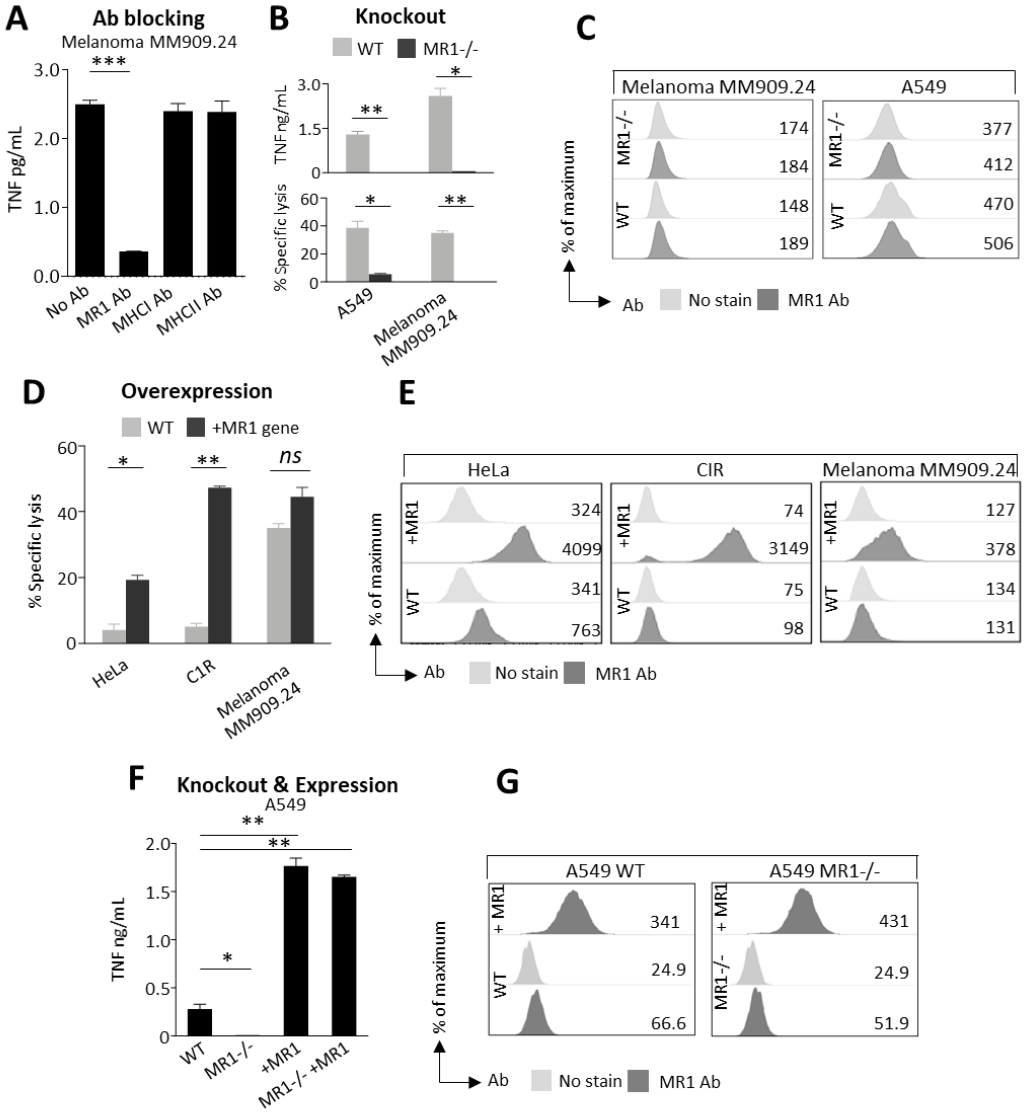

Figure 4.6 - Validation of MR1 recognition by MC.7.G5

(**A**). A T-cell activation assay with MC.7.G5 in the presence of melanoma MM909.24 cell pre-treated with anti-MR1, anti-pan-MHC-I or anti-pan-MHC-II blocking antibodies. TNF secretion quantified by ELISA. ***p = 0.0004, unpaired Student's t-test. Representative of two independent experiments, assay performed in duplicate. (**B**). Melanoma MM909.24 and A549 cells were transduced with a sgRNA to target MR1 resulting in MR1 knockout (-/-) via CRISPR/Cas9. MR1 knockout lines were single cell cloned and screened for induction of MC.7.G5. Overnight activation assay with TNF secretion quantified by ELISA. Chromium release assay performed to show specific lysis for 6 hours (MM909.24) or 18 hours (A549). *p < 0.03; **p < 0.002; Student's unpaired t-test. Representative of two independent experiments, assay performed in duplicate. (**D**). HeLa, C1R and MM909.24 cells were transduced with an MR1 transgene to induce MR1 overexpression. Chromium release assay showing specific lysis induced by MC.7.G5 for 6 hours. Assay performed once in duplicate. *p = 0.0209; **p = 0.0008; Student's t-test. (**F**). Transgene MR1 was transduced into MR1 knockout -/- A549, then screened alongside MR1 -/- A549 and wildtype A549 in an overnight T-cell activation assay with MC.7.G5. TNF secretion quantified by ELISA. (**C**, **E**, & **G**). Surface MR1 expression of cell lines, analysed by flow cytometry. All T-cell activation assays and chromium release assays were performed in duplicate with error bars shown.

4.3.7 MC.7.G5 recognises a ligand presented by MR1

Surface-expressed MR1 has previously been shown to induce a response in T-cells *without* a presented ligand; the K43A mutated form of MR1 disables Schiff-bond formation with MR1 ligand and enables antigen-independent MR1 refolding (Reantragoon et al. 2013). MR1-K43A is however still able to bind ligands that do not require Schiff bond formation such as the MAIT-activating ligand RL-6-Me-7-OH. Refolded MR1-K43A-'empty' tetramers (without added ligand) have been previously shown to bind to T-cells (Gherardin et al. 2016). Therefore, to test if MC.7.G5 simply recognised surface-expressed refolded MR1 independent of bound ligand, I assessed the binding of MR1 tetramers (MR1 monomers provided by Professor Jamie Rossjohn). MC.7.G5 did not stain with MR1-K43A-'empty' tetramer, nor MR1 tetramer loaded with the MAIT-activating ligand 5-OP-RU, whereas a conventional MAIT clone stained only with MR1-5-OP-RU tetramer (**Figure 4.7a**). An HLA-A2 tetramer loaded with ELAGIGILTV peptide was used a negative control which stained the cognate MEL5 Melan-A specific T-cell clone. I next transduced C1R cells with a lentivirus containing MR1 K43A, that when cultured with MC.7.G5 did not induce TNF secretion unlike the native MR1 counterpart (**Figure 4.7b**), despite increased surface MR1 expression. Thus, MC.7.G5 does not recognise a MAIT ligand in MR1 or empty MR1; suggesting that this T-cell clone might recognise a cancer-specific ligand within the MR1 binding groove.

To confirm that MC.7.G5 recognised an MR1-presented ligand I loaded A549 cells with *M. smegmatis,* known to be potent producers of MAIT-activating MR1 ligands (Laugel et al. 2016). The rationale for this experiment was *M. Smegmatis*-derived MAIT-activating MR1 ligands would compete for any cancer-specific ligand within these cells, thereby lowering recognition by MC.7.G5 while increasing recognition by a canonical MAIT cell. *M. Smegmatis* loading of A549 cells resulted in a decrease in TNF secretion and CD107a expression by MC.7.G5 (**Figure 4.7c**) while inducing recognition by a conventional MAIT clone.

Furthermore, the MR1 ligand Ac-6-FP, which does not activate conventional MAIT cells, has previously been used to verify the ligand specificity of MR1-restricted T-cells (Eckle et al. 2014; Lepore et al. 2017). Titration of Ac-6-FP on MM909.24 cells blocked recognition of these cells by MC.7.G5 using CD107a, TNF and IFNγ as functional readouts (**Figure 4.7d**). These data together indicate MC.7.G5 does not simply recognise folded surface MR1, but rather MR1 with bound cargo that is associated with cancer cells.

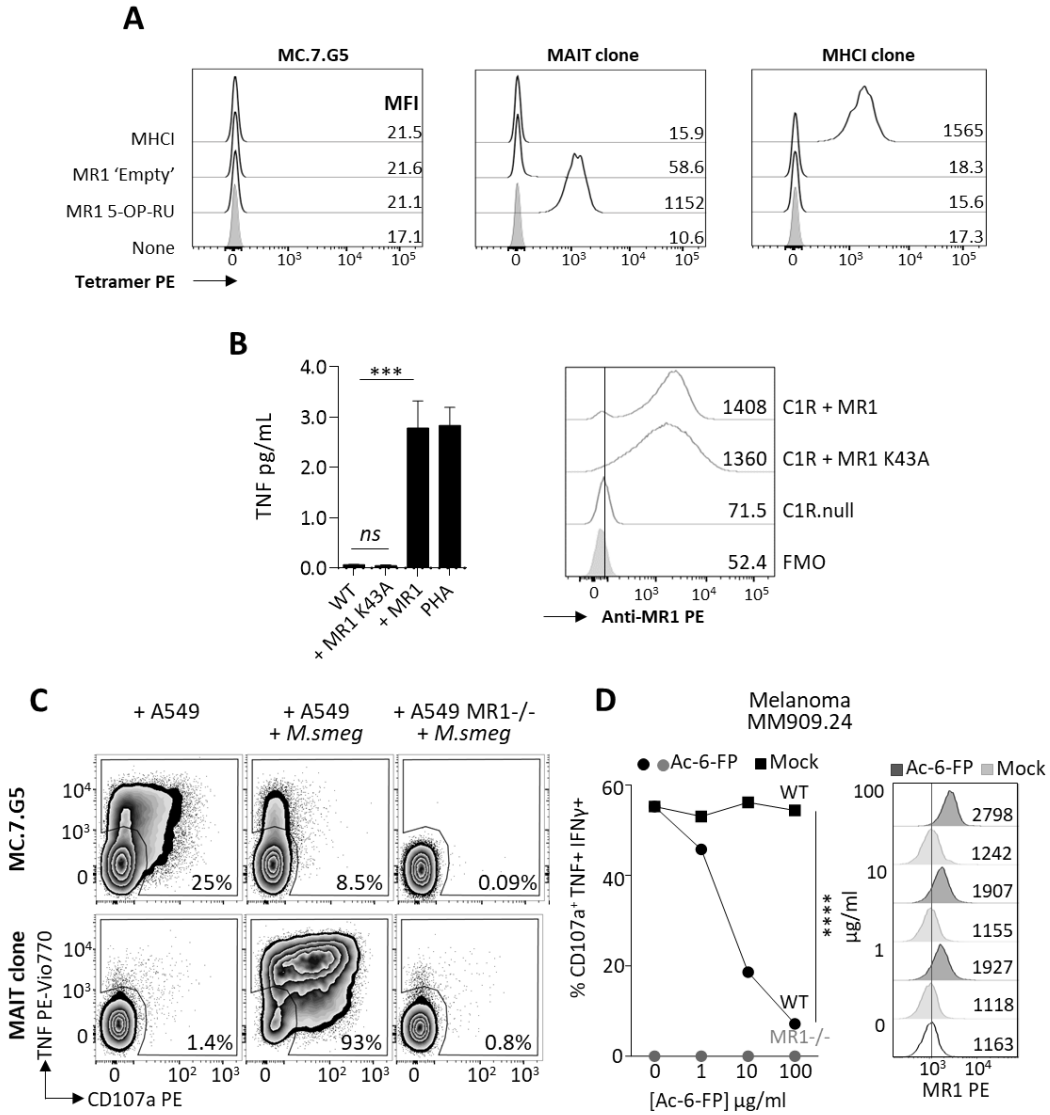

Figure 4.7 - MC.7.G5 is MR1-ligand specific

(**A**). MC.7.G5, a canonical MAIT clone and an HLA-A2 restricted clone (Mel5/13, ELAGIGILTV peptide specific) were stained with the following tetramers; MR1-OP-RU, the canonical MAIT activating ligand; MR1 'Empty', a K43A mutant that refolds without ligand; MHCI, HLA-A2-ELAGIGILTV. The latter was used as an irrelevant tetramer for MC.7.G5 and mucosal-associated invariant T-cell (MAIT) clone. Tetramer stains were boosted using PKI and anti-PE antibody. Representative of two independent experiments. (**B**). Left panel: MC.7.G5 was cultured overnight with wildtype (WT) C1R cells, C1R cells transduced with MR1 K43A, C1R cells transduced with native MR1 or PHA with TNF secretion quantified by ELISA. Assay performed in triplicate. Right panel: C1R cells were stained with anti-MR1 antibody. ***p= 0.001, Student's t-test. (**C**). A549 cells loaded with the canonical MAIT-activating bacterium *Mycobacterium smegmatis (M. smeg)* were cultured with MC.7.G5 for four hours and stained for surface CD107a and intracellular TNF. A549 without bacteria and A549 MR1 knockout loaded with bacteria were used as controls. Previous gating on $CD3^+$ alive lymphocytes. Gates set on clone alone. The canonical MAIT clone was used a positive control. (**D**). Acetyl-6-formylpterin (Ac-6-FP), a known MR1-binidng molecule, was loaded onto MM909.24 overnight before culturing with MC.7.G5 and staining for surface CD107a and intracellular TNF and IFNγ. Mock treated wildtype and MR1 knockout MM909.24 used as controls. Left panel: MC.7.G5 staining for triple positivity ($CD107a^+$ TNF^+ $IFN\gamma^+$) analysed by FlowJo. Error bars shown, smaller than plot symbols. Representative of two independent experiments. Right panel: Surface MR1 expression on Ac-6-FP treated targets cells, plus mock treated. ****p<0.0001, two-way ANOVA. Representative of two independent assays.

4.3.8 MC.7.G5 ligand requires intracellular processing before loading onto MR1

To gain insight into the origin of the MR1 ligand recognised by MC.7.G5, I sought to determine if the stimulatory ligand required intracellular processing or if recognition was dependent on the capture of culture media antigens by cell surface-expressed MR1 as shown previously (Kjer-Nielsen et al. 2012). Brefeldin-A inhibits transport of secreted and surface proteins between the endoplasmic reticulum and the Golgi complex (Misumi et al. 1986). Brefeldin-A can therefore be used to identify if a T-cell recognises newly surface-expressed proteins or if recognition is mediated through ligand exchange by proteins already surface-expressed.

MM909.24 melanoma cells were treated with Brefeldin-A overnight and then cultured with MC.7.G5 resulting in reduced recognition, and when combined with Ac-6-FP treatment, resulted in almost complete blockade of recognition (**Figure 4.8a**). The MM909.24-reactive HLA-A2-restricted Melan-A specific KTB17HI T-cell clone showed reduced recognition after brefeldin-A treatment indicating a similar pathway of presentation of an endogenous antigen (**Figure 4.8a**). These data suggested MC.7.G5 recognises MR1 that requires some form of Golgi processing, implying that the activating ligand is not the result of surface exchange of MR1 antigens found in the media. However, brefeldin-A can also affect the organisation of microtubule and actin cytoskeletons (Alvarez et al. 1999), so the ligand could still be derived from the culture medium but would require internalisation and processing before loading onto MR1. Indeed, this may be the manner in which CORO1b reduces recognition by MC.7.G5 (Föger et al. 2011). Additionally, brefeldin-A may reduce surface expression of MR1, preventing surface ligand exchange which is subsequently recognised by MC.7.G5, however this was not detectable by surface anti-MR1 staining (**Figure 4.8a**). I next hypothesised the ligand presented on MR1 might be soluble, secreted and captured by MR1. To test this, I

cultured C1R cells with supernatant harvested from MM909.24 cells followed by co-culture with MC.7.G5, however this induced no statistically significant change in recognition (**Figure 4.8b**), suggesting the MC.7.G5 ligand may be either be unstable in solution or not secreted by target cells.

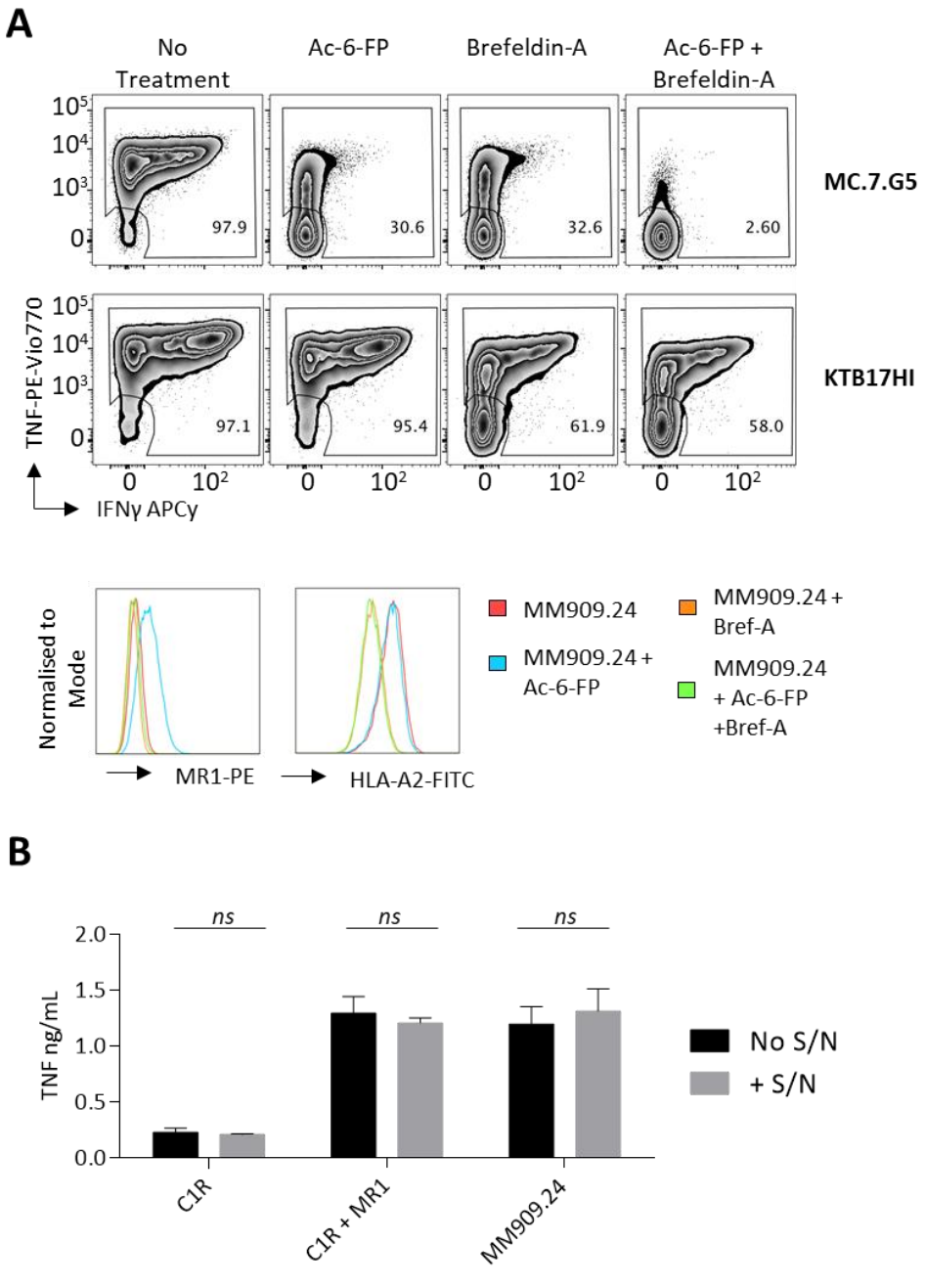

Figure 4.8 – MC.7.G5 ligand requires intracellular loading onto MR1 and is not secreted
(**A**). MM909.24 melanoma cells were treated overnight with Brefeldin-A, acetyl-6-formylpterin (Ac-6-FP) or both, before culturing with MC.7.G5 for four hours followed by intracellular cytokine staining (TNF and IFNγ). No treatment included as positive control. KTB17HI is HLA-A2 Melan-A specific T-cell clone. Surface MR1 and HLA-A2 antibody staining analysed by flow cytometry. (**C**). Supernatant from MM909.24 melanoma cells was harvested and added to C1R cells (wildtype, MR1 knockout and MR1 overexpressing) for four hours. Without washing, MC.7.G5 cells were added in an overnight activation assay, with secreted TNF quantified by ELISA. Assay performed in triplicate with error bars shown. S/N, supernatant. Student's t-test, ns – not significant. All assays were performed once.

4.3.9 MC.7.G5 cancer cell recognition is through the TCR

As MC.7.G5 recognised a wide range of tumours, there was a possibility that recognition could be through an innate-like receptor as opposed to the TCR as in the case of γδ T-cells expressing NKG2D (**Section 1.5**). Indeed, αβ T-cells are known to express NKG2D receptors and other lymphoid stress receptors (Groh et al. 2001; Wensveen et al. 2018). I therefore sought to identify if recognition of tumours occurred via the MC.7.G5 αβ-TCR by transferring the TCR to other T-cells. Sequencing of the MC.7.G5 TCR revealed a non-MAIT TCR comprised of TCR-α TRAV38.2/DV8 TRAJ31 with a CDR3α sequence of CAYRSAVNARLMF, paired with TCR-β TRBV25.1 TRBJ2.3 possessing the CDR3β sequence CASSEARGLAEFTDTQYF (**Figure 4.9**). This represents a completely novel MR1-reactive TCR, however interestingly encodes a Tyr94α - a single position shift from the Tyr95α required in canonical MAIT TCRs (Reantragoon et al. 2012).

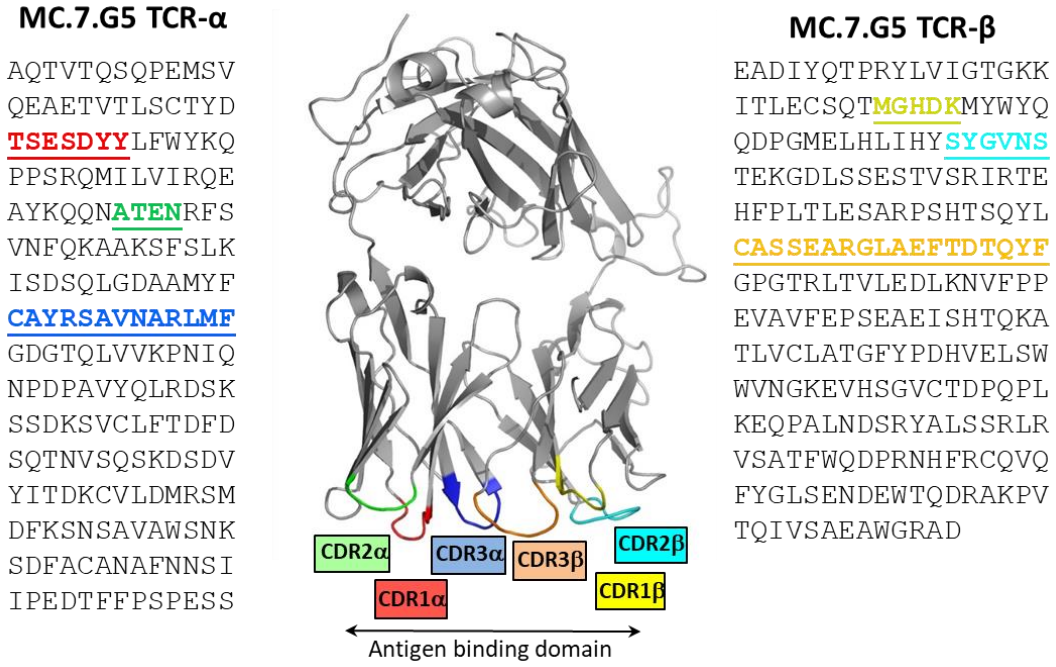

Figure 4.9 - Sequence and model of structural outline of MC.7.G5 TCR
Sequencing of MC.7.G5 TCR was performed in collaboration with Dr Meriem Attaf. TCR-α chain TRAV38.2/DV8 TRAJ31, TCR-β chain TRBV25.1 TRBJ2.3. Complementarity determining regions (CDR) underlined in bold coloured text. Example of a TCR crystal structure shown to indicate how these protein chains are thought to combine and fold to create the antigen binding domain.

I next cloned the TCR into the pELNS lentiviral vector which includes the transduction marker rat CD2 (rCD2), produced whole lentivirus particles and transduced the MC.7.G5 TCR into $CD4^+$ and $CD8^+$ T-cells from two melanoma cancer patients, MM909.11 and MM909.24 (**Figure 4.10**). $rCD2^+$ transduced T-cells were then screened against autologous and non-autologous melanoma cell lines which confirmed TCR-mediated recognition of cancer lines compared to untransduced T-cells (**Figure 4.10a**). Indeed, transduced T-cells from patient MM909.11 showed increased killing compared to untransduced T-cells against wild type cancer lines, but not to MR1 knockout non-autologous MM909.24 cancer cell line (**Figure 4.10b**). Importantly, MC.7.G5 TCR transduced T-cells did not kill healthy cells (**Figure 4.10b**).

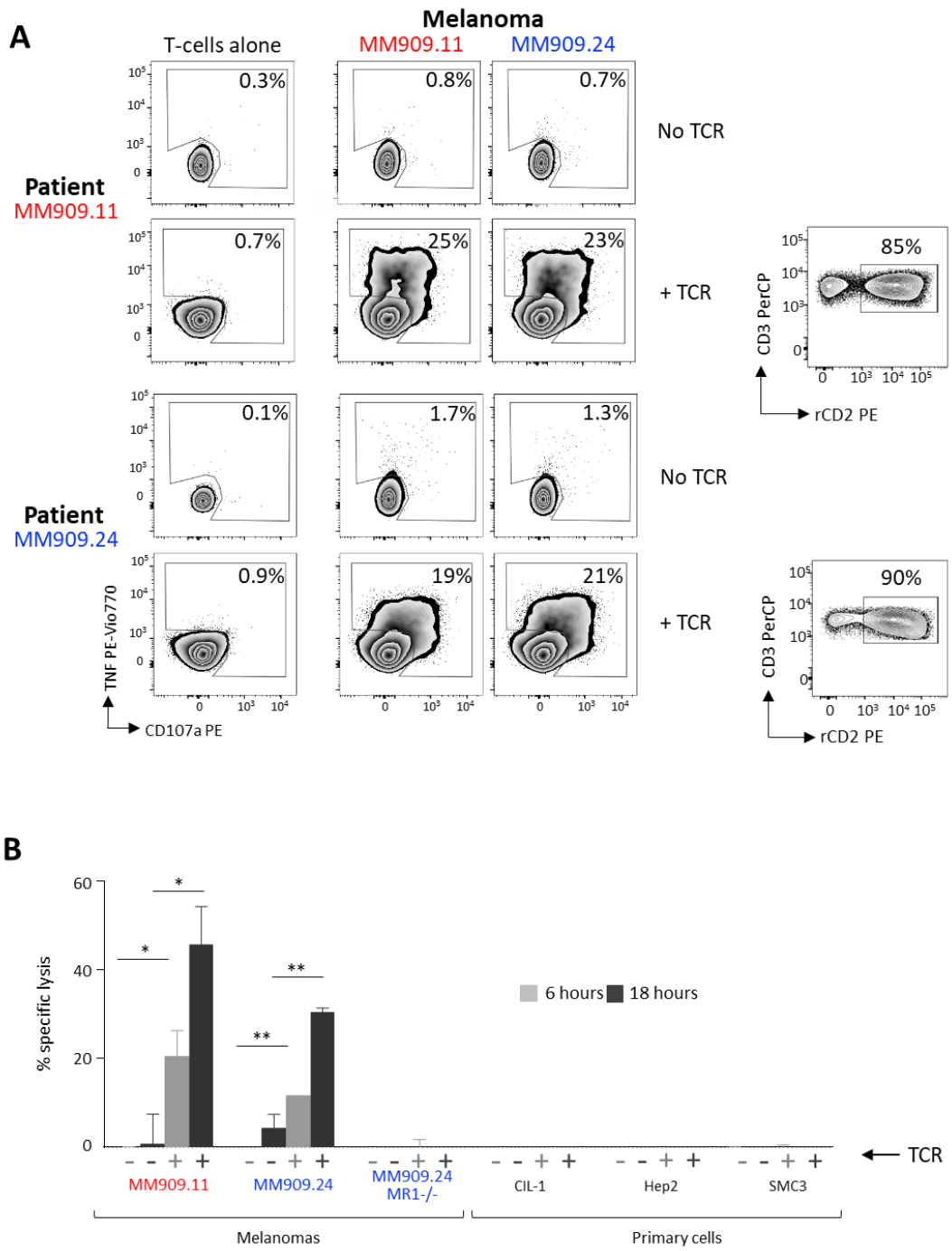

Figure 4.10 - Transfer of MC.7.G5 T-cell receptor redirects T-cells to kill autologous melanoma
(**A**). Melanoma patient (MM909.11 and MM909.24) derived T-cells transduced with the MC.7.G5 T-cell receptor (TCR) and cultured with autologous melanoma for 4 hours followed by staining surface CD107a and intracellular TNF. Rat CD2 (rCD2) expression indicates level of transduction of MC.7.G5 lentivirus. Non-transduced T-cells were included as negative control. (**B**). Chromium release cytotoxicity assay with non-transduced T-cells (-) and T-cells transduced with MC.7.G5 TCR (+) from patient MM909.11 versus autologous melanoma, melanoma from patient MM909.24 (wildtype and MR1 knockout -/-) and healthy cell lines CIL-1, Hep2 and SMC3 (ciliated epithelial, hepatocyte and smooth muscle, respectively). Performed at T-cell to target ratio of 5:1 for 6 hours and 18 hours in duplicate. *p<0.04, **p<0.008, Student's t-test. All assays were performed once.

4.4 Discussion

4.4.1 The challenges of T-cell/TCR-based cancer immunotherapies

A major challenge of current cancer immunotherapies is producing broad, safe and efficacious treatments. While personalised therapies such as adoptive tumour infiltrating lymphocyte (TIL) therapy have proven effective (Rosenberg et al. 2011), they are extremely costly and time-consuming with limited scalability. Previous examples of ubiquitous cancer-targeting immunotherapies include chimeric antigen receptor (CAR) T-cells, involving the transduction of a CAR with an antibody-like moiety to bind to surface receptors such as CD19 on B-cell malignancies resulting in tumour clearance (reviewed in (Tran et al. 2017)). However, there is evidence of harmful autoreactive side effects to such therapies (Linette et al. 2013).

4.4.2 The potential advantages of unconventional T-cell/TCR based cancer immunotherapies

HLA-independent recognition of cancer cells by unconventional T-cells is an attractive alternative approach for producing immunotherapies as these can recognise a broad range of cancer types in any individual without the need for HLA-matching. Additionally, unconventional T-cells are less susceptible to cancer evasion through changes in classical HLA antigen processing and presentation. Unfortunately, the ligands recognised by the majority of unconventional T-cells remain largely unknown; with regards to γδ T-cells, the cancer antigens so far described include the human phosphoantigen IPP bound to BTN3A1 (Gober et al. 2003), lipids bound by CD1 (Roy et al. 2016), overexpressed MICA/B and EPCR (Qi et al. 2003; Willcox et al. 2012). γδ T-cells have also been shown to directly recognise ectopically

expressed proteins such as Annexin A2 and MSH2 (Marlin et al. 2017; Dai et al. 2012). The known unconventional αβ T-cells so far described that may have a potential role in the immune response to cancer include NKT (Heczey et al. 2015), CD1-a -b and -c restricted (reviewed in (Godfrey et al. 2015)), and HLA-E restricted (Joosten et al. 2010) T-cells.

4.4.3 MR1 in cancer

With regards to T-cell responses to MR1 in cancers, infiltrations of MAIT cells have been reported in cancers with varying clinical outcomes (Peterfalvi et al. 2008; Sundström et al. 2015; Zabijak et al. 2015). MAIT cells were first identified in tumours by TCR transcript analysis of brain and renal tumours (Peterfalvi et al. 2008) where they correlated with the presence of pro-inflammatory cytokines. MAIT cell infiltrations have also been found in colorectal cancer where they possessed cell-cycle arrest functionality (Ling et al. 2016; Sundström et al. 2015; Won et al. 2016). Additionally, a recent study showed pulsing of multiple myeloma cell lines with vitamin-B derivatives enables MR1-dependent recognition by conventional MAIT cells, resulting in tumour lysis (Gherardin, Loh, et al. 2018). Indeed, a more direct role of MR1-restricted T-cells expressing non-canonical MAIT TCRs (TRAV1-2 TRAJ33^{neg}) has been observed, where they were able to directly recognise non-microbial antigens via MR1 (Lepore et al. 2017). These MR1-restricted T-cells were stimulated to produce a range of cytokines including IFNγ demonstrating the family of MR1-restricted T-cells extends beyond TRAV1-2 TRAJ33 expressing canonical MAITs. Initial experiments showed no surface expression of MR1 but ubiquitous mRNA expression (Hashimoto et al. 1995; Riegert et al. 1998), however a more recent study showed minimal amounts of MR1 could be found on the surface of cells even when cultured with Ac-6-FP-free culture media (McWilliam et al. 2016). Furthermore, surface exchanged ligand with 5-OP-RU indicated the MR1 ligand was non-covalently bound. The commercially available anti-MR1 antibody is

unable to detect this minimal surface expression, however newer anti-MR1 antibodies such as 8F2.F9 appear to show more robust MR1 staining (Chua et al. 2011), which could potentially identify MR1 expression on the surface of cancer cells.

4.4.4 Cancer-specific T-cell clone MC.7.G5 is MR1-restricted

Here, I identified a T-cell designated MC.7.G5 that induced targeted lysis in addition to cytokine secretion in response to a broad range of cancer cell lines with differing HLA types. This enabled the adoption of a whole genome CRISPR approach to identify the cancer cell-expressed restricting ligand required to facilitate MC.7.G5 recognition. My initial pilot studies suggested that β_2M was required for recognition by the MC.7.G5 T-cell. A full screen using the 293T cell line confirmed that β_2M knockout cells were enriched after two rounds of T-cell killing in addition to cells lacking MR1 and transcription factors thought to be required for expression of MHC encoded genes (**Figure 4.5**). Subsequent antibody blocking and CRISPR knockout experiments confirmed that MR1 was the target for the MC.7.G5 TCR. Staining with MR1 tetramers and MR1 K43A cellular expression showed that the MC.7.G5 TCR did not bind MR1 presenting known ligands or a mutated empty version of MR1, suggesting MC.7.G5 possessed ligand discrimination in the context of MR1. This hypothesis was supported by experiments using *M. smegmatis*-loaded cells, or addition of the MR1 ligand Ac-6-FP, that inhibited the recognition of tumour cells by MC.7.G5 (**Figure 4.7**). I therefore conclude that MC.7.G5 recognises a cancer-specific or cancer-upregulated ligand in the context of MR1. The exact nature of this ligand remains unknown.

4.4.5 Determining the nature of the MR1-presented MC.7.G5 ligand

Known MR1 ligands include 6-FP, 5-OP-RU and RL-6-Me-7-OH plus a limited range of other small molecules that occupy very little space within the MR1 binding groove (**Figure 4.11**). Consequently, there is potential for MR1 to bind and present much larger ligands than those currently identified. The majority of MR1 ligands are metabolic intermediates so it is feasible that MR1 could present elements of the cancer metabolome at the cell surface. The whole genome CRISPR screen with 293T targets proved to be a powerful means of identifying genes involved in target recognition by MC.7.G5. Despite this success, this screen did not reveal any hits within metabolic pathways or enzymes that were essential for production of the MC.7.G5 MR1-presented ligand. The reason for this may be that my screening was incomplete, but it could also signify that the pathway that produces the MC.7.G5 MR1-presented ligand is essential for cell survival but is upregulated in cancers. If this pathway is essential for cell survival, the possibility of finding clues about the ligand from a forward genetic screen like the one I performed here would not be possible.

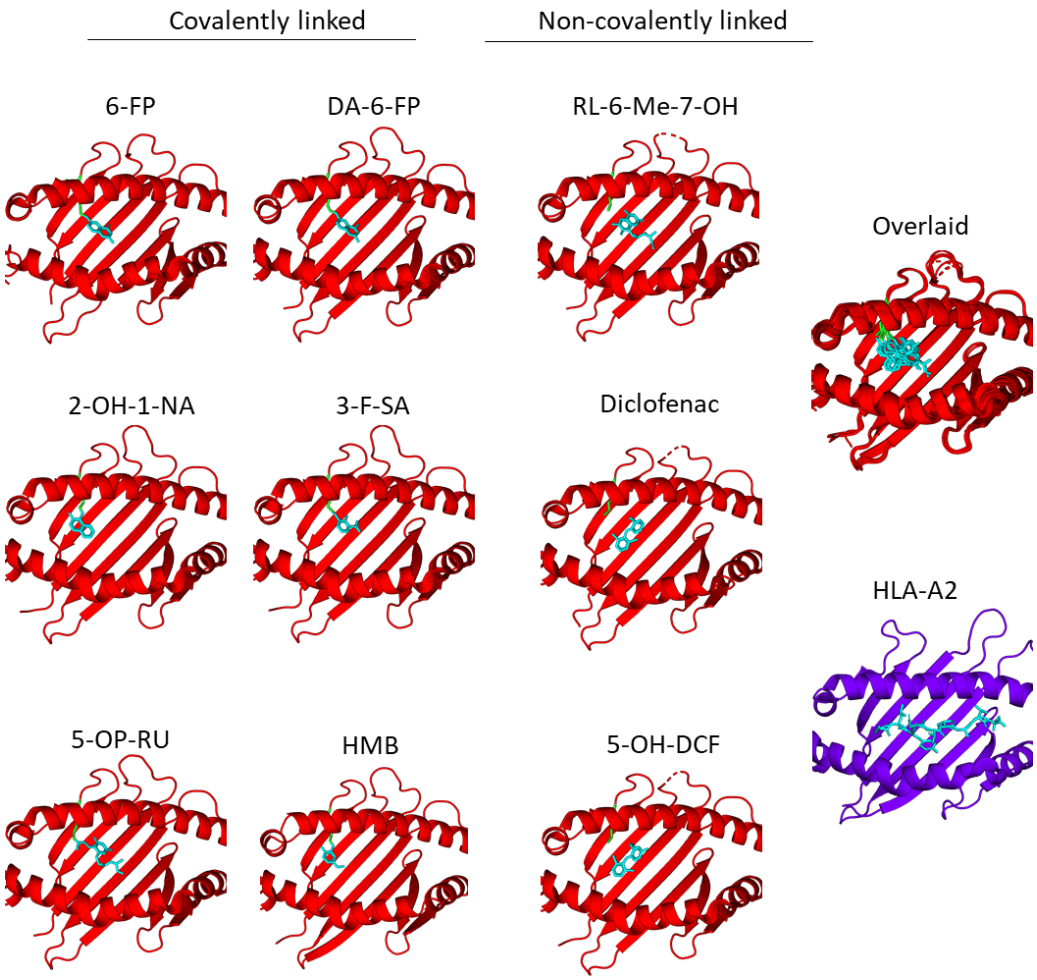

Figure 4.11 - Structure of MR1 antigen-binding groove with various ligands
MR1 structures with different ligands bound either covalent or non-covalently to MR1. MR1 molecule in red, amino acid MR1-K43 highlighted in green (essential for forming Schiff base with ligands), ligand in cyan. PDB codes: 6-formylpterin (6-FP), 4GUP; 2,4-diamino-6-formylpteridine (DA-6-FP), 5U17; 7-hydroxy-6-methyl-8-D-ribityllumazine (RL-6-Me-7-OH), 4L4V; 2-hydroxynaphthaldehyde (2-OH-NA), 5U16; 3-formylsalicylic acid (3-F-SA), 5U6Q; Diclofenac, 5U1R; 5-(2-oxopropylideneamino)-6-D-ribitylaminouracil (5-OP-RU), 5D5M; 2-hydroxy-5-methoxybenzaldehyde (HMB), 5U2V; 5-hydroxydiclofenac (5-OH-DCF), 5U72; HLA-A2, 5NMH.

Further experiments to attempt to identify the MC.7.G5 ligand bound to MR1 could consist of *in silico* rational design of compounds that fit into the MR1 antigen binding groove using kinetics elucidated from previously identified ligands, as previously performed in (Andrew N Keller et al. 2017). In this study, predicted drug-like small molecules that would be able to form a Schiff-base with the K43 residue of MR1 were found to bind to MR1 and competitively inhibit activation of MAIT cells. Indeed, it appears that the MC.7.G5 MR1-presented ligand requires Schiff-bond formation to result in activation (**Figure 4.7b**). Expanding the *in silico*

rational design to include small metabolic intermediates that can form a Schiff bond overexpressed in cancers could be viable approach. Alternatively, literature searching of small pterin-containing molecules, like 6-FP, overexpressed in cancers followed by *in vitro* screening could also yield results. A related technique would involve blocking or activation of pathways that produce molecules chemically related to known MR1 antigens that could affect the nature of antigens loaded onto MR1. One approach I am actively seeking is isolating MR1 from MM909.24 cells (which have high expression of the MC.7.G5 agonist) and elute the ligand from the MR1 antigen binding groove that can then be identified with mass spectrometry. This method was used to identify the MR1 ligand 6-FP in addition to CD1 lipid antigens (Kjer-Nielsen et al. 2012; Birkinshaw et al. 2015). Indeed, I have already supplied Professor Jamie Rossjohn with melanoma MM909.24 in the hopes he can successfully elute the MR1 ligand recognised by MC.7.G5.

4.4.6 Applications for cancer immunotherapy

The work presented in this chapter incorporates several highly original findings. It represents the first example of using whole genome CRISPR to identify unconventional T-cell ligands, as well as the first study to indicate that cancer cells might present a different MR1-bound cargo than healthy cells that can result in targeted killing by T-cells. MC.7.G5 also killed cancer cells expressing surface levels of MR1 that were undetectable using the commercially available antibody suggesting that T-cell recognition requires a very low copy number of ligand per target cell. The future applications of this discovery could revolutionise cancer immunotherapy and diagnostics. Indeed, MR1 antigens are an attractive target for characterisation – the hydrophobic antigen binding groove can facilitate larger molecules than those currently defined, and as shown here, these new antigens appear to be cancer specific. Vaccination with novel MR1 antigens, such as the one recognised by MC.7.G5, either

directly or through dendritic cell loading could provide a new avenue of therapeutic cancer vaccination. One possible therapy could be adopted from a recent clinical trial showing concomitant loading of NY-ESO-1 peptide antigen with the NKT ligand α-GalCer onto dendritic cells before reinfusing back into the patient, resulting in priming of independent cancer-specific T-cell subsets that were able to activate a greater immune response to autologous cancer targets (Gasser et al. 2017). Another possible therapy includes T-cell engineering using the TCR gene replacement system developed by my laboratory (Legut, Dolton, et al. 2018) involving CRISPR/Cas9-mediated knockout of an endogenous TCR while simultaneously transducing an antigen-specific TCR. In the context of MC.7.G5, the 'TCR replacement' approach could be used as a method to induce recognition of autologous cancer, whilst overcoming the issues associated with other T-cell based gene therapies, such as the limited efficacy of CAR T-cells in solid tumours and the HLA-restriction associated with conventional TCRs that when affinity enhanced have, in some cases, resulted in fatalities caused by off-target effects (Raman et al. 2016; Linette et al. 2013). Importantly, as MC.7.G5 was isolated from a healthy donor where it caused no obvious pathology and its TCR did not recognise healthy cell lines, it could be well tolerised in cancer patients without allogenic rejection. It is therefore feasible that such MR1-restricted T-cells exist in other healthy individuals, with research into this forming the basis of Chapter 5 of this thesis. To conclude, the MC.7.G5 TCR and its MR1-restricted ligand provide an exciting range of potential avenues for further research into possibilities for pan population therapeutic cancer treatments.

Chapter 5. MR1-Restricted Cancer-Specific T-cells

5.1. Background

In **Chapter 4** I identified an MR1-restricted T-cell clone that recognised and lysed a wide range of cancer cell lines without the requirement for a specific HLA. This T-cell clone, named MC.7.G5 appeared to show specificity for an MR1-restricted ligand produced endogenously by cancer cells but not healthy cells. The natural MC.7.G5 TCR could be useful for treating a range of cancers via adoptive T-cell transfer. It is also possible that the ligand for this type of T-cell might be useful for cancer vaccination. However, vaccination with the cancer-derived MR1-ligand would require that people to be vaccinated possess a resident population of T-cells capable of mounting a response to the putative cancer-specific ligand. As MC.7.G5 was identified from a healthy donor, I hypothesised that T-cells with similar characteristics might be present in all individuals across the population, making MC.7.G5-like T-cells potential targets for cancer vaccines.

5.1.1. Aims

For this chapter, I sought to identify if MC.7.G5-like cancer-killing MR1-restricted T-cells were present in healthy individuals. My specific aims were to:

- Optimise a system to isolate MR1-reactive T-cells adapting techniques learned in Chapter 3
- Clonotype MR1-reactive T-cells to identify patterns of TCR gene usage and CDR3 sequences
- Produce T-cell lines and clones that recognise MR1 in a similar manner to MC.7.G5

5.2. Results

5.2.1. MR1-reactive T-cells are present in low numbers in healthy donors

To identify if MR1-reactive T-cells are present in healthy donors I adapted the priming process shown in **Chapter 3**, by priming HLA-A2^{neg} PBMCs with an APC commonly used in the laboratory, C1R.A2 (Purbhoo et al. 2001), transduced with MR1 (C1R.A2.MR1) (**Figure 5.1**). Importantly, C1R cells overexpressing MR1 activated MC.7.G5 (**Section 4.4.6**). The C1R.A2.MR1 target cells were irradiated prior to T-cell priming to prevent their uncontrolled outgrowth in priming cultures. After two weeks of PBMC/C1R.A2.MR1 co-culture, I monitored if the priming conditions resulted in expansion of MR1-reactive T-cells by performing a TAPI/CD107a assay on the cultures using C1R.A2 and C1R.A2.MR1 cells (**Figure 5.1**). MR1-reactive T-cells were enriched in the healthy donor PBMCs, however there was high background to the C1R.A2 cells, likely through allogenic recognition (**Figure 5.2a**). In an attempt to increase the numbers of MR1-reactive T-cells, I performed a second round of priming on the T-cells and included labelling for IFN-γ, however this did not reveal MR1-specific enrichment (**Figure 5.2b**).

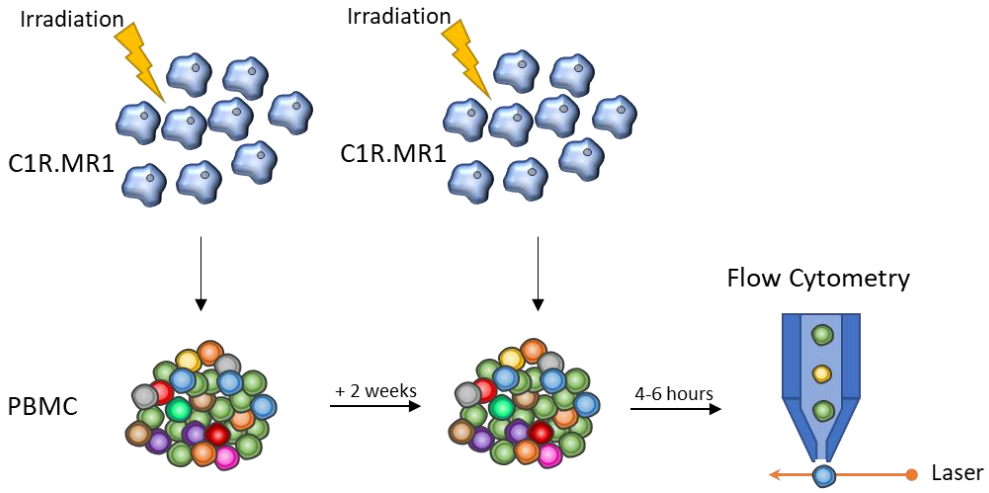

Figure 5.1 - Experimental outline of expansion of MR1-reactive T-cells
C1R cells overexpressing MR1 (C1R.MR1) were irradiated to prevent proliferation and were used to prime PBMCs from a healthy donor. 20 PBMCs were added for every C1R.MR1 cell and cultured for two weeks. Expanded T-cells were restimulated with irradiated C1R.MR1 cells, then surface markers stained and/or sorted based on reactivity to C1R.MR1 cells.

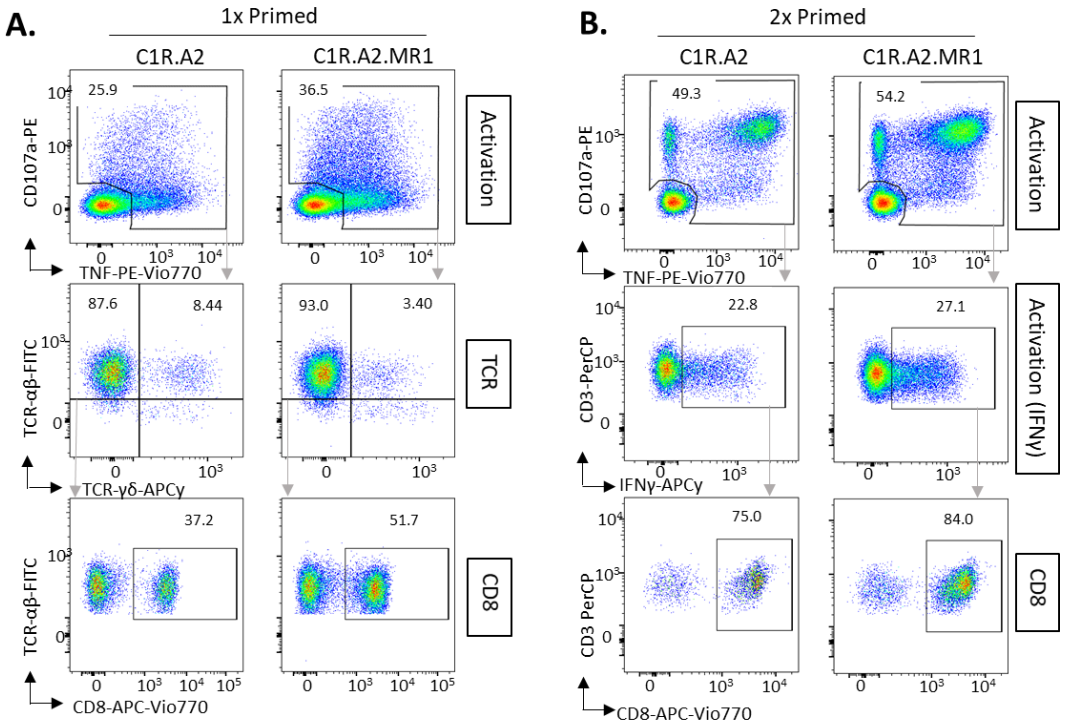

Figure 5.2 - C1R cells overexpressing MR1 prime MR1-specific T-cells
(**A**). Irradiated C1R.A2 cells overexpressing MR1 (C1R.A2.MR1) were cultured with PBMCs from a healthy donor for two weeks, then tested for reactivity in a TAPI-based assay using either C1R.A2.MR1 or C1R.A2. Cells were previously gated on alive $CD3^+$ lymphocytes with gates set on PBMCs alone. Grey arrows show sequence of gates used. (**B**). Irradiated C1R.A2.MR1 cells were cultured for 2 weeks with healthy donor PBMCs, then a fresh batch of irradiated C1R.A2.MR1 cells added and cultured for a further two weeks before being activated in an ICS using C1R.A2.MR1 or C1R.A2 cells. Cells were previously gated on alive $CD3^+$ lymphocytes with gates set on PBMCs alone. Grey arrows show sequence of gates used. Assay performed once.

5.2.2. TCR usage of MR1-reactive T-cells

As a greater number of T-cell responded to C1R.A2.MR1 cells compared to the C1R.A2 control, I aimed to identify the TCRs responsible for this potentially MR1-specific recognition. Staining with Vα7.2 antibody showed that the majority of T-cells responding to C1R.A2.MR1 targets used a Vα7.2 (TRAV1-2) αβ-TCR (**Figure 5.3**), commonly associated with MAIT cells (Reantragoon et al. 2013), and were enriched for CD8 expression.

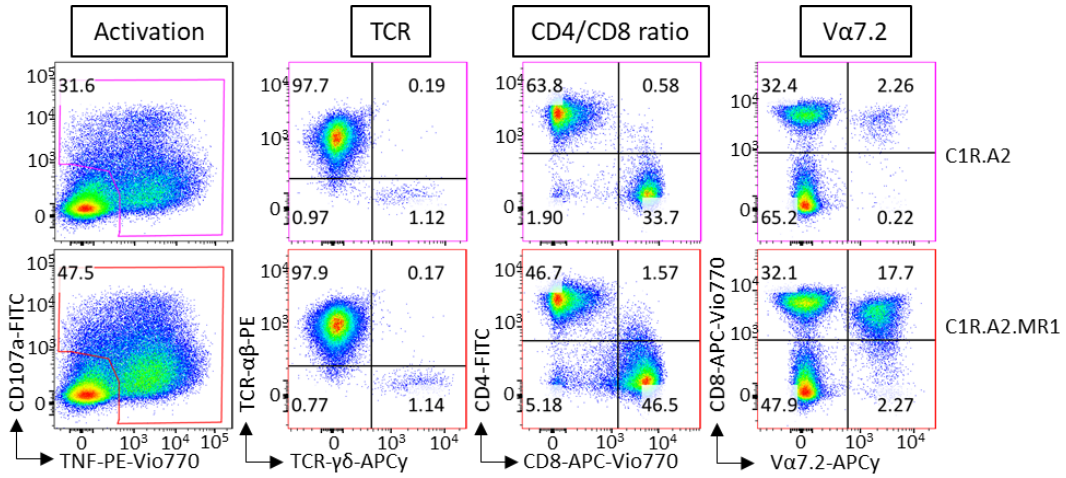

Figure 5.3 - C1R.A2.MR1 reactive T-cells are CD8⁺ Vα7.2⁺(TRAV1-2)
Healthy donor 759S T-cells were primed with irradiated C1R.A2 cells overexpressing MR1 (C1R.A2.MR1) and activated in a TAPI/CD107a assay with either C1R.A2 or C1R.A2.MR1 cells. Cells were previously gated on live CD3⁺ lymphocytes. Assay performed once.

I next sought to identify the clonotypic architecture of the TCRs recognising C1R.A2.MR1 cells in primed T-cells while removing the clonotypes that recognise C1R.A2 cells, using the python script written by Thomas Whalley (**Section 3.2.1**). For this, I flow cytometry sorted TAPI-treated C1R.A2.MR1-reactive cells after two weeks of priming, gating on CD107a and TNF expression. C1R.A2-reactive cells were concomitantly sorted with C1R.A2.MR1 reactive T-cells, sequenced and removed from the C1R.A2.MR1-reactive clonotype sequences. Corroborating the Vα7.2 (TRAV1-2) surface staining in **Figure 5.3**, the C1R.A2.MR1-reactive TCRs showed an enrichment for TRAV1-2 (**Figure 5.4**). Interestingly, the most common rearrangement pairing was to TRAJ12; a less dominant canonical MAIT-cell TCR subset

enriched in the peripheral tissues as opposed to adult peripheral blood (Lepore, Kalinicenko, et al. 2014). Indeed, such tissue localisation may the reason that these MR1-reactive T-cells are found in low numbers in PBMCs. Furthermore, the most common TRBV genes were TRBV27 and TRBV29-1, which have previously not been associated with MAIT cells. It is thought the TCR-β chain in MAIT cells mediates antigen specificity to the MR1 bound ligand (Eckle et al. 2014), here TRBV27 and TRBV29-1 may potentially be responsible for recognition of the bound ligand (or lack thereof) to MR1.

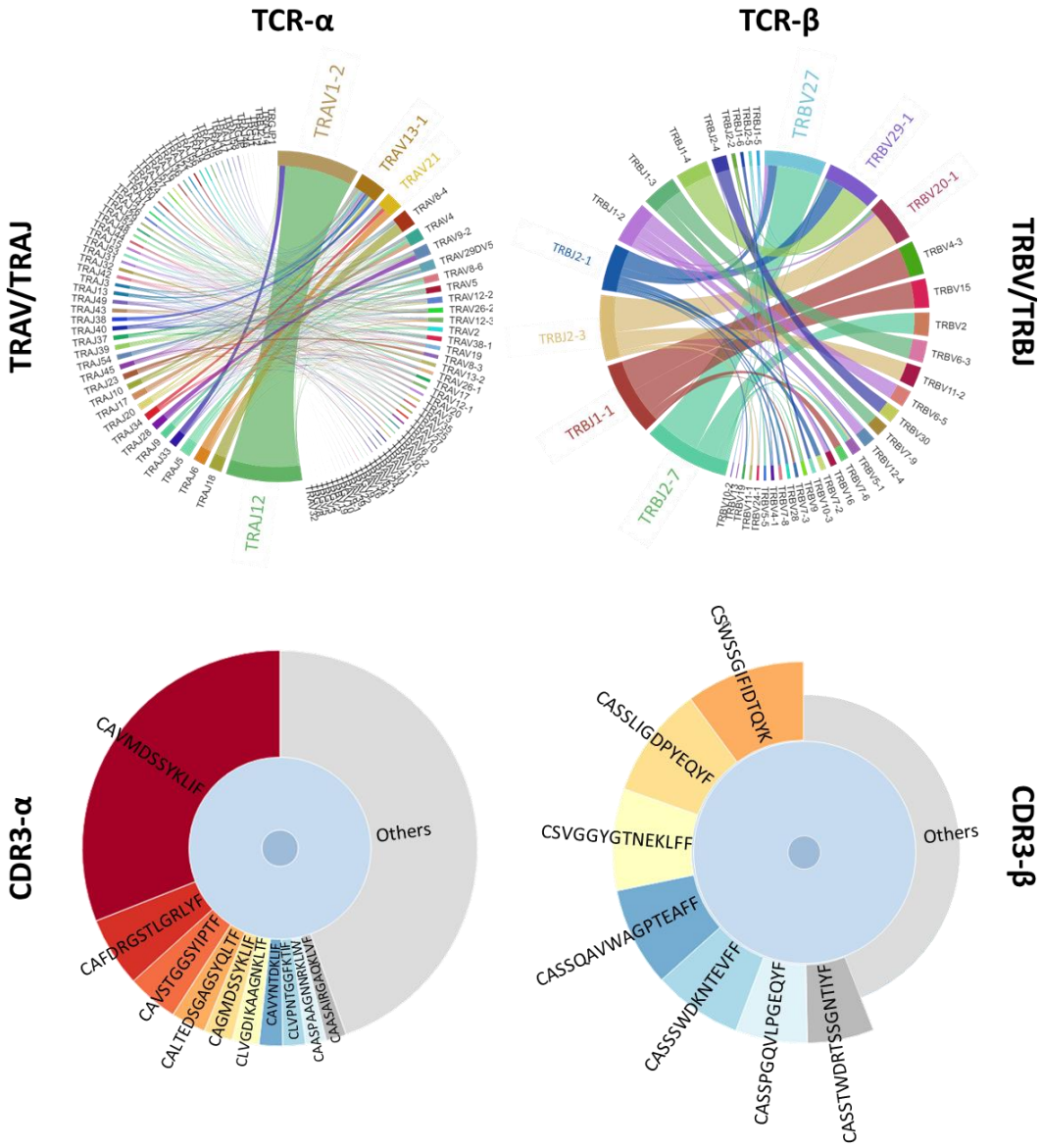

Figure 5.4 - Clonotypic architecture of T-cells activated in response to C1R.A2.MR1
PBMCs from Donor 759S were primed with C1R.A2 cells overexpressing MR1, then sorted on dual expression of TNF and CD107a in response to MM909.24 cells overexpressing MR1. TCRs were sequenced and clonotypes removed that responded to C1R.A2 cells. Top row shows rearranged gene usages of TCRα and TCRβ. The larger the arc, the greater the enrichment of gene. The greater the link between V and J genes indicates more common gene rearrangements. Bottom row shows dominant CDR3 sequences for TCRα and TCRβ chains. CDR – complementarity determining region.

While canonical MAIT TCRs were present in the sample, alternative TCRs also showed high enrichments. The third most dominant TCR clonotype present (3.2%, 825 reads) possessed a TRAV21 TRAJ6 TCR with a CAVSTGGSYIPTF CDR3α sequence, which has previously been published as part of a comment on the immune landscape of cancer, including tumour

infiltrating T-cells (Thorsson et al. 2018). This paper also identified clonotypes identified in **Chapter 3**; however, the authors did not describe the TRAV/TRAJ usage and therefore convergent clonotype sequences may have occurred. Furthermore, (Thorsson et al. 2018) also showed the presence of the CDR3α sequence CAVYNTDKLIF, here comprised of a TRAV21 TRAJ34 TCRα chain, implying these two TCR chains may be conserved in the population. Identification of this clonotype within MR1-reactive T-cell populations from other donors will be required to definitively prove that this TCR demarcates a population-invariant T-cell subset.

5.2.3. C1R.MR1 primed cells cross-react with MM909.24 overexpressing MR1

While high background can be removed from NGS data, production of clones required further enrichment of MR1-reactive cells. I therefore transduced C1R cells with MR1 (C1R.MR1), as these are HLA-A and B negative (Storkus et al. 1989) and should not induce a large HLA class-I antigen specific responses. As MC.7.G5 could recognise both C1R.MR1 cells and MM909.24 MR1 overexpressing cells (MM909.24 + MR1), I hypothesised that C1R.MR1 primed cells would cross react to MM909.24 + MR1 with reduced allogenic background activation. I performed priming of healthy PBMCs with C1R.MR1 cells, as in **Section 2.2.1**, but activated primed T-cells in an ICS using either C1R or MM909.24 cells with varying MR1 expression profiles (wild-type, knockout or overexpressing, **Figure 5.5**). Activation with MM909.24 identified a greater proportion of seemingly MR1-reactive cells with much reduced background recognition, particularly in donor 663. As in **Figure 5.2**, activated cells were skewed towards a $CD8^+$ TCR-$\alpha\beta^+$ phenotype (**Figure 5.5b**).

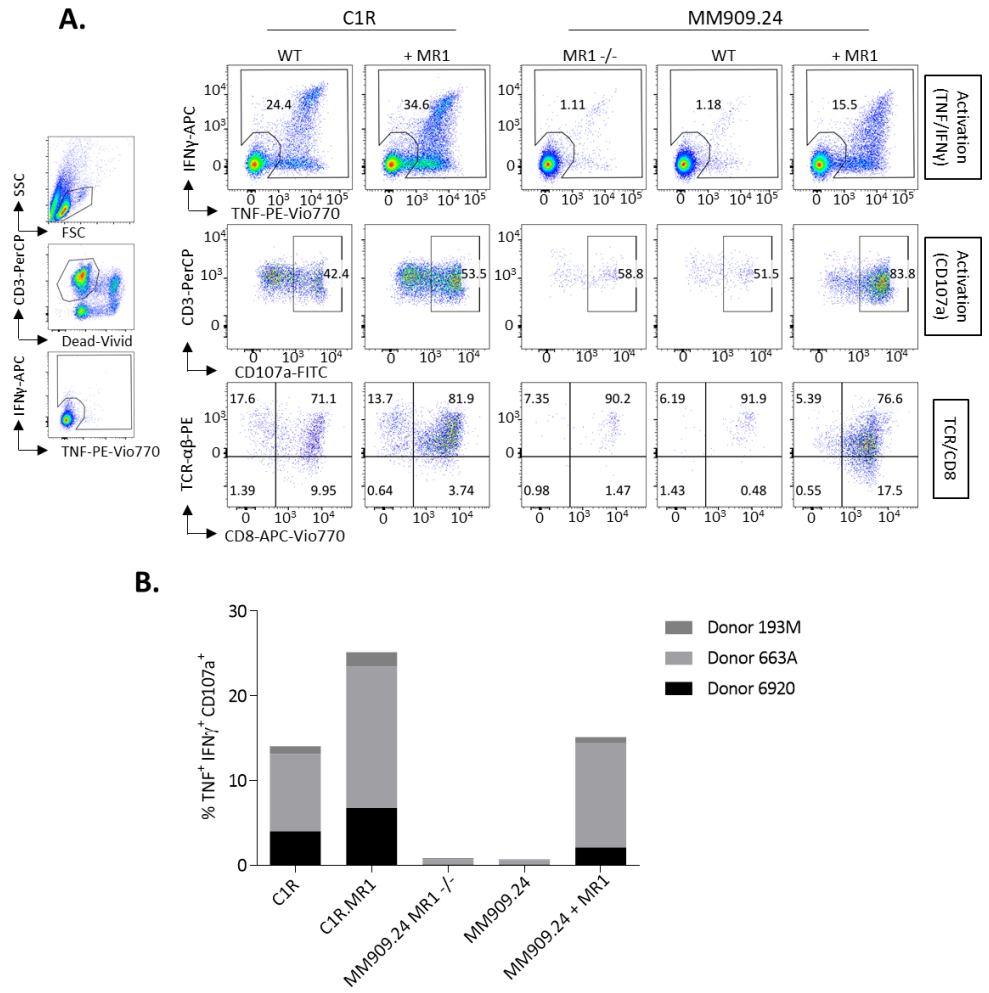

Figure 5.5 - C1R.MR1 primed T-cells are activated by MM909.24 cells overexpressing MR1
(**A**). Irradiated C1R cells overexpressing MR1 (C1R.MR1) were cultured with PBMCs from a healthy donor (663A) for two weeks, then tested for reactivity in an ICS assay using either C1R.MR1, C1R.null, melanoma MM909.24 wildtype, MR1 knockout (MR1 -/-), or MR1 overexpressing (+ MR1). Cells were previously gated on alive $CD3^+$ lymphocytes with gates set on PBMCs alone, as shown (left). Grey arrows show sequence of gates used. Donor shown is 663A. (**B**). Summary data of three independent donors using gating strategy from (A), with triple positivity determined by statistical analysis in FlowJo software. Data are not significant (t-test).

5.2.4. MM909.24 + MR1 pull-out cells do not have the same recognition profile as MC.7.G5

Despite C1R.MR1 primed T-cells showing cross-reactivity to MM909.24 + MR1 cells, they did not strongly recognise MM909.24 wildtype cells, contrasting the MC.7.G5 recognition profile. One plausible reason for this is MR1 overexpression may result in surface expression of MR1 without a bound ligand that is then recognised by T-cells. I therefore sought to enrich

for two independent populations; those T-cells that responded to overexpressed MR1 only, and those that responded to wildtype MM909.24 but are still restricted by MR1. The rationale behind this being that T-cells reactive to wildtype MM909.24 cells might exhibit an MC.7.G5-like reactivity profile. C1R.MR1-primed T-cells were pulled out by magnetic sorting based on TNF-expression in response to either MR1 overexpressing MM909.24 or wildtype MM909.24 cells and expanded, after which I performed an ICS (**Figure 5.6**) across three donors (**Figure 5.7**). In T-cells pulled out with MM909.24 + MR1 cells, isolated T-cell lines maintained reactivity to MM909.24 + MR1 cells (31.7 % ± 19.4) but had reduced reactivity to wildtype MM909.24 (7.6 % ± 4.0). In contrast, in cells pulled out with wildtype MM909.24, reactivity to wildtype MM909.24 cells (19.6 % ± 3.5) was comparable to MM909.24 + MR1 reactivity (20.8 % ± 5.3), while recognition of MM909.24 MR1 -/- was reduced (6.2 % ± 4.4). Therefore, pull out of wildtype MM909.24-reactive cells appears to select for MC.7.G5-like T-cells. **Figure 5.8** outlines the putative mechanism of the reactivity of both MC.7.G5-like cells and overexpressed MR1-reactive cells.

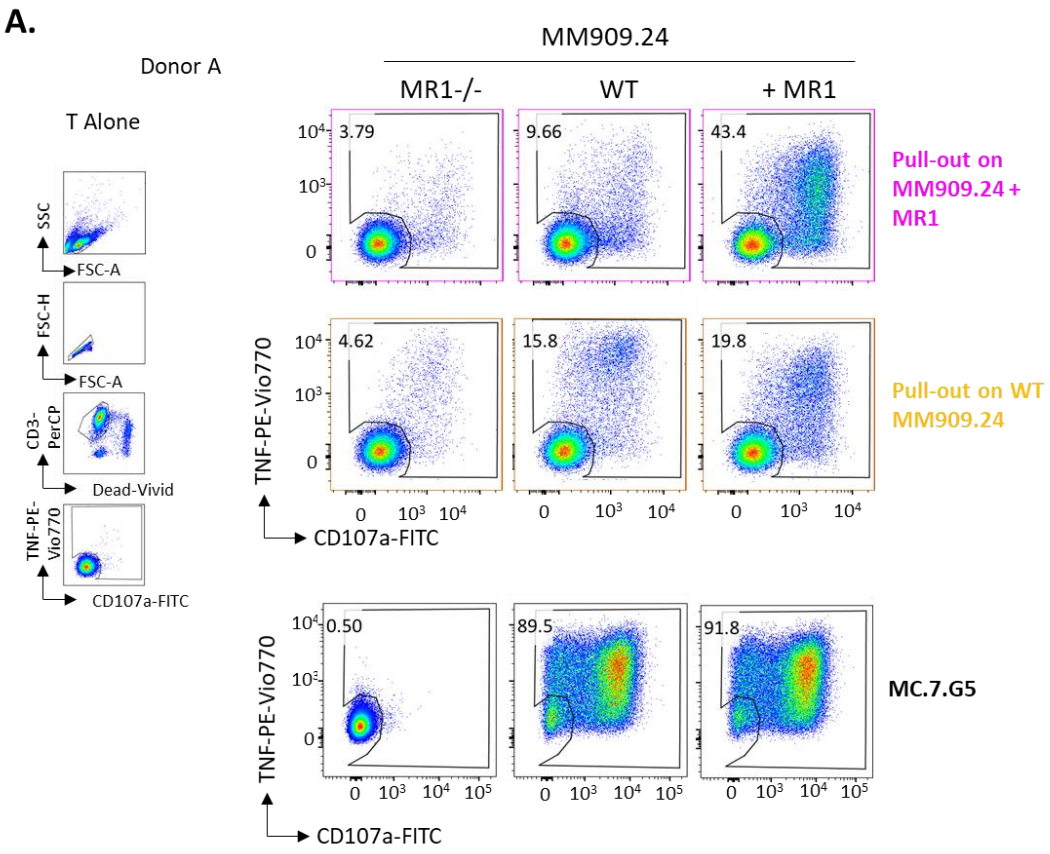

Figure 5.6 - MR1-reactive T-cells compared to MC.7.G5 T-cells

PBMCs were cultured with C1R cells overexpressing MR1 (C1R.MR1). After 14 days, T-cells were activated with either MM909.24 wildtype (WT) or overexpressing MR1 (+ MR1) with TNF-secreting cells, isolated by MACS and expanded in lines. Expanded pull-outs from Donor A were activated in an ICS with C1R or MM909.24 with differing levels of MR1 expression. Previous gating strategy shown on left with T-cells alone. MC.7.G5 was activated in a parallel assay.

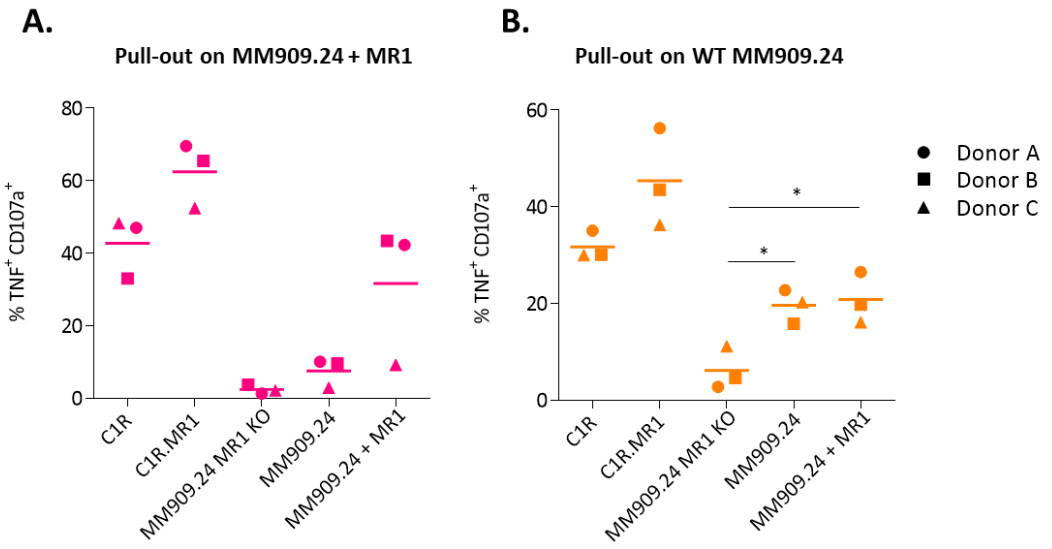

Figure 5.7 - Summary of activation of MR1-reactive cells in three donors
T-cells from three donors were primed with C1R.MR1 cells, and TNF MACS pulled out with either wild type or MR1 overexpressing MM909.24 (+ MR1) reactivity. T-cells were then activated in an ICS against C1R cells or MM909.24 cells with varying MR1 expression. (**A**). Summary of three donors (A, B and C) with the same gating shown in **Figure 5.6**, activation of T-cells originally pulled out on MM909.24 + MR1 reactivity, then screened against C1R or MM909.24 cells in an ICS. Data are not significant, Student's t-test. (**B**). Summary of three donors, activation of T-cells originally pulled out on MM909.24 WT reactivity, against C1R or MM909.24 cells. * P<0.03, unpaired two-tailed t-test. C1R data are not significant.

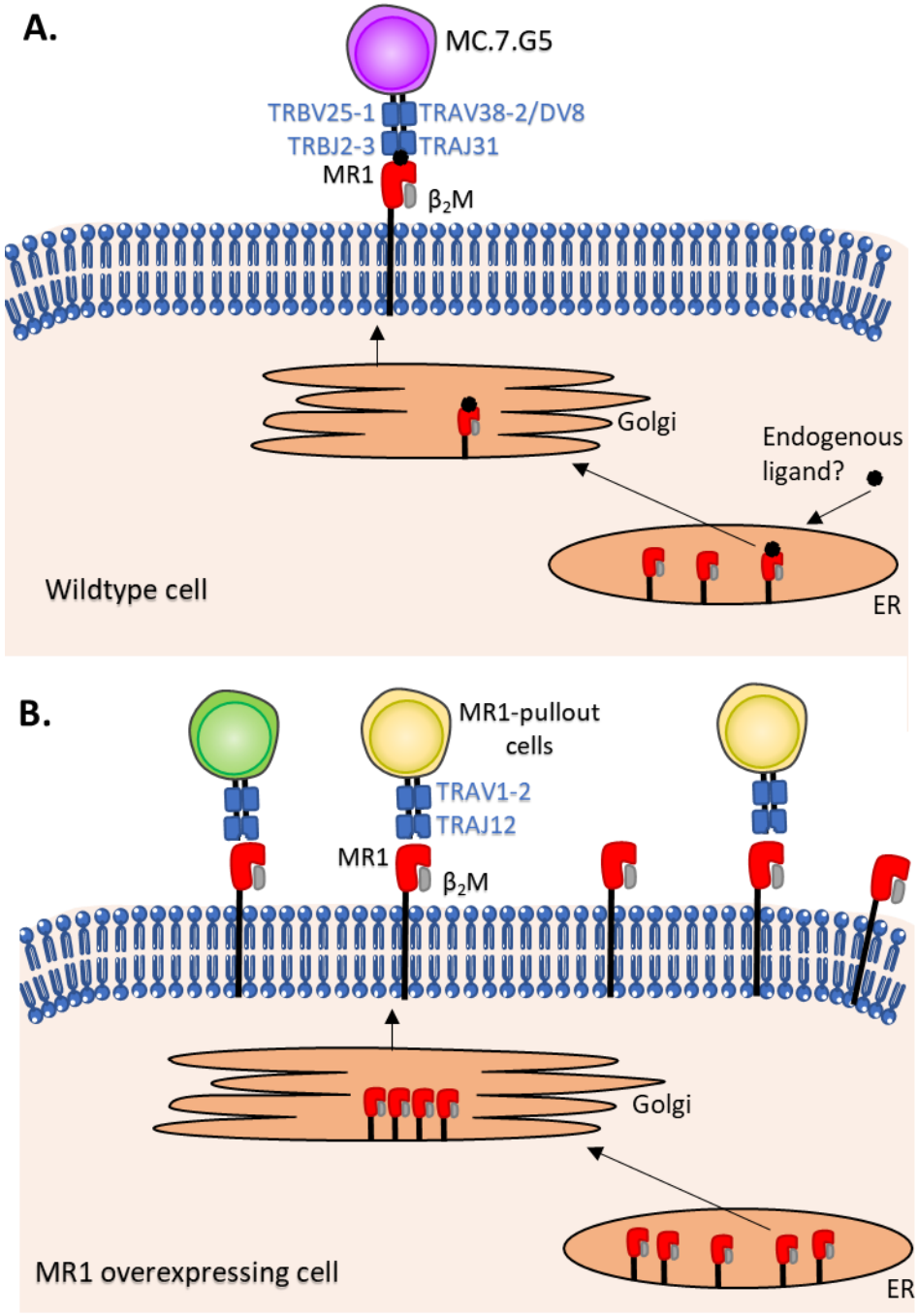

Figure 5.8 – Putative model of recognition of MR1-reactive T-cells

(**A**). MC.7.G5 recognises MR1 only when an endogenous ligand is bound. MR1 has low natural expression (undetectable by flow cytometry) (**B**). T-cells pulled out based on TNF^{+} secretion in response to MR1 overexpressing MM909.24 cells may recognise MR1 without a bound antigen, due to overexpression of MR1 enabling surface expression of ligand independent MR1. ER, endoplasmic reticulum.

5.2.5. MC.27.759S T-cell clone shows similar reactivity to MC.7.G5

I next sought to identify if MC.7.G5-like clones could be isolated from the MC.7.G5-like activated T-cell populations identified in **Figure 5.7**. One T-cell clone, designated MC.27.759S, was isolated by flow cytometry sorting on TNF^+ $CD107a^+$ T-cells in response to C1R.MR1 cells from donor 759S (**Figure 5.2**). MC.27.759S was able to secrete IFNγ and TNF cytokines and express CD107a in response to C1R.MR1, MM909.24 + MR1 and MM909.24 wildtype (**Figure 5.9a**), indicating a similar pattern of recognition to MC.7.G5. MC.27.759S exhibited higher expression of CD8 (**Figure 5.9b**). When screened against C1R cells overexpressing MR1 with a K43A mutation (i.e. unable to form Schiff bases with MR1 ligands (Reantragoon et al. 2013)), MC.27.759S was minimally stimulated, similar to MC.7.G5 recognition of MR1-K43A (**Figure 5.9c**). MC.27.759S therefore appears to show ligand specificity in the context of MR1.

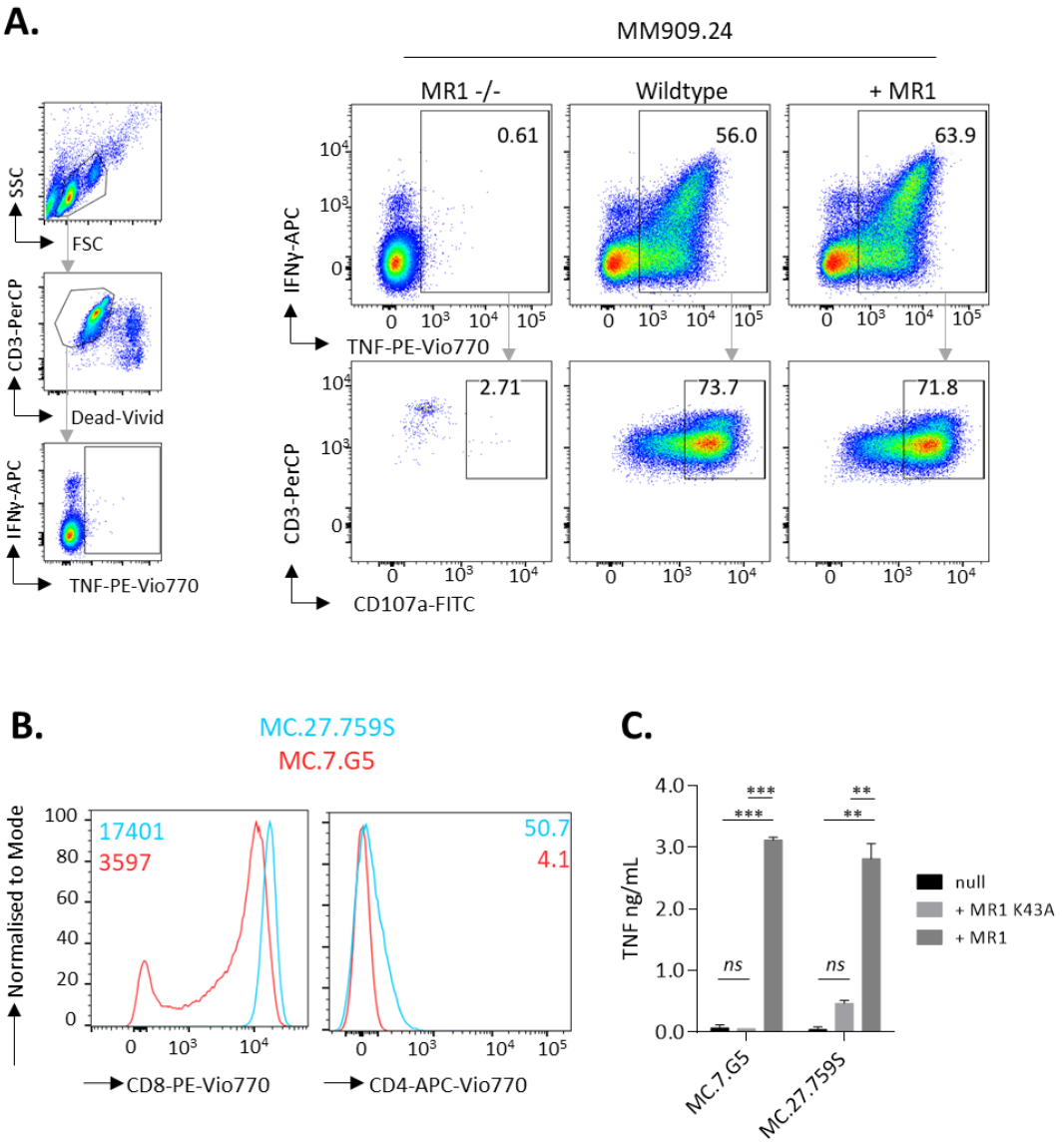

Figure 5.9 - MC.27.759S has similar reactivity to MC.7.G5
(**A**). The MC.27.759S T-cell clone was activated in an ICS using melanoma MM909.24 wildtype, MR1 knockout (MR1 -/-) or MR1 overexpressing (+ MR1). Previous gating shown on left, with gates set on T-cell alone. Representative of two independent experiments. (**B**). CD8 and CD4 co-receptor staining of MC.7.G5 and MC.27.759S. Previous gating on alive $CD3^+$ lymphocytes. Assay representative of two independent experiments. (**C**). MC.7.G5 and MC.27.759S T-cell clones were cultured with C1R cells without MR1 or transduced with either native MR1 or MR1 with a K43A mutation. Supernatants were harvested, and TNF secretion quantified by ELISA. Assay performed once in duplicate. Statistical significance determined by t-test analysis. ** P<0.006; *** P<0.0003; *ns,* not significant.

I next sought to identify the killing capabilities of MC.27.759S. A chromium release assay showed MC.27.759S could kill a range of cancer cell lines (**Figure 5.10a**). Moreover, MC.27.759S killing capacity was similar to MC.7.G5 when titrating E:T against MM909.24 wildtype, while remaining inert to MM909.24 MR1 -/- (**Figure 5.10b**).

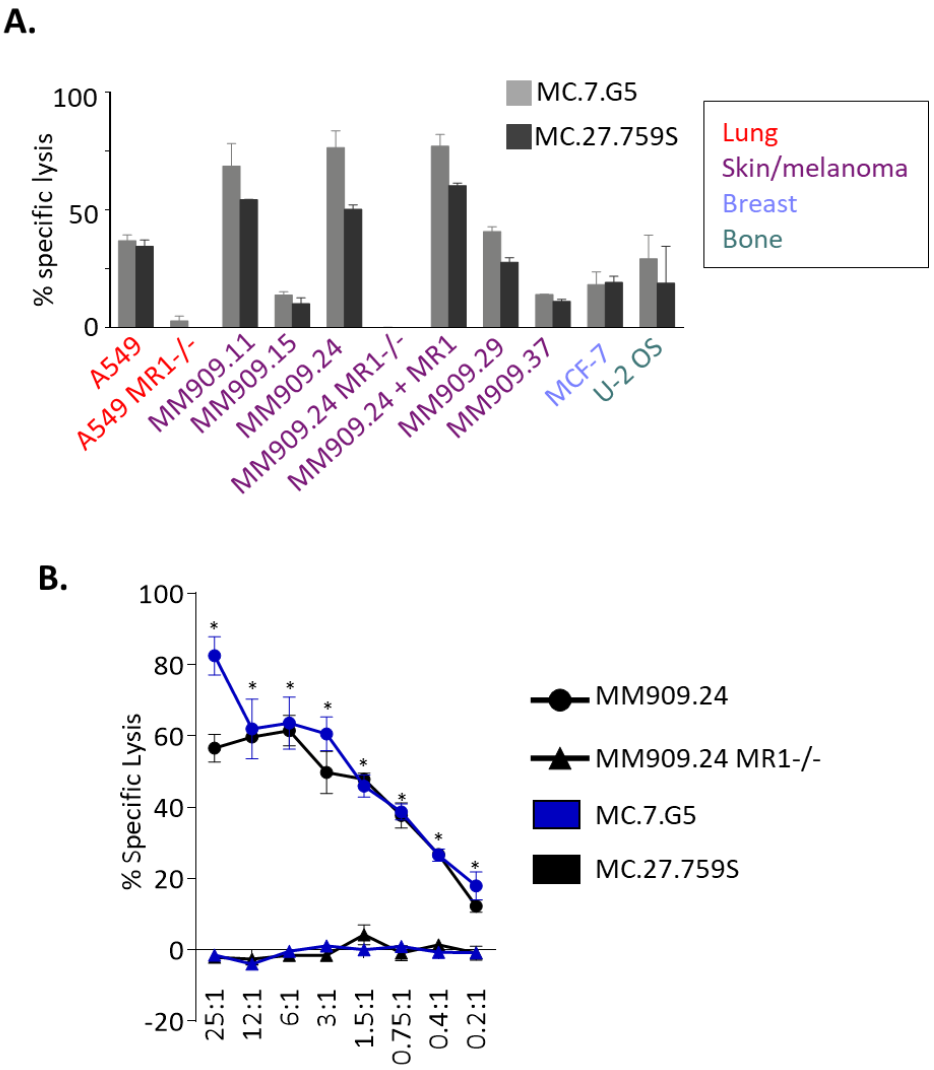

Figure 5.10 - MC.27.759S kills a similar range of cancer cells to MC.7.G5
(**A**). A cytotoxicity chromium release assay was performed with MC.7.G5 and MC.27.759S against a range of cancer cell lines at an effector to target ratio of 5:1 over 6 hours. Assay performed in duplicate with error bars shown. Representative of two independent experiments. (**B**). A cytotoxicity chromium release assay was performed with MC.7.G5 and MC.27.759S against melanoma MM909.24 wildtype or MR1 knockout (MR1 -/-) at a range of effector to target ratios over 6 hours. Assay performed once in duplicate with error bars shown. *p<0.01, multiple t-tests. Applies to both MC.7.G5 and MC.27.759S, comparing wild type to MR1 -/- lysis.

5.2.6. MC.7.G5-like T-cell clones and their TCRs

To identify if MC.27.759S used a similar TCR to MC.7.G5, Cristina Rius performed sequencing of both the TCR-α and paired TCR-β, revealing a TRAV21/TRAJ42 TCR-α with a relatively long CDR3α CAVRLAGYGGSQGNLIF sequence, and a TCR-β comprised of TRBV9/TRDB2/TRBJ2.3

with a CDR3β sequence of CASSVASTGTDTQYF. There was no obvious similarity with MC.7.G5, and pairwise sequencing alignment of TCRs showed minimal overlapping of residues, with the only shared sequences limited to TRBJ2-3 and a small section located adjacent to CDR1β, highlighted in pink (**Figure 5.11**).

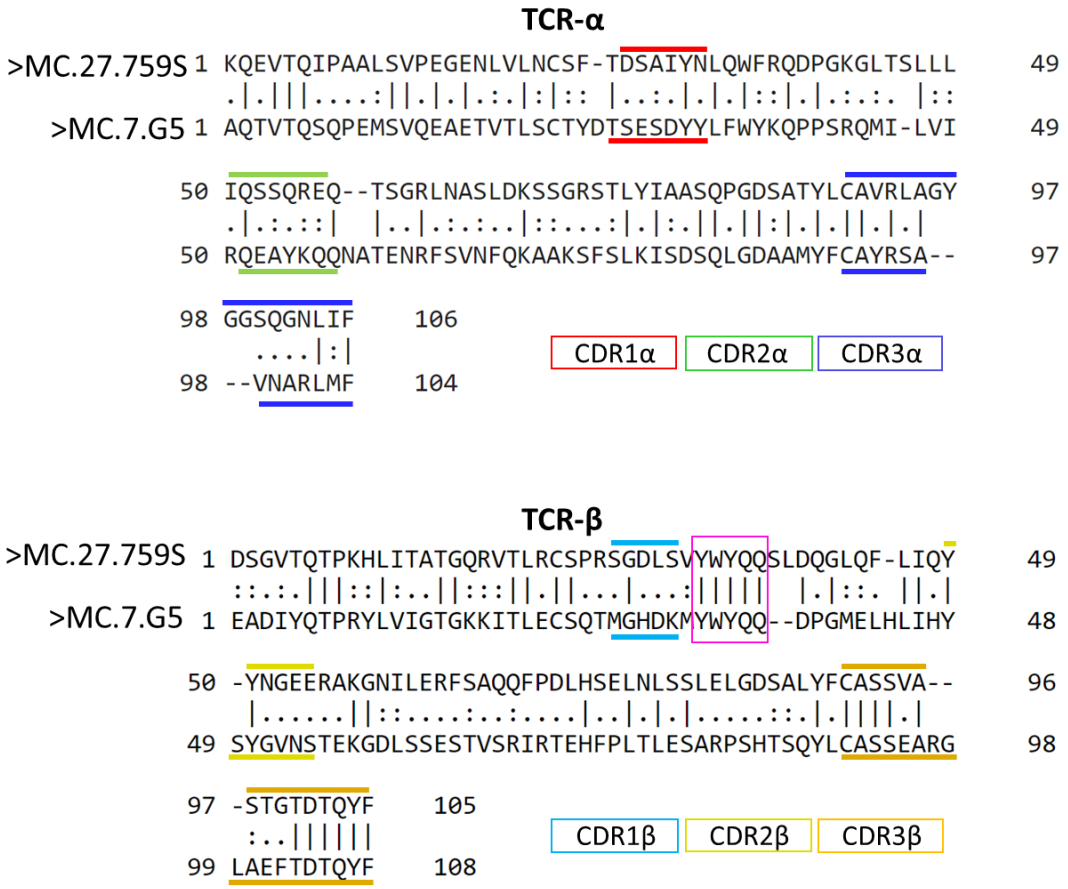

Figure 5.11 - TCR alignment of MC.7.G5 and MC.27.759S
MC.27.759S T-cell receptor (TCR) was sequenced revealing a TRAV21/TRAJ42 TCR-α paired with TRBV9/TRDB2/TRBJ2.3 TCR-β. CDR loops are highlighted in colour. MC.7.G5 TCR consists of TRAV38-2/TRAJ31 paired with TRBV25-1/TRBJ2-3. Alignment performed using EMBOSS Needle.

I also produced T-cell clones from T-cells primed on C1R.MR1 cells, that were magnetically pulled out on TNF^{+} by MACS in response MM909.24 wildtype (**Figure 5.7**). After expansion, 5 clones from Donor C showed recognition of MM909.24 wildtype but not to MM909.24 MR1 KO targets (**Figure 5.12**). These results indicate that MC.7.G5-like cells are present across the population. These new clones were less potent at cytokine secretion compared to MC.7.G5, however this might be attributed to many factors such as stage of culture, co-

receptor expression, activation state of T-cells and possible recognition of alternative MR1-ligands.

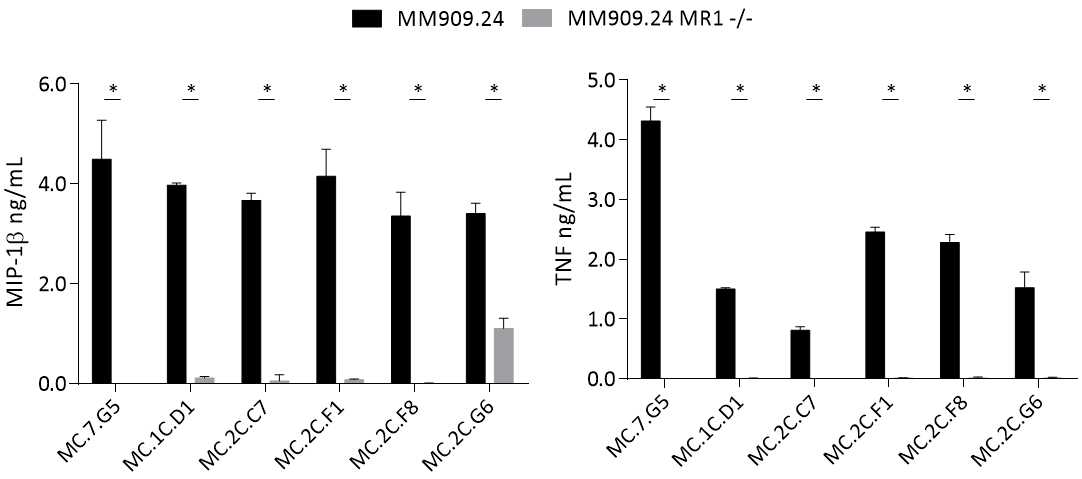

Figure 5.12 - MC.7.G5-like T-cells recognise MM909.24 targets via MR1
T-cell clones initially primed on C1R.MR1 cells were pulled out with wildtype MM909.24 and expanded. After an overnight T-cell activation assay, MIP-1β and TNF secretion by T-cell clones was quantified by ELISA. Assay performed once in triplicate with standard deviations shown. Differences between MM909.24 and MM909.24 MR1 knockout (-/-) were all statistically significant ($p<0.001$, multiple t-tests).

5.3. Discussion

5.3.1. Summary

In **Chapter 4** I identified a novel T-cell clone capable of killing cancer cells through the monomorphic MR1. In this chapter sought to identify if this discovery was unique or if such T-cells exist across the population. Initial priming experiments resulted in high background of activation by C1R.A2 cells, however there was greater recognition of C1R.A2.MR1 cells. NGS revealed that the MR1-reactive cells were enriched for the peripheral tissue-associated form of the MAIT TCR. However, while primed T-cells were activated by both C1R.MR1 and MM909.24.MR1 cells with lower recognition of MR1 knockout cells, an issue arose in that T-

cells pulled out against targets overexpressing MR1 did not exhibit MC.7.G5 T-cell-like recognition of wild type MM909.24 cells. As outlined in **Figure 5.8,** transduction with MR1 may result in MR1 surface expression without a bound ligand, and it is possible that empty MR1 may be recognised by some T-cells (Gherardin et al. 2016). Indeed, (McWilliam et al. 2016) showed MR1 transgene expression can result in misfolded MR1 without β_2M, which the authors suggested resulted in ligand-free MR1 expression. T-cells pulled out on wildtype MM909.24 cells did not respond to MR1 knockout cells but maintained reactivity to both wild type and MR1 overexpressing cells. This recognition pattern mirrored that of MC.7.G5 and was replicable across three independent donors, suggesting that MC.7.G5-like T-cells are present across the population. Clonal analysis of a new TCR (MC.27.759S) capable of recognising MR1 suggests MC.7.G5-like activity can be polyclonal unlike the invariant TCR nature of classical MAIT cells. Interestingly, the MC.7.G5-like T-cell clone MC.27.759S used a TRAV21 TCR-α gene segment which showed enrichment in both bacterial screenings in **Chapter 3** and in the NGS clonotyping of MR1-reactive T-cells (**Figure 5.4**). Finally, I identified five new T-cell clones in addition to MC.7.G5 and MC.27.759S that were able to recognise MM909.24 but not MM909.24 MR1 KO cells, indicating MR1-ligand dependent recognition.

5.3.2. Further experiments

An important next step in further studying the biology of MC.7.G5-like T-cells will be to test the specific killing capacity, as I have only shown cytokine secretion of a few MC.7.G5-like T-cell clones, with some killing data on MC.27.759S. Additionally, screening new T-cell clones with cells overexpressing the MR1 K43A mutant would reveal if these T-cell clones also require an MR1-presented ligand as with MC.7.G5 and MC.27.759S clones.

Analysis of the populations of MR1-reactive T-cells in more donors than shown here at both an NGS level and clonal level would confirm the pan-population nature of the MR1-reactive, cancer specific T-cell pool. Moreover, a greater variety of sources of T-cells could also be investigated; as identified in NGS clonotyping of donor 759S, MR1-reactive T-cells possess a TRAV1-2/TRAJ12 TCR which is associated with tissue localisation. Tissue-resident T-cells could show an enrichment of these TRAV1-2/TRAJ12 MR1-reactive cells (Lepore, Kalinicenko, et al. 2014), or provide access to a greater range of T-cells not present in the blood. However, as described earlier, the TRAV1-2/TRAJ12 T-cells may react to aberrant surface MR1 expression independent of ligand. Despite this, such T-cells may be important in the context of bacterial and viral infection, and cancer, where MR1 may be acting as a stress signal as in the case with EPCR and MICA/B (Bauer et al. 1999; Willcox et al. 2012). An obvious next step therefore is to identify if T-cells can recognise MR1 overexpressing cells in other contexts, such as those infected with bacteria e.g. *M. smegmatis*. Furthermore, testing T-cells that only recognise overexpressed MR1 with cells instead transduced with MR1-K43A, could also reveal the antigen specificity of these T-cells.

TIL populations could provide another source of MR1-reactive T-cells. It is well established that TILs harbour an enriched pool of cancer-reactive T-cells (Rosenberg et al. 2011), therefore it is feasible that the TIL population may include MC.7.G5-like MR1-reactive T-cells. In our laboratory, we already have access to TIL samples from cancer patients as part of a collaboration with Professor Inge Marie Svane at the Centre for Cancer Immune Therapy in Copenhagen. It would be interesting to determine if MC.7.G5-like T-cells form part of the repertoire of TIL populations.

It would also be interesting to determine whether MR1-restricted, cancer-reactive T-cells exhibit cross-reactivity between MR1 and HLA-I. Indeed, it has been established that T-cells

must cross-react to be able to fully cover required immunity (Sewell 2012), with documented cases of TCR recognition of disparate HLA molecules (Colf et al. 2007; Garcia et al. 1998; Yin et al. 2011) including TCRs that recognise both MHC class I and MHC class II . A way to test this would be to identify the HLA haplotypes of MC.7.G5 and MC.27.759S, then perform a combinatorial peptide screen to reveal if HLA-dependent recognition can occur using these T-cell clones (Ekeruche-Makinde et al. 2012).

It was also noticeable that both MC.7.G5 and MC.27.759S expressed the CD8 glycoprotein. The majority of MAIT cells have also been shown to express CD8 (Gherardin, Souter, et al. 2018; Walker et al. 2012). CD8 is known to play important roles in the recognition of peptide antigens bound to HLA class I as it: (i) delivers the key kinase, Lck to the intracellular side of the TCR/CD3 complex ((Purbhoo et al. 2001)); (ii) stabilises the TCR/pHLA-I interaction (Wooldridge et al. 2005) and (iii) augments TCR localisation into privileged membrane microdomains that are enriched for other TCR-mediated signalling machinery (Arcaro et al. 2000; Arcaro et al. 2001). It would be interesting to examine whether CD8 plays similar roles in the recognition of tumour cells via MR1 and to examine whether MR1 binds CD8 by surface plasmon resonance.

An exciting prospect of cancer-specific MR1-restricted T-cells appearing across the population is the possible vaccination with the cancer-derived ligand hinted at in **Chapter 4**. Not only could such a vaccination be used to increase the population of MR1-reactive T-cells while a patient is undergoing cancer treatment, but also it could be given prophylactically to prevent the development of cancer. However, this avenue of research is distant, as the ligand first needs to be identified before any experiments of this nature can be performed.

Chapter 6. General Discussion

6.1. Summary of work and implications of findings

6.1.1. Bacteria-reactive T-cells

Despite the revolutionary discovery of antibiotics for treatment of bacterial infections, bacteria such as *Mycobacterium tuberculosis* and Methicillin-resistant *Staphylococcus aureus* are increasingly resistant to antibiotics, a problem exacerbated by the fact few new classes of antibiotics have been discovered within the past three decades (Ling et al. 2015; Hover et al. 2018). Unfortunately, the alternative approach of antibody-targeting vaccines has been unsuccessful (Tameris et al. 2013; Jansen et al. 2013; Pereira et al. 2007). In contrast, T-cell-based therapies have not been thoroughly explored and may offer means to target bacteria by mechanisms they cannot escape from. The HLA-restriction associated with conventional T-cells combined with the huge variance in HLA type across the human population could greatly limit the potential of anti-bacterial vaccine approaches enlisting conventional T-cells. Targeting unconventional T-cells could circumvent this limitation to enable population-wide therapeutics. Accordingly, the field of unconventional T-cells is becoming more attractive with the known repertoire of public TCRs (i.e. shared across individuals) and the ligands restricting them ever-expanding.

In **Chapter 3**, I developed a system to procure bacteria-reactive unconventional T-cells that is straight forward and replicable across multiple donors. These bacteria-reactive T-cells were identified using upregulation of TNF and CD107a, as these outputs allowed the isolation of living cells for downstream analyses, as discussed earlier in **Chapter 3**. By using these markers, I may have inadvertently biased the pool of T-cells being studied to those that

possess these particular effector functions, which is a something that could be addressed as these studies progress by monitoring for different effector outputs and phenotypes. NGS of TCRs showed that known subsets of unconventional T-cells were sufficiently activated and prominent in bacteria-activated T-cells. Despite differences in the co-receptor expression of T-cells involved, clonotyping revealed a shared component of the bacteria-reactive T-cell repertoire across donors and bacteria that is mostly dominated by MAIT cells and Vγ9Vδ2 γδ T-cells. I also identified shared TCR-β chains that are likely associated with MAIT cells that respond to multiple distinct bacteria, contrasting previous studies that show private MAIT TCR-β chains facilitate pathogen specificity (Gold et al. 2014; Howson et al. 2018). Furthermore, additional novel invariant T-cells using TRAV13-1 and TRAV21 TCRs were enriched, suggesting the presence of new bacteria-reactive unconventional T-cell subsets. If these additional invariant T-cells are indeed important in the anti-bacterial response, when combined with therapies targeting other unconventional T-cells such as MAIT cells and Vγ9Vδ2 cells, they could encourage a multi-pronged immune attack on invading pathogens. The next step to continue this study would involve isolation and further characterisation of the other invariant TCRs I identified within the bacteria-reactive T-cell pool. Clones bearing these TCRs could also be screened against more bacteria and importantly the mode of T-cell recognition of bacteria characterised.

The exquisite specificity of T-cells may allow pathogenic bacterium to be distinguished from commensal species, which is something broad-spectrum antibiotics fail to do (Langdon et al. 2016). Additionally, the central and resident memory T-cell pool found in lymph nodes and tissues respectively could provide an enriched pool of bacteria-reactive T-cells, as these cells reside in the periphery to enable direct killing of pathogens at the site of entry (Kaech et al. 2012). The TCR repertoire and phenotype of such cells could differ from the PBMC pool and therefore warrants further study. Overall, the identification of bacteria derived agonists for

these unconventional T-cells could provide new vaccination targets for induction of broad anti-bacterial T-cell responses.

I anticipate that repertoire sequencing will become a powerful tool to answer a range of biological questions as well as generate hypotheses for future studies. Advances in the field of single cell repertoire analysis such as DropSeq and 10x Genomics Chromium provide opportunities to not just analyse the repertoire of TCR chains, but also the chain pairing of TCRs thus increasing the dimensionality of output data. Indeed, one outcome of such sequencing could provide a novel method of isolating rare invariant T-cell populations, where bacteria-reactive activated T-cells can be sequenced and identified TCR chains transduced into primary T-cells with TCR replacement (Legut, Dolton, et al. 2018; Roth et al. 2018), thus enabling investigation into the biology of such T-cells and their ligands. Moreover, as TCR sequencing becomes higher throughput and cost effective, nuances in TCR diversity could potentially be used diagnostically to identify specific bacteria responsible for pathogenic infections.

6.1.2. MR1-restricted cancer-specific T-cells

During the bacterial studies undertaken in **Chapter 3**, I isolated a T-cell clone that recognised a cancer-cell derived ligand without requirement for a specific HLA. This discovery changed the course of my project as I sought to characterise the nature of this recognition, forming **Chapters 4** and **5**. To identify the cancer-associated ligand, I adopted a whole genome CRISPR approach; the first time this has been used to identify an unconventional T-cell ligand. Recognition was revealed to require MR1, however the ligand presented by MR1 remained elusive. MR1 is a monomorphic ubiquitously expressed molecule. The MR1-restricted T-cells described to date include MAIT cells that respond to small molecules similar to riboflavin

metabolites and other molecular mimics (Gherardin et al. 2016), and MR1 T-cells that recognise non-exogenous antigens evidenced through cytokine secretion (Lepore et al. 2017). Through ligand replacement and mutation of MR1 to abrogate Schiff-bond formation with ligands, I showed that recognition required a cancer-endogenous ligand within the MR1 antigen-binding groove. My work represents the first example of targeted killing of a broad range of cancer cells through an MR1 presented ligand. MC.7.G5 T-cells did not kill all screened cancers, however, with the possible explanations for this being not all cancers express (or upregulate) the agonist ligand or preferential binding of an alternative MR1 ligand out-competing the MC.7.G5 agonist ligand (such as Ac-6-FP, **Section 4.7**). Recognition of cancers through MR1 appeared to be conserved across all individuals screened shown by isolation of MC.7.G5-like T-cells in multiple donors. These MC.7.G5-like T-cells may provide a source of exploitable cancer-reactive T-cells that could be used for treatment of many cancer types. Potential unexplored reservoirs of these MR1-restricted T-cells are the lymph nodes and tissues, which possess populations of antigen-experienced central memory and resident memory T-cells respectively (Kaech et al. 2012). These populations were overlooked for this thesis due to difficulties in isolating such cells which would require surgery, however it would be worthy of further investigation if MR1-restricted T-cells in cancer proves to be relevant.

Multiple applications of these discoveries arise. As MR1 is monomorphic, the current caveats with TCR-transfer based cancer immunotherapy requiring patient HLA-matching would not be required. Consequently, one avenue of research, which I have demonstrated an example of in **Chapter 4**, is to use TCR transduction into a cancer patient's T-cells enabling killing of autologous cancer while remaining inert to healthy cells. It is important to note that, in the steady state, human cells do not produce substantial amounts of endogenous MR1 ligands, nor do they obtain exogenous ligands from the extracellular environment (McWilliam et al.

2016), intimating that off-target effects with the MC.7.G5 TCR may be minimised. However, there is still the potential for TCR cross-reactivity, such as with the MAGE-A3-specific TCR cross-reactivity to a cardiovascular peptide (Linette et al. 2013) or alloreactivity to specific HLAs resulting in patient toxicity, so screening with a wider range of healthy cells would be required. Conceivably, TCR tetramers (Laugel et al. 2005) could be produced and used to screen cancer cells for production of the relevant TCR ligand, before taking experiments further. Unfortunately, my attempts to produce MC.7.G5 TCR tetramers were unsuccessful. An additional issue with TCR transfer is potential for TCR mis-pairing, where novel combinations of endogenous and transduced TCRs form, leading to new potentially fatal TCR specificities (Bendle et al. 2010; van Loenen et al. 2010). This can however be negated by adopting a TCR replacement method that removed the endogenously expressed TCR chain(s) from the recipient T-cell (Roth et al. 2018; Legut, Dolton, et al. 2018). Notably, MC.7.G5, MC.27.759S and other MR1-restricted T-cells were isolated from healthy donors that had no obvious pathology.

In vivo experiments in mouse models are common techniques used to show safety and efficacy in scientific research. We are currently attempting to induce sub-cutaneous MM909.24 melanoma clearance in immune deficient 'non-obese diabetic, severe combined immunodeficient, IL-2 receptor-γ' null (NSG) mice (Ito et al. 2002), by adoptive transfer of MC.7.G5 T-cells (Jespersen et al. 2017). The NSG mouse strain allows human cells to transferred without rejection, thereby allowing T-cell mediated cancer cell targeting to be studied. Initial experiments showed MC.7.G5 T-cell engrafted successfully in to the NSG mice and were not toxic, despite the high sequence homology between murine and human MR1 antigen binding grooves and purported species cross-reactivity (Riegert et al. 1998; Huang et al. 2009). We have engineered the cancer cells to express a fluorescent protein allowing sensitive *in vivo* imaging and experiments have now been initiated.

In parallel to the *in vivo* studies we are attempting to identify the cancer-derived activating ligand presented by MR1 to MC.7.G5 T-cells. My laboratory will be isolating MR1 from MM909.24 melanoma cells, eluting the ligand and then using mass spectrometry to explore the MR1 cargo. Candidate ligands could then be tested for MR1 binding and used with the MC.7.G5 clone to assess their ability to induce T-cell activation. If this process is successful, this ligand or a structural mimic of the ligand could then be used for vaccination. In the same manner as other vaccines, this would theoretically stimulate MC.7.G5-like T-cells before the development of cancer and theoretically prime a pool of cancer-specific T-cells able to clear a pre-cancerous cell before it can progress. As such antigens may be unstable and require antigen presentation, DC-loading would more than likely be required to stimulate MC.7.G5-like T-cells (Fujii et al. 2013; Gasser et al. 2017).

While MC.7.G5-like T-cells were identified in **Chapter 5**, I also discovered a population of MR1-restricted T-cells that appeared to recognise only overexpressed surface MR1. It has been documented that MR1 overexpression can lead to misfolded MR1 on the surface independent of bound antigen (McWilliam et al. 2016). As T-cells exist that appear to recognise this overexpressed form of MR1, they may be recognising aberrant surface expression and therefore may be important in pathologies that occur to increase MR1 expression, such as in bacterial-infection (Reantragoon et al. 2013). To test this hypothesis, MR1-reactive T-cells could be screened against overexpressed MR1-K43A mutants to determine if recognition is ligand dependent. It would also be reasonable to screen MR1-reactive T-cells against bacteria-loaded antigen presenting cells, as these overexpress MR1 (Salerno-Goncalves et al. 2014; Gold et al. 2010).

6.1.3. Whole genome CRISPR as a tool to discover unconventional T-cell ligands

I have shown here for the first time the use of whole genome CRISPR to investigate the biology of an unconventional T-cell clone. Not only did whole genome CRISPR identify MR1 as the restricting molecule for MC.7.G5 activation, it expanded the knowledge on MR1-dependent antigen presentation. In addition to β_2M, STAT6, RFX, RFXANK and RFXAP were all implicated in the same screen in which MR1 was identified. Furthermore, pilot screens identified CORO1b and cell adhesion molecules as being of potential importance during killing of target cells. These data provide an example of the power of forward genetic screens as a tool to discover unconventional T-cell ligands, and to improve the knowledge of antigen-presentation to unconventional T-cells. Indeed, whole genome CRISPR could be used to provide insight to the restricting molecules of the novel invariant T-cells identified in **Chapter 3**.

6.2. Concluding remarks

Unconventional T-cells provide an opportunity to develop broad immunotherapies to a range of diseases without the limitation of HLA-restriction and may represent a new era in immunotherapy and vaccine strategies to target pathogens or cancer. In this thesis, I showed shared T-cell clonotypes in response to three different bacteria possessed known invariant TCR sequences. I also identified other, new invariant sequences that might be responsible for recognising novel antigens on bacteria-infected cells. Such bacteria-reactive T-cells may be important in the fight against antibiotic resistance. Through my studies, I identified the MC.7.G5 cancer-specific T-cell clone. A whole genome CRISPR forward genetic screen was used to delineate that this T-cell clone recognised cancer targets via MR1. I further

demonstrated that MC.7.G5-like T-cell responses can be generated from the blood of multiple healthy donors suggesting that such T-cells might be harnessed for pan-population, pan-cancer therapeutics.

Chapter 7. References

Albacker, L.A., Chaudhary, V., Chang, Y.-J., Kim, H.Y., Chuang, Y.-T., Pichavant, M., DeKruyff, R.H., Savage, P.B. and Umetsu, D.T. 2013. Invariant natural killer T cells recognize a fungal glycosphingolipid that can induce airway hyperreactivity. *Nature Medicine* 19(10), pp. 1297–1304. 23995283.

Alvarez, C. and Sztul, E.S. 1999. Brefeldin A (BFA) disrupts the organization of the microtubule and the actin cytoskeletons. *European Journal of Cell Biology* 78(1), pp. 1–14. 10082419.

Anuwatnonthakate, A., Whitehead, S.J., Varma, J.K., Silachamroon, U., Kasetjaroen, Y., Moolphate, S., Limsomboon, P., Inyaphong, J., Suriyon, N., Kavinum, S., Chiengson, N., Tunteerapat, P. and Kaewkungwal, J. 2013. Effect of mycobacterial drug resistance patterns on patients' survival: a cohort study in Thailand. *Glob J Health Sci* 5(6), pp. 60–72. 24171875.

Arcaro, A., Grégoire, C., Bakker, T.R., Baldi, L., Jordan, M., Goffin, L., Boucheron, N., Wurm, F., van der Merwe, P.A., Malissen, B. and Luescher, I.F. 2001. CD8beta endows CD8 with efficient coreceptor function by coupling T cell receptor/CD3 to raft-associated CD8/p56(lck) complexes. *The Journal of experimental medicine* 194(10), pp. 1485–95. 11714755.

Arcaro, A., Gregoire, C., Boucheron, N., Stotz, S., Palmer, E., Malissen, B. and Luescher, I.F. 2000. Essential Role of CD8 Palmitoylation in CD8 Coreceptor Function. *The Journal of Immunology* 165(4), pp. 2068–2076. 10925291.

Arden, B., Clark, S.P., Kabelitz, D. and Mak, T.W. 1995. Human T-cell receptor variable gene segment families. *Immunogenetics* 42(6), pp. 455–500. 8550092.

Attaf, M., Legut, M., Cole, D.K. and Sewell, A.K. 2015. The T cell antigen receptor: The Swiss army knife of the immune system. *Clinical and Experimental Immunology* 181(1), pp. 1–18. 25753381.

Bagaev, D. V., Zvyagin, I. V., Putintseva, E. V., Izraelson, M., Britanova, O. V., Chudakov, D.M. and Shugay, M. 2016. VDJviz: a versatile browser for immunogenomics data. *BMC Genomics* 17(1), p. 453. 27297497.

Bai, L., Picard, D., Anderson, B., Chaudhary, V., Luoma, A., Jabri, B., Adams, E.J., Savage, P.B. and Bendelac, A. 2012. The majority of CD1d-sulfatide-specific T cells in human blood use a semiinvariant Vδ1 TCR. *European Journal of Immunology* 42(9), pp. 2505–2510. 22829134.

Balachandran, V.P., Łuksza, M., Zhao, J.N., Makarov, V., Moral, J.A., Remark, R., Herbst, B., Askan, G., Bhanot, U., Senbabaoglu, Y., Wells, D.K., Cary, C.I.O., Grbovic-Huezo, O., Attiyeh, M., Medina, B., Zhang, J., Loo, J., Saglimbeni, J., Abu-Akeel, M. et al. 2017. Identification of unique neoantigen qualities in long-term survivors of pancreatic cancer. *Nature* 551(7681), pp. 512–516. 29132146.

Balato, A., Unutmaz, D. and Gaspari, A.A. 2009. Natural killer T cells: An unconventional t-cell subset with diverse effector and regulatory functions. *Journal of Investigative Dermatology* 129(7), pp. 1628–1642. 19262602.

Barbee, S.D., Woodward, M.J., Turchinovich, G., Mention, J.-J., Lewis, J.M., Boyden, L.M., Lifton, R.P., Tigelaar, R. and Hayday, A.C. 2011. Skint-1 is a highly specific, unique selecting component for epidermal T cells. *Proceedings of the National Academy of Sciences* 108(8), pp. 3330–3335. 21300860.

Barry, C.E., Lee, R.E., Mdluli, K., Sampson, A.E., Schroeder, B.G., Slayden, R.A. and Yuan, Y. 1998. Mycolic acids: Structure, biosynthesis and physiological functions. *Prog. Lipid Res.* 37(2–3), pp. 143–179. 9829124.

Bassiri, H., Das, R., Guan, P., Barrett, D.M., Brennan, P.J., Banerjee, P.P., Wiener, S.J., Orange, J.S., Brenner, M.B., Grupp, S.A. and Nichols, K.E. 2014. iNKT Cell Cytotoxic Responses Control T-Lymphoma Growth In Vitro and In Vivo. *Cancer Immunology Research* 2(1), pp. 59–69. 24563871.

Battle, R., Poole, K., Haywood-Small, S., Clark, B. and Woodroofe, M.N. 2013. Molecular characterisation of the monocytic cell line THP-1 demonstrates a discrepancy with the documented HLA type. *International journal of cancer. Journal international du cancer* 132(1), pp. 246–7. 22674354.

Bauer, S., Groh, V., Wu, J., Steinle, A., Phillips, J.H., Lanier, L.L. and Spies, T. 1999. Activation of NK cells and T cells by NKG2D, a receptor for stress- inducible MICA. *Science* 285(5428), pp. 727–729. 10426993.

Bendle, G.M., Linnemann, C., Hooijkaas, A.I., Bies, L., De Witte, M.A., Jorritsma, A., Kaiser, A.D.M., Pouw, N., Debets, R., Kieback, E., Uckert, W., Song, J.Y., Haanen, J.B.A.G. and Schumacher, T.N.M. 2010. Lethal graft-versus-host disease in mouse models of T cell receptor gene therapy. *Nature Medicine* 16(5), pp. 565–570. 20400962.

Berntman, E., Rolf, J., Johansson, C., Anderson, P. and Cardell, S.L. 2005. The role of CD1d-restricted NK T lymphocytes in the immune response to oral infection with Salmonella typhimurium. *European Journal of Immunology* 35(7), pp. 2100–2109. 15940666.

Bertotto, A., Gerli, R., Spinozzi, F., Muscat, C., Scalise, F., Castellucci, G., Sposito, M., Candio, F. and Vaccaro, R. 1993. Lymphocytes bearing the gamma delta T cell receptor in acute Brucella melitensis infection. *European journal of immunology* 23(5), pp. 1177–80. 8477812.

Berzofsky, J.A. and Terabe, M. 2008. NKT Cells in Tumor Immunity: Opposing Subsets Define a New Immunoregulatory Axis. *The Journal of Immunology* 180(6), pp. 3627–3635. 18322166.

Betts, M.R., Brenchley, J.M., Price, D.A., De Rosa, S.C., Douek, D.C., Roederer, M. and Koup, R.A. 2003. Sensitive and viable identification of antigen-specific CD8+ T cells by a flow cytometric assay for degranulation. *Journal of Immunological Methods* 281(1–2), pp. 65–78. 14580882.

Bilal, M.Y., Vacaflores, A. and Houtman, J.C.D. 2015. Optimization of methods for the genetic modification of human T cells. *Immunology and Cell Biology* 93(10), pp. 896–908. 26027856.

Birkinshaw, R.W., Pellicci, D.G., Cheng, T.-Y., Keller, A.N., Sandoval-Romero, M., Gras, S., de Jong, A., Uldrich, A.P., Moody, D.B., Godfrey, D.I. and Rossjohn, J. 2015. αβ T cell antigen receptor recognition of CD1a presenting self lipid ligands. *Nature Immunology* 16(3), pp. 258–266.

Le Bourhis, L., Dusseaux, M., Bohineust, A., Bessoles, S., Martin, E., Premel, V., Coré, M., Sleurs, D., Serriari, N.E., Treiner, E., Hivroz, C., Sansonetti, P., Gougeon, M.L., Soudais, C. and Lantz, O. 2013. MAIT Cells Detect and Efficiently Lyse Bacterially-Infected Epithelial Cells. *PLoS Pathogens* 9(10), p. e1003681. 24130485.

Le Bourhis, L., Martin, E., Péguillet, I., Guihot, A., Froux, N., Coré, M., Lévy, E., Dusseaux, M., Meyssonnier, V., Premel, V., Ngo, C., Riteau, B., Duban, L., Robert, D., Huang, S., Rottman, M., Soudais, C. and Lantz, O. 2010. Antimicrobial activity of mucosal-associated invariant T cells. *Nature immunology* 11(8), pp. 701–708. 20581831.

Bowen, S., Sun, P., Livak, F., Sharrow, S. and Hodes, R.J. 2014. A Novel T Cell Subset with Trans-Rearranged V -C TCRs Shows V Expression Is Dispensable for Lineage Choice and MHC Restriction. *The Journal of Immunology* 192(1), pp. 169–177. 24307734.

Brandes, M., Willimann, K., Bioley, G., Lévy, N., Eberl, M., Luo, M., Tampé, R., Lévy, F., Romero, P. and Moser, B. 2009. Cross-presenting human γδ T cells induce robust CD8+ αβ T cell responses. *Proceedings of the National Academy of Sciences of*

the United States of America 106(7), pp. 2307–12. 19171897.

Brandes, M., Willimann, K. and Moser, B. 2005. Immunology: Professional antigen-presentation function by human γδ cells. *Science* 309(5732), pp. 264–268. 15933162.

Braud, V., Jones, E.Y. and McMichael, A. 1997. The human major histocompatibility complex class Ib molecule HLA-E binds signal sequence-derived peptides with primary anchor residues at positions 2 and 9. *European Journal of Immunology* 27(5), pp. 1164–1169. 9174606.

Braud, V.M., Allan, D.S.J., O'Callaghan, C.A., Soderstrom, K., D'Andrea, A., Ogg, G.S., Lazetic, S., Young, N.T., Bell, J.I., Phillips, J.H., Lanler, L.L. and McMichael, A.J. 1998. HLA-E binds to natural killer cell receptors CD94/NKG2A, B and C. *Nature* 391(6669), pp. 795–799. 9486650.

Britanova, O. V., Putintseva, E. V., Shugay, M., Merzlyak, E.M., Turchaninova, M.A., Staroverov, D.B., Bolotin, D.A., Lukyanov, S., Bogdanova, E.A., Mamedov, I.Z., Lebedev, Y.B. and Chudakov, D.M. 2014. Age-Related Decrease in TCR Repertoire Diversity Measured with Deep and Normalized Sequence Profiling. *The Journal of Immunology* 192(6), pp. 2689–2698. 24510963.

Bröker, B., Mrochen, D. and Péton, V. 2016. The T Cell Response to Staphylococcus aureus. *Pathogens* 5(1), p. 31. 26999219.

Brossay, L., Chioda, M., Burdin, N., Koezuka, Y., Casorati, G., Dellabona, P. and Kronenberg, M. 1998. CD1d-mediated Recognition of an α-Galactosylceramide by Natural Killer T Cells Is Highly Conserved through Mammalian Evolution. *The Journal of Experimental Medicine* 188(8), pp. 1521–1528. 9782129.

Brown, L., Wolf, J.M., Prados-Rosales, R. and Casadevall, A. 2015. Through the wall: Extracellular vesicles in Gram-positive bacteria, mycobacteria and fungi. *Nature Reviews Microbiology* 13(10), pp. 620–630. 26324094.

Burrows, S.R., Chen, Z., Archbold, J.K., Tynan, F.E., Beddoe, T., Kjer-Nielsen, L., Miles, J.J., Khanna, R., Moss, D.J., Liu, Y.C., Gras, S., Kostenko, L., Brennan, R.M., Clements, C.S., Brooks, A.G., Purcell, A.W., McCluskey, J. and Rossjohn, J. 2010. Hard wiring of T cell receptor specificity for the major histocompatibility complex is underpinned by TCR adaptability. *Proceedings of the National Academy of Sciences* 107(23), pp. 10608–10613. 20483993.

Caccamo, N., Pietra, G., Sullivan, L.C., Brooks, A.G., Prezzemolo, T., La Manna, M.P., Di Liberto, D., Joosten, S. a., van Meijgaarden, K.E., Di Carlo, P., Titone, L., Moretta, L., Mingari, M.C., Ottenhoff, T.H.M. and Dieli, F. 2015. Human CD8 T lymphocytes recognize *Mycobacterium tuberculosis* antigens presented by HLA-E during active tuberculosis and express type 2 cytokines. *European Journal of Immunology* 45(4), pp. 1069–1081. 25631937.

CDC 2013. Antibiotic resistance threats in the United States, 2013. *Current*, p. 114. 24911880.

Cheminay, C., Mohlenbrink, A. and Hensel, M. 2005. Intracellular Salmonella Inhibit Antigen Presentation by Dendritic Cells. *The Journal of Immunology* 174(5), pp. 2892–2899. 15728500.

Chen, G., Yang, X., Ko, A., Sun, X., Gao, M., Zhang, Y., Shi, A., Mariuzza, R.A. and Weng, N. ping 2017. Sequence and Structural Analyses Reveal Distinct and Highly Diverse Human CD8+TCR Repertoires to Immunodominant Viral Antigens. *Cell Reports* 19(3), pp. 569–583. 28423320.

Chiang, E. and Stroynowski, I. 2005. Protective Immunity against Disparate Tumors Is Mediated by a Nonpolymorphic MHC Class I Molecule. *Journal of immunology (Baltimore, Md : 1950)* 174(9), pp. 5367–5374. 15843534.

Chien, Y., Meyer, C. and Bonneville, M. 2014. <scp>γδ</scp> T Cells: First Line of Defense and Beyond. *Annual Review of Immunology* 32(1), pp. 121–155. 24387714.

Chiu, N.M., Wang, B., Kerksiek, K.M., Kurlander, R., Pamer, E.G. and Wang, C.R. 1999. The selection of M3-restricted T cells is dependent on M3 expression and presentation of N-formylated peptides in the thymus. *J Exp Med* 190(12), p. 1869–78.

Chua, W.-J.W.-J., Kim, S., Myers, N., Huang, S., Yu, L., Fremont, D.H., Diamond, M.S. and Hansen, T.H. 2011. Endogenous MHC-Related Protein 1 Is Transiently Expressed on the Plasma Membrane in a Conformation That Activates Mucosal-Associated Invariant T Cells. *The Journal of Immunology* 186(8), pp. 4744–4750. 21402896.

Colditz, G.A., Brewer, T.F., Berkey, C.S., Burdick, E., Fineberg, H. V and Mosteller, F. 1994. Vaccine in the Prevention of Tuberculosis Efficacy of BCG. *Jama* 271(9), pp. 698–702. 8309034.

Cole, D.K., Pumphrey, N.J., Boulter, J.M., Sami, M., Bell, J.I., Gostick, E., Price, D.A., Gao, G.F., Sewell, A.K. and Jakobsen, B.K. 2007. Human TCR-Binding Affinity is Governed by MHC Class Restriction. *The Journal of Immunology* 178(9), pp. 5727–5734. 17442956.

Colf, L.A., Bankovich, A.J., Hanick, N.A., Bowerman, N.A., Jones, L.L., Kranz, D.M.M. and Garcia, K.C. 2007. How a Single T Cell Receptor Recognizes Both Self and Foreign MHC. *Cell* 129(1), pp. 135–146. 17418792.

Compeer, E.B., Flinsenberg, T.W.H., Boon, L., Hoekstra, M.E. and Boes, M. 2014. Tubulation of endosomal structures in human dendritic cells by toll-like receptor ligation and lymphocyte contact accompanies antigen cross-presentation. *Journal of Biological Chemistry* 289(1), pp. 520–528. 24235148.

Comrie, W.A., Babich, A. and Burkhardt, J.K. 2015. F-actin flow drives affinity maturation and spatial organization of LFA-1 at the immunological synapse. *Journal of Cell Biology* 208(4), pp. 475–491. 25666810.

Cooper, A.M. 2009. Cell-Mediated Immune Responses in Tuberculosis. *Annual Review of Immunology* 27(1), pp. 393–422. 19302046.

Cosgrove, C., Ussher, J.E., Rauch, A., Gärtner, K., Kurioka, A., Hühn, M.H., Adelmann, K., Kang, Y.H., Fergusson, J.R., Simmonds, P., Goulder, P., Hansen, T.H., Fox, J., Günthard, H.F., Khanna, N., Powrie, F., Steel, A., Gazzard, B., Phillips, R.E. et al. 2013. Early and nonreversible decrease of CD161++/MAIT cells in HIV infection. *Blood* 121(6), pp. 951–961. 23255555.

Cosman, D., Müllberg, J., Sutherland, C.L., Chin, W., Armitage, R., Fanslow, W., Kubin, M. and Chalupny, N.J. 2001. ULBPs, novel MHC class I-related molecules, bind to CMV glycoprotein UL16 and stimulate NK cytotoxicity through the NKG2D receptor. *Immunity* 14(2), pp. 123–133. 11239445.

Cotton, R.N., Shahine, A., Rossjohn, J. and Moody, D.B. 2018. Lipids hide or step aside for CD1-autoreactive T cell receptors. *Current Opinion in Immunology* 52, pp. 93–99.

Dai, Y., Chen, H., Mo, C., Cui, L. and He, W. 2012. Ectopically expressed human tumor biomarker MutS homologue 2 is a novel endogenous ligand that is recognized by human γδ T cells to induce innate anti-tumor/virus immunity. *Journal of Biological Chemistry* 287(20), pp. 16812–16819. 22433851.

Das, H., Groh, V., Kuijl, C., Sugita, M., Morita, C.T., Spies, T. and Bukowski, J.F. 2001. MICA engagement by human Vγ2Vδ2 T cells enhances their antigen-dependent effector function. *Immunity* 15(1), pp. 83–93. 11485740.

Davis, M.M. and Bjorkman, P.J. 1988. T-cell antigen receptor genes and T-cell recognition. *Nature* 334(6181), pp. 395–402. 3043226.

Davodeau, F., Peyrat, M. a, Hallet, M.M., Gaschet, J., Houde, I., Vivien, R., Vie, H. and Bonneville, M. 1993. Close correlation between Daudi and mycobacterial antigen recognition by human gamma delta T cells and expression of V9JPC1 gamma/V2DJC delta-encoded T cell receptors. *Journal of immunology (Baltimore, Md. : 1950)* 151(3), pp. 1214–1223. 8393042.

Dellabona, P., Padovan, E., Casorati, G., Brockhaus, M. and Lanzavecchia, A. 1994. An

Invariant valpha24-JalphaQ/Vbeta11 T Cell Receptor Is Expressed in All Individuals by Clonally Expanded CD4-8- T Cells. *Journal of experimental medicine* 180(September), pp. 1171–1176.

Derry, M.C., Sutherland, M.R., Restall, C.M., Waisman, D.M. and Pryzdial, E.L.G. 2007. Annexin 2-mediated enhancement of cytomegalovirus infection opposes inhibition by annexin 1 or annexin 5. *Journal of General Virology* 88(1), pp. 19–27. 17170432.

Dik, W.A., Pike-Overzet, K., Weerkamp, F., de Ridder, D., de Haas, E.F.E., Baert, M.R.M., van der Spek, P., Koster, E.E.L., Reinders, M.J.T., van Dongen, J.J.M., Langerak, A.W. and Staal, F.J.T. 2005. New insights on human T cell development by quantitative T cell receptor gene rearrangement studies and gene expression profiling. *The Journal of Experimental Medicine* 201(11), pp. 1715–1723. 15928199.

Dusseaux, M., Martin, E., Serriari, N., Péguillet, I., Premel, V., Louis, D., Milder, M., Le Bourhis, L., Soudais, C., Treiner, E. and Lantz, O. 2011. Human MAIT cells are xenobiotic-resistant, tissue-targeted, CD161hi IL-17-secreting T cells. *Blood* 117(4), pp. 1250–9. 21084709.

Eberl, M., Altincicek, B., Kollas, A.K., Sanderbrand, S., Bahr, U., Reichenberg, A., Beck, E., Foster, D., Wiesner, J., Hintz, M. and Jomaa, H. 2002. Accumulation of a potent γδ T-cell stimulator after deletion of the lytB gene in Escherichia coli. *Immunology* 106(2), pp. 200–211. 12047749.

Eberl, M. and Moser, B. 2009. Monocytes and γδ T cells: close encounters in microbial infection. *Trends in Immunology* 30(12), pp. 562–568. 19853512.

Eckle, S.B.G., Birkinshaw, R.W., Kostenko, L., Corbett, a. J., McWilliam, H.E.G., Reantragoon, R., Chen, Z., Gherardin, N. a., Beddoe, T., Liu, L., Patel, O., Meehan, B., Fairlie, D.P., Villadangos, J. a., Godfrey, D.I., Kjer-Nielsen, L., McCluskey, J. and Rossjohn, J. 2014. A molecular basis underpinning the T cell receptor heterogeneity of mucosal-associated invariant T cells. *Journal of Experimental Medicine* 211(8), pp. 1585–1600. 25049336.

Ekeruche-Makinde, J., Clement, M., Cole, D.K., Edwards, E.S.J., Ladell, K., Miles, J.J., Matthews, K.K., Fuller, A., Lloyd, K. a., Madura, F., Dolton, G.M., Pentier, J., Lissina, A., Gostick, E., Baxter, T.K., Baker, B.M., Rizkallah, P.J., Price, D. a., Wooldridge, L. et al. 2012. T-cell receptor-optimized peptide skewing of the T-cell repertoire can enhance antigen targeting. *Journal of Biological Chemistry* 287(44), pp. 37269–37281. 22952231.

Elliott, J.F., Rock, E.P., Patten, P.A., Davis, M.M. and Chien, Y.H. 1988. The adult T-cell receptor delta-chain is diverse and distinct from that of fetal thymocytes. *Nature* 331(6157), pp. 627–31. 2963227.

Facciotti, F., Cavallari, M., Angénieux, C., Garcia-Alles, L.F., Signorino-Gelo, F., Angman, L., Gilleron, M., Prandi, J., Puzo, G., Panza, L., Xia, C., Wang, P.G., Dellabona, P., Casorati, G., Porcelli, S. a, de la Salle, H., Mori, L. and De Libero, G. 2011. Fine tuning by human CD1e of lipid-specific immune responses. *Proceedings of the National Academy of Sciences of the United States of America* 108(34), pp. 14228–14233. 21844346.

Faure, F., Jitsukawa, S., Miossec, C. and Hercend, T. 1990. CD1c as a target recognition structure for human T lymphocytes: Analysis with peripheral blood γ/δ cells. *European Journal of Immunology* 20(3), pp. 703–706. 1690662.

Felício, L.P., Porto, I.O.P., Mendes-Junior, C.T., Veiga-Castelli, L.C., Santos, K.E., Vianello-Brondani, R.P., Sabbagh, A., Moreau, P., Donadi, E.A. and Castelli, E.C. 2014. Worldwide HLA-E nucleotide and haplotype variability reveals a conserved gene for coding and 3' untranslated regions. *Tissue Antigens* 83(2), pp. 82–93. 24400773.

Fernandez, C.S., Amarasena, T., Kelleher, A.D., Rossjohn, J., Mccluskey, J., Godfrey, D.I. and Kent, S.J. 2015. MAIT cells are depleted early but retain functional cytokine

expression in HIV infection. *Immunology and Cell Biology* 93(2), pp. 177–188. 25348935.

Fielding, C.A., Aicheler, R., Stanton, R.J., Wang, E.C.Y., Han, S., Seirafian, S., Davies, J., McSharry, B.P., Weekes, M.P., Antrobus, P.R., Prod'homme, V., Blanchet, F.P., Sugrue, D., Cuff, S., Roberts, D., Davison, A.J., Lehner, P.J., Wilkinson, G.W.G. and Tomasec, P. 2014. Two Novel Human Cytomegalovirus NK Cell Evasion Functions Target MICA for Lysosomal Degradation. *PLoS Pathogens* 10(5). 24787765.

Föger, N., Jenckel, A., Orinska, Z., Lee, K., Chan, A.C. and Bulfone-paus, S. 2011. Differential regulation of mast cell degranulation versus cytokine secretion by the actin regulatory proteins Coronin1a and Coronin1b. 208(9), pp. 1777–1787.

Fowler, V.G. and Proctor, R.A. 2014. Where does a Staphylococcus aureus vaccine stand? *Clinical Microbiology and Infection* 20(S5), pp. 66–75. 24476315.

Fox, L.M., Cox, D.G., Lockridge, J.L., Wang, X., Chen, X., Scharf, L., Trott, D.L., Ndonye, R.M., Veerapen, N., Besra, G.S., Howell, A.R., Cook, M.E., Adams, E.J., Hildebrand, W.H. and Gumperz, J.E. 2009. Recognition of lyso-phospholipids by human natural killer T lymphocytes. *PLoS Biology* 7(10). 19859526.

Fraunholz, M. and Sinha, B. 2012. Intracellular staphylococcus aureus: Live-in and let die. *Frontiers in Cellular and Infection Microbiology* 2(April), pp. 1–10. 22919634.

Fujii, S. ichiro, Shimizu, K., Okamoto, Y., Kunii, N., Nakayama, T., Motohashi, S. and Taniguchi, M. 2013. NKT cells as an ideal anti-tumor immunotherapeutic. *Frontiers in Immunology* 4(DEC), pp. 1–7. 24348476.

Fujii, S., Shimizu, K., Smith, C., Bonifaz, L. and Steinman, R.M. 2003. Activation of Natural Killer T Cells by α-Galactosylceramide Rapidly Induces the Full Maturation of Dendritic Cells In Vivo and Thereby Acts as an Adjuvant for Combined CD4 and CD8 T Cell Immunity to a Coadministered Protein. *The Journal of Experimental Medicine* 198(2), pp. 267–279. 12874260.

Fuss, I.J., Joshi, B., Yang, Z., Degheidy, H., Fichtner-Feigl, S., De Souza, H., Rieder, F., Scaldaferri, F., Schirbel, A., Scarpa, M., West, G., Yi, C., Xu, L., Leland, P., Yao, M., Mannon, P., Puri, R.K., Fiocchi, C. and Strober, W. 2014. IL-13Rα2-bearing, type II NKT cells reactive to sulfatide self-antigen populate the mucosa of ulcerative colitis. *Gut* 63(11), pp. 1728–1736. 24515806.

Gao, Y. and Williams, A.P. 2015. Role of Innate T Cells in Anti-Bacterial Immunity. *Frontiers in immunology* 6, p. 302. 26124758.

Garcia-Alles, L.F., Giacometti, G., Versluis, C., Maveyraud, L., de Paepe, D., Guiard, J., Tranier, S., Gilleron, M., Prandi, J., Hanau, D., Heck, A.J.R., Mori, L., De Libero, G., Puzo, G., Mourey, L. and de la Salle, H. 2011. Crystal structure of human CD1e reveals a groove suited for lipid-exchange processes. *Proceedings of the National Academy of Sciences of the United States of America* 108(32), pp. 13230–5. 21788486.

Garcia-del Portillo, F., Zwick, M.B., Leung, K.Y. and Finlay, B.B. 1993. Salmonella induces the formation of filamentous structures containing lysosomal membrane glycoproteins in epithelial cells. *Proceedings of the National Academy of Sciences* 90(22), pp. 10544–10548. 8248143.

García-Pérez, B.E., Hernández-González, J.C., García-Nieto, S. and Luna-Herrera, J. 2008. Internalization of a non-pathogenic mycobacteria by macropinocytosis in human alveolar epithelial A549 cells. *Microbial Pathogenesis* 45(1), pp. 1–6. 18487035.

Garcia, K.C., Degano, M., Pease, L.R., Huang, M.D., Peterson, P.A., Teyton, L. and Wilson, I.A. 1998. Structural basis of plasticity in T cell receptor recognition of a self peptide MHC antigen. *Science* 279(5354), pp. 1166–1172.

Gasser, O., Sharples, K.J., Barrow, C., Williams, G.M., Bauer, E., Wood, C.E., Mester, B., Dzhelali, M., Caygill, G., Jones, J., Hayman, C.M., Hinder, V.A., Macapagal, J.,

McCusker, M., Weinkove, R., Painter, G.F., Brimble, M.A., Findlay, M.P., Dunbar, P.R. et al. 2017. A phase I vaccination study with dendritic cells loaded with NY-ESO-1 and α-galactosylceramide: induction of polyfunctional T cells in high-risk melanoma patients. *Cancer Immunology, Immunotherapy* (0123456789), pp. 1–14. 29094183.

Gherardin, N.A., Keller, A.N., Woolley, R.E., Le Nours, J., Ritchie, D.S., Neeson, P.J., Birkinshaw, R.W., Eckle, S.B.G., Waddington, J.N., Liu, L., Fairlie, D.P., Uldrich, A.P., Pellicci, D.G., McCluskey, J., Godfrey, D.I. and Rossjohn, J. 2016. Diversity of T Cells Restricted by the MHC Class I-Related Molecule MR1 Facilitates Differential Antigen Recognition. *Immunity* 44(1), pp. 32–45.

Gherardin, N.A., Loh, L., Admojo, L., Davenport, A.J., Richardson, K., Rogers, A., Darcy, P.K., Jenkins, M.R., Prince, H.M., Harrison, S.J., Quach, H., Fairlie, D.P., Kedzierska, K., McCluskey, J., Uldrich, A.P., Neeson, P.J., Ritchie, D.S. and Godfrey, D.I. 2018. Enumeration, functional responses and cytotoxic capacity of MAIT cells in newly diagnosed and relapsed multiple myeloma. *Scientific Reports* 8(1), p. 4159.

Gherardin, N.A., Souter, M.N.T., Koay, H.-F., Mangas, K.M., Seemann, T., Stinear, T.P., Eckle, S.B.G., Berzins, S.P., d'Udekem, Y., Konstantinov, I.E., Fairlie, D.P., Ritchie, D.S., Neeson, P.J., Pellicci, D.G., Uldrich, A.P., McCluskey, J. and Godfrey, D.I. 2018. Human blood MAIT cell subsets defined using MR1 tetramers. *Immunology and Cell Biology* 1, pp. 1–19.

Girardi, E., Maricic, I., Wang, J., Mac, T.T., Iyer, P., Kumar, V. and Zajonc, D.M. 2012. Type II natural killer T cells use features of both innate-like and conventional T cells to recognize sulfatide self antigens. *Nature Immunology* 13(9), pp. 851–856. 22820602.

Giulia, C., Loizon, S., Guenot, M., Mocan, I., Halary, F., De Saint-Basile, G., Pitard, V., Chanet-Merville, J.D., Moreau, J.F., Troye-Blomberg, M., Mercereau-Puijalon, O. and Behr, C. 2011. Control of Plasmodium falciparum erythrocytic cycle: γδ T cells target the red blood cell-invasive merozoites. *Blood* 118(26), pp. 6952–6962. 22045985.

Gober, H.-J., Kistowska, M., Angman, L., Jenö, P., Mori, L. and De Libero, G. 2003. Human T Cell Receptor γδ Cells Recognize Endogenous Mevalonate Metabolites in Tumor Cells. *The Journal of Experimental Medicine* 197(2), pp. 163–168. 12538656.

Godfrey, D.I., Le Nours, J., Andrews, D.M., Uldrich, A.P. and Rossjohn, J. 2018. Unconventional T Cell Targets for Cancer Immunotherapy. *Immunity* 48(3), pp. 453–473. 29562195.

Godfrey, D.I., Rossjohn, J. and McCluskey, J. 2008. The Fidelity, Occasional Promiscuity, and Versatility of T Cell Receptor Recognition. *Immunity* 28(3), pp. 304–314. 18342005.

Godfrey, D.I., Uldrich, A.P., Mccluskey, J., Rossjohn, J. and Moody, D.B. 2015. The burgeoning family of unconventional T cells. *Nature Immunology* 16(11), pp. 1114–1123. 26482978.

Gold, M.C., Cerri, S., Smyk-Pearson, S., Cansler, M.E., Vogt, T.M., Delepine, J., Winata, E., Swarbrick, G.M., Chua, W.J., Yu, Y.Y.L., Lantz, O., Cook, M.S., Null, M.D., Jacoby, D.B., Harriff, M.J., Lewinsohn, D.A., Hansen, T.H. and Lewinsohn, D.M. 2010. Human mucosal associated invariant T cells detect bacterially infected cells. *PLoS Biology* 8(6). 20613858.

Gold, M.C., McLaren, J.E., Reistetter, J. a., Smyk-Pearson, S., Ladell, K., Swarbrick, G.M., Yu, Y.Y.L., Hansen, T.H., Lund, O., Nielsen, M., Gerritsen, B., Kesmir, C., Miles, J.J., Lewinsohn, D. a., Price, D. a. and Lewinsohn, D.M. 2014. MR1-restricted MAIT cells display ligand discrimination and pathogen selectivity through distinct T cell receptor usage. *Journal of Experimental Medicine* 211(8), pp. 1601–1610. 25049333.

Gracey, E., Qaiyum, Z., Almaghlouth, I., Lawson, D., Karki, S., Avvaru, N., Zhang, Z., Yao, Y.,

Ranganathan, V., Baglaenko, Y. and Inman, R.D. 2016. IL-7 primes IL-17 in mucosal-associated invariant T (MAIT) cells, which contribute to the Th17-axis in ankylosing spondylitis. *Annals of the Rheumatic Diseases* 75(12), pp. 2124–2132. 27165176.

Groh, V., Rhinehart, R., Randolph-Habecker, J., Topp, M.S., Riddell, S.R. and Spies, T. 2001. Costimulation of CD8alphabeta T cells by NKG2D via engagement by MIC induced on virus-infected cells. *Nature immunology* 2(3), pp. 255–60. 11224526.

Groh, V., Rhinehart, R., Secrist, H., Bauer, S., Grabstein, K.H. and Spies, T. 1999. Broad tumor-associated expression and recognition by tumor-derived gamma delta T cells of MICA and MICB. *Proceedings of the National Academy of Sciences of the United States of America* 96(12), pp. 6879–6884. 10359807.

Groh, V., Steinle, A., Bauer, S. and Spies, T. 1998. Recognition of stress-induced MHC molecules by intestinal epithelial γδ T cells. *Science* 279(5357), pp. 1737–1740. 9497295.

Groh, V., Wu, J., Yee, C. and Spies, T. 2002. Tumour-derived soluble MIC ligands impair expression of NKG2D and T-cell activation. *Nature* 419(6908), pp. 734–738. 12384702.

Grupp, S.A., Kalos, M., Barrett, D., Aplenc, R., Porter, D.L., Rheingold, S.R., Teachey, D.T., Chew, A., Hauck, B., Wright, J.F., Milone, M.C., Levine, B.L. and June, C.H. 2013. Chimeric Antigen Receptor–Modified T Cells for Acute Lymphoid Leukemia. *New England Journal of Medicine* 368(16), pp. 1509–1518. 23527958.

Guo, T., Koo, M.Y., Kagoya, Y., Anczurowski, M., Wang, C.-H., Saso, K., Butler, M.O. and Hirano, N. 2017. A Subset of Human Autoreactive CD1c-Restricted T Cells Preferentially Expresses TRBV4-1 $^{+}$ TCRs. *The Journal of Immunology*, p. ji1700677.

Guo, Y., Ziegler, H.K., Safley, S.A., Niesel, D.W., Vaidya, S. and Klimpel, G.R. 1995. Human T-cell recognition of Listeria monocytogenes: recognition of listeriolysin O by TcR alpha beta + and TcR gamma delta + T cells. *Infect Immun* 63(6), pp. 2288–2294. 7768611.

Haeryfar, S.M.M., Shaler, C.R. and Rudak, P.T. 2018. Mucosa-associated invariant T cells in malignancies: a faithful friend or formidable foe? *Cancer Immunology, Immunotherapy* 0(0), p. 0.

Haney, D., Quigley, M.F., Asher, T.E., Ambrozak, D.R., Gostick, E., Price, D.A., Douek, D.C. and Betts, M.R. 2011. Isolation of viable antigen-specific CD8+ T cells based on membrane-bound tumor necrosis factor (TNF)-α expression. *Journal of Immunological Methods* 369(1–2), pp. 33–41. 21501617.

Hannani, D., Ma, Y., Yamazaki, T., Déchanet-Merville, J., Kroemer, G. and Zitvogel, L. 2012. Harnessing γδ T cells in anticancer immunotherapy. *Trends in Immunology* 33(5), pp. 199–206. 22364810.

Hannoun, Z., Lin, Z., Brackenridge, S., Kuse, N., Akahoshi, T., Borthwick, N., McMichael, A., Murakoshi, H., Takiguchi, M. and Hanke, T. 2018. Identification of novel HIV-1-derived HLA-E-binding peptides. *Immunology Letters* 202(August), pp. 65–72.

Hara, T., Mizuno, Y., Takaki, K., Takada, H., Akeda, H., Aoki, T., Nagata, M., Ueda, K., Matsuzaki, G., Yoshikai, Y. and Nomoto, K. 1992. Predominant activation and expansion of Vg9-bearing gd T cells in vivo as well as in vitro in salmonella infection. *Journal of Clinical Investigation* 90(1992), pp. 204–210.

Harly, C., Guillaume, Y., Nedellec, S., Peigné, C., Mönkkönen, H., Li, J., Kuball, J., Adams, E.J., Netzer, S., Déchanet-merville, J., Léger, A., Herrmann, T., Breathnach, R., Olive, D., Bonneville, M. and Scotet, E. 2012. Key implication of CD277 / Butyrophilin-3 (BTN3A) in cellular stress sensing by a major human γ δ T cell subset. *Blood* 120(11), pp. 2269–2279.

Hart, T., Chandrashekhar, M., Aregger, M., Steinhart, Z., Brown, K.R., MacLeod, G., Mis, M., Zimmermann, M., Fradet-Turcotte, A., Sun, S., Mero, P., Dirks, P., Sidhu, S., Roth, F.P.,

Rissland, O.S., Durocher, D., Angers, S. and Moffat, J. 2015. High-Resolution CRISPR Screens Reveal Fitness Genes and Genotype-Specific Cancer Liabilities. *Cell* 163(6), pp. 1515–1526. 26627737.

Hashimoto, K., Hirai, M. and Kurosawa, Y. 1995. A gene outside the human MHC related to classical HLA class I genes. *Science (New York, N.Y.)* 269(5224), pp. 693–695. 7624800.

Hayday, A.C. 2000. γδ Cells: A Right Time and a Right Place for a Conserved Third Way of Protection. *Annual Review of Immunology* 18(1), pp. 975–1026. 10837080.

Hayworth, J.L., Mazzuca, D.M., Maleki Vareki, S., Welch, I., McCormick, J.K. and Haeryfar, S.M. 2012. CD1d-independent activation of mouse and human iNKT cells by bacterial superantigens. *Immunology and Cell Biology* 90(7), pp. 699–709. 22041925.

Heczey, A., Liu, D., Tian, G., Courtney, A.N., Wei, J., Marinova, E., Gao, X., Guo, L., Yvon, E., Hicks, J., Liu, H., Dotti, G. and Metelitsa, L.S. 2015. Invariant NKT cells with chimeric antigen receptor provide a novel platform for safe and effective cancer immunotherapy. 124(18), pp. 2824–2834.

Heinzel, A.S., Grotzke, J.E., Lines, R. a, Lewinsohn, D. a, McNabb, A.L., Streblow, D.N., Braud, V.M., Grieser, H.J., Belisle, J.T. and Lewinsohn, D.M. 2002. HLA-E-dependent presentation of Mtb-derived antigen to human CD8+ T cells. *The Journal of experimental medicine* 196(11), pp. 1473–1481. 12461082.

Helke, K.L., McCrackin, M.A., Galloway, A.M., Poole, A.Z., Salgado, C.D. and Marriott, B.P. 2017. Effects of antimicrobial use in agricultural animals on drug-resistant foodborne salmonellosis in humans: A systematic literature review. *Critical Reviews in Food Science and Nutrition* 57(3), pp. 472–488. 27602884.

Heuston, S., Begley, M., Gahan, C.G.M. and Hill, C. 2012. Isoprenoid biosynthesis in bacterial pathogens. *Microbiology* 158(Pt_6), pp. 1389–1401. 22466083.

Himoudi, N., Morgenstern, D.A., Yan, M., Vernay, B., Saraiva, L., Wu, Y., Cohen, C.J., Gustafsson, K. and Anderson, J. 2012. Human γδ T lymphocytes are licensed for professional antigen presentation by interaction with opsonized target cells. *Journal of immunology (Baltimore, Md. : 1950)* 188(4), pp. 1708–16. 22250090.

Hintz, M., Reichenberg, A., Altincicek, B., Bahr, U., Gschwind, R.M., Kollas, A.K., Beck, E., Wiesner, J., Eberl, M. and Jomaa, H. 2001. Identification of (E)-4-hydroxy-3-methyl-but-2-enyl pyrophosphate as a major activator for human γδ T cells in Escherichia coli. *FEBS Letters* 509(2), pp. 317–322. 25246403.

Hirano, M., Guo, P., McCurley, N., Schorpp, M., Das, S., Boehm, T. and Cooper, M.D. 2013. Evolutionary implications of a third lymphocyte lineage in lampreys. *Nature* 501(7467), pp. 435–438. 23934109.

Hoare, H.L., Sullivan, L.C., Pietra, G., Clements, C.S., Lee, E.J., Ely, L.K., Beddoe, T., Falco, M., Kjer-Nielsen, L., Reid, H.H., McCluskey, J., Moretta, L., Rossjohn, J. and Brooks, A.G. 2006. Structural basis for a major histocompatibility complex class Ib-restricted T cell response. *Nature Immunology* 7(3), pp. 256–264. 16474394.

Holoshitz, J., Koning, F., Coligan, J.E., De Bruyn, J. and Strober, S. 1989. Isolation of CD4-CD8- mycobacteria-reactive T lymphocyte clones from rheumatoid arthritis synovial fluid. *Nature* 339(6221), pp. 226–229. 2524009.

Hover, B.M., Kim, S.H., Katz, M., Charlop-Powers, Z., Owen, J.G., Ternei, M.A., Maniko, J., Estrela, A.B., Molina, H., Park, S., Perlin, D.S. and Brady, S.F. 2018. Culture-independent discovery of the malacidins as calcium-dependent antibiotics with activity against multidrug-resistant Gram-positive pathogens. *Nature Microbiology* 3(4), pp. 415–422. 29434326.

Howson, L.J., Napolitani, G., Shepherd, D., Ghadbane, H., Kurupati, P., Preciado-Llanes, L., Rei, M., Dobinson, H.C., Gibani, M.M., Teng, K.W.W., Newell, E.W., Veerapen, N., Besra, G.S., Pollard, A.J. and Cerundolo, V. 2018. MAIT cell clonal expansion

and TCR repertoire shaping in human volunteers challenged with Salmonella Paratyphi A. *Nature Communications* 9(1), p. 253.

Huang, S., Martin, E., Kim, S., Yu, L., Soudais, C., Fremont, D.H., Lantz, O. and Hansen, T.H. 2009. MR1 antigen presentation to mucosal-associated invariant T cells was highly conserved in evolution. *Proceedings of the National Academy of Sciences of the United States of America* 106(20), pp. 8290–8295. 19416870.

Ito, M., Hiramatsu, H., Kobayashi, K., Suzue, K., Kawahata, M., Hioki, K., Ueyama, Y., Koyanagi, Y., Sugamura, K., Tsuji, K., Heike, T. and Nakahata, T. 2002. NOD/SCID/gamma(c)(null) mouse: an excellent recipient mouse model for engraftment of human cells. *Blood* 100(9), pp. 3175–82. 12384415.

Jansen, K.U., Girgenti, D.Q., Scully, I.L. and Anderson, A.S. 2013. Vaccine review: 'Staphyloccocus aureus vaccines: Problems and prospects'. *Vaccine* 31(25), pp. 2723–2730. 23624095.

Jespersen, H., Lindberg, M.F., Donia, M., Söderberg, E.M.V., Andersen, R., Keller, U., Ny, L., Svane, I.M., Nilsson, L.M. and Nilsson, J.A. 2017. Clinical responses to adoptive T-cell transfer can be modeled in an autologous immune-humanized mouse model. *Nature Communications* 8(1). 28955032.

Jin, C., Gibani, M.M., Moore, M., Juel, H.B., Jones, E., Meiring, J., Harris, V., Gardner, J., Nebykova, A., Kerridge, S.A., Hill, J., Thomaides-Brears, H., Blohmke, C.J., Yu, L.M., Angus, B. and Pollard, A.J. 2017. Efficacy and immunogenicity of a Vi-tetanus toxoid conjugate vaccine in the prevention of typhoid fever using a controlled human infection model of Salmonella Typhi: a randomised controlled, phase 2b trial. *The Lancet* 390(10111), pp. 2472–2480. 28965718.

de Jong, A., Peña-Cruz, V., Cheng, T.-Y., Clark, R.A., Van Rhijn, I. and Moody, D.B. 2010. CD1a-autoreactive T cells are a normal component of the human αβ T cell repertoire. *Nature Immunology* 11(12), pp. 1102–1109. 21037579.

Joosten, S.A., Van Meijgaarden, K.E., Van Weeren, P.C., Kazi, F., Geluk, A., Savage, N.D.L., Drijfhout, J.W., Flower, D.R., Hanekom, W.A., Klein, M.R. and Ottenhoff, T.H.M. 2010. Mycobacterium tuberculosis peptides presented by HLA-E molecules are targets for human CD8+ T-cells with cytotoxic as well as regulatory activity. *PLoS Pathogens* 6(2). 20195504.

Jouen-Beades, F., Paris, E., Dieulois, C., Lemeland, J.F., Barre-Dezelus, V., Marret, S., Humbert, G., Leroy, J. and Tron, F. 1997. In vivo and in vitro activation and expansion of gammadelta T cells during Listeria monocytogenes infection in humans. *Infect Immun* 65(10), pp. 4267–4272. 9317036.

Joung, J., Konermann, S., Gootenberg, J.S., Abudayyeh, O.O., Platt, R.J., Brigham, M.D., Sanjana, N.E. and Zhang, F. 2017. Genome-scale CRISPR-Cas9 knockout and transcriptional activation screening. *Nature Protocols* 12(4), pp. 828–863. 28333914.

Kaech, S.M. and Cui, W. 2012. Transcriptional control of effector and memory CD8+ T cell differentiation. *Nature Reviews Immunology* 12(11), pp. 749–761. 23080391.

Kain, L., Webb, B., Anderson, B.L., Deng, S., Holt, M., Constanzo, A., Zhao, M., Self, K., Teyton, A., Everett, C., Kronenberg, M., Zajonc, D.M., Bendelac, A., Savage, P.B. and Teyton, L. 2014. The Identification of the Endogenous Ligands of Natural Killer T Cells Reveals the Presence of Mammalian α-Linked Glycosylceramides. *Immunity* 41(4), pp. 543–554. 25367571.

Kasmar, A.G., van Rhijn, I., Cheng, T.-Y., Turner, M., Seshadri, C., Schiefner, A., Kalathur, R.C., Annand, J.W., de Jong, A., Shires, J., Leon, L., Brenner, M., Wilson, I.A., Altman, J.D. and Moody, D.B. 2011. CD1b tetramers bind αβ T cell receptors to identify a mycobacterial glycolipid-reactive T cell repertoire in humans. *The Journal of Experimental Medicine* 208(9), pp. 1741–1747. 21807869.

Kawakami, K., Kinjo, Y., Uezu, K., Yara, S., Miyagi, K., Koguchi, Y., Nakayama, T., Taniguchi, M.

and Saito, A. 2001. Monocyte Chemoattractant Protein-1-Dependent Increase of V 14 NKT Cells in Lungs and Their Roles in Th1 Response and Host Defense in Cryptococcal Infection. *The Journal of Immunology* 167(11), pp. 6525–6532. 11714821.

Kawano, T., Cui, J., Koezuka, Y., Toura, I., Kaneko, Y., Motoki, K., Ueno, H., Nakagawa, R., Sato, H. and Kondo, E. 1997. Activation CD1d-Restricted and TCR-Mediated of V . 14 NKT Cells by Glycosylceramides. *Science* 278(1626–1629).

Keller, A.N., Eckle, S.B.G., Xu, W., Liu, L., Hughes, V.A., Mak, J.Y.W., Meehan, B.S., Pediongco, T., Birkinshaw, R.W., Chen, Z., Wang, H., D'Souza, C., Kjer-Nielsen, L., Gherardin, N.A., Godfrey, D.I., Kostenko, L., Corbett, A.J., Purcell, A.W., Fairlie, D.P. et al. 2017. Drugs and drug-like molecules can modulate the function of mucosal-associated invariant T cells. *Nature Immunology* (January). 28166217.

Keller, A.N., Corbett, A.J., Wubben, J.M., McCluskey, J. and Rossjohn, J. 2017. MAIT cells and MR1-antigen recognition. *Current Opinion in Immunology* 46, pp. 66–74. 28494326.

Khan, M.W.A., Curbishley, S.M., Chen, H.C., Thomas, A.D., Pircher, H., Mavilio, D., Steven, N.M., Eberl, M. and Moser, B. 2014. Expanded human blood-derived γδT cells display potent antigen-presentation functions. *Frontiers in Immunology* 5(JUL), pp. 1–13. 25101086.

Kim, H.T., Nelson, E.L., Clayberger, C., Sanjanwala, M., Sklar, J. and Krensky, A.M. 1995. Gamma delta T cell recognition of tumor Ig peptide. *Journal of immunology (Baltimore, Md. : 1950)* 154(4), pp. 1614–1623. 7836746.

Kinjo, Y., Illarionov, P., Vela, J.L., Pei, B., Girardi, E., Li, X., Li, Y., Imamura, M., Kaneko, Y., Okawara, A., Miyazaki, Y., Gómez-Velasco, A., Rogers, P., Dahesh, S., Uchiyama, S., Khurana, A., Kawahara, K., Yesilkaya, H., Andrew, P.W. et al. 2011. Invariant natural killer T cells recognize glycolipids from pathogenic Gram-positive bacteria. *Nature Immunology* 12(10), pp. 966–974. 21892173.

Kinjo, Y., Wu, D., Kim, G., Xing, G.W., Poles, M.A., Ho, D.D., Tsuji, M., Kawahara, K., Wong, C.H. and Kronenberg, M. 2005. Recognition of bacterial glycosphingolipids by natural killer T cells. *Nature* 434(7032), pp. 520–525. 15791257.

Kitaura, K., Shini, T., Matsutani, T., Suzuki, R., Beemd, R., Boor, P., Lochem, E., Hop, W., Langerak, A., Wolvers-Tettero, I., Hooijkaas, H., Dongen, J., MacIsaac, C., Curtis, N., Cade, J., Visvanathan, K., Tembhare, P., Yuan, C., Xi, L. et al. 2016. A new high-throughput sequencing method for determining diversity and similarity of T cell receptor (TCR) α and β repertoires and identifying potential new invariant TCR α chains. *BMC Immunology* 17(1), p. 38. 27729009.

Kjer-Nielsen, L., Patel, O., Corbett, A.J., Le Nours, J., Meehan, B., Liu, L., Bhati, M., Chen, Z., Kostenko, L., Reantragoon, R., Williamson, N.A., Purcell, A.W., Dudek, N.L., McConville, M.J., O'Hair, R.A.J., Khairallah, G.N., Godfrey, D.I., Fairlie, D.P., Rossjohn, J. et al. 2012. MR1 presents microbial vitamin B metabolites to MAIT cells. *Nature* 491(7426), pp. 717–723. 23051753.

Klevens, R.M., Morrison, M.A., Nadle, J., Petit, S., Gershman, K., Ray, S., Harrison, L.H., Lynfield, R., Craig, A.S., Zell, E.R., Fosheim, G.E., Mcdougal, L.K., Carey, R.B. and Fridkin, S.K. 2007. Invasive Methicillin-Resistant Staphylococcus aureus Infections in the United States. 298(15), pp. 1763–1771.

Koch, M., Stronge, V.S., Shepherd, D., Gadola, S.D., Mathew, B., Ritter, G., Fersht, A.R., Besra, G.S., Schmidt, R.R., Jones, E.Y. and Cerundolo, V. 2005. The crystal structure of human CD1d with and without α-galactosylceramide. *Nature Immunology* 6(8), pp. 819–826. 16007090.

Kong, Y., Cao, W., Xi, X., Ma, C., Cui, L. and He, W. 2009. The NKG2D ligand ULBP4 binds to TCRγ9/δ2 and induces cytotoxicity to tumor cells through both TCRγδ and

NKG2D. *Blood* 114(2), pp. 310–317. 19436053.

Kroca, M., Johansson, A., Sjöstedt, A. and Tärnvik, A. 2001. V gamma 9V delta 2 T cells in human legionellosis. *Clinical and diagnostic laboratory immunology* 8(5), pp. 949–54. 11527809.

Kronenberg, M. and Zajonc, D.M. 2013. A 'GEM' of a cell. *Nature Immunology* 14(7), pp. 694–695. 23778804.

Kwiecinski, J., Rhost, S., Löfbom, L., Blomqvist, M., Månsson, J.E., Cardell, S.L. and Jin, T. 2013. Sulfatide attenuates experimental Staphylococcus aureus sepsis through a CD1d-dependent pathway. *Infection and Immunity* 81(4), pp. 1114–1120. 23340309.

Laabei, M., Recker, M., Rudkin, J.K., Aldeljawi, M., Gulay, Z., Sloan, T.J., Williams, P., Endres, J.L., Bayles, K.W., Fey, P.D., Yajjala, V.K., Widhelm, T., Hawkins, E., Lewis, K., Parfett, S., Scowen, L., Peacock, S.J., Holden, M., Wilson, D. et al. 2014. Predicting the virulence of MRSA from its genome sequence. *Genome Research* 24(5), pp. 839–849. 24717264.

De Lalla, C., Lepore, M., Piccolo, F.M., Rinaldi, A., Scelfo, A., Garavaglia, C., Mori, L., De Libero, G., Dellabona, P. and Casorati, G. 2011. High-frequency and adaptive-like dynamics of human CD1 self-reactive T cells. *European Journal of Immunology* 41(3), pp. 602–610. 21246542.

Lança, T., Correia, D. V., Moita, C.F., Raquel, H., Neves-Costa, A., Ferreira, C., Ramalho, J.S., Barata, J.T., Moita, L.F., Gomes, A.Q. and Silva-Santos, B. 2010. The MHC class Ib protein ULBP1 is a nonredundant determinant of leukemia/lymphoma susceptibility to γδ T-cell cytotoxicity. *Blood* 115(12), pp. 2407–2411. 20101024.

Langdon, A., Crook, N. and Dantas, G. 2016. The effects of antibiotics on the microbiome throughout development and alternative approaches for therapeutic modulation. *Genome Medicine* 8(1). 27074706.

Laugel, B., Boulter, J.M., Lissin, N., Vuidepot, A., Li, Y., Gostick, E., Crotty, L.E., Douek, D.C., Hemelaar, J., Price, D.A., Jakobsen, B.K. and Sewell, A.K. 2005. Design of soluble recombinant T cell receptors for antigen targeting and T cell inhibition. *The Journal of biological chemistry* 280(3), pp. 1882–92. 15531581.

Laugel, B., Lloyd, A., Meermeier, E.W., Crowther, M.D., Connor, T.R., Dolton, G., Miles, J.J., Burrows, S.R., Gold, M.C., Lewinsohn, D.M. and Sewell, A.K. 2016. Engineering of Isogenic Cells Deficient for MR1 with a CRISPR/Cas9 Lentiviral System: Tools To Study Microbial Antigen Processing and Presentation to Human MR1-Restricted T Cells. *The Journal of Immunology* 197(3), pp. 971–982. 27307560.

Leeansyah, E., Ganesh, A., Quigley, M.F., Sönnerborg, A., Andersson, J., Hunt, P.W., Somsouk, M., Deeks, S.G., Martin, J.N., Moll, M., Shacklett, B.L. and Sandberg, J.K. 2013. Activation, exhaustion, and persistent decline of the antimicrobial MR1-restricted MAIT-cell population in chronic HIV-1 infection. *Blood* 121(7), pp. 1124–1135. 23243281.

Lefranc, M.P., Giudicelli, V., Duroux, P., Jabado-Michaloud, J., Folch, G., Aouinti, S., Carillon, E., Duvergey, H., Houles, A., Paysan-Lafosse, T., Hadi-Saljoqi, S., Sasorith, S., Lefranc, G. and Kossida, S. 2015. IMGT R, the international ImMunoGeneTics information system R 25 years on. *Nucleic Acids Research* 43(D1), pp. D413–D422. 25378316.

Legut, M., Dolton, G., Mian, A.A., Ottmann, O.G. and Sewell, A.K. 2018. CRISPR-mediated TCR replacement generates superior anticancer transgenic t cells. *Blood* 131(3), pp. 311–322. 29122757.

Legut, M. and Sewell, A.K. 2018. Designer T-cells and T-cell receptors for customized cancer immunotherapies. *Current Opinion in Pharmacology* 41(Table 1), pp. 96–103.

Lepore, M., de Lalla, C., Gundimeda, S.R., Gsellinger, H., Consonni, M., Garavaglia, C., Sansano, S., Piccolo, F., Scelfo, A., Häussinger, D., Montagna, D., Locatelli, F., Bonini,

C., Bondanza, A., Forcina, A., Li, Z., Ni, G., Ciceri, F., Jenö, P. et al. 2014. A novel self-lipid antigen targets human T cells against CD1c + leukemias. *The Journal of Experimental Medicine* 211(7), pp. 1363–1377. 24935257.

Lepore, M., Kalinicenko, A., Colone, A., Paleja, B., Singhal, A., Tschumi, A., Lee, B., Poidinger, M., Zolezzi, F., Quagliata, L., Sander, P., Newell, E., Bertoletti, A., Terracciano, L., De Libero, G. and Mori, L. 2014. Parallel T-cell cloning and deep sequencing of human MAIT cells reveal stable oligoclonal TCRβ 2 repertoire. *Nature Communications* 5(May), p. 3866. 24832684.

Lepore, M., Kalinichenko, A., Calogero, S., Kumar, P., Paleja, B., Schmaler, M., Narang, V., Zolezzi, F., Poidinger, M., Mori, L. and De Libero, G. 2017. Functionally diverse human T cells recognize non-microbial antigens presented by MR1. *eLife* 6, pp. 1–22. 28518056.

Li, W., Xu, H., Xiao, T., Cong, L., Love, M.I., Zhang, F., Irizarry, R.A., Liu, J.S., Brown, M. and Liu, X.S. 2014. MAGeCK enables robust identification of essential genes from genome-scale CRISPR/Cas9 knockout screens. *Genome Biology* 15(12), p. 554. 25476604.

Linette, G.P., Stadtmauer, E.A., Maus, M. V, Rapoport, A.P., Levine, B.L., Emery, L., Litzky, L., Bagg, A., Carreno, B.M., Cimino, P.J., Binder-scholl, G.K., Smethurst, D.P., Gerry, A.B., Pumphrey, N.J., Bennett, A.D., Brewer, J.E., Dukes, J., Harper, J., Tayton-martin, H.K. et al. 2013. Cardiovascular toxicity and titin cross-reactivity of af fi nity-enhanced T cells in myeloma and melanoma. *Blood* 122(6), pp. 863–872.

Ling, L., Lin, Y., Zheng, W., Hong, S., Tang, X., Zhao, P., Li, M., Ni, J., Li, C., Wang, L. and Jiang, Y. 2016. Circulating and tumor-infiltrating mucosal associated invariant T (MAIT) cells in colorectal cancer patients. *Scientific Reports* 6(February), p. 20358.

Ling, L.L., Schneider, T., Peoples, A.J., Spoering, A.L., Engels, I., Conlon, B.P., Mueller, A., Schäberle, T.F., Hughes, D.E., Epstein, S., Jones, M., Lazarides, L., Steadman, V.A., Cohen, D.R., Felix, C.R., Fetterman, K.A., Millett, W.P., Nitti, A.G., Zullo, A.M. et al. 2015. A new antibiotic kills pathogens without detectable resistance. *Nature* 517(7535), pp. 455–459. 25561178.

Lipsitch, M. and Siber, G.R. 2016. How can vaccines contribute to solving the antimicrobial resistance problem? *mBio* 7(3), pp. 1–8. 27273824.

Lissina, A., Ladell, K., Skowera, A., Clement, M., Edwards, E., Seggewiss, R., van den Berg, H. a., Gostick, E., Gallagher, K., Jones, E., Melenhorst, J.J., Godkin, A.J., Peakman, M., Price, D. a., Sewell, A.K. and Wooldridge, L. 2009. Protein kinase inhibitors substantially improve the physical detection of T-cells with peptide-MHC tetramers. *Journal of Immunological Methods* 340(1), pp. 11–24. 18929568.

Liuzzi, A.R., Kift-Morgan, A., Lopez-Anton, M., Friberg, I.M., Zhang, J., Brook, A.C., Roberts, G.W., Donovan, K.L., Colmont, C.S., Toleman, M.A., Bowen, T., Johnson, D.W., Topley, N., Moser, B., Fraser, D.J. and Eberl, M. 2016. Unconventional Human T Cells Accumulate at the Site of Infection in Response to Microbial Ligands and Induce Local Tissue Remodeling. *Journal of immunology (Baltimore, Md. : 1950)* 197(6), pp. 2195–207. 27527598.

Liuzzi, A.R., McLaren, J.E., Price, D. a and Eberl, M. 2015. Early innate responses to pathogens: pattern recognition by unconventional human T-cells. *Current Opinion in Immunology* 36, pp. 31–37.

van Loenen, M.M., de Boer, R., Amir, A.L., Hagedoorn, R.S., Volbeda, G.L., Willemze, R., van Rood, J.J., Falkenburg, J.H.F. and Heemskerk, M.H.M. 2010. Mixed T cell receptor dimers harbor potentially harmful neoreactivity. *Proceedings of the National Academy of Sciences* 107(24), pp. 10972–10977. 20534461.

López-Sagaseta, J., Sibener, L. V., Kung, J.E., Gumperz, J. and Adams, E.J. 2012. Lysophospholipid presentation by CD1d and recognition by a human Natural Killer T-

cell receptor. *EMBO Journal* 31(8), pp. 2047–2059. 22395072.

Luoma, A.M., Castro, C.D., Mayassi, T., Bembinster, L.A., Bai, L., Picard, D., Anderson, B., Scharf, L., Kung, J.E., Sibener, L. V., Savage, P.B., Jabri, B., Bendelac, A. and Adams, E.J. 2013. Crystal Structure of Vδ1T Cell Receptor in Complex with CD1d-Sulfatide Shows MHC-like Recognition of a Self-Lipid by Human γδ T Cells. *Immunity* 39(6), pp. 1032–1042. 24239091.

Ly, D., Kasmar, A.G., Cheng, T.-Y., de Jong, A., Huang, S., Roy, S., Bhatt, A., van Summeren, R.P., Altman, J.D., Jacobs, W.R., Adams, E.J., Minnaard, A.J., Porcelli, S.A. and Moody, D.B. 2013. CD1c tetramers detect ex vivo T cell responses to processed phosphomycoketide antigens. *The Journal of Experimental Medicine* 210(4), pp. 729–741. 23530121.

Macho-Fernandez, E. and Brigl, M. 2015. The extended family of CD1d-restricted NKT cells: Sifting through a mixed bag of TCRs, antigens, and functions. *Frontiers in Immunology* 6(JUL). 26284062.

Macosko, E.Z., Basu, A., Satija, R., Nemesh, J., Shekhar, K., Goldman, M., Tirosh, I., Bialas, A.R., Kamitaki, N., Martersteck, E.M., Trombetta, J.J., Weitz, D.A., Sanes, J.R., Shalek, A.K., Regev, A. and McCarroll, S.A. 2015. Highly parallel genome-wide expression profiling of individual cells using nanoliter droplets. *Cell* 161(5), pp. 1202–1214. 26000488.

Mao, C., Mou, X., Zhou, Y., Yuan, G., Xu, C., Liu, H., Zheng, T., Tong, J., Wang, S. and Chen, D. 2014. Tumor-activated TCRγδ^{+} T cells from gastric cancer patients induce the antitumor immune response of TCRαβ^{+} T cells via their antigen-presenting cell-like effects. *Journal of Immunology Research* 2014.

Marlin, R., Pappalardo, A., Kaminski, H., Willcox, C.R., Pitard, V., Netzer, S., Khairallah, C., Lomenech, A.-M., Harly, C., Bonneville, M., Moreau, J.-F., Scotet, E., Willcox, B.E., Faustin, B. and Déchanet-Merville, J. 2017. Sensing of cell stress by human γδ TCR-dependent recognition of annexin A2. *Proceedings of the National Academy of Sciences* 114(12), pp. 3163–3168. 28270598.

Marrack, P. and Kappler, J. 1990. The staphylococcal enterotoxins and their relatives. *Science* 248(4956), pp. 705–711. 2343314.

Matsuda, J.L., Gapin, L., Fazilleau, N., Warren, K., Naidenko, O. V and Kronenberg, M. 2001. Natural killer T cells reactive to a single glycolipid exhibit a highly diverse T cell receptor beta repertoire and small clone size. *Proceedings of the National Academy of Sciences of the United States of America* 98(22), pp. 12636–12641. 11592984.

Mcmurtrey, C., Harriff, M.J., Swarbrick, G.M., Duncan, A., Cansler, M., Null, M., Bardet, W., Jackson, K.W., Lewinsohn, A., Hildebrand, W. and Lewinsohn, D.M. 2017. T cell recognition of Mycobacterium tuberculosis peptides presented by HLA-E derived from infected human cells. , pp. 1–19.

McWilliam, H.E.G., Eckle, S.B.G., Theodossis, A., Liu, L., Chen, Z., Wubben, J.M., Fairlie, D.P., Strugnell, R.A., Mintern, J.D., McCluskey, J., Rossjohn, J. and Villadangos, J.A. 2016. The intracellular pathway for the presentation of vitamin B–related antigens by the antigen-presenting molecule MR1. *Nature Immunology* advance on(October 2015), pp. 1–9. 27043408.

Medalla, F., Gu, W., Mahon, B.E., Judd, M., Folster, J., Griffin, P.M. and Hoekstra, R.M. 2017. Estimated Incidence of Antimicrobial Drug – Resistant Nontyphoidal Salmonella. *Emerging Infectious Diseases* 23(1), pp. 2004–2012.

Meermeier, E.W., Laugel, B.F., Sewell, A.K., Corbett, A.J., Rossjohn, J., McCluskey, J., Harriff, M.J., Franks, T., Gold, M.C. and Lewinsohn, D.M. 2016. Human TRAV1-2-negative MR1-restricted T cells detect S. pyogenes and alternatives to MAIT riboflavin-based antigens. *Nature Communications* 7, p. 12506. 27527800.

Meraviglia, S., Eberl, M., Vermijlen, D., Todaro, M., Buccheri, S., Cicero, G., La Mendola, C.,

Guggino, G., D'Asaro, M., Orlando, V., Scarpa, F., Roberts, A., Caccamo, N., Stassi, G., Dieli, F. and Hayday, A.C. 2010. In vivo manipulation of V9V2 T cells with zoledronate and low-dose interleukin-2 for immunotherapy of advanced breast cancer patients. *Clinical and Experimental Immunology* 161(2), pp. 290–297. 20491785.

Messaoudi, I., Guevara Patiño, J.A., Dyall, R., LeMaoult, J. and Nikolich-Žugich, J. 2002. Direct link between mhc polymorphism, T cell avidity, and diversity in immune defense. *Science* 298(5599), pp. 1797–1800. 12459592.

Mirzaei, H.R., Rodriguez, A., Shepphird, J., Brown, C.E. and Badie, B. 2017. Chimeric antigen receptors T cell therapy in solid tumor: Challenges and clinical applications. *Frontiers in Immunology* 8(DEC). 29312333.

Misumi, Y., Misumi, Y., Miki, K., Takatsuki, A., Tamura, G. and Ikehara, Y. 1986. Novel blockade by brefeldin A of intracellular transport of secretory proteins in cultured rat hepatocytes. *Journal of Biological Chemistry* 261(24), pp. 11398–11403. 2426273.

Mogasale, V., Maskery, B., Ochiai, R.L., Lee, J.S., Mogasale, V. V., Ramani, E., Kim, Y.E., Park, J.K. and Wierzba, T.F. 2014. Burden of typhoid fever in low-income and middle-income countries: A systematic, literature-based update with risk-factor adjustment. *The Lancet Global Health* 2(10), pp. e570–e580. 25304633.

Molloy, P.E., Sewell, A.K. and Jakobsen, B.K. 2005. Soluble T cell receptors: Novel immunotherapies. *Current Opinion in Pharmacology* 5(4 SPEC. ISS.), pp. 438–443. 15939669.

Montgomery, C.P., Daniels, M., Zhao, F., Alegre, M.L., Chong, A.S. and Daum, R.S. 2014. Protective immunity against recurrent Staphylococcus aureus skin infection requires antibody and interleukin-17A. *Infection and Immunity* 82(5), pp. 2125–2134. 24614654.

Moody, D.B., Rosat, J., Roura-mir, C., Connor, P.B.O., Zajonc, D.M., Walz, A., Miller, M.J., Levery, S.B., Wilson, I.A., Costello, C.E. and Brenner, M.B. 2004. T Cell Activation by Lipopetide antigens. *Science* 303(January), p. 527.

Mookerjee-Basu, J., Vantourout, P., Martinez, L.O., Perret, B., Collet, X., Perigaud, C., Peyrottes, S. and Champagne, E. 2010. F1-Adenosine Triphosphatase Displays Properties Characteristic of an Antigen Presentation Molecule for V 9V 2 T Cells. *The Journal of Immunology* 184(12), pp. 6920–6928. 20483757.

Munk, M.E., Gatrill, A.J. and Kaufmann, S.H.E. 1990. Target cell lysis and IL-2 secretion by gamma / delta T lymphocytes after activation with bacteria . This information is current as Email Alerts Information about subscribing to The Journal of Immunology is online at : TARGET CELL LYSIS AND IL-2 SECRETION.

Murphy, A.G., O'Keeffe, K.M., Lalor, S.J., Maher, B.M., Mills, K.H.G. and McLoughlin, R.M. 2014. Staphylococcus aureus infection of mice expands a population of memory γδ T cells that are protective against subsequent infection. *Journal of immunology (Baltimore, Md. : 1950)* 192(8), pp. 3697–708. 24623128.

Nicol, A., Nieda, M., Koezuka, Y., Porcelli, S., Suzuki, K., Tadokoro, K., Durrant, S. and Juji, T. 2000. Human invariant Valpha24+ natural killer T cells activated by alpha-galactosylceramide (KRN7000) have cytotoxic anti-tumour activity through mechanisms distinct from T cells and natural killer cells. *Immunology* 99(2), pp. 229–234. 10692041.

Nizet, V., Bradley, J.S. and NHS 2015. Staphylococcal infections [Online] Available at: https://www.nhs.uk/conditions/staphylococcal-infections/ [Accessed: 15 November 2015].

Noto Llana, M., Sarnacki, S.H., Morales, A.L., Aya Castañeda, M. del R., Giacomodonato, M.N., Blanco, G. and Cerquetti, M.C. 2017. Activation of iNKT Cells Prevents Salmonella-Enterocolitis and Salmonella-Induced Reactive Arthritis by Downregulating IL-17-Producing γδT Cells. *Frontiers in Cellular and Infection Microbiology* 7(September),

pp. 1–10.

Le Nours, J., Praveena, T., Pellicci, D.G., Gherardin, N.A., Ross, F.J., Lim, R.T., Besra, G.S., Keshipeddy, S., Richardson, S.K., Howell, A.R., Gras, S., Godfrey, D.I., Rossjohn, J. and Uldrich, A.P. 2016. Atypical natural killer T-cell receptor recognition of CD1d-lipid antigens. *Nature Communications* 7. 26875526.

Oganesyan, V., Oganesyan, N., Terzyan, S., Qu, D., Dauter, Z., Esmon, N.L. and Esmon, C.T. 2002. The crystal structure of the endothelial protein C receptor and a bound phospholipid. *Journal of Biological Chemistry* 277(28), pp. 24851–24854. 12034704.

Pardoll, D.M. 2012. The blockade of immune checkpoints in cancer immunotherapy. *Nature Reviews Cancer* 12(4), pp. 252–264. 22437870.

Parra-Cuadrado, J.F., Navarro, P., Mirones, I., Setién, F., Oteo, M. and Martínez-Naves, E. 2000. A study on the polymorphism of human MHC class I-related MR1 gene and identification of an MR1-like pseudogene. *Tissue antigens* 56(2), pp. 170–2. 11019920.

Patel, O., Kjer-Nielsen, L., Le Nours, J., Eckle, S.B.G., Birkinshaw, R., Beddoe, T., Corbett, A.J., Liu, L., Miles, J.J., Meehan, B., Reantragoon, R., Sandoval-Romero, M.L., Sullivan, L.C., Brooks, A.G., Chen, Z., Fairlie, D.P., McCluskey, J. and Rossjohn, J. 2013. Recognition of vitamin B metabolites by mucosal-associated invariant T cells. *Nature communications* 4(May), p. 2142. 23846752.

Patel, S.J., Sanjana, N.E., Kishton, R.J., Eidizadeh, A., Vodnala, S.K., Cam, M., Gartner, J.J., Jia, L., Steinberg, S.M., Yamamoto, T.N., Merchant, A.S., Mehta, G.U., Chichura, A., Shalem, O., Tran, E., Eil, R., Sukumar, M., Guijarro, E.P., Day, C.P. et al. 2017. Identification of essential genes for cancer immunotherapy. *Nature* 548(7669), pp. 537–542. 28783722.

Pecora, N.D., Fulton, S.A., Reba, S.M., Drage, M.G., Simmons, D.P., Urankar-Nagy, N.J., Boom, W.H. and Harding, C. V. 2009. Mycobacterium bovis BCG decreases MHC-II expression in vivo on murine lung macrophages and dendritic cells during aerosol infection. *Cellular Immunology* 254(2), pp. 94–104. 18762288.

Pellicci, D.G., Clarke, A.J., Patel, O., Mallevaey, T., Beddoe, T., Le Nours, J., Uldrich, A.P., McCluskey, J., Besra, G.S., Porcelli, S.A., Gapin, L., Godfrey, D.I. and Rossjohn, J. 2011. Recognition of β-linked self glycolipids mediated by natural killer T cell antigen receptors. *Nature Immunology* 12(9), pp. 827–833. 21804559.

Pellicci, D.G., Uldrich, A.P., Le Nours, J., Ross, F., Chabrol, E., Eckle, S.B.G., de Boer, R., Lim, R.T., McPherson, K., Besra, G., Howell, A.R., Moretta, L., McCluskey, J., Heemskerk, M.H.M., Gras, S., Rossjohn, J. and Godfrey, D.I. 2014. The molecular bases of δ/αβ T cell–mediated antigen recognition. *The Journal of Experimental Medicine* 211(13), pp. 2599–2615. 25452463.

Pereira, S.M., Dantas, O.M.S., Ximenes, R. and Barreto, M.L. 2007. BCG vaccine against tuberculosis: Its protective effect and vaccination policies. *Revista de Saude Publica* 41(SUPPL. 1), pp. 1–7. 18038092.

Peterfalvi, A., Gomori, E., Magyarlaki, T., Pal, J., Banati, M., Javorhazy, A., Szekeres-Bartho, J., Szereday, L. and Illes, Z. 2008. Invariant Vα7.2-Jα33 TCR is expressed in human kidney and brain tumors indicating infiltration by mucosal-associated invariant T (MAIT) cells. *International Immunology* 20(12), pp. 1517–1525. 18927318.

Pietra, G., Romagnani, C., Mazzarino, P., Falco, M., Millo, E., Moretta, A., Moretta, L. and Mingari, M.C. 2003. HLA-E-restricted recognition of cytomegalovirus-derived peptides by human CD8+ cytolytic T lymphocytes. *Proceedings of the National Academy of Sciences of the United States of America* 100(19), pp. 10896–901. 12960383.

Porcelli, S., Yockey, C.E., Brenner, M.B. and Balk, S.P. 1993. Analysis of T cell antigen receptor (TCR) expression by human peripheral blood CD4-8- alpha/beta T cells

demonstrates preferential use of several V beta genes and an invariant TCR alpha chain. *The Journal of experimental medicine* 178(1), pp. 1–16. 8391057.

Porter, D.L. and Levine, Bruce L, et. al 2011. Chimeric Antigen Receptor–Modified T Cells in Chronic Lymphoid Leukemia. *The New England Journal of Medicine* 356(8), pp. 725–733. 21830940.

Prezzemolo, T., van Meijgaarden, K.E., Franken, K.L., Caccamo, N., Dieli, F., Ottenhoff, T.H. and Joosten, S.A. 2017. Detailed characterization of human *Mycobacterium tuberculosis* specific HLA-E restricted CD8 $^{+}$ T-cells. *European Journal of Immunology*, pp. 293–305.

Puan, K.J., Jin, C., Wang, H., Sarikonda, G., Raker, A.M., Lee, H.K., Samuelson, M.I., Märker-Hermann, E., Pasa-Tolic, L., Nieves, E., Giner, J.L., Kuzuyama, T. and Morita, C.T. 2007. Preferential recognition of a microbial metabolite by human Vγ2Vδ2 T cells. *International Immunology* 19(5), pp. 657–673. 17446209.

Purbhoo, M.A., Boulter, J.M., Price, D.A., Vuidepot, A.L., Hourigan, C.S., Rod Dunbar, P., Olson, K., Dawson, S.J., Phillips, R.E., Jakobsen, B.K., Bell, J.I. and Sewell, A.K. 2001. The Human CD8 Coreceptor Effects Cytotoxic T Cell Activation and Antigen Sensitivity Primarily by Mediating Complete Phosphorylation of the T Cell Receptor η Chain. *Journal of Biological Chemistry* 276(35), pp. 32786–32792. 11438524.

Qi, J., Zhang, J., Zhang, S., Cui, L. and He, W. 2003. Immobilized MICA could expand human Vdelta1 gammadelta T cells in vitro that displayed major histocompatibility complex class I chain-related A-dependent cytotoxicity to human epithelial carcinomas. *Scandinavian journal of immunology* 58(2), pp. 211–20. 12869143.

Rajasingham, R., Smith, R.M., Park, B.J., Jarvis, J.N., Govender, N.P., Chiller, T.M., Denning, D.W., Loyse, A. and Boulware, D.R. 2017. Global burden of disease of HIV-associated cryptococcal meningitis: an updated analysis. *The Lancet Infectious Diseases* 17(8), pp. 873–881. 28483415.

Raman, M.C.C., Rizkallah, P.J., Simmons, R., Donnellan, Z., Dukes, J., Bossi, G., Le Provost, G.S., Todorov, P., Baston, E., Hickman, E., Mahon, T., Hassan, N., Vuidepot, A., Sami, M., Cole, D.K. and Jakobsen, B.K. 2016. Direct molecular mimicry enables off-target cardiovascular toxicity by an enhanced affinity TCR designed for cancer immunotherapy. *Scientific Reports* 6(September 2015), pp. 1–10. 26758806.

Rapoport, A.P., Stadtmauer, E.A., Binder-Scholl, G.K., Goloubeva, O., Vogl, D.T., Lacey, S.F., Badros, A.Z., Garfall, A., Weiss, B., Finklestein, J., Kulikovskaya, I., Sinha, S.K., Kronsberg, S., Gupta, M., Bond, S., Melchiori, L., Brewer, J.E., Bennett, A.D., Gerry, A.B. et al. 2015. NY-ESO-1-specific TCR-engineered T cells mediate sustained antigen-specific antitumor effects in myeloma. *Nature Medicine* 21(8), pp. 914–921. 26193344.

Reantragoon, R., Corbett, A.J., Sakala, I.G., Gherardin, N. a, Furness, J.B., Chen, Z., Eckle, S.B.G., Uldrich, A.P., Birkinshaw, R.W., Patel, O., Kostenko, L., Meehan, B., Kedzierska, K., Liu, L., Fairlie, D.P., Hansen, T.H., Godfrey, D.I., Rossjohn, J., McCluskey, J. et al. 2013. Antigen-loaded MR1 tetramers define T cell receptor heterogeneity in mucosal-associated invariant T cells. *The Journal of experimental medicine* 210(11), pp. 2305–20. 24101382.

Reantragoon, R., Kjer-Nielsen, L., Patel, O., Chen, Z., Illing, P.T., Bhati, M., Kostenko, L., Bharadwaj, M., Meehan, B., Hansen, T.H., Godfrey, D.I., Rossjohn, J. and McCluskey, J. 2012. Structural insight into MR1-mediated recognition of the mucosal associated invariant T cell receptor. *Journal of Experimental Medicine* 209(4), pp. 761–774. 22412157.

Reith, W., LeibundGut-Landmann, S. and Waldburger, J.-M. 2005. Regulation of MHC class II gene expression by the class II transactivator. *Nature Reviews Immunology* 5(10), pp. 793–806. 16200082.

Van Rhijn, I., van Berlo, T., Hilmenyuk, T., Cheng, T.-Y., Wolf, B.J., Tatituri, R.V. V., Uldrich, A.P., Napolitani, G., Cerundolo, V., Altman, J.D., Willemsen, P., Huang, S., Rossjohn, J., Besra, G.S., Brenner, M.B., Godfrey, D.I. and Moody, D.B. 2015. Human autoreactive T cells recognize CD1b and phospholipids. *Proceedings of the National Academy of Sciences*, p. 201520947.

Van Rhijn, I., Gherardin, N.A., Kasmar, A., de Jager, W., Pellicci, D.G., Kostenko, L., Tan, L.L.L.L., Bhati, M., Gras, S., Godfrey, D.I., Rossjohn, J. and Moody, D.B. 2014. TCR Bias and Affinity Define Two Compartments of the CD1b-Glycolipid-Specific T Cell Repertoire. *The Journal of Immunology* 192(9), pp. 4054–4060. 24683194.

Van Rhijn, I., Kasmar, A., De Jong, A., Gras, S., Bhati, M., Doorenspleet, M.E., De Vries, N., Godfrey, D.I., Altman, J.D., De Jager, W., Rossjohn, J. and Moody, D.B. 2013. A conserved human T cell population targets mycobacterial antigens presented by CD1b. *Nature Immunology* 14(7), pp. 706–713. 23727893.

Van Rhijn, I., Young, D.C., Im, J.S., Levery, S.B., Illarionov, P. a, Besra, G.S., Porcelli, S. a, Gumperz, J., Cheng, T.-Y. and Moody, D.B. 2004. CD1d-restricted T cell activation by nonlipidic small molecules. *Proceedings of the National Academy of Sciences of the United States of America* 101(37), pp. 13578–13583. 15342907.

Richardson, M.W., Carroll, R.G., Stremlau, M., Korokhov, N., Humeau, L.M., Silvestri, G., Sodroski, J. and Riley, J.L. 2008. Mode of Transmission Affects the Sensitivity of Human Immunodeficiency Virus Type 1 to Restriction by Rhesus TRIM5 . *Journal of Virology* 82(22), pp. 11117–11128. 18768965.

Riegert, P., Wanner, V. and Bahram, S. 1998. Genomics, isoforms, expression, and phylogeny of the MHC class I-related MR1 gene. *Journal of immunology (Baltimore, Md. : 1950)* 161(8), pp. 4066–77. 9780177.

Roark, C.L., Simonian, P.L., Fontenot, A.P., Born, W.K. and O'Brien, R.L. 2008. gammadelta T cells: an important source of IL-17. *Current opinion in immunology* 20(3), pp. 353–7. 18439808.

Rodgers, J.R. and Cook, R.G. 2005. MHC class Ib molecules bridge innate and acquired immunity. *Nature reviews. Immunology* 5(6), pp. 459–471. 15928678.

Rohrlich, P.S., Fazilleau, N., Ginhoux, F., Firat, H., Michel, F., Cochet, M., Laham, N., Roth, M.P., Pascolo, S., Nato, F., Coppin, H., Charneau, P., Danos, O., Acuto, O., Ehrlich, R., Kanellopoulos, J. and Lemonnier, F.A. 2005. Direct recognition by alphabeta cytolytic T cells of Hfe, a MHC class Ib molecule without antigen-presenting function. *Proceedings of the National Academy of Sciences of the United States of America* 102(36), pp. 12855–60. 16123136.

Romagnani, C., Pietra, G., Falco, M., Millo, E., Mazzarino, P., Biassoni, R., Moretta, A., Moretta, L. and Mingari, M.C. 2002. Identification of HLA-E-specific alloreactive T lymphocytes: a cell subset that undergoes preferential expansion in mixed lymphocyte culture and displays a broad cytolytic activity against allogeneic cells. *Proc Natl Acad Sci U S A* 99(17), pp. 11328–11333. 12167676.

Rosenberg, S.A., Yang, J.C., Sherry, R.M., Kammula, U.S., Hughes, M.S., Phan, G.Q., Citrin, D.E., Restifo, N.P., Robbins, P.F., Wunderlich, J.R., Morton, K.E., Laurencot, C.M., Steinberg, S.M., White, D.E. and Dudley, M.E. 2011. Durable complete responses in heavily pretreated patients with metastatic melanoma using T-cell transfer immunotherapy. *Clinical Cancer Research* 17(13), pp. 4550–4557. 21498393.

Roth, T.L., Puig-Saus, C., Yu, R., Shifrut, E., Carnevale, J., Li, P.J., Hiatt, J., Saco, J., Krystofinski, P., Li, H., Tobin, V., Nguyen, D.N., Lee, M.R., Putnam, A.L., Ferris, A.L., Chen, J.W., Schickel, J.-N., Pellerin, L., Carmody, D. et al. 2018. Reprogramming human T cell function and specificity with non-viral genome targeting. *Nature* 559(7714), pp. 405–409. 29995861.

Roy, S., Ly, D., Castro, C.D., Li, N.-S., Hawk, A.J., Altman, J.D., Meredith, S.C., Piccirilli, J.A.,

Moody, D.B. and Adams, E.J. 2016. Molecular Analysis of Lipid-Reactive Vδ1 γδ T Cells Identified by CD1c Tetramers. *The Journal of Immunology* 196(4), pp. 1933–1942. 26755823.

Roy, S., Ly, D., Li, N.-S., Altman, J.D., Piccirilli, J.A., Moody, D.B. and Adams, E.J. 2014. Molecular basis of mycobacterial lipid antigen presentation by CD1c and its recognition by ab T cells. *Proceedings of the National Academy of Sciences* 111(43), pp. E4648–E4657. 25298532.

Russano, A.M., Bassotti, G., Agea, E., Bistoni, O., Mazzocchi, A., Morelli, A., Porcelli, S.A. and Spinozzi, F. 2007. CD1-restricted recognition of exogenous and self-lipid antigens by duodenal gammadelta+ T lymphocytes. *Journal of immunology (Baltimore, Md. : 1950)* 178(6), pp. 3620–6. 17339459.

Russo, D.M., Armitage, R.J., Barral-Netto, M., Barral, A., Grabstein, K.H. and Reed, S.G. 1993. Antigen-reactive gamma delta T cells in human leishmaniasis. *Journal of immunology (Baltimore, Md. : 1950)* 151(7), pp. 3712–8. 8376802.

Sada-Ovalle, I., Chiba, A., Gonzales, A., Brenner, M.B. and Behar, S.M. 2008. Innate invariant NKT cells recognize Mycobacterium tuberculosis-infected macrophages, produce interferon-γ, and kill intracellular bacteria. *PLoS Pathogens* 4(12). 19079582.

Salerno-Goncalves, R., Fernandez-Vina, M., Lewinsohn, D.M. and Sztein, M.B. 2004. Identification of a Human HLA-E-Restricted CD8+ T Cell Subset in Volunteers Immunized with Salmonella enterica Serovar Typhi Strain Ty21a Typhoid Vaccine. *The Journal of Immunology* 173(9), pp. 5852–5862. 12165550.

Salerno-Goncalves, R., Rezwan, T. and Sztein, M.B. 2014. B Cells Modulate Mucosal Associated Invariant T Cell Immune Responses. *Frontiers in Immunology* 4(January), pp. 1–15. 24432025.

Salim, M., Knowles, T.J., Hart, R., Mohammed, F., Woodward, M.J., Willcox, C.R., Overduin, M., Hayday, A.C. and Willcox, B.E. 2016. Characterization of a putative receptor binding surface on skint-1, a critical determinant of dendritic epidermal t cell selection. *Journal of Biological Chemistry* 291(17), pp. 9310–9321. 26917727.

Sandstrom, A., Peigné, C.M., Léger, A., Crooks, J., Konczak, F., Gesnel, M.C., Breathnach, R., Bonneville, M., Scotet, E. and Adams, E.J. 2014. The intracellular B30.2 domain of butyrophilin 3A1 binds phosphoantigens to mediate activation of human Vγ9Vδ2T Cells. *Immunity* 40(4), pp. 490–500. 24703779.

Scalise, F., Gerli, R., Castellucci, G., Spinozzi, F., Fabietti, G.M., Crupi, S., Sensi, L., Britta, R., Vaccaro, R. and Bertotto, A. 1992. Lymphocytes bearing the gamma delta T-cell receptor in acute toxoplasmosis. *Immunology* 76(4), pp. 668–70. 1398756.

Scallan, E., Hoekstra, R.M., Angulo, F.J., Tauxe, R. V., Widdowson, M.A., Roy, S.L., Jones, J.L. and Griffin, P.M. 2011. Foodborne illness acquired in the United States-Major pathogens. *Emerging Infectious Diseases* 17(1), pp. 7–15. 21192848.

Schulte, D., Vogel, M., Langhans, B., Krämer, B., Körner, C., Nischalke, H.D., Steinberg, V., Michalk, M., Berg, T., Rockstroh, J.K., Sauerbruch, T., Spengler, U. and Nattermann, J. 2009. The HLA-E ^{R} /HLA-E ^{R} Genotype Affects the Natural Course of Hepatitis C Virus (HCV) Infection and Is Associated with HLA-E–Restricted Recognition of an HCV-Derived Peptide by Interferon-γ–Secreting Human CD8 $^{+}$ T Cells. *The Journal of Infectious Diseases* 200(9), pp. 1397–1401. 19780673.

Scotet, E., Martinez, L.O., Grant, E., Barbaras, R., Jenö, P., Guiraud, M., Monsarrat, B., Saulquin, X., Maillet, S., Estève, J.P., Lopez, F., Perret, B., Collet, X., Bonneville, M. and Champagne, E. 2005. Tumor recognition following Vγ9Vδ2 T cell receptor interactions with a surface F1-ATPase-related structure and apolipoprotein A-I. *Immunity* 22(1), pp. 71–80. 15664160.

Seaman, M.S., Wang, C.-R. and Forman, J. 2000. MHC Class Ib-Restricted CTL Provide Protection Against Primary and Secondary Listeria monocytogenes Infection. *The*

Journal of Immunology 165(9), pp. 5192–5201. 11046052.

Serriari, N.E., Eoche, M., Lamotte, L., Lion, J., Fumery, M., Marcelo, P., Chatelain, D., Barre, A., Nguyen-Khac, E., Lantz, O., Dupas, J.L. and Treiner, E. 2014. Innate mucosal-associated invariant T (MAIT) cells are activated in inflammatory bowel diseases. *Clinical and Experimental Immunology* 176(2), pp. 266–274. 24450998.

Seshadri, C., Thuong, N.T.T., Mai, N.T.H., Bang, N.D., Chau, T.T.H., Lewinsohn, D.M., Thwaites, G.E., Dunstan, S.J. and Hawn, T.R. 2016. A polymorphism in human MR1 is associated with mRNA expression and susceptibility to tuberculosis. *Nature Publishing Group* 18(1), pp. 8–14.

Seshadri, C., Thuong, N.T.T., Yen, N.T.B., Bang, N.D., Chau, T.T.H., Thwaites, G.E., Dunstan, S.J. and Hawn, T.R. 2014. A polymorphism in human CD1A is associated with susceptibility to tuberculosis. *Genes & Immunity* 15(3), pp. 195–198.

Sewell, A.K. 2012. Why must T cells be cross-reactive? *Nature reviews. Immunology* 12(9), pp. 669–77. 22918468.

Shalem, O., Sanjana, N.E., Hartenian, E., Shi, X., Scott, D.A., Mikkelsen, T.S., Heckl, D., Ebert, B.L., Root, D.E., Doench, J.G. and Zhang, F. 2014. Genome-scale CRISPR-Cas9 knockout screening in human cells. *Science* 343(6166), pp. 84–87. 24336571.

Sharma, M., Bose, M., Abhimanyu, Sharma, L., Diwakar, A., Kumar, S., Gaur, S.N. and Banavalikar, J.N. 2012. Intracellular survival of Mycobacterium tuberculosis in macrophages is modulated by phenotype of the pathogen and immune status of the host. *International Journal of Mycobacteriology* 1(2), pp. 65–74. 26787058.

Sherwood, A.M., Desmarais, C., Livingston, R.J., Andriesen, J., Haussler, M., Carlson, C.S. and Robins, H. 2011. Deep sequencing of the human TCRγ and TCRβ repertoires suggests that TCRβ rearranges after αβ and γδ T cell commitment. *Science Translational Medicine* 3(90), p. 90ra61-90ra61. 21734177.

Shugay, M., Bagaev, D. V., Zvyagin, I. V., Vroomans, R.M., Crawford, J.C., Dolton, G., Komech, E.A., Sycheva, A.L., Koneva, A.E., Egorov, E.S., Eliseev, A. V., Van Dyk, E., Dash, P., Attaf, M., Rius, C., Ladell, K., McLaren, J.E., Matthews, K.K., Clemens, E.B. et al. 2018. VDJdb: A curated database of T-cell receptor sequences with known antigen specificity. *Nucleic Acids Research* 46(D1), pp. D419–D427. 28977646.

Sims, J.S., Grinshpun, B., Feng, Y., Ung, T.H., Neira, J.A., Samanamud, J.L., Canoll, P., Shen, Y., Sims, P.A. and Bruce, J.N. 2016. Diversity and divergence of the glioma-infiltrating T-cell receptor repertoire. *Proceedings of the National Academy of Sciences* 113(25), pp. E3529–E3537. 27261081.

Spellberg, B., Guidos, R., Gilbert, D., Bradley, J., Boucher, H.W., Scheld, W.M., Bartlett, J.G. and Edwards, J. 2008. The Epidemic of Antibiotic-Resistant Infections: A Call to Action for the Medical Community from the Infectious Diseases Society of America. *Clinical infectious diseases : an official publication of the Infectious Diseases Society of America* 46(2), pp. 155–164. 18171244.

Storkus, W.J., Alexander, J., Payne, J. a, Dawson, J.R. and Cresswell, P. 1989. Reversal of natural killing susceptibility in target cells expressing transfected class I HLA genes. *Proceedings of the National Academy of Sciences of the United States of America* 86(7), pp. 2361–4. 2784569.

Sun, X., Shi, Y., Akahoshi, T., Fujiwara, M., Gatanaga, H., Schönbach, C., Kuse, N., Appay, V., Gao, G.F., Oka, S. and Takiguchi, M. 2016. Effects of a Single Escape Mutation on T Cell and HIV-1 Co-adaptation. *Cell Reports* 15(10), pp. 2279–2291. 27239036.

Sundström, P., Ahlmanner, F., Akéus, P., Sundquist, M., Alsén, S., Yrlid, U., Börjesson, L., Sjöling, Å., Gustavsson, B., Wong, S.B.J. and Quiding-Järbrink, M. 2015. Human Mucosa-Associated Invariant T Cells Accumulate in Colon Adenocarcinomas but Produce Reduced Amounts of IFN-γ. *The Journal of Immunology* 195(7), pp. 3472–3481. 26297765.

Sutherland, C.L., Rabinovich, B., Chalupny, N.J., Brawand, P., Miller, R. and Cosman, D. 2006. ULBPs, human ligands of the NKG2D receptor, stimulate tumor immunity with enhancement by IL-15. *Blood* 108(4), pp. 1313–1319. 16621962.

Swanson, P.A., Pack, C.D., Hadley, A., Wang, C.-R., Stroynowski, I., Jensen, P.E. and Lukacher, A.E. 2008. An MHC class Ib–restricted CD8 T cell response confers antiviral immunity. *The Journal of Experimental Medicine* 205(7), pp. 1647–1657. 18541714.

Szymczak, A.L., Workman, C.J., Wang, Y., Vignali, K.M., Dilioglou, S., Vanin, E.F. and Vignali, D.A.A. 2004. Correction of multi-gene deficiency in vivo using a single 'self-cleaving' 2A peptide-based retroviral vector. *Nature Biotechnology* 22(5), pp. 589–594. 15064769.

Tameris, M.D., Hatherill, M., Landry, B.S., Scriba, T.J., Snowden, M.A., Lockhart, S., Shea, J.E., McClain, J.B., Hussey, G.D., Hanekom, W.A., Mahomed, H. and McShane, H. 2013. Safety and efficacy of MVA85A, a new tuberculosis vaccine, in infants previously vaccinated with BCG: A randomised, placebo-controlled phase 2b trial. *The Lancet* 381(9871), pp. 1021–1028. 23391465.

Tan, M.P., Dolton, G.M., Gerry, A.B., Brewer, J.E., Bennett, A.D., Pumphrey, N.J., Jakobsen, B.K. and Sewell, A.K. 2017. Human leucocyte antigen class I-redirected anti-tumour CD4+ T cells require a higher T cell receptor binding affinity for optimal activity than CD8+ T cells. *Clinical and Experimental Immunology* 187(1), pp. 124–137. 27324616.

Tan, M.P., Gerry, A.B., Brewer, J.E., Melchiori, L., Bridgeman, J.S., Bennett, A.D., Pumphrey, N.J., Jakobsen, B.K., Price, D.A., Ladell, K. and Sewell, A.K. 2015. T cell receptor binding affinity governs the functional profile of cancer-specific CD8 $^{+}$ T cells. *Clinical & Experimental Immunology* 180(2), pp. 255–270. 25496365.

Tatituri, R.V. V., Watts, G.F.M., Bhowruth, V., Barton, N., Rothchild, A., Hsu, F.-F., Almeida, C.F., Cox, L.R., Eggeling, L., Cardell, S., Rossjohn, J., Godfrey, D.I., Behar, S.M., Besra, G.S., Brenner, M.B. and Brigl, M. 2013. Recognition of microbial and mammalian phospholipid antigens by NKT cells with diverse TCRs. *Proceedings of the National Academy of Sciences* 110(5), pp. 1827–1832. 23307809.

Teunissen, M.B.M., Yeremenko, N.G., Baeten, D.L.P., Chielie, S., Spuls, P.I., De Rie, M.A., Lantz, O. and Res, P.C.M. 2014. The IL-17A-producing CD8 + T-cell population in psoriatic lesional skin comprises mucosa-associated invariant t cells and conventional t cells. *Journal of Investigative Dermatology* 134(12), pp. 2898–2907. 24945094.

Thorsson, V., Gibbs, D.L., Brown, S.D., Wolf, D., Bortone, D.S., Ou Yang, T.H., Porta-Pardo, E., Gao, G.F., Plaisier, C.L., Eddy, J.A., Ziv, E., Culhane, A.C., Paull, E.O., Sivakumar, I.K.A., Gentles, A.J., Malhotra, R., Farshidfar, F., Colaprico, A., Parker, J.S. et al. 2018. The Immune Landscape of Cancer. *Immunity* 48(4), p. 812–830.e14. 29628290.

Tilloy, F., Treiner, E., Park, S.H., Garcia, C., Lemonnier, F., de la Salle, H., Bendelac, A., Bonneville, M. and Lantz, O. 1999. An invariant T cell receptor alpha chain defines a novel TAP-independent major histocompatibility complex class Ib-restricted alpha/beta T cell subpopulation in mammals. *The Journal of experimental medicine* 189(12), pp. 1907–21. 10377186.

Tran, E., Longo, D.L. and Urba, W.J. 2017. A Milestone for CAR T Cells. *New England Journal of Medicine*, p. NEJMe1714680. 29226781.

Treiner, E., Duban, L., Bahram, S., Radosavljevic, M., Wanner, V., Tilloy, F., Affaticati, P., Gilfillan, S. and Lantz, O. 2003. Selection of evolutionarily conserved mucosal-associated invariant T cells by MR1. *Nature* 422(6928), pp. 164–169. 12634786.

Treiner, E. and Liblau, R.S. 2015. Mucosal-associated invariant T cells in multiple sclerosis: The jury is still out. *Frontiers in Immunology* 6(SEP), pp. 1–7. 26483793.

Tungatt, K., Bianchi, V., Crowther, M.D., Powell, W.E., Schauenburg, a. J., Trimby, A., Donia, M., Miles, J.J., Holland, C.J., Cole, D.K., Godkin, a. J., Peakman, M., Straten, P.T.,

Svane, I.M., Sewell, a. K. and Dolton, G. 2014. Antibody Stabilization of Peptide-MHC Multimers Reveals Functional T Cells Bearing Extremely Low-Affinity TCRs. *The Journal of Immunology* 194(1), pp. 463–474. 25452566.

Tuovinen, H., Pöntynen, N., Gylling, M., Kekäläinen, E., Perheentupa, J., Miettinen, A. and Arstila, T.P. 2009. γδ T cells develop independently of Aire. *Cellular Immunology* 257(1–2), pp. 5–12.

Tupin, E., Kinjo, Y. and Kronenberg, M. 2007. The unique role of natural killer T cells in the response to microorganisms. *Nature Reviews Microbiology* 5(6), pp. 405–417. 17487145.

Uchida, R., Ashihara, E., Sato, K., Kimura, S., Kuroda, J., Takeuchi, M., Kawata, E., Taniguchi, K., Okamoto, M., Shimura, K., Kiyono, Y., Shimazaki, C., Taniwaki, M. and Maekawa, T. 2007. γδT cells kill myeloma cells by sensing mevalonate metabolites and ICAM-1 molecules on cell surface. *Biochemical and Biophysical Research Communications* 354(2), pp. 613–618. 17250803.

Uldrich, A.P., Le Nours, J., Pellicci, D.G., Gherardin, N. a, McPherson, K.G., Lim, R.T., Patel, O., Beddoe, T., Gras, S., Rossjohn, J. and Godfrey, D.I. 2013. CD1d-lipid antigen recognition by the γδ TCR. *Nature immunology* 14(11), pp. 1137–45. 24076636.

Vantourout, P. and Hayday, A. 2013. Six-of-the-best: Unique contributions of γδ T cells to immunology. *Nature Reviews Immunology* 13(2), pp. 88–100. 23348415.

Vavassori, S., Kumar, A., Wan, G.S., Ramanjaneyulu, G.S., Cavallari, M., El Daker, S., Beddoe, T., Theodossis, A., Williams, N.K., Gostick, E., Price, D.A., Soudamini, D.U., Voon, K.K., Olivo, M., Rossjohn, J., Mori, L. and De Libero, G. 2013. Butyrophilin 3A1 binds phosphorylated antigens and stimulates human γδ T cells. *Nature Immunology* 14(9), pp. 908–916. 23872678.

Verboogen, D.R.J., Dingjan, I., Revelo, N.H., Visser, L.J., Ter Beest, M. and Van Den Bogaart, G. 2016. The dendritic cell side of the immunological synapse. *Biomolecular Concepts* 7(1), pp. 17–28. 19833055.

Vermijlen, D., Brouwer, M., Donner, C., Liesnard, C., Tackoen, M., Van Rysselberge, M., Twité, N., Goldman, M., Marchant, A. and Willems, F. 2010. Human cytomegalovirus elicits fetal γδ T cell responses in utero. *The Journal of Experimental Medicine* 207(4), pp. 807–821. 20368575.

Vermijlen, D., Gatti, D., Kouzeli, A., Rus, T. and Eberl, M. 2018. γδ T cell responses : How many ligands will it take till we know ? *Seminars in Cell and Developmental Biology*, pp. 1–49.

Walker, L.J., Kang, Y.H., Smith, M.O., Tharmalingham, H., Ramamurthy, N., Fleming, V.M., Sahgal, N., Leslie, A., Oo, Y., Geremia, A., Scriba, T.J., Hanekom, W.A., Lauer, G.M., Lantz, O., Adams, D.H., Powrie, F., Barnes, E. and Klenerman, P. 2012. Human MAIT and CD8αα cells develop from a pool of type-17 precommitted CD8+T cells. *Blood* 119(2), pp. 422–433. 22086415.

Wang, L., Kamath, A., Das, H., Li, L. and Bukowski, J.F. 2001. Antibacterial effect of human Vγ2Vδ2 T cells in vivo. *The Journal of Clinical Investigation* 108(9), pp. 1349–1357. 11696580.

Wang, T., Birsoy, K., Hughes, N.W., Krupczak, K.M., Post, Y., Wei, J.J., Lander, E.S. and Sabatini, D.M. 2015. Identification and characterization of essential genes in the human genome. *Science* 350(6264), pp. 1096–1101. 26472758.

Wang, T., Wei, J.J., Sabatini, D.M. and Lander, E.S. 2014. Genetic screens in human cells using the CRISPR-Cas9 system. *Science* 343(6166), pp. 80–84. 24336569.

Wang, Y., Sedimbi, S., Löfbom, L., Singh, A.K., Porcelli, S.A. and Cardell, S.L. 2018. Unique invariant natural killer T cells promote intestinal polyps by suppressing TH1 immunity and promoting regulatory T cells. *Mucosal Immunology* 11(1), pp. 131–143. 28401935.

Wasylnka, J.A. and Moore, M.M. 2002. Uptake of Aspergillus fumigatus Conidia by phagocytic and nonphagocytic cells in vitro: quantitation using strains expressing green fluorescent protein. *Infection and immunity* 70(6), pp. 3156–63. 12011010.

Wensveen, F.M., Jelenčić, V. and Polić, B. 2018. NKG2D: A master regulator of immune cell responsiveness. *Frontiers in Immunology* 9(MAR). 29568297.

WHO 2016. Salmonella (non-typhoidal) [Online] Available at: http://www.who.int/mediacentre/factsheets/fs139/en/ [Accessed: 15 November 2017].

WHO 2017. *Global Tuberculosis Report 2017*.

Wilgenburg, B. van, Scherwitzl, I., Hutchinson, E.C., Leng, T., Kurioka, A., Kulicke, C., Lara, C. de, Cole, S., Vasanawathana, S., Limpitikul, W., Malasit, P., Young, D., Denney, L., Consortium, S.-H., Moore, M.D., Fabris, P., Giordani, M.T., Oo, Y.H., Laidlaw, S.M. et al. 2016. MAIT cells are activated during human viral infections. *Nature Communications* 7, p. 11653. 27337592.

Wilgenburg, B. van, Loh, L., Chen, Z., Pediongco, T.J., Wang, H., Shi, M., Zhao, Z., Koutsakos, M., Nüssing, S., Sant, S., Wang, Z., D'Souza, C., Jia, X., Almeida, C.F., Kostenko, L., Eckle, S.B.G., Meehan, B.S., Kallies, A., Godfrey, D.I. et al. 2018. MAIT cells contribute to protection against lethal influenza infection in vivo. *Nature Communications* 9(1). 30413689.

Willcox, C.R., Pitard, V., Netzer, S., Couzi, L., Salim, M., Silberzahn, T., Moreau, J.F., Hayday, A.C., Willcox, B.E. and Déchanet-Merville, J. 2012. Cytomegalovirus and tumor stress surveillance by binding of a human γδ T cell antigen receptor to endothelial protein C receptor. *Nature Immunology* 13(9), pp. 872–879. 22885985.

Williams, H.C., San Martín, A., Adamo, C.M., Seidel-Rogol, B., Pounkova, L., Datla, S.R., Lassègue, B., Bear, J.E. and Griendling, K. 2012. Role of coronin 1B in PDGF-induced migration of vascular smooth muscle cells. *Circulation research* 111(1), pp. 56–65. 22619279.

Wolf, B.J., Tatituri, R.V. V., Almeida, C.F., Le Nours, J., Bhowruth, V., Johnson, D., Uldrich, a. P., Hsu, F.-F., Brigl, M., Besra, G.S., Rossjohn, J., Godfrey, D.I. and Brenner, M.B. 2015. Identification of a Potent Microbial Lipid Antigen for Diverse NKT Cells. *The Journal of Immunology* (AUGUST).

Won, E.J., Ju, J.K., Cho, Y., Jin, H., Park, K.-J., Kim, T.-J., Kwon, Y., Kee, H.J., Kim, J., Kee, S. and Park, Y. 2016. Clinical relevance of circulating mucosal-associated invariant T cell levels and their anti-cancer activity in patients with mucosal-associated cancer. *Oncotarget* 7(46), pp. 76274–76290. 27517754.

Wooldridge, L., Van Den Berg, H.A., Glick, M., Gostick, E., Laugel, B., Hutchinson, S.L., Milicic, A., Brenchley, J.M., Douek, D.C., Price, D.A. and Sewell, A.K. 2005. Interaction between the CD8 coreceptor and major histocompatibility complex class I stabilizes T cell receptor-antigen complexes at the cell surface. *Journal of Biological Chemistry* 280(30), pp. 27491–27501. 15837791.

Wooldridge, L., Laugel, B., Ekeruche, J., Clement, M., van den Berg, H.A., Price, D.A. and Sewell, A.K. 2010. CD8 Controls T Cell Cross-Reactivity. *The Journal of Immunology* 185(8), pp. 4625–4632. 20844204.

World Health Organization 2015. Global action plan on antimicrobial resistance. *WHO Press*, pp. 1–28. 25801559.

World Health Organization 2018. Typhoid vaccines: WHO position paper, March 2018 – Recommendations. *Vaccine* (13), pp. 153–172. 22919737.

Wun, K.S., Reijneveld, J.F., Cheng, T.-Y., Ladell, K., Uldrich, A.P., Le Nours, J., Miners, K.L., McLaren, J.E., Grant, E.J., Haigh, O.L., Watkins, T.S., Suliman, S., Iwany, S., Jimenez, J., Calderon, R., Tamara, K.L., Leon, S.R., Murray, M.B., Mayfield, J.A. et al. 2018. T cell autoreactivity directed toward CD1c itself rather than toward carried self lipids.

Nature Immunology. 29531339.

Xing, Y. and Hogquist, K.A. 2012. T-Cell Tolerance : Central and Peripheral. *Cold Spring Harbour Perspectivies Biology* 4, pp. 1–16.

Xu, B., Pizarro, J.C., Holmes, M.A., McBeth, C., Groh, V., Spies, T. and Strong, R.K. 2011. Crystal structure of a gammadelta T-cell receptor specific for the human MHC class I homolog MICA. *Proceedings of the National Academy of Sciences of the United States of America* 108(6), pp. 2414–9. 21262824.

Yang, S.H., Lee, J.P., Jang, H.R., Cha, R. -h., Han, S.S., Jeon, U.S., Kim, D.K., Song, J., Lee, D.-S. and Kim, Y.S. 2011. Sulfatide-Reactive Natural Killer T Cells Abrogate Ischemia-Reperfusion Injury. *Journal of the American Society of Nephrology* 22(7), pp. 1305–1314.

Yazdi, M.T., van Riet, S., van Schadewijk, A., Fiocco, M., van Hall, T., Taube, C., Hiemstra, P.S. and van der burg, S.H. 2016. The positive prognostic effect of stromal CD8+ tumor-infiltrating T cells is restrained by the expression of HLA-E in non-small cell lung carcinoma. *Oncotarget* 7(3). 26658106.

Yin, L., Huseby, E., Scott-Browne, J., Rubtsova, K., Pinilla, C., Crawford, F., Marrack, P., Dai, S. and Kappler, J.W. 2011. A single T cell receptor bound to major histocompatibility complex class I and class II glycoproteins reveals switchable TCR conformers. *Immunity* 35(1), pp. 23–33. 21683626.

Yu, W., Yao, D., Yu, S., Wang, X., Li, X., Wang, M., Liu, S., Feng, Z., Chen, X., Li, W., Wang, L., Liu, W., Ma, J., Yu, L., Tong, C., Song, B. and Cui, Y. 2018. Protective humoral and CD4+T cellular immune responses of Staphylococcus aureus vaccine MntC in a murine peritonitis model. *Scientific Reports* 8(1), pp. 1–13.

Zabijak, L., Attencourt, C., Guignant, C., Chatelain, D., Marcelo, P., Marolleau, J.P. and Treiner, E. 2015. Increased tumor infiltration by mucosal-associated invariant T cells correlates with poor survival in colorectal cancer patients. *Cancer Immunology, Immunotherapy* 64(12), pp. 1601–1608. 26497850.

Zajonc, D.M., Crispin, M.D.M., Bowden, T.A., Young, D.C., Cheng, T.-Y., Hu, J., Costello, C.E., Rudd, P.M., Dwek, R.A., Miller, M.J., Brenner, M.B., Moody, D.B. and Wilson, I.A. 2005. Molecular mechanism of lipopeptide presentation by CD1a. *Immunity* 22(2), pp. 209–19. 15723809.

Zajonc, D.M., Elsliger, M.A., Teyton, L. and Wilson, I.A. 2003. Crystal structure of CD1a in complex with a sulfatide self antigen at a resolution of 2.15 Å. *Nature Immunology* 4(8), pp. 808–815. 12833155.

Zarnitsyna, V.I., Evavold, B.D., Schoettle, L.N., Blattman, J.N. and Antia, R. 2013. Estimating the diversity, completeness, and cross-reactivity of the T cell repertoire. *Frontiers in Immunology* 4(DEC), pp. 1–11. 24421780.

Zeissig, S., Murata, K., Sweet, L., Publicover, J., Hu, Z., Kaser, A., Bosse, E., Iqbal, J., Hussain, M.M., Balschun, K., Röcken, C., Arlt, A., Günther, R., Hampe, J., Schreiber, S., Baron, J.L., Branch Moody, D., Jake Liang, T. and Blumberg, R.S. 2012. Hepatitis B virus-induced lipid alterations contribute to natural killer T cell-dependent protective immunity. *Nature Medicine* 18(7), pp. 1060–1068. 22706385.

Zeng, X., Meyer, C., Huang, J., Newell, E.W., Kidd, B.A., Wei, Y.L. and Chien, Y. hsiu 2014. Gamma delta T cells recognize haptens and mount a hapten-specific response. *eLife* 3, p. e03609. 25255099.

Zeng, X., Wei, Y.L., Huang, J., Newell, E.W., Yu, H., Kidd, B.A., Kuhns, M.S., Waters, R.W., Davis, M.M., Weaver, C.T. and Chien, Y.H. 2012. γδ T Cells Recognize a Microbial Encoded B Cell Antigen to Initiate a Rapid Antigen-Specific Interleukin-17 Response. *Immunity* 37(3), pp. 524–534. 22960222.

Zeng, Z. and Castan, A.R. 1997. Crystal Structure of Mouse CD1:An MHC-Like Fold with a LargeHydrophobic Binding Groove. *Science* 277(July), pp. 339–345. 9219685.

Zhang, J., Huang, J.Y., Chen, Y.N., Yuan, F., Zhang, H., Yan, F.H., Wang, M.J., Wang, G., Su, M., Lu, G., Huang, Y., Dai, H., Ji, J., Zhang, J.N., Jiang, Y.N., Chen, S.J., Zhu, Z.G. and Yu, Y.Y. 2015. Whole genome and transcriptome sequencing of matched primary and peritoneal metastatic gastric carcinoma. *Scientific reports* 5, p. 13750. 26330360.

Zhang, X.M., Tonnelle, C., Lefranc, M.P. and Huck, S. 1994. T cell receptor gamma cDNA in human fetal liver and thymus: variable regions of gamma chains are restricted to V gamma I or V9, due to the absence of splicing of the V10 and V11 leader intron. *European journal of immunology* 24(3), pp. 571–8. 8125127.

Zheng, G.X.Y., Lau, B.T., Schnall-Levin, M., Jarosz, M., Bell, J.M., Hindson, C.M., Kyriazopoulou-Panagiotopoulou, S., Masquelier, D.A., Merrill, L., Terry, J.M., Mudivarti, P.A., Wyatt, P.W., Bharadwaj, R., Makarewicz, A.J., Li, Y., Belgrader, P., Price, A.D., Lowe, A.J., Marks, P. et al. 2016. Haplotyping germline and cancer genomes with high-throughput linked-read sequencing. *Nature Biotechnology* 34(3), pp. 303–311. 26829319.

Zheng, G.X.Y., Terry, J.M., Belgrader, P., Ryvkin, P., Bent, Z.W., Wilson, R., Ziraldo, S.B., Wheeler, T.D., McDermott, G.P., Zhu, J., Gregory, M.T., Shuga, J., Montesclaros, L., Underwood, J.G., Masquelier, D.A., Nishimura, S.Y., Schnall-Levin, M., Wyatt, P.W., Hindson, C.M. et al. 2017. Massively parallel digital transcriptional profiling of single cells. *Nature Communications* 8, pp. 1–12. 28091601.

Appendix

Table 8.1 - Primer sequences for PCR and sequencing

Primer name	Application	Sequence
Cα-R1	NGS	CCATAGACCTCATGTCTAGCACAG
Cα-R2	NGS	GGTGAATAGGCAGACAGACTTGTC
Cα-R3	TCR clone sequencing	CTCTCAGCTGGTACACGGCAGG
Cβ-R1	NGS	GAGACCCTCAGGCGGCTGCTC
Cβ-R2	NGS	TGTGGCCAGGCACACCAGTGTG
Cβ-R3	TCR clone sequencing	TTCTGATGGCTCAAACACAGCGAC
Cγ-R1	NGS	CATGTCTGACGATACATCTGTG
Cγ-R2	NGS	CATGTATGTGTCGTTAGTCTTC
Cδ-R1	NGS	CAGTCTTTGCAAACAGCATTC
Cδ-R2	NGS	AGAGATGACAATAGCAGGATC
Universal A	NGS	CTAATACGACTCACTATAGGGCAA GCAGTGGTATCAACGCAGAGT
Universal Short	NGS	CTAATACGACTCACTATAGGGC
M13 F	TOPO PCR and Sequencing	GTAAAACGACGGCCAG
M13 R	TOPO PCR and Sequencing	CAGGAAACAGCTATGAC
pELNS F1	pELNS PCR	GAGTTTGGATCTTGGTTCATTC
pELNS F2	pELNS insert sequencing	CTTCCATTTCAGGTGTCGTG
pELNS R1	pELNS PCR	GCATTAAAGCAGCGTATCCAC
pELNS R2	pELNS insert sequencing	CCAGAGGTTGATTGTCGAC
pELNS R3	pELNS insert sequencing	AGAAACTTGCACCGCATATG
Adaptor F	GeCKO library PCR	AATGGACTATCATATGCTTACCGTA ACTTGAAAGTATTTCG
Adaptor R	GeCKO library PCR	TCTACTATTCTTTCCCCTGCACTGTT GTGGGGCGATGTGCGCTCTG

Table 8.2 - Sequences of forward primers for HiSeq of GeCKO libraries

Primer name	Sequence & stagger	Barcode F
Illumina F01	TAATGATACGGCGACCACCGAGATCTACACTCTTT CCCTACACGACGCTCTTCCGATCT	AAGTAGAG
Illumina F02	ATAATGATACGGCGACCACCGAGATCTACACTCTT TCCCTACACGACGCTCTTCCGATCT	CATGCTTA
Illumina F03	GATAATGATACGGCGACCACCGAGATCTACACTCT TTCCCTACACGACGCTCTTCCGATCT	GCACATCT
Illumina F04	CGATAATGATACGGCGACCACCGAGATCTACACTC TTTCCCTACACGACGCTCTTCCGATCT	TGCTCGAC

Staggers are shown in red text. Priming site: TCTTGTGGAAAGGACGAAACACC.

Table 8.3 - Sequences of reverse primers for HiSeq of GeCKO libraries

Primer name	Sequence	Barcode R	Illumina seq R
Illumina R01	CAAGCAGAAGAC GGCATACGAGAT	TCGCCTTG	GTGACTGGAGTTCAGACGT GTGCTCTTCCGATCT
Illumina R02	CAAGCAGAAGAC GGCATACGAGAT	ATAGCGTC	GTGACTGGAGTTCAGACGT GTGCTCTTCCGATCT

Priming site: CCGACTCGGTGCCACTTTTTCAA

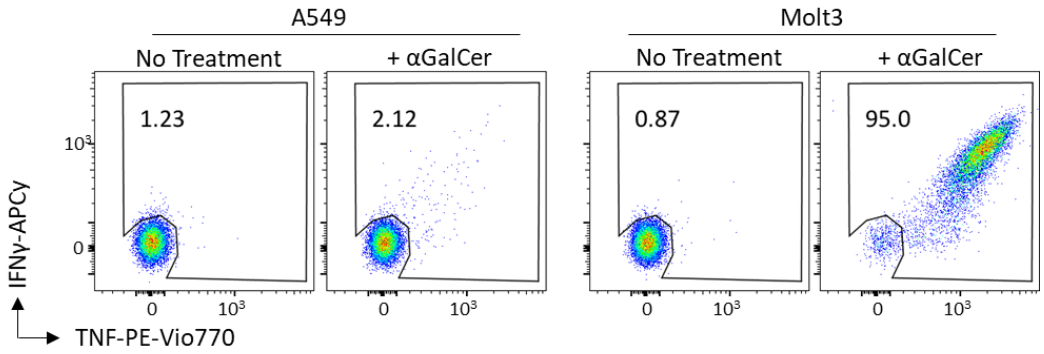

Figure 8.1 - A549 cells are unable to activate iNKT cells

A549 cells or Molt3 cells were loaded with α-galactosylceramide (αGalCer) overnight. Loaded or unloaded cells were subsequently cultured with an iNKT clone in an ICS. Cells were previously gated on single alive $CD3^+$ cells. Original FCS files provided by Mat Legut.

Table 8.4 - Cells sorted based on expression of CD107a and TNF and their corresponding TCR chain usage.

	778M			**759S**			**779K**		
	M. smegmatis	*Salmonella*	*S. aureus*	*M. smegmatis*	*Salmonella*	*S. aureus*	*M. smegmatis*	*Salmonella*	*S. aureus*
No. of cells sorted	99297	98989	50715	142609	416108	64450	471125	72672	27834
Diversity of **α-chains**	1189	714	1304	1354	736	1794	1043	291	941
No. **α-chains** sequenced	47152	36837	36771	29170	6644	46216	33924	2143	25603
Diversity of **β-chains**	1173	652	1161	2241	602	1926	1547	1095	1216
No. **β-chains** sequenced	9829	9067	9850	20155	3793	13691	15037	11193	12775
Diversity of **γ-chains**	121	85	48	254	377	77	134	71	24
No. **γ-chains** sequenced	19743	22870	25681	22316	30346	21556	33620	17654	15598
Diversity of **δ-chains**	98	126	94	188	154	140	164	117	75
No. **δ-chains** sequenced	1115	2198	1274	884	778	700	877	492	449

```
#!/usr/bin/env python
"""
this script takes an 'excel' type file of MIXCR output of clontypes
and normalises them against each other
"""
import argparse
import sys
def parse_args():
   """take parse arguments"""
   parser = argparse.ArgumentParser()
   parser.add_argument('--reference', '-R', dest = "reference_file", required = True, help = 'Baseline
file from which values will be substituted')
   parser.add_argument('--alter', '-A', dest = "input_file", required = True, help = 'Second file which
will have values altered')
   args = parser.parse_args()
   return args
def read_file(file):
   """read in tab delimited file"""
   out = []
   with open(file, 'r') as f:
      lines = f.readlines()
      for line in lines:
         elements = line.strip().split("\t")
         out.append(elements)
   return out
def column(matrix, i):
   return [row[i] for row in matrix]
def get_interesting_bit(mixcr_array):
   """gets the bit we need; the CDR3b AA sequence
     and the frequency"""
   clone_fraction_col = 2
   CDR3_col          = 32
   clone = column(mixcr_array, clone_fraction_col)
   CDR3  = column(mixcr_array, CDR3_col)
   out = []
   out.append(clone)
   out.append(CDR3)
   return out

def main():
   """main function"""
   args = parse_args()
   reference = args.reference_file
   alter = args.input_file
   files = [alter, reference]
   body = []
   full = []
   for f in files:
      full_table   = read_file(f)
      full.append(full_table)
      CDR3_freq    = get_interesting_bit(full_table)
      body.append(CDR3_freq)
   interest = body[0]
   baseline = body[1]
   full_interest = full[0]
```

```
    full_baseline = full[1]
    colnames = full_interest[0]
    out_list = []
    for i in range(1, len(interest[0])):
        CDR3_of_interest = interest[1][i]
        freq_of_interest = interest[0][i]
        for j in range(1, len(baseline[0])):
            CDR3_reference = baseline[1][j]
            freq_reference = baseline[0][j]
            if CDR3_reference == CDR3_of_interest:
                frequency = float(freq_of_interest) - float(freq_reference)
                if frequency >= 0:
                    full_interest[i][2] = frequency
                else:
                    full_interest[i][2] = 0
    outfile = alter.rsplit(".", 1)[0]
    outfile = outfile + "_normalised.txt"
    with open(outfile, 'w') as file:
        file.writelines('\t'.join(str(j) for j in i) + '\n' for i in full_interest)
    print("Output written to " + outfile)


if __name__ == "__main__":
    main()
```

Figure 8.2 - Python script for removing background clonotypes in MiXCR files

Script written by Thomas Whalley, cross references two MiXCR output files and removes frequency of clonotypes from sample. Used in this thesis to remove clonotypes present in T-cells responding to A549 alone from bacteria + A549 cells.

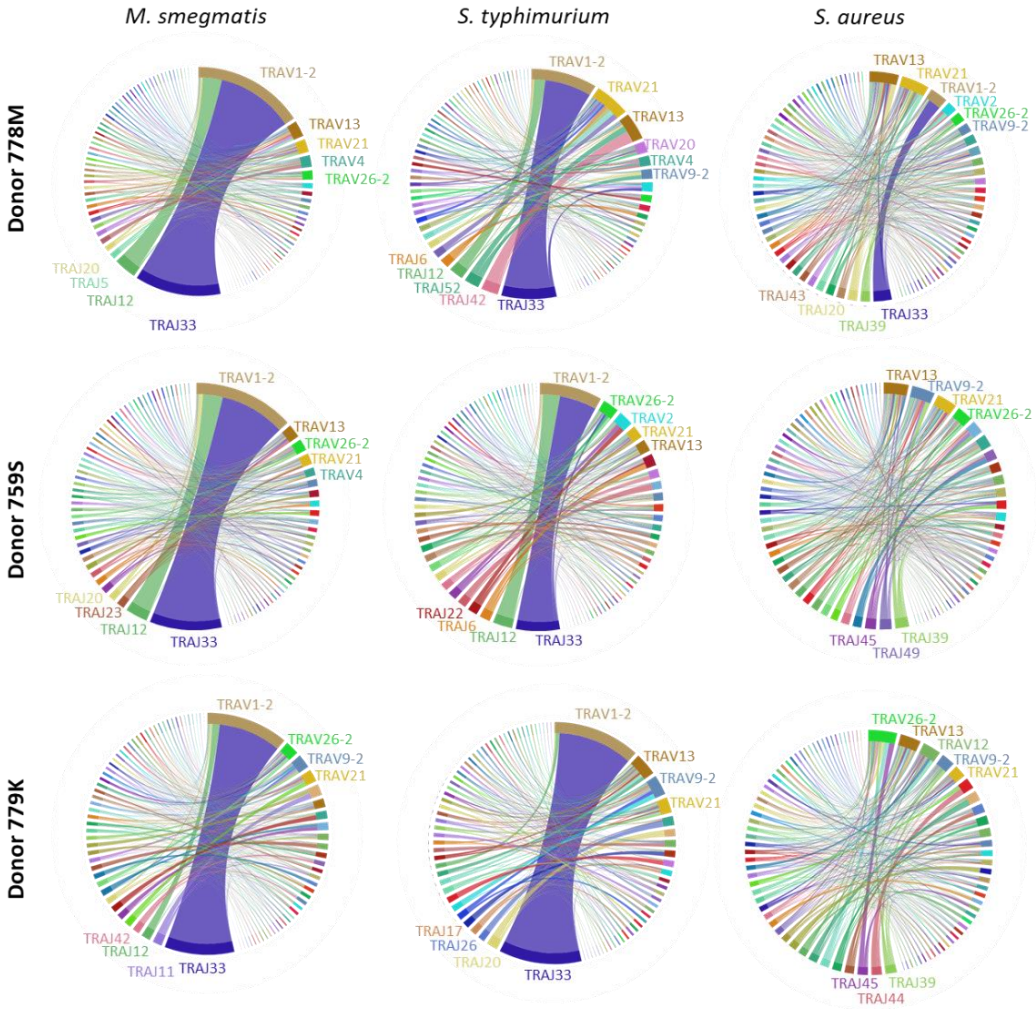

Figure 8.3 – TCR-α gene rearrangements across individual samples
NGS data from clonotyped T-cells in response to bacteria. Data analysed using VDJViz. Less common genes are hidden due to small text size.

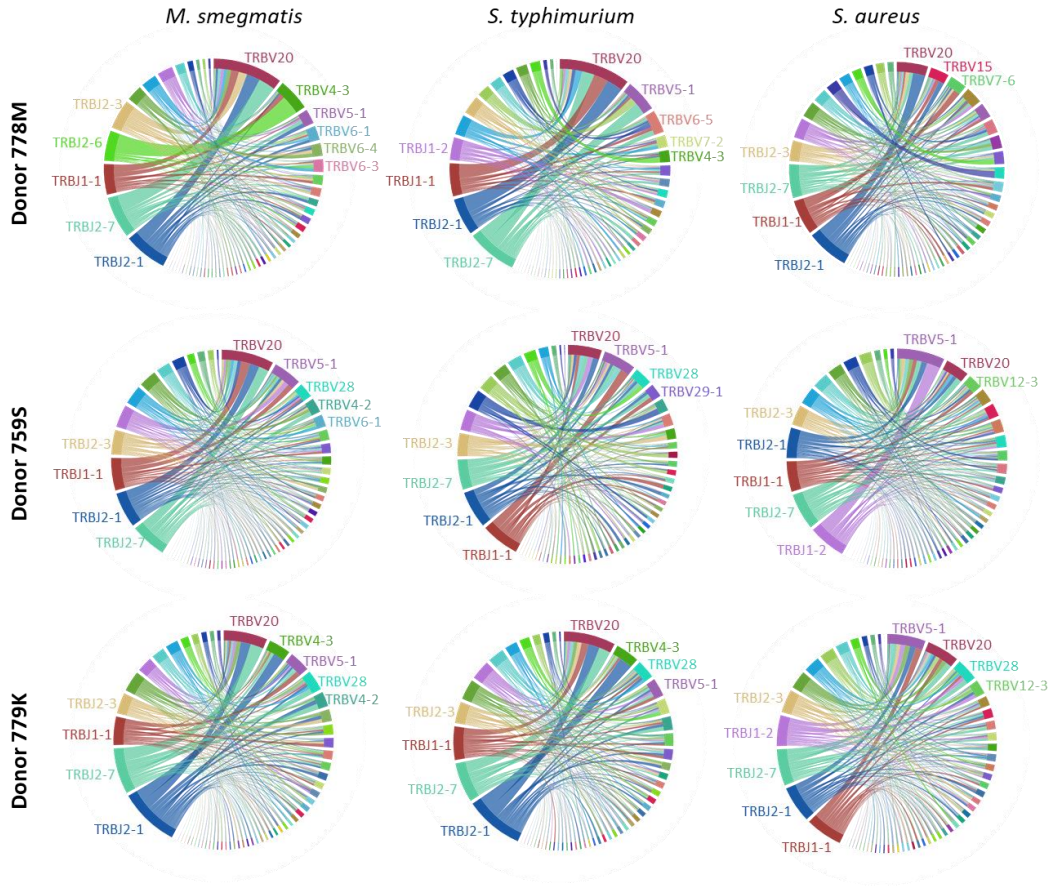

Figure 8.4 - TCR-β gene rearrangements across individual samples
NGS data from clonotyped T-cells in response to bacteria. Data analysed using VDJViz. Less common genes are hidden due to small text size.

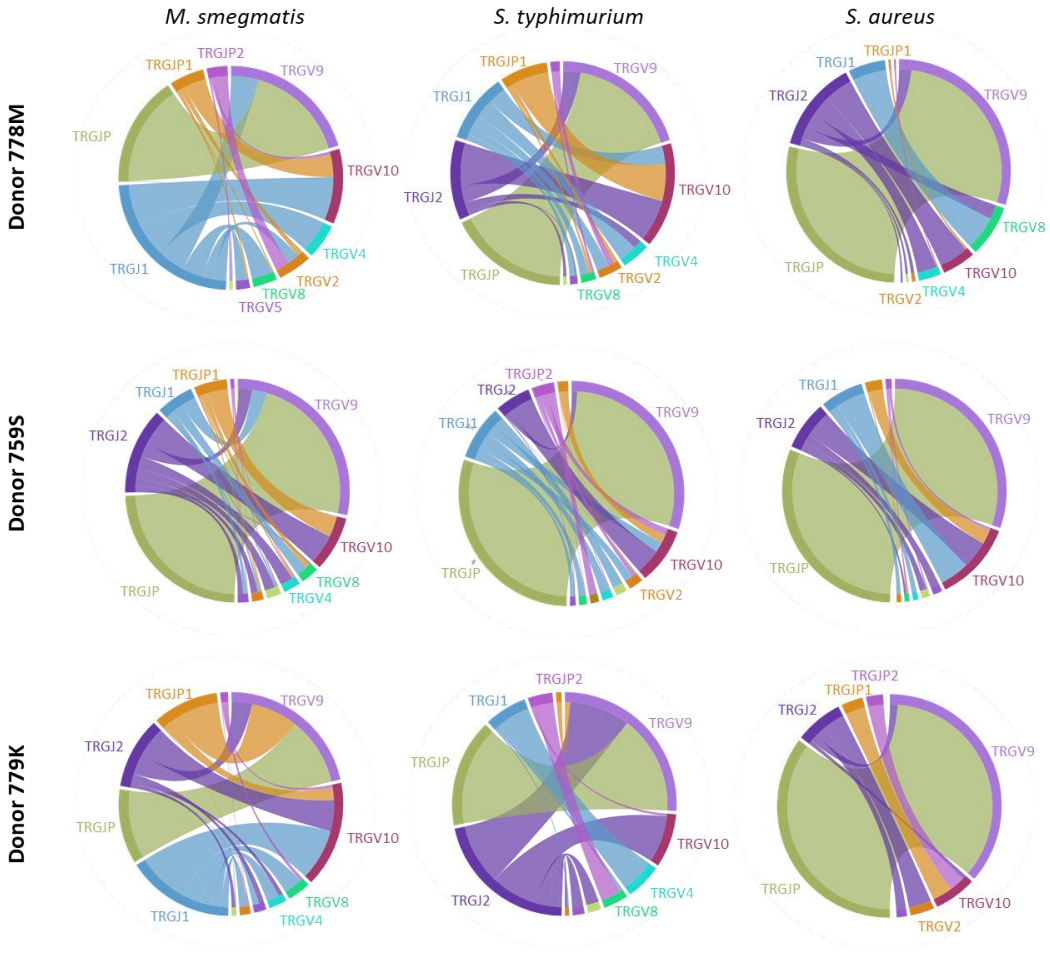

Figure 8.5 - TCR-γ gene rearrangements across individual samples
NGS data from clonotyped T-cells in response to bacteria. Data analysed using VDJViz. Less common genes are hidden due to small text size.

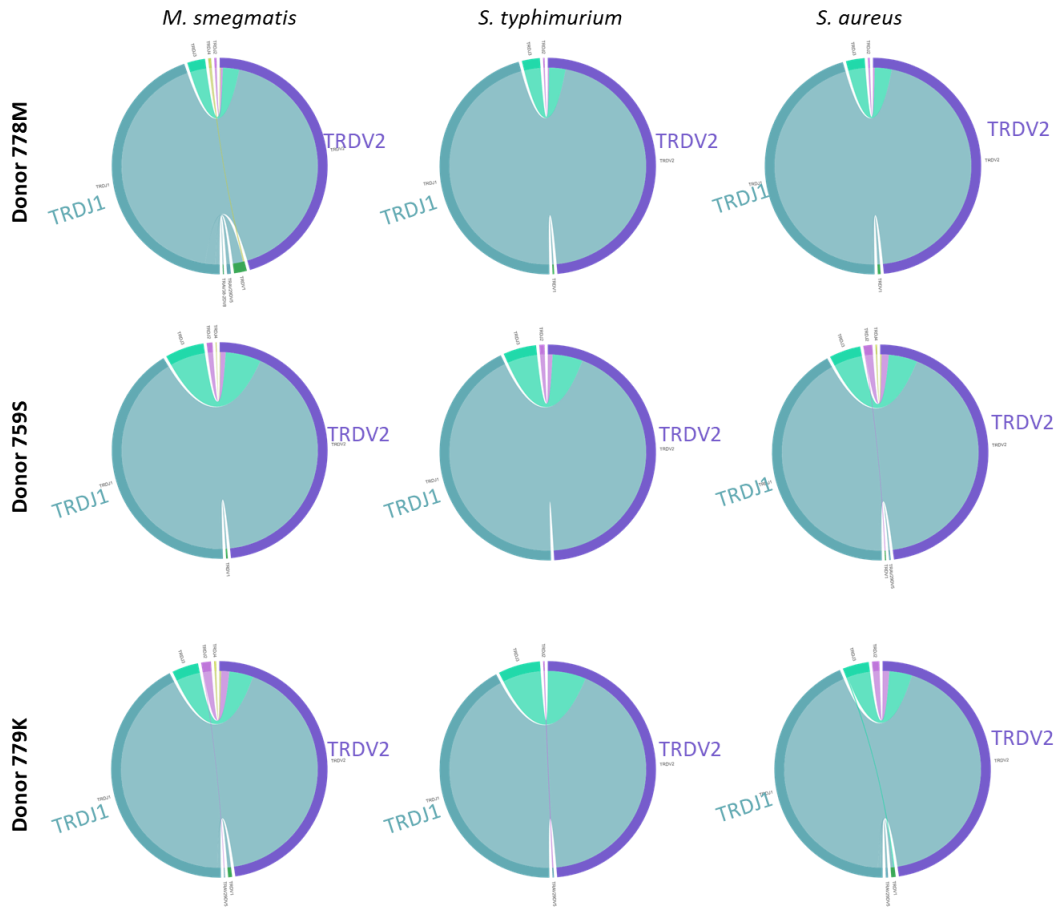

Figure 8.6 - TCR-δ gene rearrangements across individual samples
NGS data from clonotyped T-cells in response to bacteria. Data analysed using VDJViz. Less common genes are hidden due to small text size.